

A CRITICAL EVALUATION OF BRIDGE SCOUR FOR MICHIGAN SPECIFIC CONDITIONS

Submitted to

Michigan Department of Transportation
Office of Research & Best Practices
Murray D. Van Wagoner Building
Lansing MI 48909

By

Donald D. Carpenter, Ph.D., P.E., LEED AP
Associate Professor, Department of Civil Engineering
Lawrence Technological University
(Project #108493 – Contract 2007-0436)

And

Carol Miller, Ph.D., P.E.
Professor and Chair, Civil Engineering Department
Wayne State University
(Project #85106 – Contract 2006-0413)



February 2011

TECHNICAL REPORT DOCUMENTATION PAGE

1. REPORT NO. RC-1547	2. GOVERNMENT ACCESSION NO.	3. MDOT PROJECT MANAGER David Juntunen	
4. TITLE AND SUBTITLE A Critical Evaluation of Bridge Scour for Michigan Specific Conditions		5. REPORT DATE February 1, 2011	
		6. PERFORMING ORGANIZATION CODE	
7. AUTHOR(S) Donald D. Carpenter and Carol Miller		8. PERFORMING ORG. REPORT NO.	
9. PERFORMING ORGANIZATION NAME AND ADDRESS Department of Civil Engineering, Lawrence Technological University, Southfield, MI 48075 Civil Engineering Department, Wayne State University, Detroit, MI 48202		10. WORK UNIT NO. (TRAIS)	
		11. CONTRACT NO. 2007-0436 and 2006-0413	
		11a. AUTHORIZATION NO. Z1/R1	
12. SPONSORING AGENCY NAME AND ADDRESS Michigan Department of Transportation Office of Research & Best Practices PO Box 30050 Lansing, MI 48909		13. TYPE OF REPORT & PERIOD COVERED	
		14. SPONSORING AGENCY CODE	
15. SUPPLEMENTARY NOTES Additional Authors: Timothy Calappi, Hiroshan Hettiarachchi, and Matthew McClarren			
16. ABSTRACT <p>The overall goal of this research was to improve MDOTs bridge scour prediction capability. In an effort to achieve this goal, the research team evaluated scour prediction methods utilized by state DOTs, conducted a field data collection project, and proposed an alternative approach for pier scour prediction. Nine locations and twelve unique spans were selected for monitoring. During the investigation, seven episodic measurements resulted in detectable pier scour. Scour depths ranged from 0.7 to 1.5 feet with the maximum return period corresponding to a seven-year flood event. No detectable scour events occurred at the continuous scour monitoring locations. This investigation also included the use of a Jet Erosion Test (JET) to experimentally determine if in-situ soil conditions could be correlated with measured bridge scour. The JET was able to correlate erodibility with geotechnical properties such as dry unit weight, soil type, and shear strength, but was not able to aid in the calibration and/or modification of the scour prediction equations. In conclusion, a modified HEC-18 pier scour prediction equation was developed for application in Michigan using the National Bridge Scour Database (NBSD). This revised scour prediction procedure could allow MDOT to more accurately predict bridge scour and subsequently more efficiently design new bridge crossings and/or modify existing bridges. Finally, experimental and analytical approaches developed during this investigation provides a foundation for future research in the field of scour prediction.</p>			
17. KEY WORDS Bridge Scour, Soil Erosion, HEC-18, HEC-RAS		18. DISTRIBUTION STATEMENT No restrictions. This document is available to the public through the Michigan Department of Transportation.	
19. SECURITY CLASSIFICATION - report	20. SECURITY CLASSIFICATION - page	21. NO. OF PAGES 238	22. PRICE

Table of Contents

Table of Contents.....	ii
List of Figures.....	v
List of Tables.....	x
Acknowledgments.....	xii
1.0 EXECUTIVE SUMMARY	1
2.0 INTRODUCTION.....	3
3.0 LITERATURE REVIEW	5
4.0 CURRENT SCOUR EVALUATION PROCEDURES.....	9
4.1 Review of MDOT’s Scour Evaluation Procedures.....	9
4.1.1 Data.....	9
4.1.2 Scour Calculations.....	10
4.1.3 Assessment Steps.....	13
4.2 Review of Scour Evaluation Methods Utilized by other States.....	15
4.3 Database Management.....	16
5.0 BRIDGE SITE SELECTION.....	19
6.0 EQUIPMENT AND TEST METHODOLOGIES.....	23
6.1 Geotechnical Investigations.....	23
6.1.1 Sample Collection.....	23
6.1.2 Unit Weight Determination in the Field.....	24
6.1.3 Geotechnical Characterization of Soil Samples.....	26
6.1.4 Grain Size Analysis.....	26
6.1.5 Atterberg Limits.....	27
6.1.6 Direct Shear Test.....	27
6.1.7 Geotechnical Properties of Streambed Material.....	28
6.2 JET Apparatus.....	30
6.2.1 Fabrication of the Jet Apparatus.....	30
6.2.2 <i>In Situ</i> Test Setup.....	34

6.2.3 Laboratory Test Setup.....	37
6.2.4 Test Procedure.....	38
6.3 Scour Measurement.....	39
6.4 Acoustic Doppler Current Profiler.....	42
7.0 JET EROSION TEST (JET) RESULTS.....	45
7.1 Site Selection for Detailed Field JET Investigations.....	45
7.1.1 Pawpaw River at Coloma Road near Riverside, MI.....	46
7.1.2 Grand River at M-99 near Lansing, MI.....	47
7.1.3 Thornapple River at McKeown Road near Hastings, MI.....	47
7.2 Preparation of Laboratory JET Specimens.....	48
7.3 Laboratory JET.....	49
7.4 Geotechnical Properties Compared with Erodibility.....	49
7.5 Variation of Erodibility with Dry Unit Weight.....	50
7.5.1 JET Results for Control Soil.....	51
7.5.2 JET Results for Pawpaw River.....	52
7.5.3 JET Results for Grand River.....	54
7.5.4 JET Results for Thornapple River.....	55
7.5.5 Overall Comparison of Erodibility with Dry Unit Weight.....	56
7.6 Erodibility and Soil Type.....	57
7.7 Bank and Streambed Soil Comparison.....	59
7.7.1 Pawpaw River Streambed and Bank Material Comparison.....	59
7.7.2 Grand River Streambed and Bank Material Comparison.....	60
7.8 Erodibility and Shear Strength Properties.....	62
7.9 Concluding Remarks on JET Results.....	65
7.10 Recommendations for Further Research.....	67
8.0 SCOUR MEASUREMENT RESULTS.....	69
8.1 Episodic Measurements.....	70
8.1.1 Pigeon River.....	70
8.1.2 Thornapple River at M-43.....	72
8.1.3 Thornapple River at McKeown Road.....	76
8.1.4 Pine River at Lumberjack Road.....	78

8.2 Continuous Measurements.....	84
8.2.1 Flint River.....	85
8.2.2 Grand River.....	86
8.2.3 Paw Paw River.....	89
9.0 HEC-18 EQUATION MODIFICATION	91
9.1 Data Description.....	92
9.2 Regression Types.....	94
9.3 Results.....	95
9.4 Conclusion.....	99
9.5 Application to Michigan-Specific Conditions.....	100
9.6 Recommendations for future work.....	102
10.0 SCOUR PREDICTIONS USING HEC-RAS.....	103
10.1 Introduction	103
10.2 Procedure	103
10.3 Modeling Details	104
10.4 Simulation Results	108
10.5 Conclusion	111
11.0 CONCLUSION	113
References.....	117
Appendix 4.A MDOT Guidelines for Evaluation of Scour.....	121
Appendix 4.B Scour Evaluation Methods Practiced by Other States.....	139
Appendix 4.C Bridge Fact Sheets for Selected Sites.....	155
Appendix 6.A JET Apparatus Specifications.....	180
Appendix 6.B JET Excel Spreadsheet.....	188
Appendix 7.A Confidence Interval Development.....	193
Appendix 7.B Mohr-Coulomb Envelopes.....	196
Appendix 7.C Erodibility vs. Friction Angle Calculations.....	199
Appendix 8.A Hydrographs for Sites during Measurements.....	202
Appendix 9.A Detailed Results from Regression Analyses.....	217

List of Figures

Figure 4.1 Sample query of scour-critical bridges in Michigan built before 1925.....	17
Figure 4.2 All scour critical bridges in Michigan with an overlay of multi-span bridges...	18
Figure 4.3 All scour-critical bridges in the University Region.....	18
Figure 5.1 Location of nine scour monitoring locations and the additional sites visited....	20
Figure 6.1 Shelby tube schematic.....	25
Figure 6.2 Dr. Greg Hanson demonstrating the jet erosion test.....	30
Figures 6.3 (a) Submergence tank and lid (b) Lab tank and lid.....	31
Figure 6.4 Jet tube.....	32
Figure 6.5 Head pole and head tank.....	33
Figure 6.6 Head pole gusset plate.....	34
Figures 6.7(a) Site preparation (b) Submergence tank.....	35
Figure 6.8 JET apparatus in the field.....	36
Figure 6.9 Lab JET setup	37
Figures 6.10 (a) Deployed front view (b) Deployed side view	40
Figures 6.11(a) Enclosure and solar panel (b) Pier with conduit.....	41
Figures 6.12(a) Microsounder (b) Schematic drawing of continuous setup	42
Figure 6.13 Example of acoustic Doppler current profiler data.....	43
Figure 7.1 Pawpaw River field JET.....	46
Figure 7.2 Grain-size distributions of the 3 JET experiments.....	50
Figure 7.3 Control soil JET results.....	52
Figure 7.4 Pawpaw River JET results.....	53
Figure 7.5 Grand River JET results.....	55
Figure 7.6 Combined data.....	57
Figure 7.7 Combined data comparison.....	58
Figure 7.8 Pawpaw River grain-size distribution by season.....	60
Figure 7.9 Grand River grain-size distribution by season.....	61
Figure 7.10 Grand River streambed and bank material JET comparison.....	62
Figure 7.11 Pawpaw River erodibility and friction angle.....	63
Figure 7.12 Grand River erodibility and friction angle.....	64

Figure 7.13 Erodibility vs. friction angle.....	65
Figure 8.1 Measured bed elevation on the Pigeon River during 7 year return event.....	71
Figure 8.2 Bed elevation measurements upstream side of the Pigeon River at U.S.-131....	71
Figure 8.3 Pigeon River hydrograph at US-131 (USGS data)	72
Figure 8.4 Velocity contours (ft/sec) for the Pigeon River at US-131.....	72
Figure 8.5 Bed elevation on the Thornapple River at M-43 during 2 year return event.....	73
Figure 8.6 Thornapple River hydrograph at M-43.....	74
Figure 8.7 Thornapple River hydrograph at M-43.....	74
Figure 8.8 Velocity contours (ft/sec) for the Thornapple River at M-42 5/1/2009.....	75
Figure 8.9 Velocity contours (ft/sec) for the Thornapple River at M-43 3/11/2010.....	75
Figure 8.10 Velocity contours (ft/sec) for the Thornapple River at M-43 3/15/2010.....	76
Figure 8.11 Measured bed elevation on the Thornapple River at McKeown Road.....	77
Figure 8.12 Thornapple River hydrograph at McKeown.....	77
Figure 8.13 Velocity contours (ft/sec) for the Thornapple River 3/11/2010.....	78
Figure 8.14 Velocity contours (ft/sec) for the Thornapple River 3/15/2010.....	78
Figure 8.15 Mid-channel bar upstream of Pine River, north.....	79
Figure 8.16 Measured bed elevation on the Pine River (north) near Lumberjack.....	80
Figure 8.17 Pine River (north) hydrograph	80
Figure 8.18 Velocity contours (ft/sec) for the Pine River (north) 4/22/2009	81
Figure 8.19 Velocity contours (ft/sec) for the Pine River (north) 4/28/2009.....	81
Figure 8.20 Pine River at Lumberjack Road (south) with debris pile on north pier.....	82
Figure 8.21 Measured bed elevation for Pine River (south) during 3 year return event.....	83
Figure 8.22 Pine River (south) hydrograph	83
Figure 8.23 Velocity contours (ft/sec) for the Pine River (south) 4/22/2009.....	84
Figure 8.24 Velocity contours (ft/sec) for the Pine River (south) 4/28/2009	84
Figure 8.25 Bed elevation measured during maximum recorded flow event.....	86
Figure 8.26 Extended pier with data collection platform on the upstream side of bridge on M-99 over the Grand River.....	87
Figure 8.27 Continuous monitoring on the Flint, setup under the bridge deck and inaccessible during high flows.....	88
Figure 8.28 Bed elevation measured during maximum recorded flow event.....	89

Figure 8.29 Bed elevation measured during maximum recorded flow event	90
Figure 9.1 Residual comparisons for the final version of the modified HEC-18 family of equations case 1 (top) and case 2 (bottom).....	98
Figure 9.2 Residual comparisons for the final version of the modified HEC-18 family of equations case 1 (top) and case 2 (bottom).....	101
Figure 10.1 HEC-RAS scour evaluation input Cass River Crossing	105
Figure 10.2 Cass River Crossing	105
Figure 10.3 Flint River Crossing	105
Figure 10.4 Grand River	106
Figure 10.5 Paw Paw River.....	106
Figure 10.6 Raisin River.....	106
Figure 10.7 Rogue River	107
Figure 10.8 Thornapple River at M-43.....	107
Figure 10.9 Pine River (North).....	107
Figure 10.10 Cross Section of Pine River (Middle).....	108
Figure 10.11 Pine River (South)	108
Figure 4.C.1 Grand River Site.....	156
Figure 4.C.2 Cass River Site.....	158
Figure 4.C.3 Flint River Site.....	160
Figure 4.C.4 Pine River (North) Site.....	162
Figure 4.C.5 Pine River (Middle) Site.....	164
Figure 4.C.6 Pine River (South) Site.....	166
Figure 4.C.7 Rogue River Site.....	168
Figure 4.C.8 Thornapple River at M-43 Site.....	170
Figure 4.C.9 Thornapple River at McKeown Site.....	172
Figure 4.C.10 River Raisin Site.....	174
Figure 4.C.11 Paw Paw River Site.....	176
Figure 4.C.12 Pigeon River Site.....	178
Figure 6.A.1 JET apparatus	181
Figure 6.A.2 Jet tube assembly	182
Figure 6.A.3 Jet tube guide assembly.....	183

Figure 6.A.4 Lid assembly.....	184
Figure 6.A.5 Stream deflector and jet mount.....	185
Figure 6.A.6 Tank assembly.....	186
Figure 6.A.7 Tank assembly	187
Figure 6.B.1 JET input worksheet	189
Figure 6.B.2 JET asymptote plot	190
Figure 6.B.3 JET Blaisdell Method plot	191
Figure 6.B.4 JET results	192
Figure 7.A.1 Example of confidence interval for the Pawpaw River.....	194
Figure 7.A.2 Example of the linear regression for the Pawpaw River.....	195
Figure 7.B.1 Pawpaw River Mohr-Coulomb envelope.....	197
Figure 7.B.2 Grand River Mohr-Coulomb envelope.....	198
Figure 8.A.1 Hydrograph for Thornapple at McKeown (1)	203
Figure 8.A.2 Hydrograph for Thornapple at McKeown (2)	203
Figure 8.A.3 Hydrograph for Thornapple at M-43 (1).....	204
Figure 8.A.4 Hydrograph for Thornapple at M-43 (2)	204
Figure 8.A.5 Hydrograph for Rouge River at Edgerton (1)	205
Figure 8.A.6 Hydrograph for Rouge River at Edgerton (2)	205
Figure 8.A.7 Hydrograph for River Raisin at Academy (1)	206
Figure 8.A.8 Hydrograph for River Raisin at Academy (2)	206
Figure 8.A.9 Hydrograph for River Raisin at Academy (3)	207
Figure 8.A.10 Hydrograph for Pine River (South) (1)	207
Figure 8.A.11 Hydrograph for Pine River (South) (2)	208
Figure 8.A.12 Hydrograph for Pine River (Middle) (1)	208
Figure 8.A.13 Hydrograph for Pine River (Middle) (2).....	209
Figure 8.A.14 Hydrograph for Pine River (North) (1)	209
Figure 8.A.15 Hydrograph for Pine River (North) (2)	210
Figure 8.A.16 Hydrograph for Pigeon River (1)	210
Figure 8.A.17 Hydrograph for Pigeon River (2).....	211
Figure 8.A.18 Hydrograph for Grand River (1)	211
Figure 8.A.19 Hydrograph for Grand River (2).....	212

Figure 8.A.20 Hydrograph for Grand River (3)	212
Figure 8.A.21 Hydrograph for Grand River (4)	213
Figure 8.A.22 Hydrograph for Flint River (1)	213
Figure 8.A.23 Hydrograph for Flint River (2)	214
Figure 8.A.24 Hydrograph for Flint River (3)	214
Figure 8.A.25 Hydrograph for Flint River (4)	215
Figure 8.A.26 Hydrograph for Cass River at M-15 (1)	215
Figure 8.A.27 Hydrograph for Cass River at M-15 (2)	216

List of Tables

Table 4.1 State DOTs Surveyed.....	15
Table 5.1 Bridges selected for scour monitoring.....	21
Table 6.1 Laboratory tests used to characterize soils.....	26
Table 6.2 Soil parameters for selected monitoring locations.....	29
Table 7.1 Soil characteristics.....	50
Table 8.1 Episodic Scour Measurement Locations.....	69
Table 8.2 Episodic measurements that resulted in discernable pier scour.....	70
Table 9.1 Descriptive statistics.....	93
Table 9.2 Average mean square error across all four trials.....	96
Table 9.3 Descriptive statistics for Michigan sites versus the NBS Database.....	100
Table 10.1 HEC-RAS Scour Predictions.....	109
Table 10.2 Period of Study Comparisons	110
Table 10.3 Period of Record Comparison	110
Table 9.A.1 Key to following tables.....	218
Table 9.A.2 Mean square error for trials 1 to 4 from models developed with unrestricted, ordinary least-squares regression for both Case one and Case two.....	219
Table 9.A.3 Number of over predictions for original and modified models.....	220
Table 9.A.4 Modified exponents b_1 and b_2 with corresponding 95% confidence limits for each trial.....	220
Table 9.A.5 Mean square error for trials 1 to 4 from models developed with unrestricted, weighted least-squares regression for both Case one and Case two.....	221
Table 9.A.6 Number of over predictions for original and modified models.....	222
Table 9.A.7 Modified exponents b_1 and b_2 with corresponding 95% confidence limits for each trial.....	222
Table 9.A.8 Mean square error for trials 1 to 4 from models developed with restricted, ordinary least-squares regression for both Case one and Case two.....	223
Table 9.A.9 Number of over predictions for original and modified models.....	224
Table 9.A.10 Modified exponents b_1 and b_2 with corresponding 95% confidence limits for each trial.....	224

Table 9.A.11 Mean square error for trials 1 to 4 from models developed with restricted, weighted least-squares regression for both Case one and Case two.	225
Table 9.A.12 Number of over predictions for original and modified models.....	226
Table 9.A.13 Modified exponents b_1 and b_2 with corresponding 95% confidence limits for each trial.....	226

Acknowledgements

The authors would like to express their appreciation to the Michigan Department of Transportation (MDOT) for sponsoring this research project under Contract No. 2006-0413 (Wayne State University) and Contract No. 2007-0436 (Lawrence Technological University). The technical advice and direction provided by the Bridge Scour Technical Advisory Group and Project Manager David Juntunen were helpful for the successful completion of this investigation. In addition, the technical assistance by Dr. Peggy Johnson of Penn State University and Greg Hanson of the US Department of Agriculture were critical in improving our analysis. Dr. Jason Barrett of Lawrence Tech served as Technical Editor and provided final editorial review and typesetting of the report. Dr. Carpenter and Dr. Miller would also like to acknowledge the contributions of the many student research assistants including Tim Calappi, Matt McClerren, Laura Hallam, Will Fowler, Lynn Trabulsi, Adam Lacey, and Robert Feister. Without the efforts of these students, the successful completion of this project would not have been possible. Finally, the opinions expressed in this project report are those of the authors and do not necessarily reflect the views of the Michigan Department of Transportation.

1.0 EXECUTIVE SUMMARY

The Michigan Department of Transportation (MDOT) and many other state DOTs utilize the methods documented in HEC-18 to predict bridge scour for the design of new bridges as well as for the evaluation of existing bridges. However, there is documented evidence that suggests HEC-18 does not accurately predict scour for many regions of the country (Richardson & Davis, 1995; Mueller & Wagner, 2002). The overall goal of this research was to improve MDOT's bridge scour prediction capability. In an effort to achieve this goal, the research team evaluated scour prediction methods utilized by regional state DOTs, conducted a field data collection project, and proposed an alternative approach for pier scour prediction.

The project team visited 56 bridge spans at 42 unique locations across the southern half of the Lower Peninsula of Michigan. From those visits, nine locations and twelve unique spans were selected for monitoring. Eleven sites were monitored episodically with a wire-weighted gauge across the entire cross section. Three sites were monitored continuously with an acoustic device and a data logger mounted to a bridge pier. This two part data collection strategy maximized the number of sites included in the study and offered spatially and temporally varied data. In addition, a complete soil characterization was performed for the samples collected at the selected monitoring locations. Finally, all monitoring locations have a USGS gauge within several river miles of the study to monitor hydrologic conditions.

A total of 79 episodic measurements from eleven sites and more than 40 months (total) of continuous data from three different sites were collected during the project. During the investigation, seven episodic measurements resulted in measureable pier scour. Scour depths ranged from 0.7 to 1.5 ft. with the maximum return period corresponding to a seven-year flood event. No measureable scour events occurred at the continuous scour monitoring locations. This data was used to evaluate the predictive capabilities of the original and revised HEC-18 Equation.

The HEC-18 pier scour prediction equation was modified utilizing the National Bridge Scour Database (NBSD). This analysis demonstrated that developing a family of equations in a similar format to the current HEC-18 equation reduces the mean square error of prediction and reduces the overall level of over-prediction. While the study team is optimistic about the family of equations approach, these equations were developed and validated with a limited number of

data points from the NBSD. As such, application of these equations should be undertaken with caution. Additional field data will allow further validation of the equations developed in this investigation and an expansion of the approach to include more bridge types and sediment conditions.

This investigation also included the use of a Jet Erosion Test (JET) to experimentally determine if *in situ* soil conditions could be correlated with measured bridge scour. The JET was able to correlate erodibility with geotechnical properties such as dry unit weight, soil type, and shear strength, but was not able to aid in the calibration and / or modification of the scour-prediction equations. However, a laboratory procedure for JET testing has been developed and soil borings could be collected at the scour critical bridge sites for erodibility analysis in the laboratory. Future research could expand on the work completed to include additional soil types, thus improving decision making regarding erosion of soils due to flowing water.

The US Army Corps of Engineers' Hydrologic Engineering Center - River Analysis System (HEC-RAS) model was used to compute bridge scour for flood events at locations corresponding to the field measurements. The HEC-18 Equation was the predictive method selected for the HEC-RAS calculations. These values were compared against scour predicted by the modified HEC-18 equation developed during this investigation. The two scour prediction approaches were also compared to scour measurements observed during the project period. Overall, it was determined that the modified HEC-18 equation was a less conservative predictor of scour than the HEC-RAS simulation for larger flood events and that both equations predicted more scour than observed for events that occurred during this investigation.

In conclusion, a modified HEC-18 pier-scour-prediction equation was developed for application in Michigan. This revised scour-prediction procedure will allow MDOT more accurately to predict bridge scour and subsequently more efficiently and confidently design new bridge crossings and / or modify existing bridges. Finally, experimental and analytical approaches were developed during this investigation provide a foundation for future research in the field of scour prediction.

2.0 INTRODUCTION

Bridge scour is a significant concern in the United States, causing approximately 60 percent of all U.S. highway bridge failures (Lagasse & Richardson, 2001). In 1993 alone, more than 2500 bridges were destroyed or severely damaged due to scour caused by severe flooding (Mueller & Wagner, 2002) and damage or failure occurred at more than 3600 bridges between 1985 and 1995 (Mueller & Wagner, 2005b). However, scour due to severe flooding is not the only concern. The high-profile, catastrophic collapse of the Schoharie Creek Bridge in New York in 1997, in which 10 people died, was caused more by the cumulative effect of pier scour of glacial till than the severe flood which ultimately caused its collapse (NTSB, 1988; Lagasse & Richardson, 2001).

Direct costs associated with scour are significant as well. Damages due to bridge failures associated with rainfall from Hurricane Alberto, in 1994, cost Georgia more than \$130 million (Richardson & Davis, 2001). After the 1993 flooding of the Upper Mississippi River basin, more than \$258 million in federal funding was requested for replacement or repair to bridge-related infrastructure (Parola et al., 1998). In addition to the unacceptable loss of life and the direct costs associated with bridge repair, the Federal Highway Administration (FHWA) estimates that indirect costs suffered by the public and local business because of long detours and lost production are five times greater than the direct costs of bridge repair (Lagasse & Richardson, 2001).

In response to these issues, the FHWA established a national scour evaluation program as a component of the National Bridge Inspection Program, resulting in the development of the National Bridge Inspection Standards (NBIS). The NBIS requires more than 588,000 U.S. bridges to be inspected every two years for scour and structural stability, and with divers every five years if underwater members are not visible (USDOT, 1991; Lagasse & Richardson, 2001). In addition, the FHWA has published three reports that define bridge scour technology and provide guidance to state DOTs: “Hydraulic Engineering Circular No. 18 (HEC-18) Evaluating Scour at Bridges” (Richardson & Davis, 2001), “HEC-20 Stream Stability at Highway Structures” (Lagasse et al., 2001a), and “HEC-23 Bridge Scour and Stream Instability Countermeasures” (Lagasse et al., 2001b).

The methods documented in HEC-18 are utilized in Michigan by engineers both in the private sector and within the Michigan Department of Transportation (MDOT) to predict bridge scour for the design of new bridges as well as for the evaluation of existing bridges (see Chapter 4 for additional details). However, documented evidence suggests that HEC-18 does not accurately predict scour for many regions of the country (Richardson & Davis, 1995; Mueller & Wagner, 2002). Therefore, it is of specific interest to MDOT (as well as other state DOTs) for the equations to be modified and/or calibrated to yield more accurate calculations of scour for Michigan-specific conditions.

The overall goal of this research was to improve the MDOT bridge scour prediction capability. In an effort to achieve this goal, the following tasks were undertaken:

- Scientific literature review;
- Evaluate MDOT's current scour evaluation procedures;
- Review scour evaluation procedures utilized by other states;
- Revise Level 2 (HEC-18) scour prediction equations for Michigan-specific use:
 - Select bridges for episodic and continuous monitoring;
 - Geotechnical investigation of selected sites and JET scour testing;
 - HEC-RAS modeling and scour prediction of selected sites;
 - Evaluation and modification of HEC-18 Pier Scour Equation based on National Bridge Scour Database (NBSD).

3.0 LITERATURE REVIEW

The Federal Highway Administration (FHWA) requires engineers to design bridges over waterways to withstand the effects of a 500-year super flood or a series of smaller floods if the series simulation causes greater scour depths (Richardson & Davis, 2001). To facilitate the design process, the FHWA issued Hydraulic Engineering Circular (HEC) 18 (Richardson & Davis, 2001), HEC-20 (Lagasse et al, 2001a) and HEC-23 (Legasse, 2001b) to provide guidance. HEC-18 provides specific guidance regarding the prediction of scour depth primarily through an empirically derived equation (Richardson & Davis, 2001). The HEC-18 Scour Prediction Equation represents the state of the practice and is included in popular one-dimensional hydraulic models as the default pier-scour equation. The HEC-18 pier-scour equation is not the only common empirical equation (Mueller & Wagner, 2002). Other notable examples include Jain & Fischer (1979), Laursen & Toch (1956), Sheppard (2006), and Melville (1988, 1997). These equations were developed with data from laboratory experiments and have inherent errors due to scaling and/or unrealistic representation of field conditions. As such, these equations are prone to gross over estimates of scour depth prediction (Wagner et al, 2006, Benedict & Caldwell, 2005; Mueller & Wagner, 2002).

Errors in predicting scour primarily stem from one of three sources: estimation of hydraulic parameters, determination of scour-prediction variables, and application of scour-prediction equations (Wagner et al, 2006). Hydraulic parameters are commonly estimated from simplified hydraulic models that distribute flow across the approach section and do not accurately capture complex velocity patterns found in the field. Commonly used scour-prediction variables include bridge geometry, channel geometry, hydraulic characteristics and sediment properties, but their individual contributions to scour are not always accurately captured. Regarding scour-prediction equations, simplifications made to estimate scour based on laboratory measurements have made scour prediction less accurate when applied in field settings. Finally, uncertainty stems from the fact that the ranges of the various parameters over which the equations are valid are typically unknown (Johnson, 1995).

Over the last few decades, physical modeling has dominated scour research with the goal of more accurately relating hydraulic characteristics, geometry, and sediment data to scour depth.

Although laboratory data is the most common source of data used to define relationships (Mueller & Wagner, 2005), there is an inherent complexity of bridge scour due to difficulties in scaling the effects of sediment and hydraulics (Hopkins & Vance, 1980; Ettema et al., 1998). Regarding sediment, scaled physical models often use sediment of similar size as the field conditions they represent. Sediment is difficult to scale due to cohesive effects and the presence of bed forms determined by particle size relative to the height of the viscous sub-layer (Ettema et al., 1998). For example, Sheppard (2006) evaluated the predictive ability of four common empirical models in a large flume. The tests were conducted under live-bed conditions with uniform sediment size and a single cylindrical pier. All four equations were found to over-predict scour depth in this study, in some instances by as much as 100 percent. This leads to amplified over-prediction at field scale due to an increased pier-width-to-sediment-grain-size term in each equation.

Attempts to improve fit and reduce uncertainty in commonly used equations began in the 1990s when researchers, such as Johnson (1995), tried using field data to determine valid ranges for typical parameters. Johnson compared several competing models based on computed bias in predictions. She concluded that some equations were not fit for design purposes because they often under-predict scour. Conversely, equations used for design purposes over-predict with a large, positive bias leading to an improved design from a safety perspective while unnecessarily increasing construction costs (Johnson, 1995).

Recent regional investigations have also explored the potential use of field data to improve predictive capability, including studies conducted in South Carolina (Benedict & Caldwell, 2005), Georgia (Gotvald, 2003), Michigan (Holtschlag & Miller, 1997), Wisconsin (Walker & Hughes, 2005), and North Dakota (Williams-Sether, 1997). While these investigations have led to insightful observations on scour, most have not led to the development of an improved scour-prediction methodology. A common finding in all of these investigations is that current scour-prediction equations overestimate scour depth, and each recommends collecting additional field data. Of these investigations, perhaps the most insightful is Benedict & Caldwell (2005). They developed a modified version of the HEC-18 pier-scour equation using historic scour data from South Carolina bridges. They found that clear-water pier scour as predicted by HEC-18 exceeded measured scour 70% of the time with over-predictions being as excessive as 26 ft. However, under-predictions occurred 30% of the time and were under by as

much as 7 ft. To improve the accuracy of predictions, they modified HEC-18 to reduce excessive predictions of pier scour associated with skew and pier width. Finally, they used historic artifacts of field-scour data to develop a series of envelope curves which included pier width, contraction ratio, and flow velocity as the primary explanatory variables across two different physiographic regions of South Carolina. These envelope curves could then be utilized to set limits on scour prediction.

Regional investigations have allowed for the creation of the US Geologic Survey (USGS) National Bridge Scour Database (NBSD) which provides field-collected measurements of scour. In 2005, Mueller and Wagner used the NBSD to evaluate and rank a suite of 26 pier scour equations, including five variants of the popular HEC-18 equation. This study utilized metrics (such as sum-square error, number of under-predictions, and sum-square error of the under-predictions) to evaluate the effectiveness of these equations. The study found that no single equation predicted scour best, but concluded the best equations were the Froehlich Design Equation, HEC-18, HEC-18-K4, HEC-18K4Mu, HEC-18-K4Mo (>2mm), and Mississippi (Mueller & Wagner, 2005). Mueller and Wagner also investigated the range of exponents on various equations. The pier-width exponent in non regime equations, such as HEC-18, range from 0.6 to 0.75, while the exponent on the velocity factor ranges from 0.2 to 0.68. The wide ranging exponent on the velocity factor indicates a lack of agreement on the importance of velocity in determining scour depth. Through the use of residual analysis, they also concluded that equation modification can alter the importance of other parameters. For example, the K4 modification proposed by Mueller (1996) reduces the effect of the Froude number.

Many historic scour data sets, such as those included in the NBSD, have sufficient hydraulic and geometric information to apply scour-prediction equations (Johnson, 1995) but lack detailed sediment characteristics which were not routinely collected (Landers et al., 1996). As such, most scour-prediction equations use median grain size as the sole predictive sediment property. However, due to armoring affects, graded sediment under live-bed conditions causes shallower equilibrium scour depth (Mueller & Wagner, 2005). In addition, scour-prediction equations were developed in the laboratory with cohesionless soil, but applied to bridge locations exhibiting cohesive soil characteristics. A soil need only contain 10 percent clay before cohesive properties dominate the soil (Raudkivi, 1998) and cohesive soil erodes more slowly than cohesionless soil, further exaggerating predicted scour depths.

Calappi et al. (2009) used NBSD records that included grain-size characteristics to determine if improvements to a scour-prediction equation, the Froehlich equation, were possible. They found that slight modifications to the independent variables led to marginal improvements in error. More importantly, the re-derivation of this equation shed light on the statistical significance of common parameters included in common scour equations. All parameters included in the re-derived Froehlich equation had high statistical significance (p-values less than 0.06). However, the same cannot be said for the original equation. When the original data set was used to derive the Froehlich equation, the Froude number had a p-value of 0.29 and pier-width-to-median-grain-size ratio had a p-value of 0.46. Both values are statistically insignificant, yet were included in the final derivation (Calappi et al., 2009).

Probabilistic characterizations of scour events are another option to improve safety. Typically, bridge designers are interested in the probability of exceeding a given scour depth over the lifespan of the bridge. Exceedance probabilities are computed using Monte Carlo simulations, which model thousands of realizations of an observed time series, capturing the ultimate scour depth over the length of each (Brandimarte, 2006).

In addition to the scientific literature review that informed this investigation, several additional project tasks were related to published information, including:

- Summarizing existing USGS, FHWA, ASCE, and regional reports that are available through online portals;
- Determining state DOT contacts responsible for hydraulic engineering design and bridge scour programs;
- Identifying research being conducted and scour prediction methodologies employed by DOTs in neighboring states.

These task deliverables were provided to MDOT in semi-annual progress reports with the final annotated bibliography and state DOT contact lists provided as separate documents. State DOT scour prediction methodologies and research are described in Chapter 4 and Appendix 4.B.

4.0 CURRENT SCOUR EVALUATION PROCEDURES

This chapter provides a summary of currently employed scour evaluation procedures. A majority of the chapter is devoted to current methods utilized by the Michigan Department of Transportation (MDOT) as a foundation for this investigation. In addition, scour evaluation practices from sixteen Midwestern and Mid-Atlantic states that have similar conditions to Michigan are discussed. Finally, a recommended database management system that employs a geographic information system (GIS) is presented.

4.1 Review of MDOT's Scour Evaluation Procedures

The Michigan Department of Transportation utilizes the MDOT Drainage Manual (2006) which supplements the Federal Highway Administration (FHWA) "Evaluating Scour at Bridges," Forth Edition of HEC -18 (2001) and "Stream Stability at Highway Structures," Third Edition of HEC - 20 (2001) for bridge scour evaluation.

4.1.1 Data

Bridge inspection and maintenance records, hydraulic analysis including flood insurance studies, and bridge construction drawings are needed for scour analysis. Aerial photographs, soil gradation results for streams and abutments, and topographic maps are also required for scour analysis.

Hydraulics and Hydrology: If hydraulic reports are not available, a worst case scenario is suggested. MDOT recommends the use of the U.S. Army Corps of Engineers' Hydraulic Engineering Center (HEC) River Analysis System (RAS) computer program (Brunner, 2010) for the computation of water surface profiles and hydraulic parameters.

The discharge estimate used in the scour screening procedure is not used for scour design. For drainage areas less than 20 square miles, MDOT requires the use of "Computing Flood Discharges for Small Ungaged Watersheds" (Sorrell, 2001). For drainage areas greater than twenty square miles, MDOT requires "DNR/USGS Peak Flow Regression" (Croskey, 1985). Finally, an accompanying report is "Statistical Models for Estimating Flow Characteristics of Michigan Streams," U.S. Geological Survey, Water-Resources Investigations

Report 84-4207 (Holtzschlag, 1984). This accompanying report contains methodology for the estimation of flow characteristics of ungauged locations in Michigan.

Geotechnical data: A soil gradation curve of streambed and overbank material is needed to determine the D50 and D84 particle sizes for use in the respective contraction scour and pier scour equations.

4.1.2 Scour Calculations

The scour calculations for contraction, live bed, clear water contraction, pier scour and abutment scour described here are detailed in Chapter 6 of the MDOT Bridge Design Manual.

HEC-18 is used to determine the overall depth of scour and should be referenced for a thorough discussion. However, several important equations are included in this section for reference. Present technology dictates that bridge scour be evaluated by interrelated components, including:

- Long-term profile changes (aggradation / degradation);
- Plan form change (lateral channel movement);
- Contraction scour / deposition;
- Local scour (piers and abutments).

Upon determining the total scour depth, structural engineers need to determine the stability of the structure.

Contraction Scour: Contraction scour occurs from a contraction of the natural stream's flow area such as occurs at a bridge. One contraction scour equation is used for live bed (bed sediment moving) and another for clear water (no bed sediment moving). Live bed scour occurs when the shear velocity, V^* , exceeds the fall velocity, ω (fall velocity of sand-sized particles, found in Figure 6-4 in the MDOT Bridge Manual).

$$V^* = (g y_1 S_1)^{1/2} \quad \text{(Equation 4.1)}$$

Where:

- y_1 = average flow depth in upstream channel
- S_1 = slope of energy grade line or main channel
- g = acceleration due to gravity (32.2 feet/s²)

Live Bed Equation:

$$y_2/y_1 = (Q_2/Q_1)^{6/7} (W_1/W_2)^{K_1} \quad \text{(Equation 4.2)}$$

$$y_s = y_2 - y_0 \text{ (average scour depth)}$$

Where:

y_s = average contraction scour depth

y_1 = average flow depth in the upstream main channel, feet

y_0 = existing flow depth in the contracted section before scour, feet

y_2 = average flow depth in the contracted section, feet

W_1 = bottom width of the upstream main channel, feet

W_2 = bottom width of the main channel in the contracted section, feet

Q_1 = flow in the upstream channel transporting sediment, cfs

Q_2 = flow in the contracted channel, cfs

K_1 = exponent determined in Table 6-1 (MDOT Bridge Manual)

Clear Water Contraction Scour:

$$y_2 = [(K_u Q^2)/(D_m^{2/3} W^2)]^{3/7} \quad \text{(Equation 4.3)}$$

$$y_s = y_2 - y_0 \text{ (average contraction scour depth)}$$

Where:

y_0 = existing depth in the contracted section before scour, feet

y_2 = average equilibrium depth in the contracted section after contraction scour, feet

y_s = depth of scour, feet

Q = discharge through the bridge or on the overbank at the bridge, cfs

D_m = diameter of the smallest nontransportable particle in the bed material

($D_m = 1.25 D_{50}$) in the contracted section, feet

D_{50} = median diameter of bed material in the bridge opening or on the floodplain, ft.

W = bottom width of the bridge, less pier widths or overbank width (set back distance), feet

$K_u = 0.0077$ (English units)

Pier Scour: Pier scour occurs due to vortices produced by the obstruction. The pier scour equation takes the form of:

$$y_s/y_1 = 2.0 K_1 K_2 K_3 K_4 (a/y_1)^{0.65} Fr_1^{0.43} \quad \text{(Equation 4.4)}$$

Where:

y_s = scour depth, feet

y_1 = flow depth directly upstream of the pier, feet

K_1 = Correction factor for pier nose shape from Table 6-2 (MDOT Bridge Manual)

K_2 = correction factor for angle of attack of flow from Table 6-3 (MDOT Bridge Manual)

K_3 = correction factor for bed condition from Table 6-2 (MDOT Bridge Manual)

K_4 = correction factor for armoring by bed material size from the equation

$K_4 = 0.4V_R$

a = pier width, feet

L = length of pier, feet

$Fr_1 = \text{Froude number} = V_1 / (gy_1)^{1/2}$

$V_1 = \text{mean velocity of flow directly upstream of the pier, fps}$

The correction factor K_4 decreases scour depths for armoring of the scour hole for bed materials that have a D_{50} equal to or larger than 0.079 inch (2.0 mm) and D_{95} equal to or larger than 0.79 inch (20 mm). The correction factor results from recent research by Molinas and Mueller. Molinas' research for FHWA showed that when the approach velocity (V_1) is less than the critical velocity (VC_{90}) of the D_{90} size of the bed material and there is a gradation in sizes in the bed material, the D_{90} will limit the scour depth. Mueller and Jones (year) developed a K_4 correction coefficient from a study of 384 field measurements of scour at 56 bridges.

The equation developed by Jones given in HEC-18 Third Edition should be replaced with the following:

- If $D_{50} < 0.079$ inch (2 mm) or $D_{95} < 0.79$ inch (20 mm),

then $K_4 = 1$

- If $D_{50} \geq 0.079$ inch (2 mm) or $D_{95} \geq 0.79$ inch (20 mm),

then $K_4 = 0.4 (V_R) 0.15 (6.5)$ (Equation 4.5)

Where:

$V_R = (V_1 - VicD_{50}) / (VcD_{50} - VicD_{95}) > 0$ (Equation 4.6)

and:

$VicD_x = \text{The approach velocity, fps, required to initiate scour at the pier for the grain size } D_x \text{ feet}$

$VicD_x = 0.645 (D_x/a)^{0.053} VcD_x$ (Equation 4.7)

$VcD_x = K_u (y_1)^{1/6} (D_x)^{1/3}$ (Equation 4.8)

$VcD_x = \text{the critical velocity, fps, for incipient motion for the grain size } D_x, \text{ feet}$

$y_1 = \text{depth of flow just upstream of the pier, excluding local scour, feet}$

$V_1 = \text{velocity of the approach flow just upstream of the pier, n/s fps}$

$D_x = \text{grain size for which } x \text{ percent of the bed material is finer, feet (mm)}$

$K_u = 11.17$ (English units)

The minimum value of K_4 is 0.4, and it should only be used when $V_1 < VicD_{50}$.

Abutment Scour: Abutment scour is caused by the constriction of flow at the sides of a channel created by the abutments of the bridge. The abutment scour equation is:

$y_s/y_a = 2.27K_1K_2(a'/y_a)^{0.43} Fr^{0.61} + 1$ (Equation 4.9)

Where:

K_1 = coefficient for abutment shape (see Table 6-5, MDOT Bridge Manual)
 K_2 = coefficient for angle of embankment to flow (see Table 6-3, MDOT Bridge Manual)
 $= (\theta/90)^{0.13}$ (see Figure 6-5, MDOT Bridge Manual, Adjustment of Abutment Scour Estimate
for Skew, for definition of θ)
 $\theta < 90$ degrees if embankment points downstream
 $\theta > 90$ degrees if embankment points upstream
 a' = length of abutment projected normal to flow, feet
 A_e = flow area of the approach cross section obstructed by the
embankment, sf
 Fr = Froude number of approach flow upstream of the abutment $= V_e / (g y_a)^{1/2}$
 V_e = Q_e / A_e , ft./s
 Q_e = flow obstructed by the abutment and approach embankment, cfs
 y_a = average depth of flow in the overbank, feet
 y_s = scour depth, feet

4.1.3 Assessment Steps

Scour analysis procedures for the design of a new bridge or evaluation of an existing bridge utilized worksheets based on HEC-20 and NBIS. Level One and Level Two worksheets are included in Appendix 4A. Assessment steps begin with a site visit to complete the Level One scour worksheet. Level Two analysis is conducted for all new bridges or for existing bridges if warranted from Level One analysis (Lagasse, 2001).

For state trunkline structures, the worksheet with the appropriate code should be forwarded to the Hydraulics/Hydrology Unit for review after each level of analysis. Documentation for MDOT scour evaluation procedure includes updating Item 113 of the National Bridge Inspection Systems (NBIS) at each level of analysis and action, and retaining the Level One and Level Two Worksheets (see Appendix 4A). Level One, Level Two and Level Three analyses are briefly discussed in the following subsections.

Level One Analysis: A Level One analysis is an information gathering effort consisting of office and field reviews of the structure. The Level One analysis procedure is outlined in Chapter 3 of HEC-20. The following information should be obtained, reviewed, and commented on:

- Bridge inspection reports;
- Underwater inspection reports (if available);
- Items 60, 61, 71, 92, 93, and 113 of the NBIS (see HEC-18, Appendix J, for

definitions);

- Construction, design, and maintenance files for repair and maintenance on the structure;
- Hydraulic data (flood insurance study or original design analysis).

Level Two Analysis: The Level Two scour analysis is an eight-step process to define stream stability and scour problems. These steps cover:

- Hydrology or flood history;
- Hydraulic conditions;
- Geotechnical - bed and bank material evaluation;
- Watershed sediment yield;
- Incipient motion analysis;
- Armoring potential;
- Rating curve shifts.

If it is determined that scour countermeasures are required to reduce vulnerability due to either damage or failure from scour, then recommended countermeasures include:

- Riprap at piers and abutments with monitoring (visual, cross sections, instrumentation, etc.) during and after flood events;
- Guide banks;
- Channel improvements;
- Strengthening bridge foundations;
- Relief bridges.

Action plans can be part of the Level Two documentation, if needed. Action plans should be developed among the hydraulic, geotechnical, and structural engineers. Examples include:

- Monitor for scour during regular bridge inspection;
- Increase monitoring frequency;
- Temporary countermeasures - riprap and monitor;
- Selection of scour countermeasures;
- Scheduling of scour countermeasure construction.

Level Three Analysis: Level three analysis includes a mathematical or physical model of scour potential. This analysis is typically beyond the scope / monetary funding of the majority of Michigan projects.

4.2 Review of Scour Evaluation Methods Utilized by other States

The study team performed contacted sixteen states in the Midwest and mid-Atlantic to determine scour evaluation methods utilized in adjacent regions (Table 4.1). This process was first conducted in 2007 and then repeated in late 2010 to determine if any states had updated their procedures or research programs.

Procedures and protocols followed by these states were compared to scour estimation practices used in Michigan. It was found out that similar to Michigan, the FHWA HEC manuals are standard procedures applied by each state surveyed.

Table 4.1 – State DOTs Surveyed

Illinois	Nebraska
Indiana	New Jersey
Iowa	New York
Kansas	Ohio
Kentucky	Pennsylvania
Maryland	Virginia
Minnesota	West Virginia
Missouri	Wisconsin

Three states (Indiana, Maryland and New Jersey) use the AASHATO Drainage Manual in addition to the guidance in the HEC manuals. Five other states (Illinois, Kentucky, Pennsylvania, Virginia and West Virginia) include guidance from state drainage manuals. Several states in the region have active scour research program and are either currently funding projects or previously funded scour evaluation projects. Indiana, Missouri, Nebraska, New York, Virginia and West Virginia list no current or previous research. Details for each state can be found in Appendix 4.B.

Illinois and Maryland have looked into Scour Rates in Cohesive Sediments (SRICOS) for their cohesive scour needs. SRICOS is an accepted method developed at Texas A&M University and has been used on large projects around the country (Wang, 2004). The main idea behind this method is to extract Shelby tubes of cohesive sediment at specific locations and use a specially designed flume called the Erosion Function Apparatus to determine the critical shear stress for

the specific site. The study team found that SRICOS is the most widely used scour estimation method developed specifically for cohesive material.

Pennsylvania worked with the USGS to develop techniques for Bridge Scour Assessment. The assessment consists of two parts - a scour critical bridge indicator code and a scour assessment rating. Ratings for each subunit of the bridge are aggregated into an overall score. This score helps the bridge owner rank the threat of failure due to hydraulic forces.

4.3 Database Management

The study team found that storing bridge information in a geographic information system (GIS) is particularly useful for managing the large number of structures considered in this investigation. There are two possible methods to create a GIS application, either a Google Earth application or a full featured geo-spatial and relational database. The project team relied on both for this investigation.

A Google Earth database is cheap to implement and easily shared among users. However, it is a decentralized application which might be difficult to maintain and update. Also problematic would be the potential for numerous versions of the database to exist among staff. A professional application such as ESRI® ArcGIS Desktop allows for an easily maintained central database and more robust features. However, due to expensive licensing and a difficult interface, compared to Google Earth, it is not as easily shared or used.

ArcGIS can also provide a mechanism to visualize results from a standard relational database (Figure 4.1). ArcGIS is used to detail attributes in Figure 4.1 and are automatically highlighted in the tabular results and simultaneously highlighted on a map depicting spatial distribution. An example of how GIS was used for this project was to identify where the multi-span, scour-critical bridges in the Bay, Grand, Southwest, University and Metro regions were located (Figure 4.2). Since local pier scour was the focus of this study, the team only needed to visit bridges with at least one pier which will have two or more main spans. The map in Figure 4.2 was used to help choose potential study sites and prevented the team from visiting single span sites. Google Earth was also used by the team for ease of identifying bridge locations, logistical planning, and sharing aerial imagery. Figure 4.3 is an example of how Google Earth was used to map bridges by MDOT region and examples of Google Earth satellite images and

maps can be found Appendix 4.C. Appendix 4C also contains information on bridge condition from inspection reports and USGS gauge station data.

Another option in a professional GIS system is mobility. A mobile GIS application used by a trained field crew could update the GIS database in real time. As an example of how a mobile GIS system could be useful, during the reconnaissance phase of this project the research team, along with MDOT engineers, visited a site listed on the scour critical database and unexpectedly found a new structure. The scour critical bridge database used to select sites for inspection had not been updated when the new bridge was completed. A mobile GIS application would have allowed an MDOT engineer instantly update the bridge status and prevent further use of stale data.

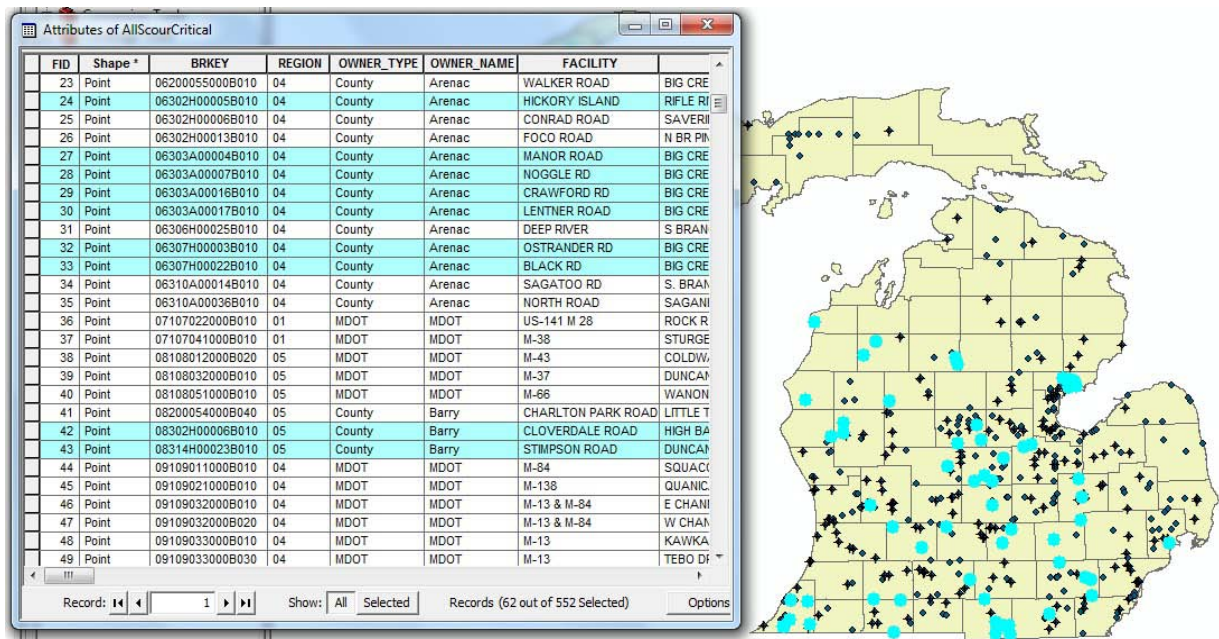


Figure 4.1 Sample query of scour-critical bridges in Michigan built before 1925.

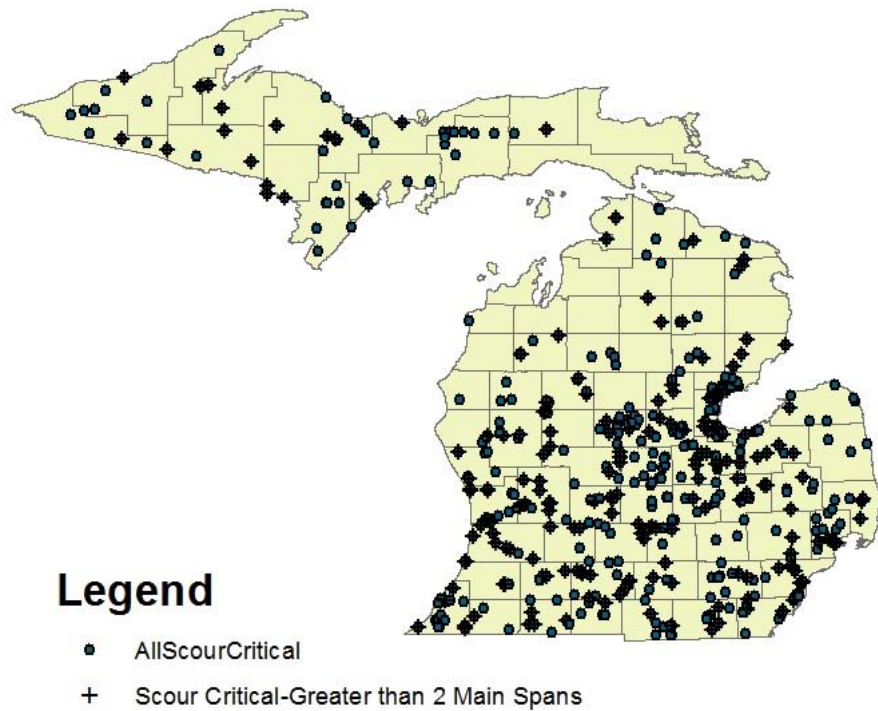


Figure 4.2 All scour critical bridges in Michigan with an overlay of multi-span bridges.

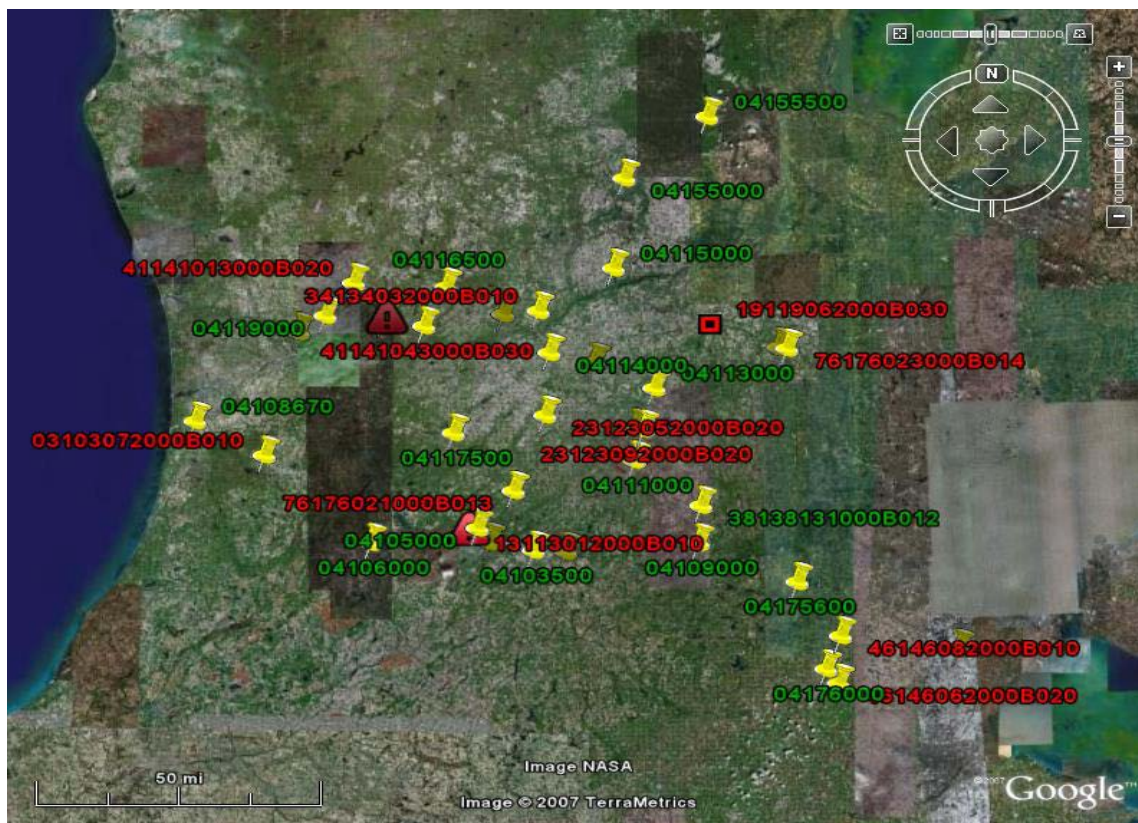


Figure 4.3 All scour-critical bridges in the University Region.

5.0 BRIDGE SITE SELECTION

The Michigan Department of Transportation (MDOT) supplied the study team with a list of hundreds of potential bridges to include in the study. A geographic information system (GIS) created for the project determined which locations required a site visit. The GIS is laptop based and was used to keep notes and make decisions in the field. During 2008 and 2009, the project team visited 56 bridge spans at 42 locations (Figure 5.1) across five of the seven MDOT regions (Metro, University, Grand, Southwest, and Bay). Based on these visits, fourteen locations (some with multiple spans) were identified for monitoring.

However, in subsequent visits to those locations for data collection and cross-sectional profiling under low-flow conditions, several sites were removed based on soil conditions and / or the existence of scour countermeasures. The criteria for the final selection of locations included:

- Bridges on the MDOT scour critical list (State and County trunk line roads);
- Lower Peninsula;
- Soil characteristics - cohesive or semi-cohesive conditions at some depth;
- Proximity to USGS gauge;
- Access to and ease of monitoring data collection;
- Absence of scour counter measures to allow for monitoring;
- Wade-able under low flow conditions for baseline profiling and access to equipment for continuous monitoring sites.

The team developed two strategies for data collection: episodic and continuous monitoring. All sites are monitored episodically with a wire-weighted gauge, with data recorded along the upstream and downstream face of the bridge. These data provide some spatial and temporal scour information. In addition, three of the sites are continuously monitored with an acoustic device and a data logger. These data provide scour information at a point location, but at one to two hour intervals. Chapter 6 details the instruments and methods utilized for episodic and continuous monitoring.

Table 5.1 lists the bridge spans and the type of data collection undertaken. Appendix 4.C includes location maps and photographs of all nine sites and twelve spans. Study locations were distributed throughout the southern half of Michigan's Lower Peninsula for ease of access.

However, the study area is broad enough to allow for spatially varying hydrologic conditions, increasing the chances of meaningful data collection during a significant flood event. Finally, all study locations have a USGS gauge within several river miles of the study to monitor hydrologic conditions, but only four locations have a gauge at the site. Acoustic Doppler data were collected at all sites, but were of greatest importance at the un-gauged sites.

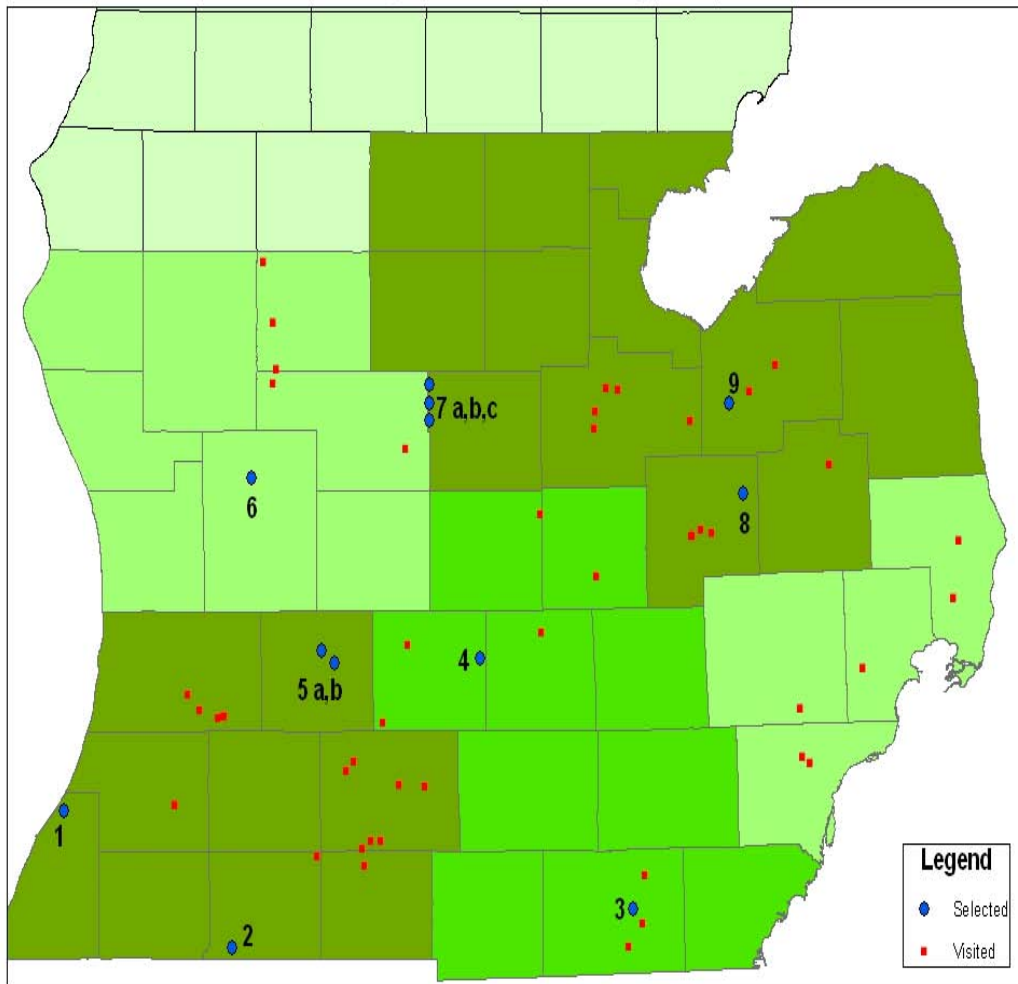


Figure 5.1: Location of nine scour monitoring locations (numbered blue circles) and the additional 56 sites visited (red squares).

Table 5.1 Bridges selected for scour monitoring.

Map Index	MDOT Region and Site Name	Episodic	Continuous
UNIVERSITY REGION			
4	Grand River @ M99	X	X
3	River Raisin @ USGS Site Adrian	X	
BAY REGION			
8	Flint River @ M15	X	X
9	Cass River @ M15	X	
7 a	Pine River @ Lumberjack Road	X	
7 b	Pine River @ Lumberjack Road	X	
7 c	Pine River @ Lumberjack Road	X	
GRAND REGION			
6 a	Rogue River @ Edgerton Road	X	
SOUTHWEST REGION			
5 a	Thornapple River @ M-43	X	
5 b	Thornapple River @ USGS Site Hastings	X	
1	Paw Paw River @ Coloma Rd	X	X
2	Pigeon River @ US-131	X	

6.0 EQUIPMENT AND TEST METHODOLOGIES

This chapter summarizes the equipment and test methodologies utilized during this investigation. The first section covers soil sample collection and the index tests used to characterize bed and bank material. The second section describes the Jet Erosion Test (JET). Section three details scour measurements, and the final section explains discharge and velocity measurements.

6.1 Geotechnical Investigations

Determining the geotechnical properties of the streambed material at each monitoring site is critical to (1) the calculation of scour using existing and modified HEC-18 methodology (such as D_{50} and D_{84}), and (2) the correlation of scour potential to geotechnical features of the soil (e.g. shear strength).

Soils samples collected from streambeds and banks of selected sites were analyzed at the Geotechnical & Materials Laboratory at Lawrence Technological University using the following standard tests:

- Sieve analysis (ASTM D-421);
- Hydrometer analysis (ASTM D-422);
- Atterberg limit tests (ASTM D-4318);
- Direct shear test (ASTM D-3080).

The following sub-sections provide information on the geotechnical investigations conducted during the project including sample collections, measurement of in situ soil density, as well as the standard soil tests conducted.

6.1.1 Sample Collection

Soil sampling was carried out in order to conduct geotechnical characterization in the laboratory. Bulk soil samples were collected using a soil auger to drill into the bed and obtain a core. The bottom of the auger is open to allow the auger to cut into the ground and collect a core. The bottom of the auger was immediately covered in order to minimize the loss of fine sediment. Approximately four pounds of soil were collected from each location to ensure that

standard geotechnical tests could be completed. The collected samples were then sealed in a plastic, one-gallon bag and transported to the lab for testing.

Initial soil samples retrieved from the field were used to determine if the soil was suitable for JETs. Once suitability for testing was confirmed, further samples were collected. Soil samples taken from a particular site were not always homogeneous. In order to collect samples that accurately represented the soil tested with the JET, samples were retrieved from the exact location that JET testing had occurred.

6.1.2 Unit Weight Determination in the Field

Field density was used to simulate the field conditions in the laboratory, so precautions were taken to ensure the correct density was known. Two techniques were applied to determine the density of the soil *in situ*. The first method was the sand cone test (ASTM D1556 – 07). This method proved difficult for testing soils located below the water table because it was necessary to keep the sand used in the test free from moisture. A plastic cellophane sheet was placed tightly within the hole to prevent moisture from contaminating the calibrated sand. The calibrated sand used for the test was then collected and weighed in the laboratory. The test was successfully completed on the banks of streams when a JET was completed on the bank. However, many of the tests were completed below the water table. This situation led to the development of a second method using a Shelby tube.

An empty Shelby tube (Figure 6.1) was cut to a length of 28 inches. Using a sliding hammer, the tube was pounded into the ground to a depth deemed sufficient to collect a sample and then extruded. The soil around the Shelby tube was removed to a depth that allowed for undisturbed removal of the soil sample. The length of the core sample was then recorded to determine the *in situ* density and the sample was sealed in a bag for transport to the lab for further testing. These core samples were obtained within the footprint of the JET tank so that the unit weight of the soil represents the soil tested during the JET.

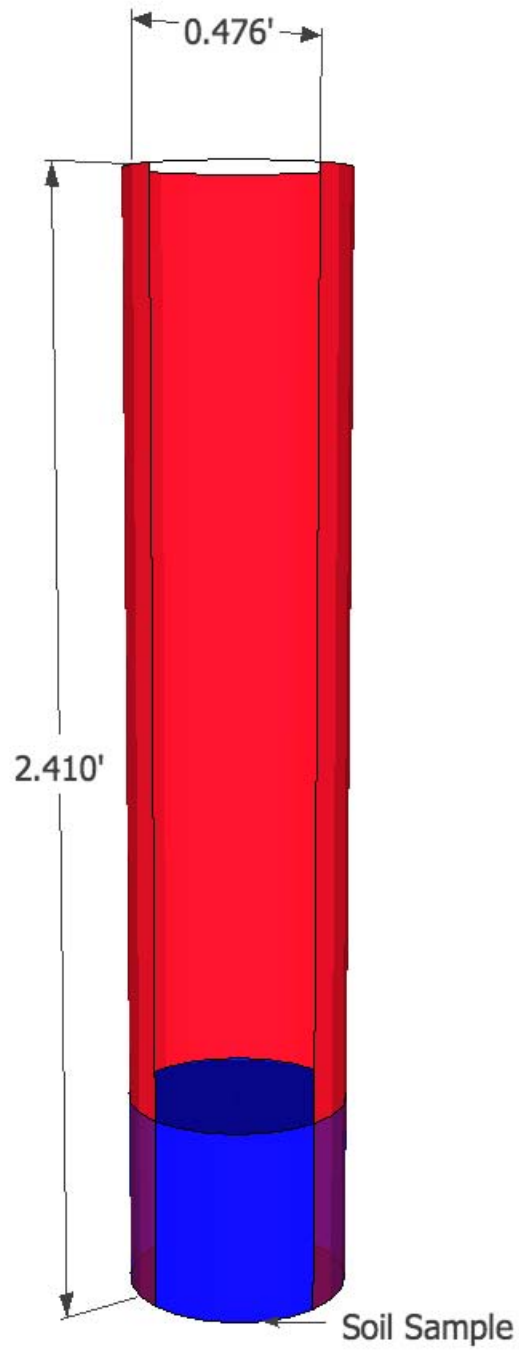


Figure 6.1 Shelby tube schematic

6.1.3 Geotechnical Characterization of Soil Samples

A complete particle-size analysis (sieve analysis combined with hydrometer analysis) and Atterberg-limits analysis (liquid limit and plastic limit) were conducted on each sample to classify soils as per the Unified Soil Classification System (USCS). Direct shear tests were conducted on samples collected from selected sites to find their shear strength properties. Table 6.1 shows the tests completed and their associated ASTM test designations.

Table 6.1 Laboratory tests used to characterize soils

Laboratory test	ASTM test designation
Sieve analysis	ASTM D-422
Hydrometer analysis	ASTM D-422
Liquid limit and plastic limit	ASTM D-4318
USCS	ASTM D-2487
Direct shear test	ASTM D-3080

6.1.4 Grain Size Analysis

Particle-size analysis was initiated by oven drying a soil sample of at least 500 grams and with soil particles smaller than a 200 sieve washed out. This produced two pans: one with soil larger than a 200 sieve and one with smaller soil. This soil was then oven dried for two days, ensuring that little or no moisture remained. The soil sized greater than the 200 sieve was then passed through a series of sieves and weighed, while the soil that passed through the 200 sieve was used in the hydrometer analysis.

The hydrometer analysis consisted of mixing a dispersion agent in water and then mixing approximately 50g of soil that passed the number 200 sieve. The mix was combined in a 1000ml tube and kept at a constant temperature. Once the mixture was prepared, a hydrometer was placed in the tube and readings were taken at set time intervals.

A recurring issue appeared with large pieces of organic material such as roots or leaves. While conducting the sieve analysis procedure, organic particles large enough to be easily spotted and picked out by hand were removed. This process reduced the clogging of the sieve and prepared the soils samples for laboratory JET, because it was thought that the roots would skew the erodibility of the soil.

Once the hydrometer analysis and sieve analyses were completed, data were combined to create a gradation curve for the soil sample.

6.1.5 Atterberg Limits

The last piece of information needed to classify the soil using the USCS was the Atterberg limit. The Atterberg limit is determined by two measurements of the plasticity of soil: the liquid limit and the plastic limit.

The liquid limit finds the point at which a soil no longer acts like a solid and begins acting more like a liquid. This is determined using a Casagrande liquid-limit device. By varying the moisture levels in the soil, the Casagrande liquid-limit device graphically represents the soil's liquid limit. The plastic-limit test shows the point at which a soil no longer acts like a plastic and begins acting like a semisolid. The limit is reached by rolling a moist soil sample into a thin thread of soil. Once the soil reaches a certain diameter without falling apart but nearing the point of failure, the soil is weighed, then dried and weighed again to attain the moisture content. This provides the user with the plastic limit. The plastic limit is then subtracted from the liquid limit to find the plasticity index.

6.1.6 Direct Shear Test

Direct shear testing identified the shear strength properties of the soil samples. These properties are the friction angle (ϕ) and the cohesion (c). This test was carried out using the DigiShear® direct shear-testing machine. Soil samples were compacted to their *in situ* unit weight in the shear box. To simulate fully saturated field conditions, the basin outside the shear box was filled with water. The test was initiated using a computer program that varied the normal force for three different tests, which allowed for the shear strengths at failure to be determined. The shear box is made of two halves of one-inch thick aluminum and connected with screws. Both halves of the shear box have a hole 2.5 inches in diameter that align with one another. A porous stone is placed on both ends of the soil specimen, which allows for the release of the excess pore water pressure. The test can now be initiated on the computer which records the friction of the soil sample to affect maximum shear strength. The maximum shear strength is then plotted against the normal force used to seat the sample and the resulting curve defines the shear strength parameters.

6.1.7 Geotechnical Properties of Streambed Material

Using the tests described in the previous sections, a complete soil characterization was performed for the samples collected at the selected monitoring locations. Table 6.2 summarizes the soil properties including USCS classification. The table also includes two other data points reported by Hanson (2007).

Table 6.2 Soil parameters for selected monitoring locations.

Sample	Dry Unit Weight (KN/m ³)	T _c (Pa)	K (cm ³ /N-s)	% Sand	% Fines	PI	USCS	Liquid Limit	Plastic Limit
Cass River @ M-15	N/A	N/A	N/A	37.7	1.3	NP	GP (Poorly Graded Gravel With Sand)	N/A	N/A
Flint River @ M-15	N/A	N/A	N/A	77.5	22.5	NP	SM (Silty Sand)	N/A	N/A
Grand River @ M-99				58.7	29.2	4.28	SM-SC (Silty Clayey Sand)	16.65	12.37
Pawpaw River @ Coloma Rd. Lab test 1	18.5	1.121	0.598	81.8	15.9	5.23	SM-SC (Silty Clayey Sand)	17.9	12.67
Pawpaw River @ Coloma Rd. Lab test 2	17.1	0.442	1.01	81.8	15.9	5.23	SM-SC (Silty Clayey Sand)	17.9	12.67
Pawpaw River @ Coloma Rd. Lab test 3.17.09	18	4.183	0.308	81.8	15.9	5.23	SM-SC (Silty Clayey Sand)	17.9	12.67
Pawpaw River @ Coloma Rd. Lab Test 3.27.09	17.8	2.938	0.365	81.8	15.9	5.23	SM-SC (Silty Clayey Sand)	17.9	12.67
Pigeon River @ US-131	N/A	N/A	N/A	90.7	9.3	NP	SP-SM (Well Graded Sand With Silt)	N/A	N/A
Pine River @ Lumberjack Rd									
River Raisin @ Academy Rd	N/A	N/A	N/A	94.8	4	NP	SP (Poorly Graded Sand With Gravel)	N/A	N/A
Rogue River @ Edgerton Rd.	N/A	N/A	N/A	58.1	0.4	NP	SP (Poorly Graded Sand With Gravel)	N/A	N/A
Thornapple River @ McKeown Lab test 3.17.09	20	1.273	0.659	63.5	27.1	1.04	SM (Silty Sand)	12.99	11.95
Hanson 2007	17.68	N/A	1.9	63	37	NP	SM (Silty Sand)	N/A	N/A
Hanson 2007	17.61	N/A	6.1	63	37	NP	SM (Silty Sand)	N/A	N/A

Definitions:

- T_c (Critical Shear Stress) is the stress that should be exceeded for incipient motion to occur.
- K (Erodibility Coefficient) is the degree to which the material is resistant to erosion by flowing water.
- % Sand is all of the soil that passes the # 4 sieve but is retained above the # 200 sieve.
- % Fines is all of the soil that passes the # 200 sieve
- PI (Plasticity Index) is the difference between the liquid limit and the plastic limit of a soil.
- USCS (Unified Soil Classification System)
- Liquid Limit is the moisture content of a soil at the point of transition from a plastic state to liquid state.
- Plastic Limit is the moisture content of a soil at the point of transition from semisolid to plastic state.
- N/A (Not Applicable)
- NP (Non Plastic)

6.2 JET Apparatus

Construction of a JET apparatus began by obtaining a working version of the device developed by Dr. Greg Hanson (United States Department of Agriculture, Stillwater, OK), along with specifications for construction (Appendix 6.A). The device may be used *in situ* or in the lab. It is comprised of seven parts: *in situ* tank, lab tank, constant head tank, head support pole, lid, jet tube, and point gauge. Figure 6.2 shows Greg Hanson demonstrating the device he provided for this research. The spreadsheet in which the data on soil erodibility is input was also obtained from Dr. Hanson.



Figure 6.2 Dr. Greg Hanson demonstrating the jet erosion test.

6.2.1 Fabrication of the Jet Apparatus

The *in situ* submergence tank (Figure 6.3a) was made from a 9-in. long, 12-in. outside diameter, and 0.125-in. thick steel tube welded inside a 0.5-in. thick steel support ring, located 3-in. from the bottom of the tube in order to ensure the tank was properly seated in the soil and to

prevent piping of water underneath the tank. Welded to the outside of the tank were three clamp hooks at 120° from one another.



Figures 6.3 (a) Submergence tank and lid **(b)** Lab tank and lid

The lab tank (Figure 6.3b) was made from an 11-in. long, 12-in. outside diameter, and 0.25-in. thick acrylic tube. The tube was set within a 15-by-15-in., 1.0-in. thick acrylic base with a 0.25-in. deep, 12-in. diameter circular recess cut into the base. The tube was then attached into the circular recess and silicone was used to ensure a watertight fit around the base connection. Acrylic blocks for the clamp hooks were cut, drilled, tapped and attached to the tank at 120° from one another and clamp hooks were then screwed into the blocks.

The lid was made from 0.5-in. thick acrylic cut to a diameter of 13.25-in. (Figure 6.3a). A straight cut was made 3.5-in. inward from the outside edge of the circle and pieced back together using a brass hinge. This opening allows access to the sample during testing. A 0.5-in. hole was drilled 3.5-in. from the center of the lid for the stream deflector which protects the sample while the device is filling with water. The stream deflector was made of a 0.125-in. thick stainless steel plate cut in an egg shape. The plate attaches to a 0.5-in. diameter, 4.0-in. long stainless steel rod. A 3.0-in. hole was cut in the center of the lid and eight holes were drilled and tapped to 1/4-20 screw size evenly around the perimeter of the hole. A 0.25-in. thick, 2.5-in. inside-diameter pipe was cut to 2.5-in. long and welded to a 5-in. outside diameter and 3.0-in. inside-diameter ring. The ring had eight 0.25-in. holes drilled to allow for attachment to the lid. The pipe was then cut at the top and a hinge and latch were fabricated.

The jet tube (Figure 6.4) was fabricated from a 17-in. long, 0.25-in. thick acrylic tube with an outside diameter of 2.5-in. A nozzle plate was made of 0.5-in. thick acrylic cut to an outside diameter of 2.5-in. A 0.25-in. diameter hole with a 0.5-in. radius bevel was cut in the center of the nozzle plate. Four holes were drilled through the nozzle plate into the jet tube and the tube was tapped to attach the nozzle plate with screws. A guide was created using a 13.5-in. long acrylic tube with an inside diameter of 0.75-in. The bottom end of the tube had a 0.75-in. outside diameter, and a 0.25-in. inside-diameter insert was epoxied inside. The tube was epoxied inside a 0.5-in. thick acrylic insert shaped to fit inside the jet tube. Epoxied to the top of the insert was a spacer and clamp to hold the point gauge. A 2.25-in. by 4.0-in. block was then fashioned to fit the outside of the jet tube in a manner similar to the block for the head tank. Three holes were drilled and tapped through the jet tube to allow for screws to center the point gauge guide. A final hole was then drilled to allow for the evacuation of air at the top of the jet tube.

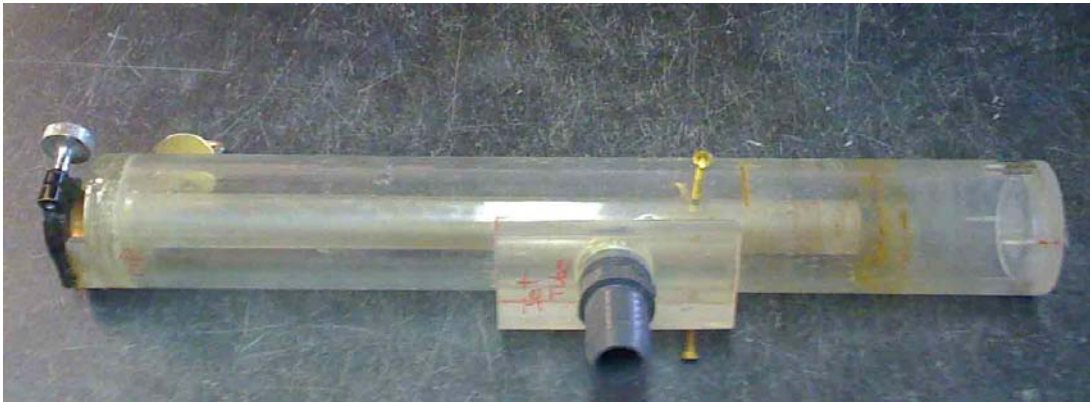


Figure 6.4 Jet tube

The constant head tank (Figure 6.5) was made from a 20-in. long, 2.5-in. outside diameter, and 0.25-in. thick acrylic tube. A 4.0-in. by 2.0-in. acrylic block, used for filling the tank, was cut and shaped to fit along the outside of the 2.5-in. acrylic head tank. This block was then drilled and tapped to allow for a 1.25-in. to 1.0-in. hose reducer to be attached. A 1.5-in. hole was drilled into the constant head tank and the previous block was then epoxied over the hole, centering the hole in the block over the hole in the head tank. At the bottom of the head tank, a 0.5-in. thick acrylic plate was fabricated, drilled, and tapped to accept a 1.25-in. to 1.0-in. hose reducer, which would lead a 1.0-in. hose to the jet tube, and was epoxied to the bottom of the constant head tank.



Figure 6.5 Head pole and head tank

The head pole was made from 1.5-in. by 0.5-in. “C” channel steel with a length of 3.0-ft. The “C” channel steel was welded to a 4.0-in. by 6.0-in. steel plate with a thickness of 0.5-in. A hole was drilled and tapped into the steel plate in order to be screwed onto an adjustable survey tripod. The plate and the pole were reinforced with 6.0-in. by 4.0-in. triangular steel gusset plate pictured in Figure 6.6. The head tank was then attached to the head pole with two 3.0-in muffler clamps.

A few modifications were made to the JET-apparatus specifications obtained from Dr. Hanson. In the construction of the *in situ* tank, the square support used to attach the head tank to the head tank support was left off. This support was left off because of the modification to the head tank design and setup. Also, this tubing was used originally as a guide for seating the tank in to the soil, but this was unnecessary for this project.

The constant head pole and constant head tank were modified simultaneously during the construction of the device. The head pole was made of “C” channel steel instead of slip form square tubing. The “C” channel was also welded to a steel plate, unlike the slip form steel that slid into the square support tubing on the *in situ* tank. Because of these modifications, it was unnecessary to attach a plastic clamping block to the outside of the constant head tube, which

appeared on the original device. The modifications performed to the head tank setup allow for considerable ease and flexibility when changing the pressure head applied to the jet nozzle.



Figure 6.6 Head pole gusset plate

Another modification was to use a screw in the top of the jet tube to release built up air in the tube. Hanson originally used an air relief valve, but because the valve was not easily purchased, a screw was used instead. To accept the screw, the jet tube was drilled and tapped on its top end. While the JET is reaching equilibrium the screw can be taken out of the hole to allow air to flush from the system, but when testing is occurring, the screw needs to be inserted so that there is no unaccounted head loss.

The modifications made were minor but helped improve the functionality of the device for the research being completed. However, none of the modifications change the device's performance from its original conception.

6.2.2 *In Situ* Test Setup

To successfully set up the JET, it is necessary to explore the site and locate soil that is not deemed depositional. Also, the streambed is often covered with loose soil, sand, and / or gravel.

To capture the most accurate erodibility, the area for testing was prepared by carefully removing the loose layers of soil and plant matter, being sure to minimize the disturbance of the underlying soil to be tested. When material on the bank needed to be tested, it was necessary to remove the soil down to a suitable depth to reveal the cohesive soil to be tested as shown in Figure 6.7a.



Figures 6.7 (a) Site preparation



(b) Submergence tank

Immediately after preparing the site, the submergence tank was seated into the ground up to the bottom ring (Figure 6.7b). In gravelly soils it was necessary to use force, such as a sledgehammer, to ensure that the tank was properly seated.

The lid and jet tube were then installed on the submergence tank. The lid has three hooks spaced evenly around the top, which allows the clamps on the submergence tank to seat firmly on it. On the lid is a metal tube that allows the jet tube to slide into, hold and center the jet tube in the submergence tank. It was important to ensure that the spacing between the soil surface and the end of the jet nozzle is greater than 1.5-in. Finally the point gauge was installed in the top end of the jet tube and then clamped down. It was important to ensure that the point gauge has plenty of range of motion. The point gauge was adjusted by turning the screw that holds the rod within the point gauge in place. Once loosened, the rod can be extended or retracted as necessary.

The head tank and the survey legs were set near the submergence tank. The head tank was created so that the tank could slide up and down the head pole by loosening or tightening a pair of muffler clamps. The pole fits upright or upside down on the survey legs allowing for a

great range of positions. This is important because some soils are more susceptible to erosion and therefore need to be tested using less pressure.

A small gasoline-powered water pump was used to pump water to the head tank. The pump was positioned near the head tank, but out of the water. It is crucial that the water pump be positioned so that it is not in the water. Because the length of hose is limited to ten feet, a relatively close proximity to shore is necessary. Once the pump is in position, hoses can be run from the pump to the head tank and from the head tank to the jet tube. After completing this setup (Figure 6.8), the deflection plate must be placed below the jet nozzle. This prevents the jet nozzle from eroding the soil before the submergence tank has a chance to fill with water and reach equilibrium. Without the tank reaching equilibrium before starting the test, the head pressure would be constantly changing as the tank fills with water.



Figure 6.8 JET apparatus in the field

6.2.3 Laboratory Test Setup

Setup of the lab device (Figure 6.9) is similar to that of the *in situ* setup. The major modification is that the lab tank is used instead of the submergence tank. The lid, jet tube and point gauge attach to the lab tank in the same fashion as they attach to the submergence tank. Setting up the lab tank involves placing it in an area near a floor drain and near a source of water. For this research, tap water was used without consideration of water chemistry. A Proctor mold was used to contain the sample for testing in the laboratory. The sample was created ahead of time and all of the soil characteristics are known at the time of testing. Before the sample was tested, the characterization and preparation technique was recorded in the notes section of the testing sheet. The sample within its mold was then placed inside the lab tank and centered, making sure that the jet of water will make contact directly in the center of the sample. The lid, jet tube, and point gauge can then be attached as described above.

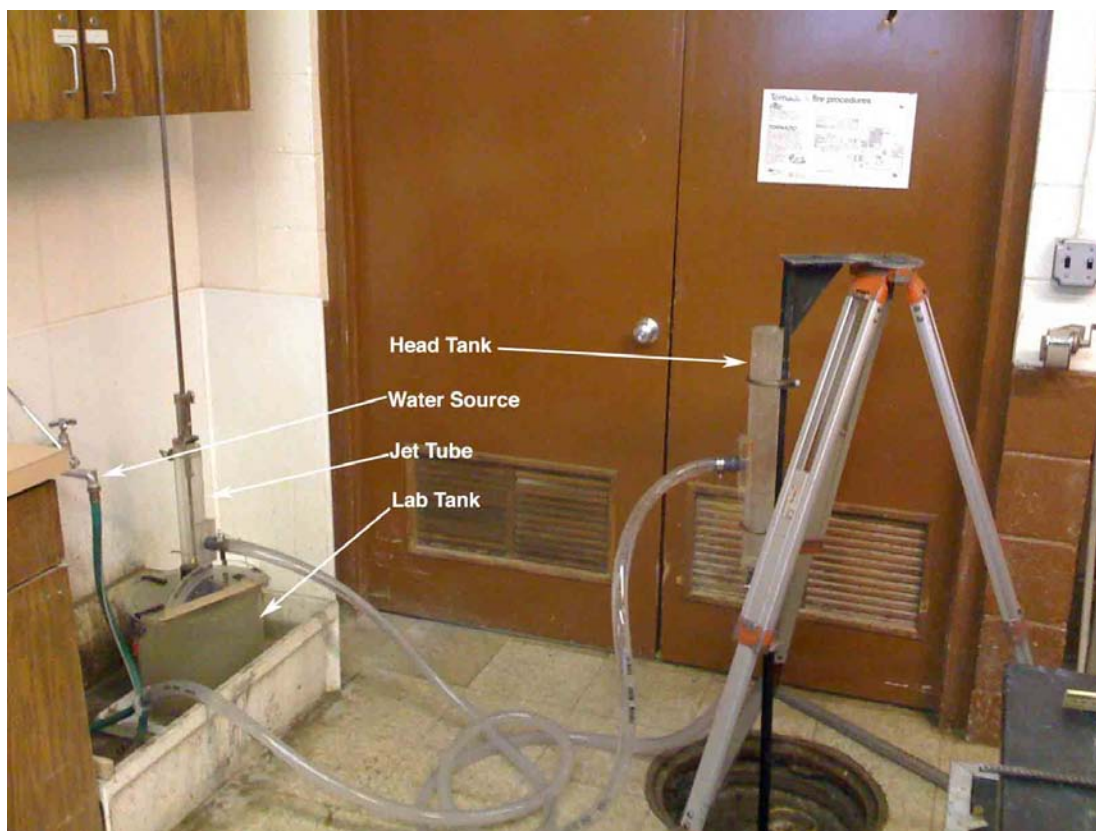


Figure 6.9 Lab JET setup

The head tank is setup in the same fashion in the lab as it is in the field. A surveyor's triangle is used to hold the feet of the tripod in place while on the tile, ensuring constant head pressure.

The hoses are then run from the head tank to the jet tube. A major difference is that the pump is not used and therefore a connection has to be made between the spigot and the head tank, which was solved using a hose reducer. The water spigot used provided plenty of pressure to maintain head pressure in the tank.

6.2.4 Test Procedure

Once the system is up and running, the first step is to record the amount of head pressure desired. The amount of head pressure varies depending on how quickly the soil erodes. The desire was to carry out a JET for two hours without eroding the soil greater than a depth of four inches. If this occurs, the test should be restarted with a lower head pressure. The pump maintains constant head pressure by being designed to overflow on the top of the head tank. This means that the water overflowing provided a datum that could be assumed at zero and maintained by gravity. Head pressure is measured from the top of the head tank where the water is overflowing, vertically to the top of the submergence / lab tank where the water flows.

Next, the nozzle height, and initial ground height need to be recorded. To do this, the stream deflector plate is moved clear of where the stream of water and the point gauge will travel. The point gauge fits tightly in the jet nozzle preventing water from passing through during the reading. The difference between the ground height and nozzle height determine the initial starting position of the test. The rest of the readings during the test are then associated with that initial position. The point gauge has a precision of one one-thousandth of a foot, which accounts for even the smallest amount of erosion. However, it is important to develop a feel for the point gauge so that the user knows when to stop the point gauge at the top of the soil surface. Otherwise, this could create a false reading that inadvertently increases the erodibility of the soil.

At this point, the submergence / lab tank needs to be filled. The deflector plate is placed underneath the nozzle of the jet and the point gauge is fully retracted. Either the pump is started or the water is turned on at the faucet. After the tank is full, the deflector plate is retracted from in front of the jet nozzle. As soon as the jet nozzle is free from obstruction, testing begins. A time / reading schedule is used that is sensitive to the beginning of testing. Soils being sampled

generally erode quicker in the first few moments of the test, while the jet nozzle is still relatively close to the surface and providing a maximum stress on the soil. But as the soil erodes and the nozzle is further away, the energy applied to the surface is reduced. The typical time scheme used is shown in Appendix 6.B, including the zero time point gauge reading and the maximum depth of scour calculated. The point-gauge readings are taken at the times shown in the “diff time” column. With every point-gauge reading, the water is cut off from passing through the nozzle and therefore stalls the test. Also, if loose gravel is identified in the depression left by the JET, it should be gently removed so as not to interfere further with the test. This is important because the user is trying to identify the erosion rate of fine cohesive soils, and the small gravel that may be mixed into that soil may skew the overall results. Once the reading is taken and the point gauge is retracted from the jet nozzle, the test begins immediately and the stopwatch is started.

Once the test is completed in the field, a soil density and soil sample is taken from within the submergence tank, to ensure consistency of soil, and is later tested in the lab. The submergence tank and all of the equipment is then moved to the next testing area. It is good practice to leave several feet of space between the old test site and the new one to reduce unnatural disturbance of the area.

6.3 Scour Measurement

This project was conducted with a two-part data collection strategy: episodic and continuous. This strategy was developed to maximize the number of sites included in the study and the potential for collecting meaningful scour measurements. Episodic measurements required minimal equipment cost but were labor intensive, while greater capital costs were associated with continuous data collection but required little labor after the initial investment. This two-part approach also offered a variety of spatially and temporally varied data. Episodic data provided a spatial component to collected data, but only two or three measurements were associated with each event. Continuous data provided data from a single location within the river, but at hourly resolution during both flood and non-flood events.

Episodic data was collected with a wire-weighted gauge from eleven of the twelve bridges. The Paw Paw River Bridge has piers that extend 12 to 15 feet beyond the bridge facing in both the upstream and downstream directions and prohibited episodic monitoring because

wire-weighted gauge would not extend more than a few feet beyond the bridge rail. A baseline riverbed survey was conducted in the vicinity of the bridge piers prior to expected high flow events. The relative movement between these two measurements is attributed to scour. Each set of measurements also includes a distance to the water surface used to determine total water depth.

The episodic measurements were made with a bridge board and a sounding reel, both purchased from Rickly Hydrological Company. The sounding reel holds 75-ft. of 0.10-in. cable and is capable of holding 100 pounds of weight. The bridge board is four feet long and has an adjustable foot rest to adapt to bridge railings of varying height (Figures 6.10a and 6.10b).



Figures 6.10 (a) Deployed front view **(b)** Deployed side view

Episodic data was collected from both the upstream and downstream sides of the bridges. A zero station was designated, marked and recorded for each bridge. For each cross-sectional measurement, a tape measure was deployed across the bridge deck starting from the zero station. The horizontal distance from the zero station accompanies each measurement made with the wire-weighted gauge. A full cross section for each bridge was measured at the onset of the project and subsequent baseline and flood measurements focused in the vicinity of the piers with increasing horizontal resolution near the pier.

Continuous data was collected from three of the twelve bridges. The continuous monitoring data collection platform consists of three systems: power supply, data logger and transmitter, and the sensor suite. The data collection platform was purchased through Fondriest Environmental, with the exception of the echo sounder as Fondriest does not provide a model that would meet required specifications. A third party supplied the echo sounder for this project and the data collection equipment was customized to accommodate it.

The power supply system includes a battery and solar panel (Figure 6.11a). Power is supplied by a 55 amp-hr, deep cycle, marine battery. It resides inside a plastic battery box on top of the bridge pier and below the bridge steel. One wire enters the box from the solar panel while another leaves the box and connects to the data logger via a MS-2 connector. The battery box is held shut with a nylon strap and the weight of the battery holds it in place. The solar panel is approximately 40-cm square and supplies 30-watts of power. The solar panel is mounted with hose clamps on 2-in. aluminum pipe and attached to the bridge with a floor flange and 1.5-in. long, 3/8-in. diameter rock bolts.



Figures 6.11(a) Enclosure and solar panel **(b)** Pier with conduit

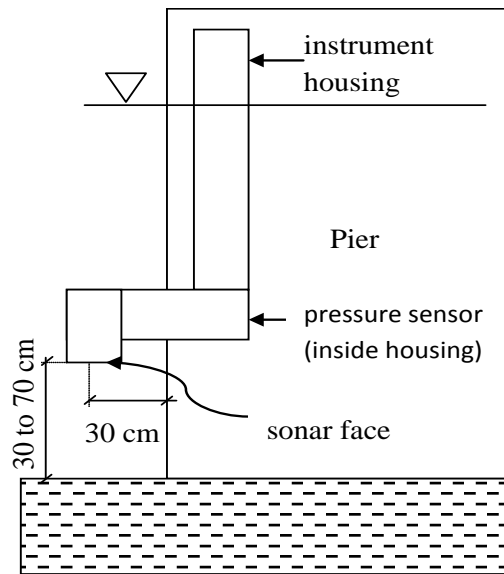
The data logger and transmitter are housed in a NEMA 4X enclosure composed of heavy-duty fiberglass (Figure 6.11a). The data logger allows four RS-232 devices, one RS-485 device, 8 analog inputs and ten SDI-12 devices to be connected at the same time. A separate terminal strip is used to connect the analog and SDI-12 devices. The high-gain cellular antenna is connected to the transmitter with a micro-loss RF cable and transmits to a server in the Wayne State University Hydraulics Laboratory fifteen minutes after being recorded.

Data is obtained with a small cylindrical microsounder (Figure 6.12a) 50-mm. in diameter and 59-mm. high. The surface of the microsounder has a diameter of 34-mm. and operates at 500 kHz. The beam width is 6 degrees conical (at 500kHz), is capable of resolving

depths to 1mm. and outputs data in ASCII, NEMA or DBT format. The microsounder is positioned approximately 35 to 70cm from the river bottom. The microsounder is attached to the end of a 1.5-in. diameter aluminum conduit. The conduit, attached to the pier (Figure 6.11b), has a 90-degree sweeping elbow and a short, 90-degree elbow on the bottom. The two elbows enable the microsounder to be positioned up to 30cm. away from the front of the bridge pier (Figure 6.12b). The sounder is capable of returning distances up to 50m. and operating in depths up to 500m. In addition to depth-to-riverbed measurements, the height of the water column above the microsounder is collected with a piezoresistive pressure sensor. The pressure sensor is corrected for water temperature and barometric pressure, is rated for 0 to 5m. of water and has $\pm 0.1\%$ full-scale accuracy. The total depth of water is obtained by adding the readings from the microsounder and the pressure sensor.



Figures 6.12(a) Microsounder



(b) Schematic drawing of continuous setup

6.4 Acoustic Doppler Current Profiler

Ideally, each study location should have a real-time USGS gauge to provide the hydraulic information necessary to apply various scour models. However, only three of the 12 locations have a gauge on site. Discharge and velocity measurements were made at each study site with an

acoustic Doppler current profiler (ADCP), but these were especially important at the ungauged study sites.

The ADCP provides three dimensional velocity measurements in water up to 13-ft. deep. The profiler was deployed from a bridge and floated across the section. Velocity was collected in vertical ensembles and integrated as the boat moved across the river. Basic output includes average velocity and total discharge. The basic output combined with water surface elevations taken during episodic measurements provided the basis for HEC-RAS model calibration.

In order to optimize data collection and obtain the most accurate information possible from the ADCP, some initial setup was required before each measurement. First, the ADCP needs the maximum depth of water at the cross section. The episodic measurements provided this information. Second, an initial pass with the instrument was made in order to determine the maximum velocity. With these two parameters, the ADCP was configured for use. Each bin (pixel) in Figure 6.13 represents approximately eight inches of depth and a single velocity is assigned to each bin. The ADCP was acquired by Wayne State in April 2009 and most scour measurements made since then have an associated velocity contour.

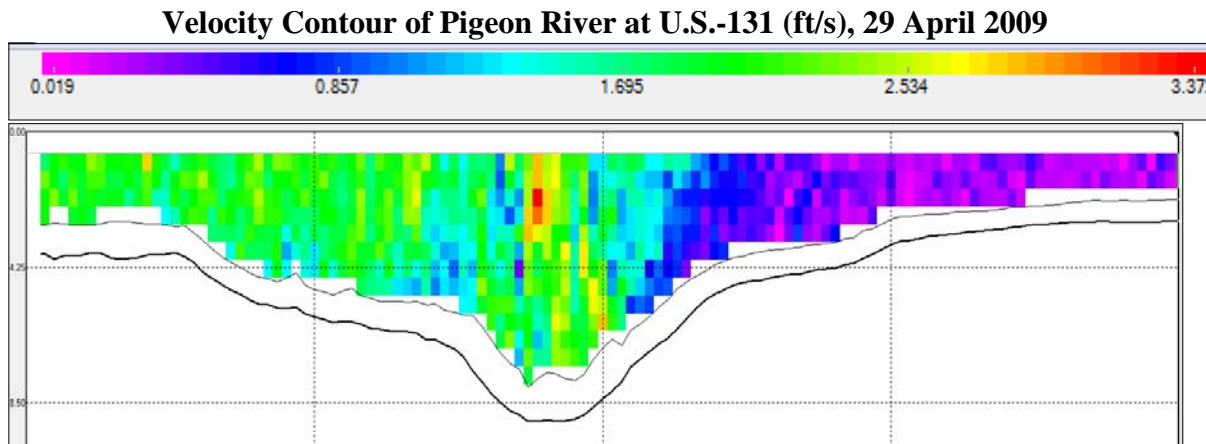


Figure 6.13 Example of acoustic Doppler current profiler data.

7.0 JET EROSION TEST (JET) RESULTS

The JET portion of this project was conducted in the expectation that knowing the potential of a soil to erode could help to predict scour more accurately. Engineers might identify potential erosion-related problems if we can relate erodibility to other geotechnical properties. The specific objectives of JETs were: 1) to correlate erodibility to other geotechnical properties; 2) to use JET results to supplement the data necessary for the process of calibration/verification of scour equations; and 3) to correlate observed scour with *in situ* soil conditions.

The following sections describe site selection for field JET investigations, sample preparation for laboratory versions of the JET, and how erodibility is correlated to other measured geotechnical characteristics. The final section is an assessment of objective achievements, limitations of JET, and recommendations for further research.

7.1 Site Selection for Detailed Field JET Investigations

The JET device has been developed to test the erodibility of cohesive soils. One goal of this investigation was to test the effectiveness of the JET beyond cohesive soils into silty and sandy fine-grained soils. Therefore, soil type was a main consideration in choosing locations for testing. Using boring logs obtained from MDOT, sites with fine soils were selected for further analysis. Field inspections that yielded fine soils in close proximity to the surface, which allowed soil samples to be obtained and a JET to be completed, was the final determining factor. Fine soils located deeper than one foot made samples difficult to retrieve and to complete the JET. This was a limitation because extensive excavation would be needed and may compromise the undisturbed soils condition.

Geotechnical tests including sieve analysis, hydrometer tests and Atterberg limits resulted in the selection of three sites for detailed JET testing: Pawpaw River at Coloma Road near Riverside, Thornapple River at McKeown Road near Hastings, and the Grand River at M-99 near Lansing. Two additional sites (Flint River at M-36 and Evan's Drain on Lawrence Tech's campus) were also tested to establish field protocols for the JETs.

7.1.1 Pawpaw River at Coloma Road near Riverside, MI

The soil at the Pawpaw River is classified as “silty clayey sand” (SM-SC) according to the Unified Soil Classification System (USCS). Soil samples were taken to determine if performing a JET was viable. The soil type at this location varied from the bank to the streambed. The streambed contained large amounts of depositional silts, which made carrying out a JET very difficult.

The first *in situ* test, illustrated in Figure 7.1, was completed on top of the bank in a material that was previously unclassified. A head of over five feet was used as was established through testing protocols and sufficient for previous JETs. A sand cone density test was performed near the site of the test and a unit weight of 20 kN/m^3 was discovered. Although this density can be considered on the higher side for naturally occurring soils, it is not out of the ordinary. The test lasted the full two hours, but the total erosion was minimal, which raised some questions about the validity of the first test.



Figure 7.1 Pawpaw River field JET

The second JET conducted was near the previous test. However, approximately one foot of material was excavated from around the location to be tested. This was done to reveal soil not measured by the previous test. This test also lasted the full two hours and provided more expected results. The dry unit weight was found to be near 16 kN/m^3 using the Shelby tube method described in Chapter 6.

7.1.2 Grand River at M-99 near Lansing, MI

Soil samples were obtained from the Grand River during two separate trips. On the first visit, soil samples were taken from the edge of the river near the bank and from the center of the river. These first samples were used to classify the soil, test its shear strength properties, and complete a laboratory JET. The USCS soil classification for the Grand River was SM-SC. It was found that the soil in the center of the river closely matched the soil near the edge of the river. This is important because it suggested that a JET near the edge or on the bank would provide a result similar to a test in the center of the river and therefore would accurately represent the section.

The second trip to the Grand River was used to collect additional soil samples and complete an *in situ* JET. An *in situ* JET was completed on the bank of the Grand River because the water level of the river was too high to complete a test within the river itself. To execute this test the soil on the bank was excavated nearly two feet. This was necessary to reach the same soil type that was found on previous trips. After the *in situ* JET was completed, the dry unit weight was measured and a bulk sample was collected from the test area to be classified and tested using the laboratory JET.

7.1.3 Thornapple River at McKeown Road near Hastings, MI

The soil at the Thornapple River was tested and classified using USCS and was identified as “silty sand” (SM). The clay content of the soil was near ten percent. Several attempts were made during repeated visits to the site to conduct an *in situ* JET. However, all attempts failed as the soil did not exhibit significant cohesive properties.

7.2 Preparation of Laboratory JET Specimens

To study the behavior of the laboratory JET, a silty clay soil with known characteristics was used as a control soil. The control soil was used to calibrate the JET apparatus for laboratory conditions. In establishing the protocol, several iterations of the procedure were attempted.

With the idea that each soil has its own individual compaction curve, where maximum compaction could be reached, a specimen of soil was prepared. Using a standard four-inch Proctor mold, a dry unit weight of 20 kN/m^3 was attempted first. To reach the desired dry unit weight, it was calculated that 1.9 kilograms of soil would be needed to fill the mold. In order to pack that amount of soil into the given volume, a 5.5-pound Proctor compaction hammer was used at twenty-five blows per lift and three lifts. Before compacting the soil in the mold, the soil was passed through a # 4 sieve to remove any gravel. The soil was premixed with a percentage of water in comparison with the total amount of soil to make it more receptive to the energy being applied. This was the basic procedure for preparing a specimen to be tested.

In order to achieve the proper dry unit weight for different soils, the procedure was modified to use varying water contents and blows per lift. Certain soil specimens required significantly less water than others, so it was often necessary to make several attempts at reaching compaction with a single soil. The same was true with the number of blows per lift. In the end, a minimum water content of 10% was used for compaction of all soil specimens, and the number of blows per lift was varied depending on the desired dry unit weight.

After the soil was compacted to the desired dry unit weight, the first JET was attempted. A maximum depth of scour of four inches was met well before a full two hour test was completed. Therefore, the first procedural change was to allow the soil to strengthen for a few days. Specimens were covered with plastic to prevent them from drying out. Specimens were tested every day for five days of strengthening to see how their erodibilities would differ. From these preliminary tests, it was decided to allow samples to strengthen no less than three days before testing.

Because the soils tested in the field were generally located below the water table and considered saturated, it was necessary to saturate the soil. Therefore, the second procedural change involved saturating the soil specimen. Saturation happened after the specimen was

allowed to strengthen for a minimum of three days. It is also important to note that saturation was generally initiated the evening before the actual JET so that the specimen was only soaked for one evening.

7.3 Laboratory JET

Setup and use of the laboratory version of the JET is very similar to that of the *in situ* version of the device. Once the specimen is prepared as specified above, the lab tank is filled with water and the specimen is placed in the center of the lab tank. The lid is then placed on the lab tank and the rest of the device is set up. The head tank is set to a height of 24 inches for all of the tests to ensure consistent results and to make sure that a complete test of two hours is completed.

Jet testing was completed on specimens from the Pawpaw River, Grand River, Thornapple River, and a controlled sample of cohesive material that existed in the lab. The control specimen from the lab was the first to be tested because it was used to calibrate the test procedure. The lab soil had cohesive properties which made it an excellent choice for calibration. It was tested over a variety of dry unit weights ranging from 16 kN/m^3 to 19 kN/m^3 .

7.4 Geotechnical Properties Compared with Erodibility

For this research, the erodibility versus dry unit weight was compared by site to their classification by the Unified Soil Classification System (USCS). The idea to compare the erodibility of soil based on the classification came from the common problem of identifying one property that controlled erodibility. Previous research has found it likely that more than one property controls erodibility (Paaswell, 1973). USCS addresses this issue by classifying soils by numerous properties, with each classification of soil having a similar composition. Therefore, the composition of each classification may exhibit somewhat similar erodibility characteristics.

Table 7.1 shows the breakdown of the general soil properties from each of the samples tested. For each case the classification is discussed more completely in the following sections. Several soil types were tested using the lab JET apparatus in this study. Their general forms are shown in Table 7.1 and their grain size distributions are featured in Figure 7.2.

Table 7.1 Soil characteristics

Soil	Gradation			Atterberg Limits			USCS Classification
	% Gravel	% Sand	% Fines	Liquid Limit	Plastic Limit	Plasticity Index	
Control Soil	0.8	41.9	57.3	22.7	16.4	6.3	CL-ML (Sandy □ Silty Clay)
Pawpaw River	2.3	81.8	15.9	17.9	12.7	5.2	SM-SC (Silty □ Clayey Sand)
Grand River	12.1	58.7	29.2	16.7	12.4	4.3	SM-SC (Silty □ Clayey Sand)
Thornapple □ River	9.4	63.5	27.1	13	12	1	SM (Silty Sand)

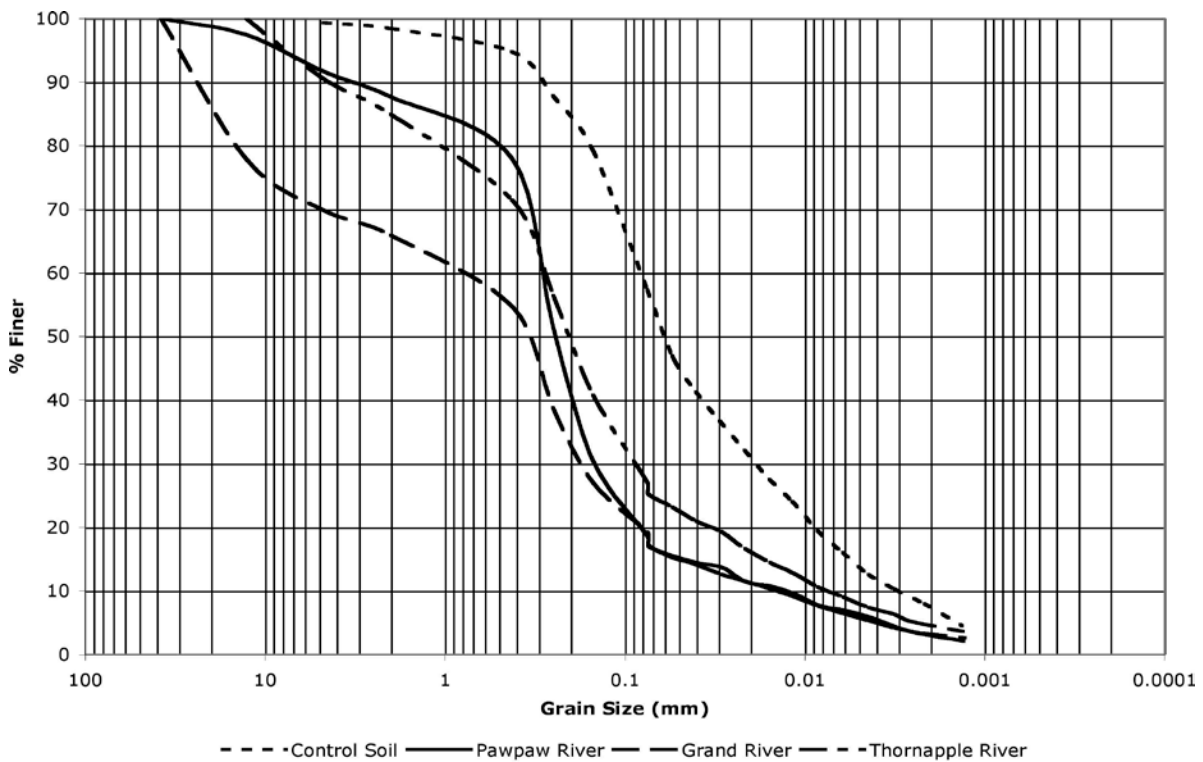


Figure 7.2 Grain-size distributions of the 3 JET experiments.

7.5 Variation of Erodibility with Dry Unit Weight

The variation of erodibility with respect to dry unit weight was compared. The logarithm of erodibility exhibited a linearly inverse relationship to the dry unit weight. For each specimen,

excluding the Thornapple River sample, a statistical analysis was completed to develop an envelope that would encapsulate 95% of the data. The upper and lower bounds of this envelope were developed using a standard linear regression. This was done by transforming the erodibility data into \log_{10} form. Once the transformation was complete, a linear regression comparing the \log_{10} of erodibility to the associated dry unit weight could be completed. The regression was executed using Excel, with a confidence level of 95%. Next, a t-statistic was used to correct for a small sample size. Choosing the t-statistic was also based on use of a two sided t-distribution. The standard error found by linear regression with the t-statistic was subtracted. The confidence intervals found were then converted back from log form and plotted using the y-axis in log form. Details of confidence interval development are presented in Appendix 7.A.

7.5.1 JET Results for Control Soil

The control soil was more cohesive than each of the other soils tested. Several tests were carried out on the control soil sample with densities from 16 to 19 kN/m^3 . These data points showed a trend indicating that the logarithm of erodibility may be linearly related to dry unit weight (Figure 7.3). Reinforcing the previous statement, the data points collected fit within the 95% confidence interval. The coefficient of determination, or R^2 value, also indicated that the data points were closely related for a single specimen tested.

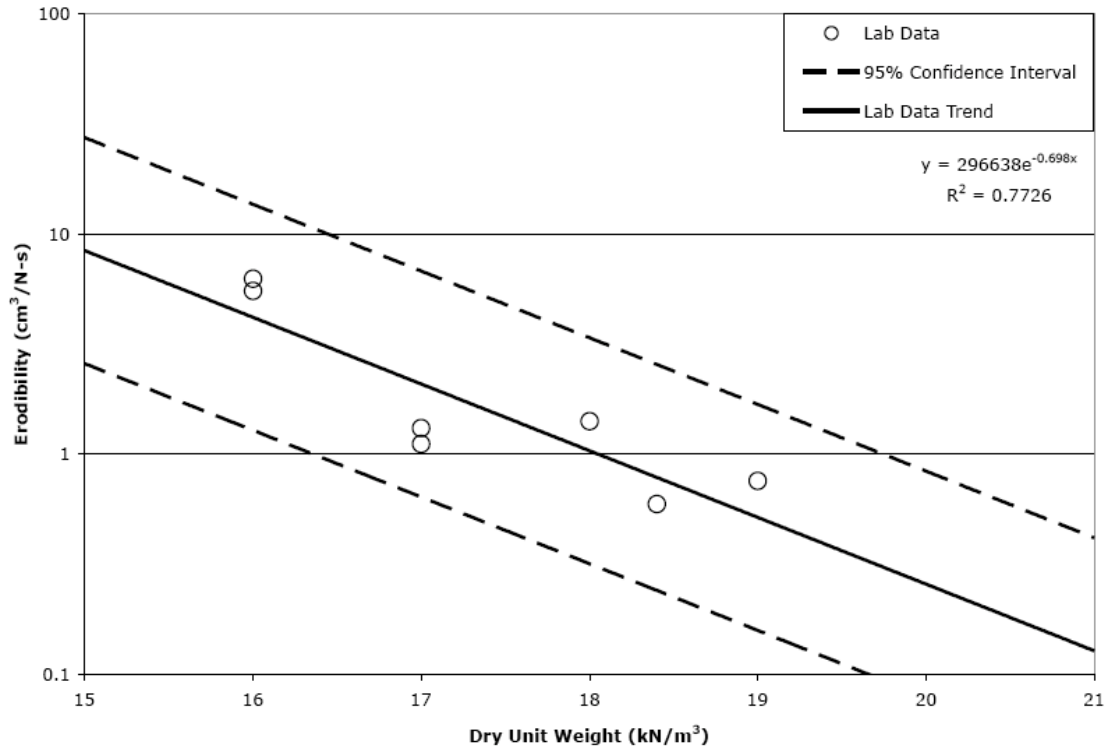


Figure 7.3 Control soil JET results

7.5.2 JET Results for Pawpaw River

Testing for the erodibility at the Pawpaw River was more extensive than any other of the selected field sites for several reasons. First, the field conditions were very conducive to the goals of this project because the tested soil was located only a few inches below the surface on the top of the bank and the site was easy to access. Although the soil was saturated, it was easy to access without concern for the water table. Second, the conditions at the Pawpaw River also made it easy to obtain an accurate density and collect bulk samples for testing in the laboratory.

The three JETs completed *in situ* at the Pawpaw River also yielded similar results. This is important because it helped to calibrate the protocol to establish laboratory testing of the collected field samples. A density of 16.44 kN/m³ was found at the site and the erodibility ranged from just below 1 cm³/N-s to just over 2 cm³/N-s. Each of the tests completed at the Pawpaw River site lasted a full two hours, which may have assured more accurate results. Another important factor affecting JETs in the field is the lack of gravel at the Pawpaw River site. The scarcity of gravel helped match the field results to the lab results where the gravel was to be removed for compaction in Proctor molds.

Laboratory JETs on the Pawpaw River sample closely mimicked the results of the field tests. Laboratory JETs were completed on the Pawpaw River sample ranging in dry unit weights from 16.5 kN/m³ to 18.5 kN/m³. Like some of the tests explained previously, lower dry unit weights were tested with the same results.

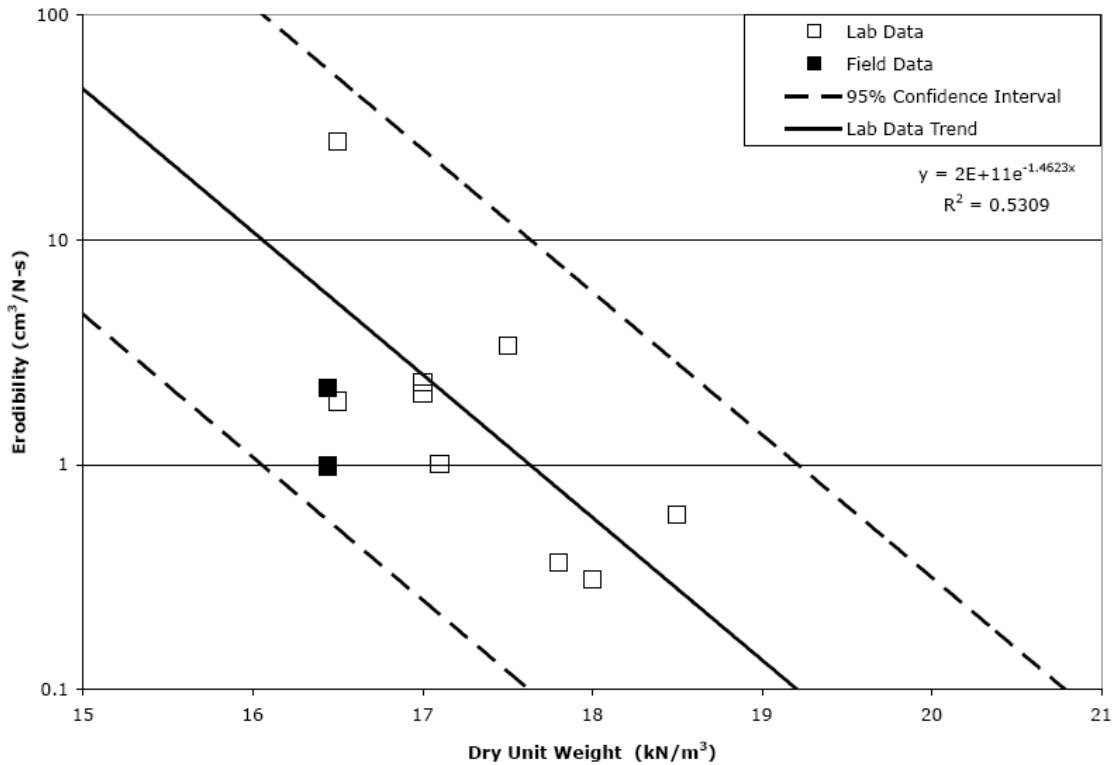


Figure 7.4 Pawpaw River JET results

The confidence interval for the Pawpaw River sample is wider than that of the control soil, which may indicate the inconsistencies in the soil sample itself or that the difference in soil properties is having an effect on the soil's erodibility. However, when the field data points are removed from the figure, the confidence interval became smaller. This is likely caused by variation in the *in situ* soil unlike that of the same soil sample when it is tested in the lab. Soil samples tested in the lab are broken down and reassembled several times in the process of testing for erodibility and characterizing the soil. It is important to note that the confidence intervals for the Pawpaw River samples were developed for the laboratory data only and do not include data from the field. However, inspection of Figure 7.4 shows that the data collected in the field falls within the 95% confidence interval found with the laboratory data. The R² value shows the

reason for this. The R^2 value is smaller, because of more scatter in the data, which causes the standard error to be larger and the confidence intervals to be wider.

7.5.3 JET Results for Grand River

Soil was taken from the Grand River at two separate times. The first soil sample was used to classify the soil and check for cohesive properties, but there were insufficient quantities of the soil to continue with laboratory JETs. A second trip was made to the location to collect more soil for further testing. On the return trip to the Grand River an *in situ* JET was performed and another sample was obtained to estimate the *in situ* unit weight.

The *in situ* JET revealed an erodibility of $3.37 \text{ cm}^3/\text{N}\cdot\text{s}$ and a density of 16.67 kN/m^3 . The density found was in the range of undisturbed soil that could be expected and because the erodibility of the soil is unknown it was deemed acceptable. Laboratory JETs could then be used to replicate expand upon the field results.

Lab testing began after completing the grain-size analysis and classifying the soil. Initial lab tests were unsuccessful because of incorrect compaction techniques that did not ensure enough initial moisture while compacting. These tests led to structurally weak samples, which were quickly scoured by the JET. The next set of tests used samples that, when compacted, contained a higher initial moisture content. Complete JETs were finished on these samples with successful results (Figure 7.5). Initially a trend did not appear obvious and an envelope was not apparent. However, once the field data point was removed from the set, an envelope became visible and conducive to the original hypothesis. Similar to the Pawpaw River, the Grand River's erodibility found in the field was lower than that of the erodibility found in the laboratory. However, unlike the Pawpaw River, the field data point from the Grand River did not fall within the 95% confidence interval developed for the laboratory data. This likely occurred because the laboratory data from the Grand River was much more consistent than the data from the Pawpaw River. This can be seen by the trend line for the Grand River samples that has a R^2 value of 0.7048 while the Pawpaw River samples' R^2 value was only 0.5309.

Multiple tests were completed for the Grand River, but none of the initial results were included in Figure 7.5 because of tests ending prematurely, especially for the lower densities. Results from tests that ended prematurely could not be used because they did not represent a full

set of data which the spreadsheet required in order to be accurate. Difficulty was also encountered while trying to calibrate the lab tests with the field tests.

Reasons for the inconsistency are unclear but are likely related to the process of compaction. In the laboratory, compaction follows the protocol of a standard proctor compaction test (ASTM D-698) where the proctor mold is compacted in three lifts of soil using equal force on each lift. This differs significantly from the field where the soil has been built up with very small lifts over a long period of time and compacted with ever increasing force over that same time period.

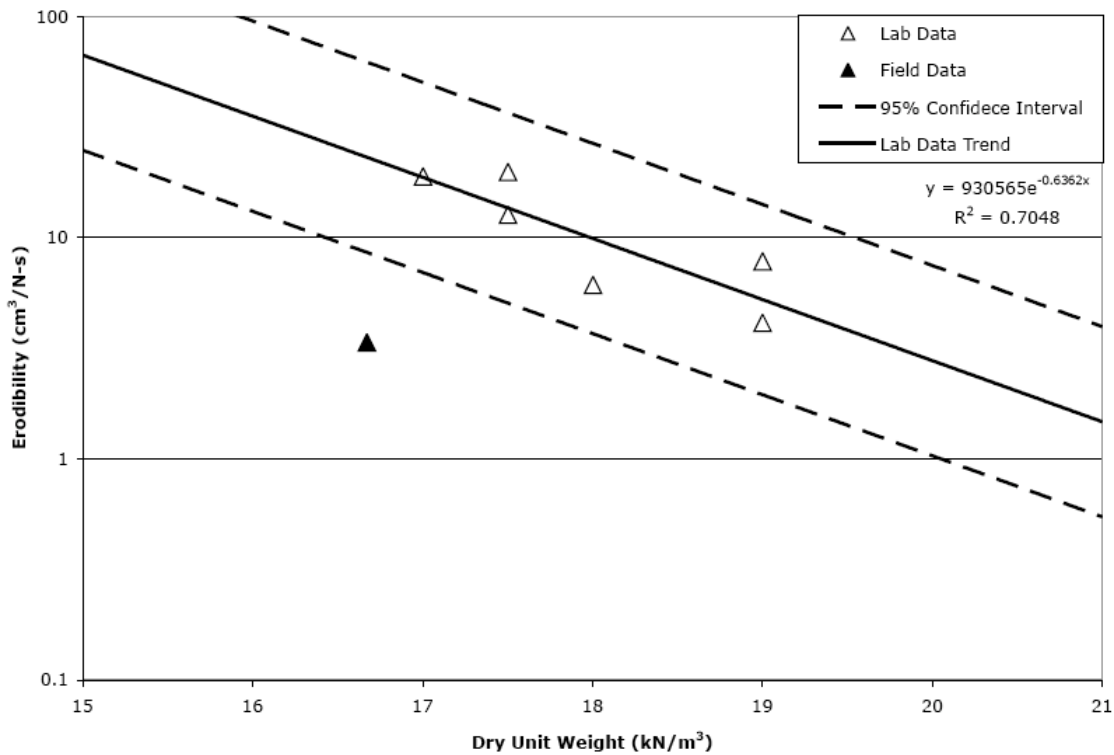


Figure 7.5 Grand River JET results

7.5.4 JET Results for Thornapple River

The Thornapple River soil was classified as silty sand. Though not cohesive, it was decided to attempt a laboratory JET. The sample continued to have issues reaching the desired dry unit weight in the proctor compaction mold. A dry unit weight of 20 kN/m³ was used, which in turn used up the entire soil sample from the Thornapple River. Only one test was completed for this sample because of the lack of *in situ* soil to continue with further tests.

Though the Thornapple River sample was quickly depleted, a set of data produced by Hanson (2007) using silty sand that was prepared in a manner similar to that of the Thornapple River sample was found. The two data sets were combined to see if there was a correlation. The data collected from Hanson and Hunt (2007) was also laboratory data, which is the reason it was used to develop a trend. Further laboratory and *in situ* JETs of silty sand samples are needed to draw a strong conclusion.

7.5.5 Overall Comparison of Erodibility with Dry Unit Weight

Testing the erodibility of soil and comparing it to its associated density has shown a likely relationship between the two properties. Comparing the erodibility of one particular soil sample generally shows the best correlation but an envelope is visible when comparing the erodibility of multiple soil samples. Figure 7.6 shows data points collected during testing for this research. Although there are differences in the soil types, there is still a general envelope that surrounds the data. Within this envelope, one can identify each type of soil and its trend. The trend for each soil helps determine the size of the envelope, but the slope of the envelope is maintained. Knowing the upper and lower bounds could give designers an idea of where to expect the erodibility of any soil. However, one issue with the presentation of this data is that it spans over two orders of magnitude. The wide range of erodibilities makes it difficult to compare multiple data sets at once. Further testing could define the bounds and improve correlation.

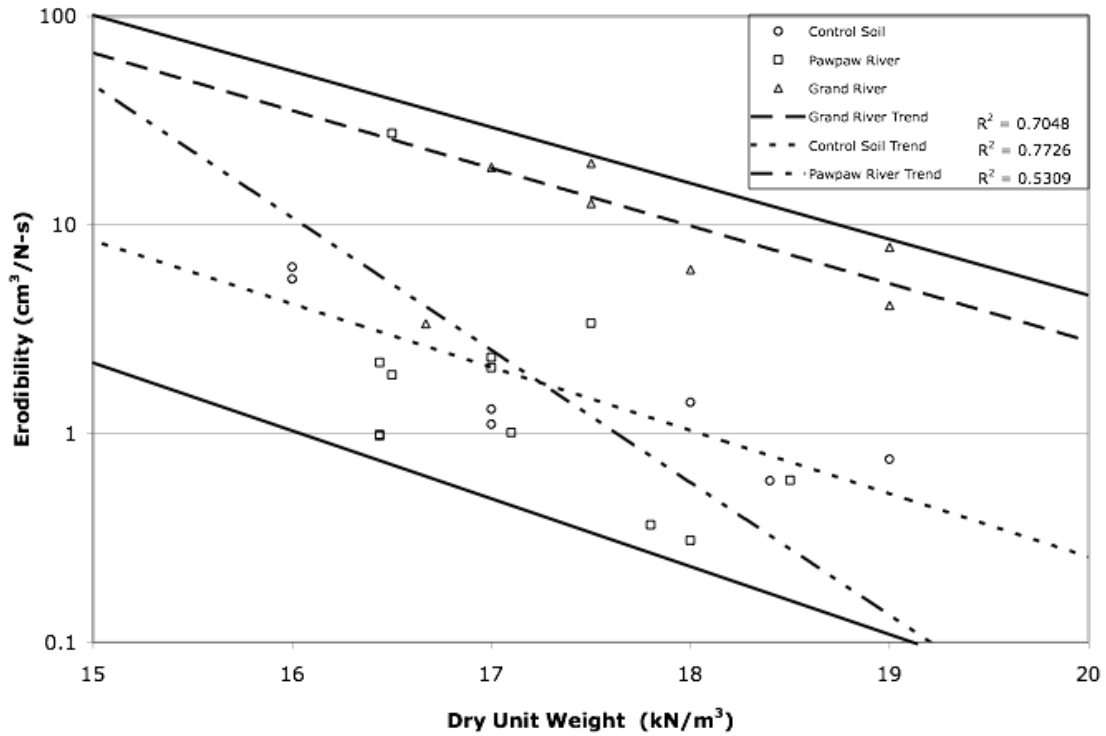


Figure 7.6 Combined data

7.6 Erodibility and Soil Type

Figure 7.7 shows data collected during this research along with data attained from previous research plotted together and each subset of data is encircled. A visually clear correlation between erodibility and dry unit weight was difficult to see until each of the subsets was outlined. Each of the subsets is labeled with its soil type, except for data from Allen et al. (1999), which was not classified. The data from Allen et al. (1999) has been separated into the percentage of fines contained in each sample tested. The Pawpaw River sample, control sample and data from Allen et al. (1999) show the most convincing trends. The most important finding in Figure 7.7 is its ability to provide a representative range of erodibilities for different classes of soils.

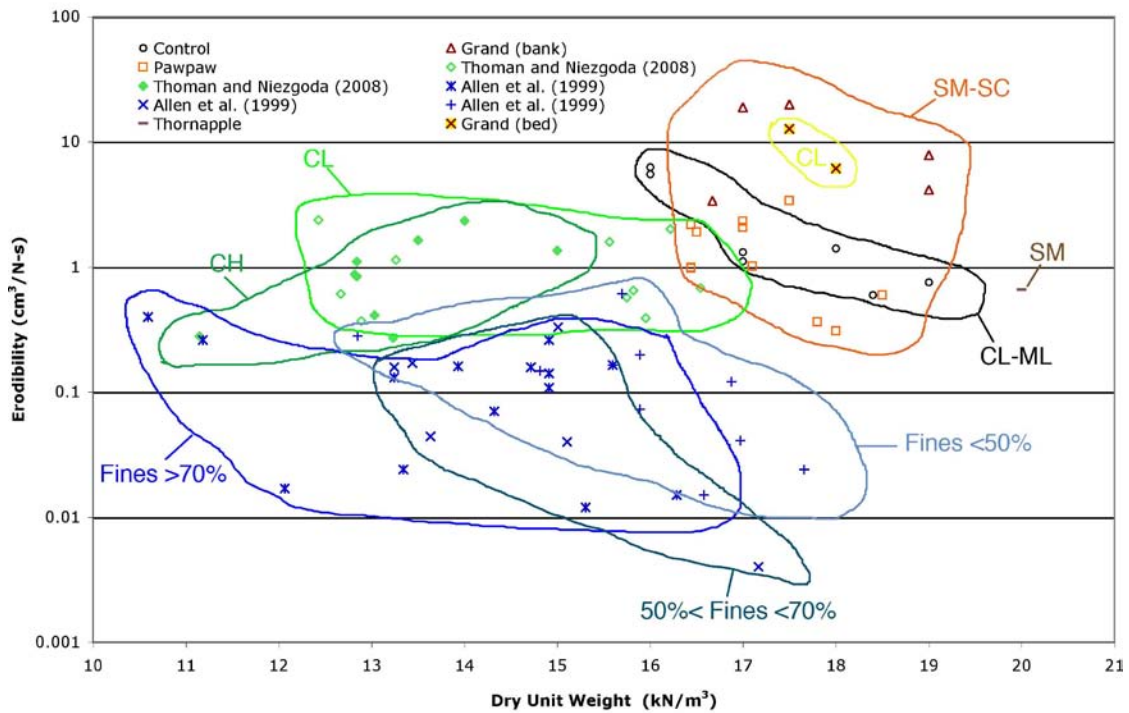


Figure 7.7 Combined data comparison

Thoman and Niezgoda (2008) provided data for the CL classification of soil and during this research, laboratory JETs were performed on CL-classified soils. The data collected in this research did not fit in with the data from Thoman and Niezgoda (2008). The reason for this is unclear, but by definition, CL can range from a lean clay to a sandy lean clay to a gravelly lean clay and everything in between. Changes in the ratio of sand to clay to gravel is likely the cause of the discrepancy. This suggests that the erodibility of soil cannot be easily identified based solely on characterization and dry unit weight. However, further testing may provide insight into other controlling factors of erodibility.

A comparison is likely to be found when utilizing the classification of soil in JET. Each class of soil has unique properties and erodibility is another unique property. Figure 7.7 shows the difference in erodibility between several different types of soil. Although there may be significant differences in a particular soil type's erodibility, the comparison of erodibility as a whole between different soil types can help engineers identify the erodibility of soil.

In this study, specific care was taken to ensure that each soil type tested was documented so it could be compared more effectively. Where possible, data from other sources was

combined with information found in this study to create a more complete set of data. Such was the case in Figure 7.7, where data from Hanson and Hunt (2007) was combined with data found in this study. The data was combined because the information provided by Hanson and Hunt (2007) was classified using the USCS method, which is the same method used in this study. This allowed for the comparison of two like soils. Unfortunately, more data could not be obtained for the data set in question, but it led to a research question. Do similar soil types have similar values of erodibility?

More information on this particular facet of erodibility could be valuable. Other studies have tried to break down erodibility by particular soil properties. If one focuses on the relationship between erodibility and a particular classification of soil it may be easier to estimate the erodibility of soil. The theory behind this idea is that soils are classified based on a set of properties distinct to a certain classification rather than a single property. Therefore, one class of soil should behave similarly no matter its original source.

7.7 Bank and Streambed Soil Comparison

Field testing of erodibility during this research took place near the banks of rivers. It became apparent that, in order to use erodibility to predict the erosion of streambed material, a comparison had to be made with the streambed material and the bank material. To complete this comparison, a number of laboratory JETs were completed on streambed material and a comparison was made between the soil characteristics of streambed material and that of the bank material.

7.7.1 Pawpaw River Streambed and Bank Material Comparison

JETs were only completed on bank material from the Pawpaw River, but soil was collected from the streambed to compare. A simple grain-size distribution, featured in Figure 7.8, may be the easiest way to compare the different materials. In particular, the percent of material passing the number 200 sieve, or the fines, is most relevant. The material taken from the bank yielded a fines percent that ranged from 17% to 19%. However, the material taken from the streambed had a much wider range from 5% to 25%. The range of percentage of fines can be expected to be greater within the river because it is a dynamic environment.

The bed material with a lower percentage of fines may be located in an area with higher shear stresses that have eroded away the fines, while the bed material with a higher percentage of fines may be located in an area where deposition is occurring. The major differences in soil characteristics should be taken into consideration and further JETs should be completed to get a complete view. In such a case, the bank material may not be a good indication of the total erodibility of the river system.

At the Pawpaw River location, it is important to remember that the bank material was taken several inches below the surface. This may have bigger implications in predicting the erodibility of the river as a whole. The material taken from the streambed was taken near the surface of the streambed, which may not fully represent the erodibility at the locations which the samples were taken. The streambed is a dynamic environment, but below the surface it may be possible to locate soil that closely mimics the soil which was found on the bank.

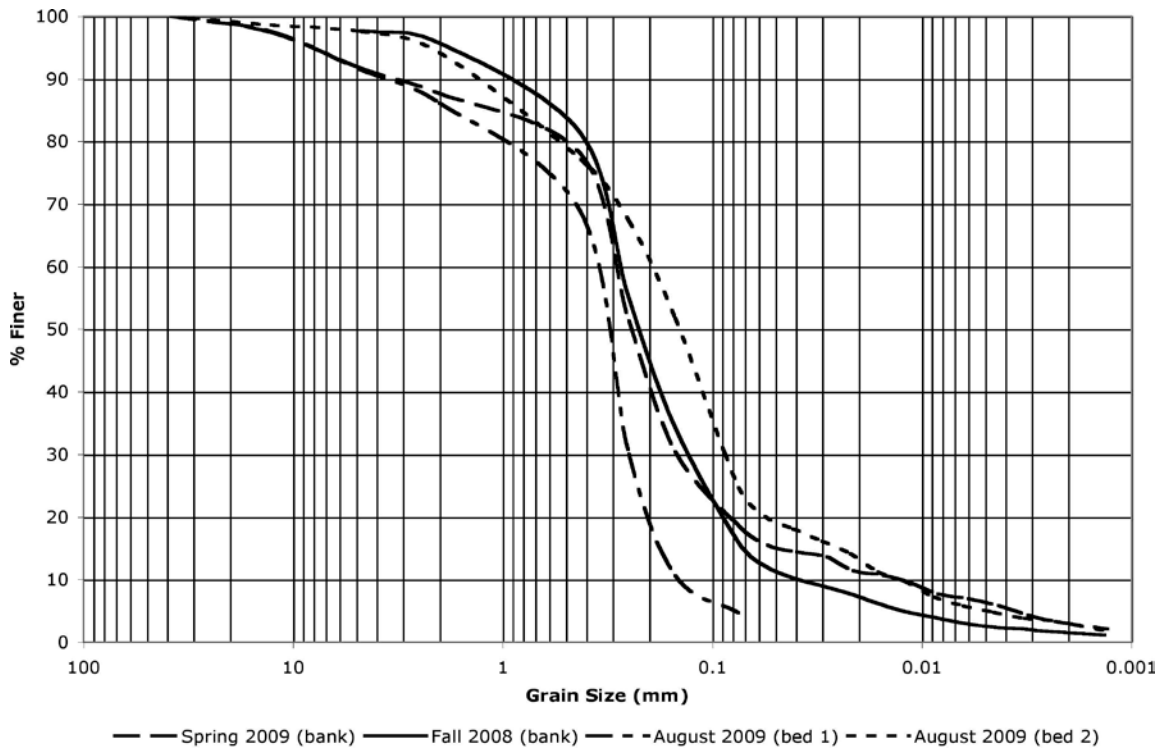


Figure 7.8 Pawpaw River grain-size distribution by season

7.7.2 Grand River Streambed and Bank Material Comparison

The grain-size distribution from the Grand River also showed variation in percentage of fines among the samples obtained (Figure 7.9). The samples taken in the fall of 2008 and the

spring of 2009 were taken from the bed and bank respectively and yielded similar grain-size distributions. The percent fines for these two samples ranged from 18% for the bank and nearly 28% for the streambed in the fall of 2008. However, the biggest difference was found when a sample was taken from the bed in August of 2009. The percentage of fines was nearly 65%.

This major difference meant that testing the erodibility of this new soil was imperative. The Atterberg limits found for this soil classified it completely. The new specimen was classified as “sandy lean clay” whereas the other samples were classified as “silty clayey sand.”

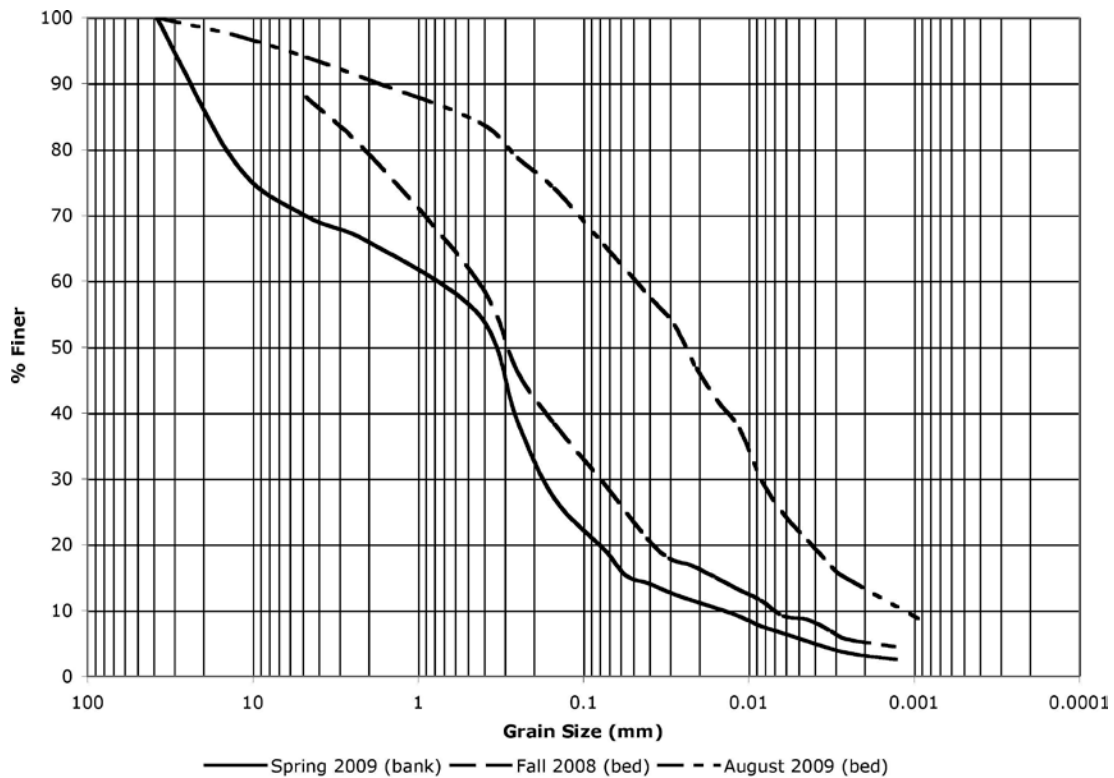


Figure 7.9 Grand River grain-size distribution by season

JETs were completed on this new soil type and were found to coincide closely with the results for the bank material. These results are shown in Figure 7.10 and support two conclusions. For this situation, material tested on the banks represents the erodibility of this section of river. The results suggest that testing bank material may be a viable method for testing the erodibility of a section of a given river. Perhaps the most important finding from testing the bank and the streambed material at this location is that even though their characteristics are significantly different, they erode in a similar manner. In this case, there are two different classifications of soil taken from locations adjacent to one another with similar erodibilities. A

thorough comparison of these two soils may show differences that could be tested to narrow down the mechanism that drives erodibility.

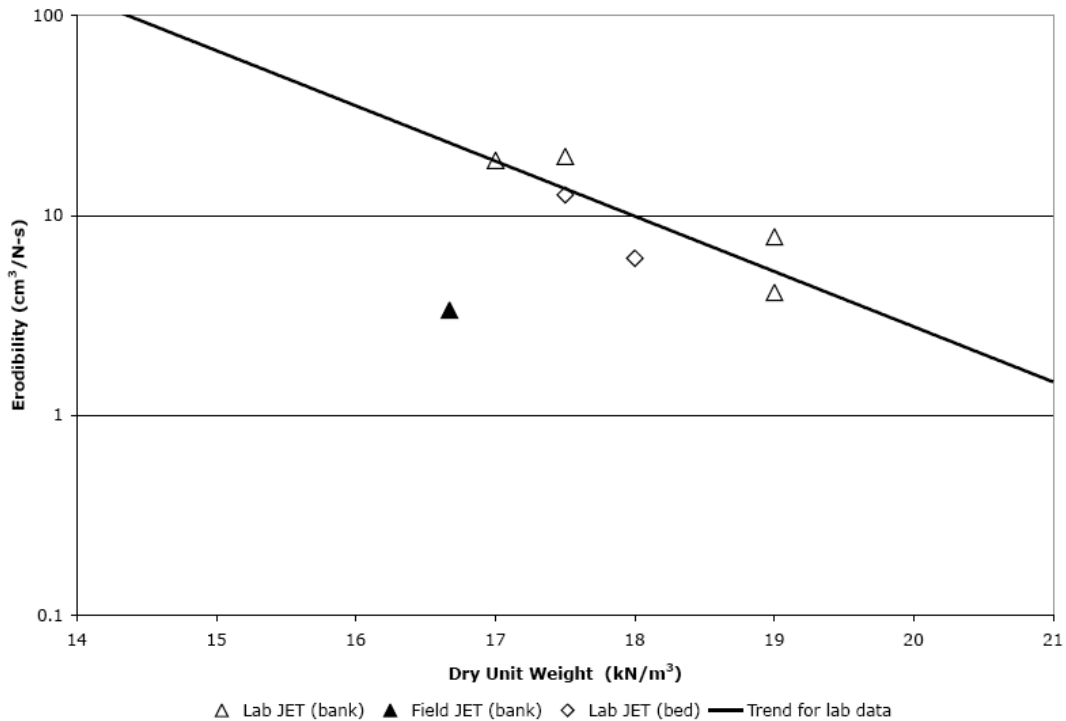


Figure 7.10 Grand River streambed and bank material JET comparison

7.8 Erodibility and Shear Strength Properties

The friction angle and the cohesion of a soil are defined as its shear strength properties. Erodibility has been compared to many soil properties, but a thorough literature review yielded very little information comparing erodibility to shear-strength properties. Finding the shear strength properties is important to geotechnical engineers because it describes how a soil will fail. Shear-strength properties of coarse-grained soils are typically found by completing a series of direct shear tests. The direct shear test measures the resistance of soil to shearing across a plane.

In simple terms, a soil erodes similarly to how a soil shears. The main difference between these two mechanisms of failure is the mediums that are causing the failure. Comparing shear-strength properties to erodibility was difficult because there was no direct way to compare the two properties. Each test had to be completed separately and the only characteristic that could be held constant was the dry unit weight of the soil specimen. The friction angle was

chosen for comparison because it had a more linear relationship than the apparent cohesion. When the comparison was made, the relationship was nearly identical to that of erodibility and the dry unit weight.

This issue made it difficult to understand the relationship between erodibility and the friction angle because the dry unit weight was dictating the results of each property. It was determined that the two properties had to be analyzed individually and compared. Figures 7.11 and 7.12 show the relationships between erodibility, friction angle and dry unit weight (details of shear-strength envelopes can be found in Appendix 7.B). Each case shows a similar relationship: as density increases the erodibility decreases and the friction angle increases. In other words, as the angle of friction of soil increases to resist failure, the erodibility decreases.

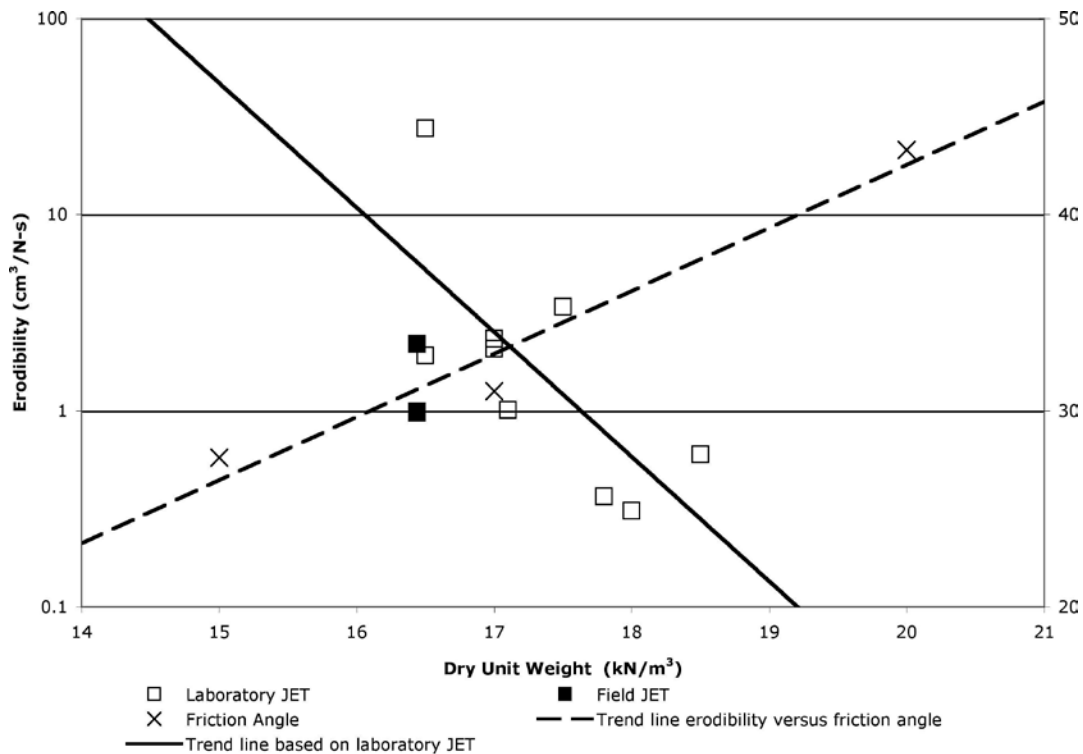


Figure 7.11 Pawpaw River erodibility and friction angle

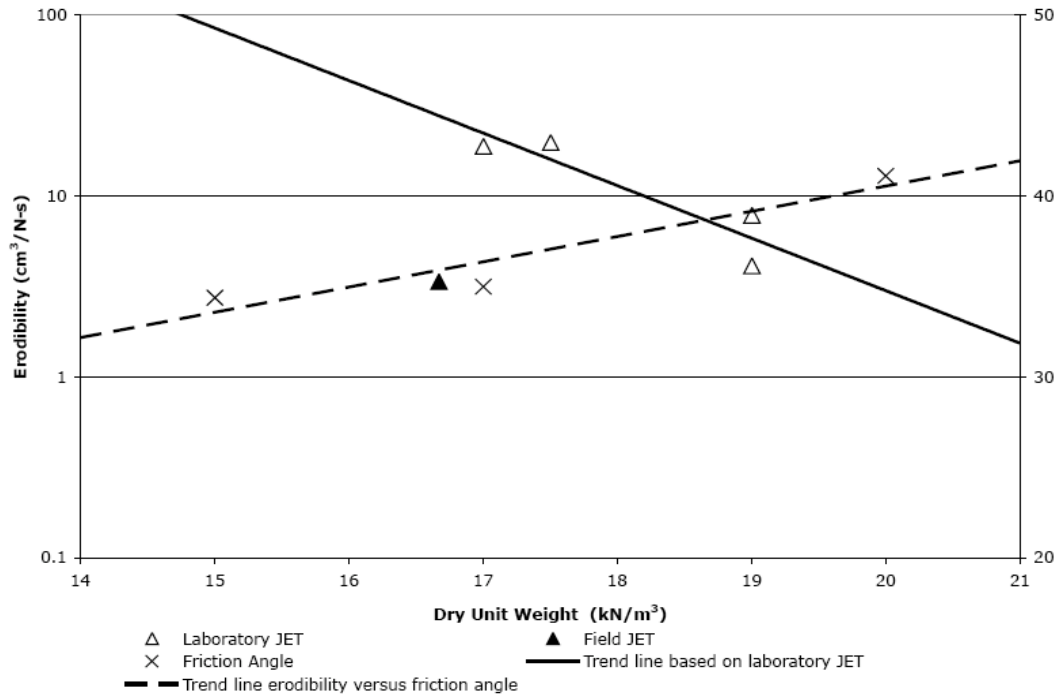


Figure 7.12 Grand River erodibility and friction angle

A relationship was developed between soil erodibility and friction angle by combining the trend-line equation for erodibility versus dry unit weight with the trend-line equation for friction angle versus dry unit weight. The equations could be equated because they both contained dry unit weight. This made it possible to develop two equations, one for the Pawpaw River (Equation 7.1) and one for the Grand River (Equation 7.2). These relationships are plotted in Figure 7.13. These equations allow the user to input a known friction angle (ϕ) to find a corresponding erodibility (k). They also illustrate a relationship showing that as the friction angle increases the erodibility decreases. Details of the formation of this relationship are given in Appendix 7C.

$$k = 2 \times 10^{11} (e^{-0.455\phi - 9.901}) \quad \text{(Equation 7.1)}$$

$$k = 2 \times 10^6 (e^{-0.478\phi + 4.02}) \quad \text{(Equation 7.2)}$$

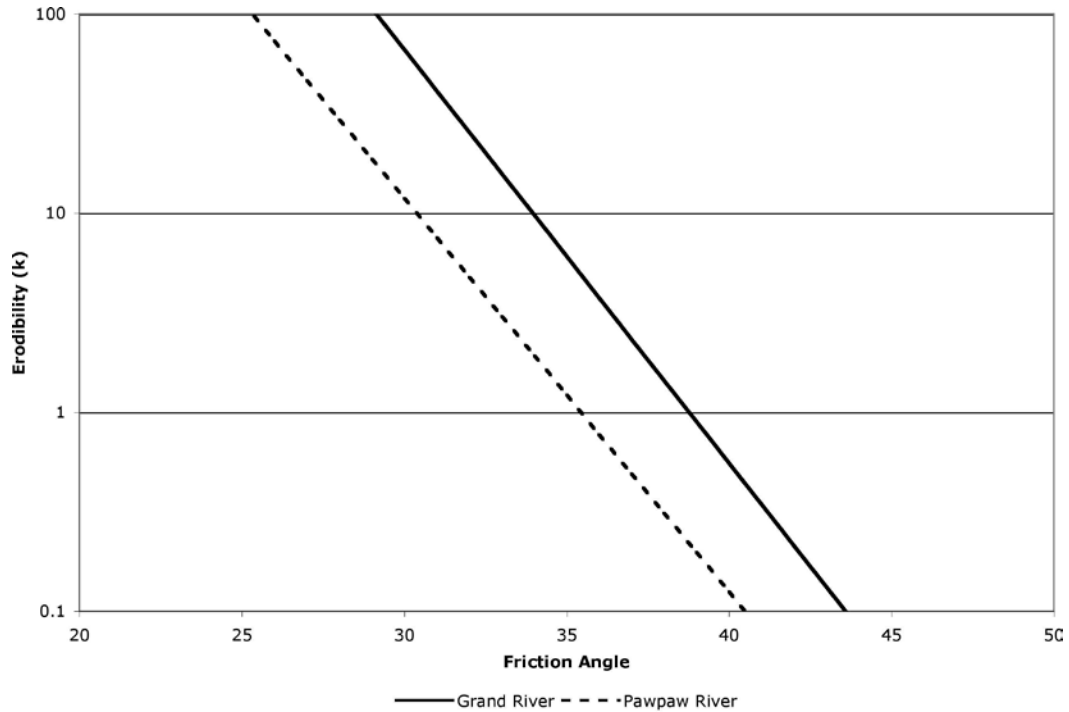


Figure 7.13 Erodibility vs. friction angle

7.9 Concluding Remarks on JET Results

Of the three JET-related objectives identified in the proposal, only the first objective (i.e. correlate erodibility to other geotechnical properties) was met fully. The second objective (use JET results to supplement the data necessary for the process of calibration / verification of scour equations) and the third objective (correlate observed scour with in situ soil conditions) were not met due to lack of sufficient data both in terms of measured scour events (see Chapter 8) and sites that had exhibited the appropriate soil conditions near the surface.

From data gathered in the field and in the laboratory, the following limitations have been identified as the main reasons for not being able to collect sufficient data:

- (a) First, testing soils with cohesive properties is necessary for the equipment to function as designed. Therefore, selection of sites to complete *in situ* jet testing was limited to three locations that exhibit cohesive properties.
- (b) Another limitation related to the cohesive properties of the sites is the depth of cohesive materials. The top surface of these and many other sites is composed of

non-cohesive sediment that cannot be tested. In order to complete jet tests at these sites, the top surface of sediment must be removed to expose the cohesive materials.

- (c) A third limitation is gathering the correct density of the soil that is being tested. The density is significant in finding the shear strength of the soil so that it can be compared to the erodibility coefficient. It is difficult to complete because the density needed is below the water surface, and our techniques require the soil to be above the water table.

During this research, steps were taken to compare erodibility with other geotechnical characteristics on a broader basis. The groundwork has been laid for civil engineers to recreate field samples in the laboratory and test them with the JET. A summary of findings on erodibility versus other geotechnical properties is given below.

Dry Unit Weight versus Erodibility

Numerous tests *in situ* and in the laboratory confirmed that the dry unit weight of a material has an inverse linear relationship with the logarithm of its erodibility. Each soil type tested had a fair coefficient of determination for data tested in the laboratory.

Testing also provided some insight into the effectiveness of laboratory testing. For both the Pawpaw River and the Grand River, soil erodibility was lower in the field than in the laboratory. Further testing is needed to confirm this occurrence and discover the degree of magnitude by which the tests differ.

Results obtained from this research confirm the effectiveness of the laboratory test sample preparation protocol. Three *in situ* test results from the Pawpaw River showed erodibilities near that of laboratory results.

Erodibility versus Soil Type

Results found in this research and in the literature review provided positive evidence that soil type may be an indicator of the erodibility of a soil. Current research has not shown exact erodibilities for any particular soil, but it has shown that different soil types erode at different rates over similar densities. Extensive research is still needed to confirm fully this hypothesis and to determine the range of erodibility for particular soils.

The erodibility of a river system may also be determined by testing material located on the banks. However, caution should be used. Determining erodibility based on a specific soil type may be inaccurate for a single location because of other soil characteristics that may be playing a role. In a case where erodibility is being predicted along a stretch of river, there may be a need to test samples from the river bed to confirm that the bank material is related. Testing soil up and down stream may also be needed in a few locations to confirm erodibilities and soil types.

Erodibility versus Shear Strength Properties

Erodibility and the shear-strength properties of soil is a very complex relationship and are difficult to compare because the two properties cannot be tested simultaneously. However, based on the testing methods presented in this research it can be concluded that that the logarithm of erodibility is inversely related to the friction angle of a soil, or that as the friction angle of a soil increases the erodibility decreases.

Few tests were completed during this research to compare the erodibility and friction angles of several different soil types. Comparing the results from the Pawpaw River and the Grand River is also difficult because their slopes are similar and the only conclusion one can make is that the Pawpaw River is less erodible than the Grand River.

7.10 Recommendations for Further Research

During this project, the samples were mostly collected using a hand auger in shallow soil layers (less than 3ft.) at or near the upstream bridge piers. The soil profiles received from MDOT indicated cohesive subsurface conditions. However, the material collected at or near the streambed was mostly granular. During some scour events, more than a few feet of streambed material can be subjected to degradation and aggregation. These scour holes can also be backfilled by loose soil deposits transported by the flow after a flood event which is why samples collected at the scour-critical bridges did not agree with the soil profiles in the as-built construction drawings. In addition, filling scour holes with coarse granular material has also been used as a counter measure at some bridge locations. Therefore, it is evident that the geotechnical properties of the material collected at or near the surface may not represent the entire soil profile that is subjected to scour.

Answers to these problems may be found through a detailed geotechnical characterization conducted on undisturbed soils samples. In future research, soil samples should be collected at the scour-critical bridge sites, in Shelby tubes, in the 0-10ft. depth range. Samples should be collected at the existing scour holes as well as at adjacent sites to evaluate the impact that the scour has had upon the soil profile.

Future research could expand on the work completed to include all soil types and tabulate their erodibilities for comparison, thus helping engineers make better decisions regarding erosion of soils. It would be useful to complete more laboratory JETs and compare them to *in situ* JETs to insure that the method for compacting samples to achieve realistic results is used. Improved laboratory testing techniques could lead to consistent testing, which could help develop a set of curves for the erodibility of different soil types. The curves could indicate the erodibility for different soil classifications so civil engineers could properly design structures that would resist erosion due to flowing water.

Finally, designers could benefit from further research determining the relationship between shear strength properties and erodibility because shear-strength properties are easily determined. Shear strength properties provide insight into the resistance of soil to move against itself, while erodibility shows the resistance of soil to move due to flowing water. If a relationship between erodibility and the shear strength of soils could be developed, it could help engineers decide whether a soil is resistant to erosion by completing a common direct shear test.

8.0 SCOUR MEASUREMENT RESULTS

This investigation included a two-part data collection strategy for pier scour and included continuous and episodic data collection. As detailed in Section 6.3, episodic measurements were taken utilizing a wire-weight gauge and continuous monitoring was performed with a microsounder and data collection system. Episodic data collection began June 27, 2008 and ended October 15, 2010. Continuous monitoring started July 11, 2008 and ended November 30, 2010. A total of 79 episodic measurements from eleven sites (Table 8.1) and more than 40 months (total) of continuous data from three different sites were collected during the project. In total, seven episodic measurements resulted in measureable pier scour. Scour depths ranged from 0.7 to 1.5ft., with the maximum return period corresponding to a seven-year flood event (Table 8.2). No measureable scour events occurred at the continuous scour monitoring locations. Short descriptions of the episodic measured scour events (Section 8.1) organized by location are in subsequent sections with similar data for all measurements are available in Appendix 8A. Section 8.2 details the continuous monitoring for this investigation.

Table 8.1 Episodic Scour Measurement Locations

Site Location	Number of Data Sets
Grand River at Lansing	10
Raisin River in Adrian	7
Flint River at M-15	12
Cass River at M-15	6
Pine River at Lumberjack Road (North)	6
Pine River at Lumberjack Road (Middle)	6
Pine River at Lumberjack Road (South)	5
Rogue River Edgerton Road (near US 131)	5
Thornapple River at M-43 in Hastings	8
Thornapple River at Mckeown Road	8
Pigeon River at US-131	6

Table 8.2 Episodic measurements that resulted in discernable pier scour

Location	Dates of Survey	Pier ID #	Scour Depth (ft)	Event Return Interval (yr)
Pine River at Lumberjack Road (North)	April 22 & 28, 2009	1	1.2	3
Pine River at Lumberjack Road (South)	April 22 & 28, 2009	1 (south pier)	0.7	3
Pine River at Lumberjack Road (South)	April 22 & 28, 2009	2 (north pier)	0.8	3
Thornapple River at M-43	March 11 & 15, 2010	1 (south pier)	0.8	2
Thornapple River at Mckeown Road	March 11 & 15, 2010	1	0.9	2
Pigeon River at U.S.-131	March 12 & 29, 2009	1	1.5	7

8.1 Episodic Measurements

8.1.1 Pigeon River

The Pigeon River at U.S.-131 represents an ungauged location with vertical control being referenced to an arbitrary benchmark near the top of the concrete guardrail of the bridge. The elevation of the concrete wall and the zero point for wire-weight measurements is 1000.39ft. However, as is the case with all measurements, only the relative difference between measurements is important for computations of scour. The first episodic measurement on the Pigeon River was during a seven-year flood (March 12, 2009) and occurred before a baseline cross-section was taken for this location. However, subsequent scour measurements (March 29, 2009) indicate the river bed at higher elevations. A comparison of bed elevations between the two events yields an estimate scour of 1.5ft. (Figure 8.1). Later measurements, all made during relatively low flow conditions, indicate a one-foot range in bed elevation adjustment (Figure 8.2). This range of normal bed adjustment suggests scour depth associated with the March event could be as low as 0.5 ft. However, since the April 29, 2009 measurement is temporally the closest to the March 12, 2009 measurement (and to provide a worst case scenario for later equation modification), the 1.5-ft. estimate of scour depth was used in the analysis. The hydrograph for the Pigeon River is shown in Figure 8.3 with time of episodic measurements marked as triangles. Figure 8.4 shows the velocity contours for the episodic measurement on April 29, 2009. The episodic measurement on March 12, 2009 was made prior to acquisition of the ADCP and no velocity contours are available.

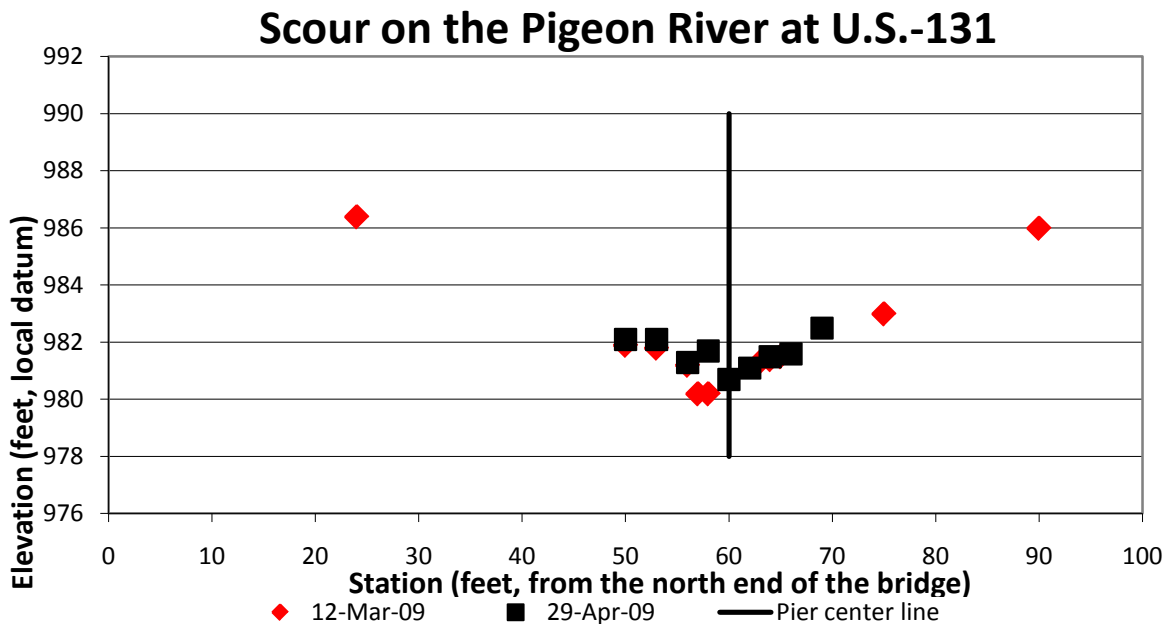


Figure 8.1 Measured bed elevation on the Pigeon River during 7 year return event.

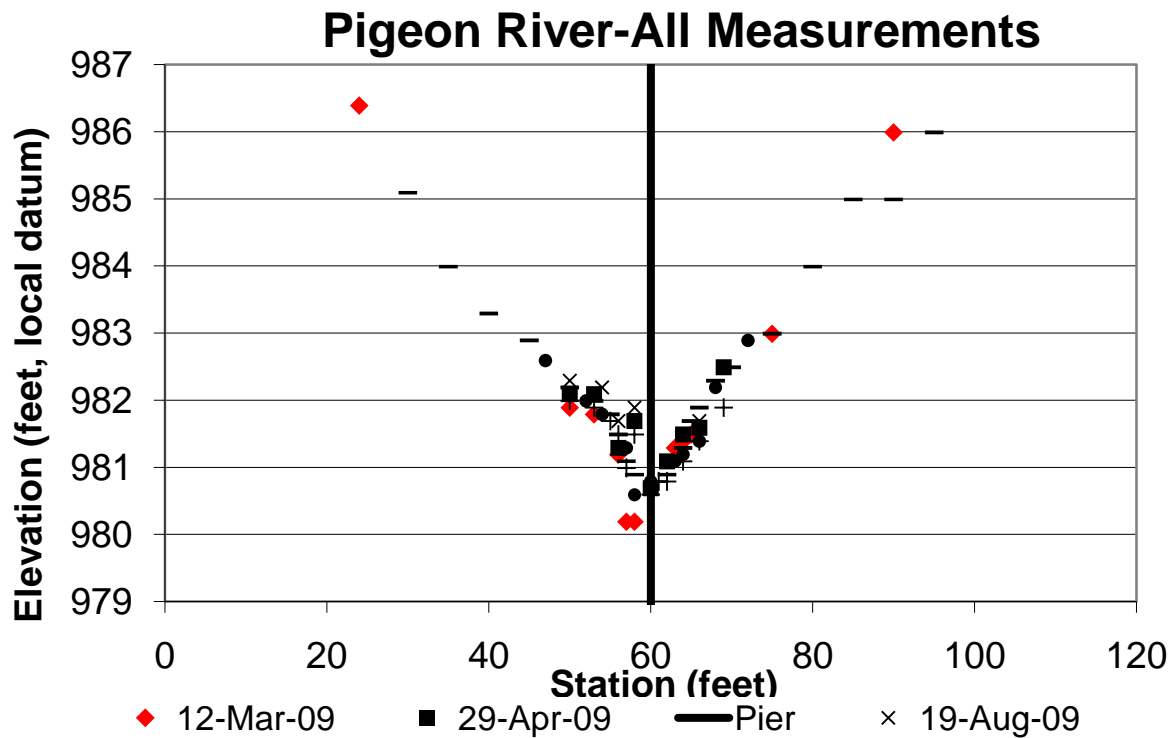


Figure 8.2 All bed elevation measurements on the upstream side of the Pigeon River at U.S.-131

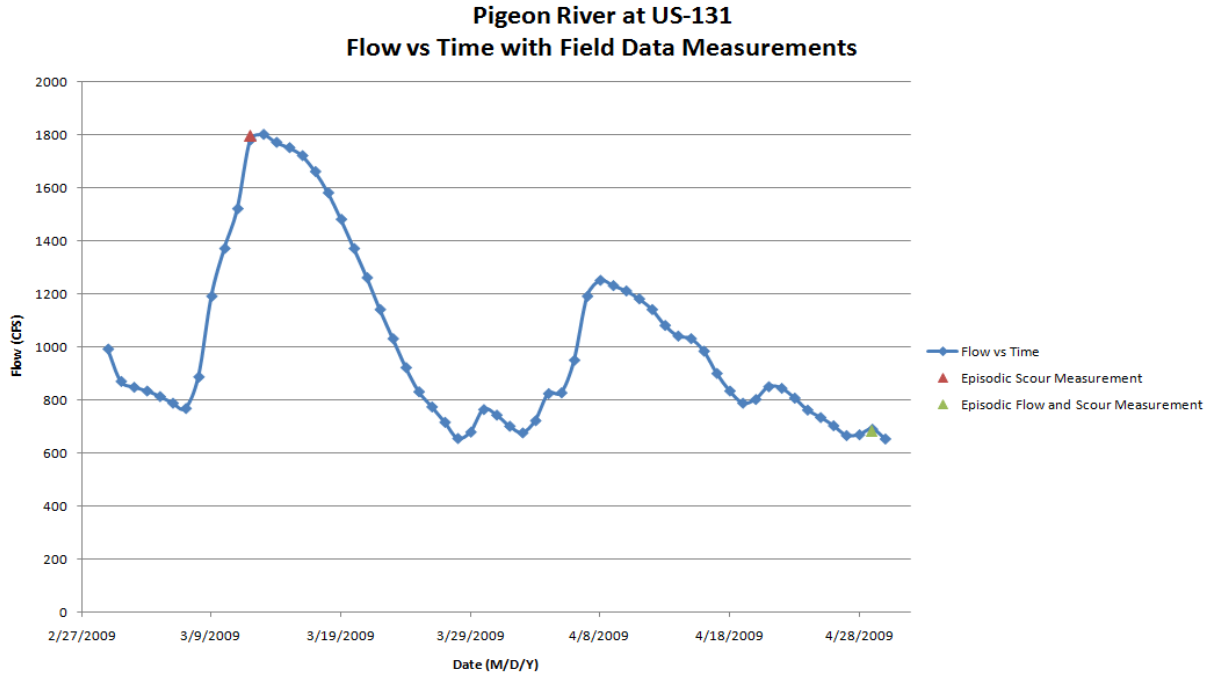


Figure 8.3 Pigeon River hydrograph at US-131 (USGS data) with time of measurement and associated discharge of depicted as triangles

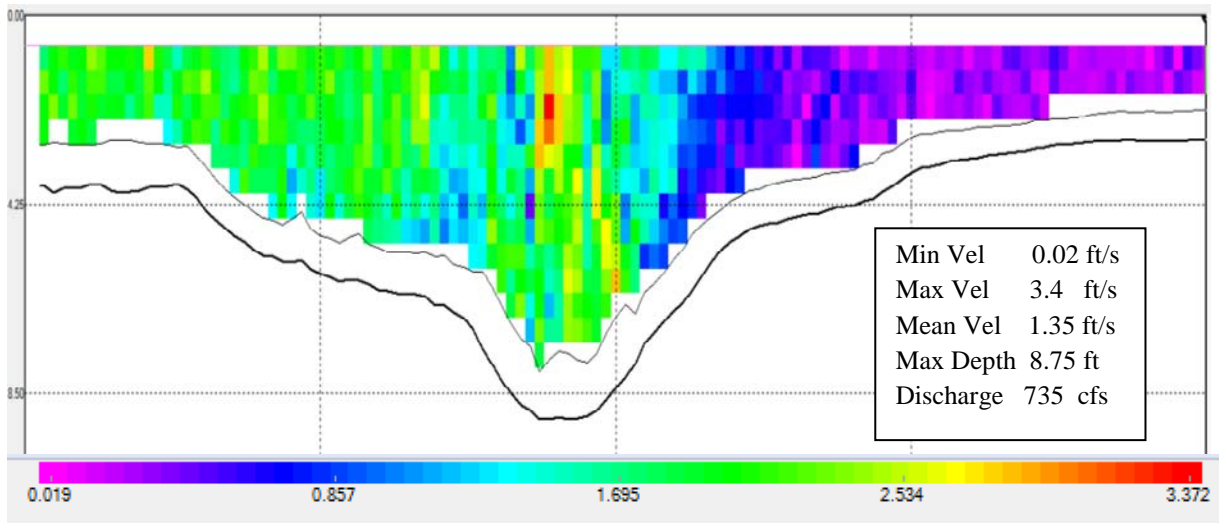


Figure 8.4 Velocity contours (ft/sec) for the Pigeon River at US-131.

8.1.2 Thornapple River at M-43

The Thornapple River at M-43 north of Hastings, Michigan, is an ungauged location. However, a USGS real-time gauge is located about four miles upstream and provides discharge information for this location. Eight episodic measurements were collected at this location with

four occurring during elevated discharges. The maximum flow (reported at the upstream gauge) during monitoring at this location was 2,350 cfs (March 15, 2010) and corresponds with a two-year return period. The gauge recorded a similar flow on May 1, 2009 (2,250 cfs). Measurements indicate 0.8ft. and 0.7ft. of scour, respectively, during these events (Figure 8.5). Figures 8.6 and 8.7 indicate when episodic measurements were conducted (time of measurement and magnitude of the discharge at the bridge are marked as triangles) relative to the peak discharge event. Velocity contours associated with the episodic measurements are shown in Figures 8.8, 8.9, and 8.10. These measurements show an increase in average cross section velocity of 1.5 ft/s. The ADCP recorded a total discharge of 2,550 cfs which is similar to the upstream gauge-recorded discharge of 2,270 cfs (Figure 8.7).

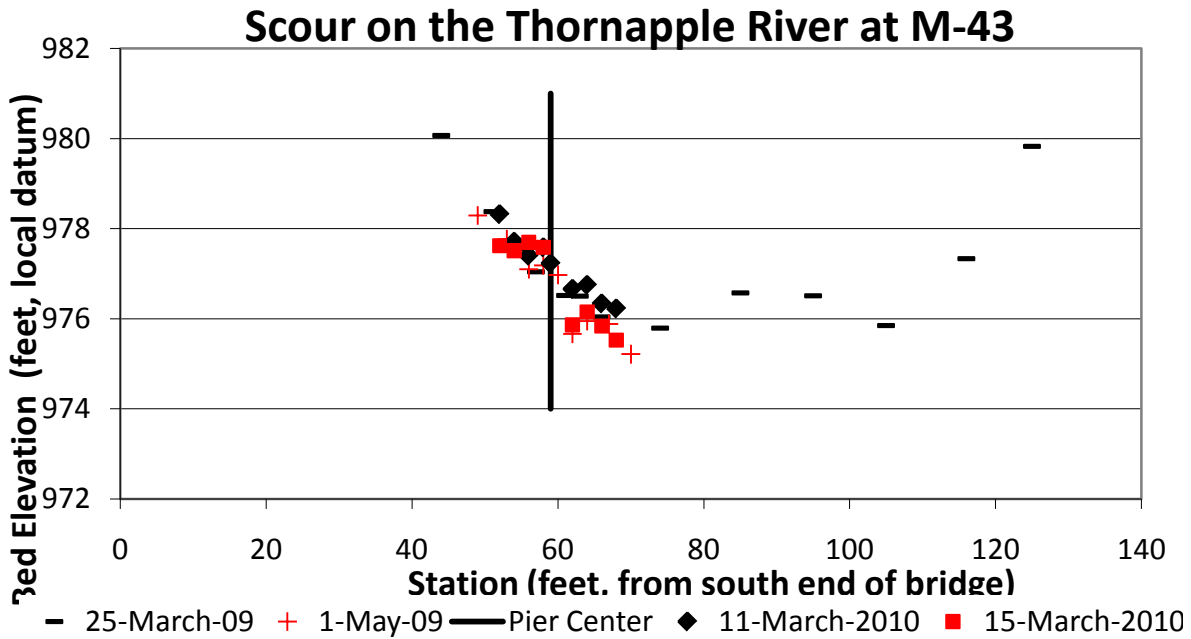


Figure 8.5 Measured bed elevation on the Thornapple River at M-43 during 2 year return event

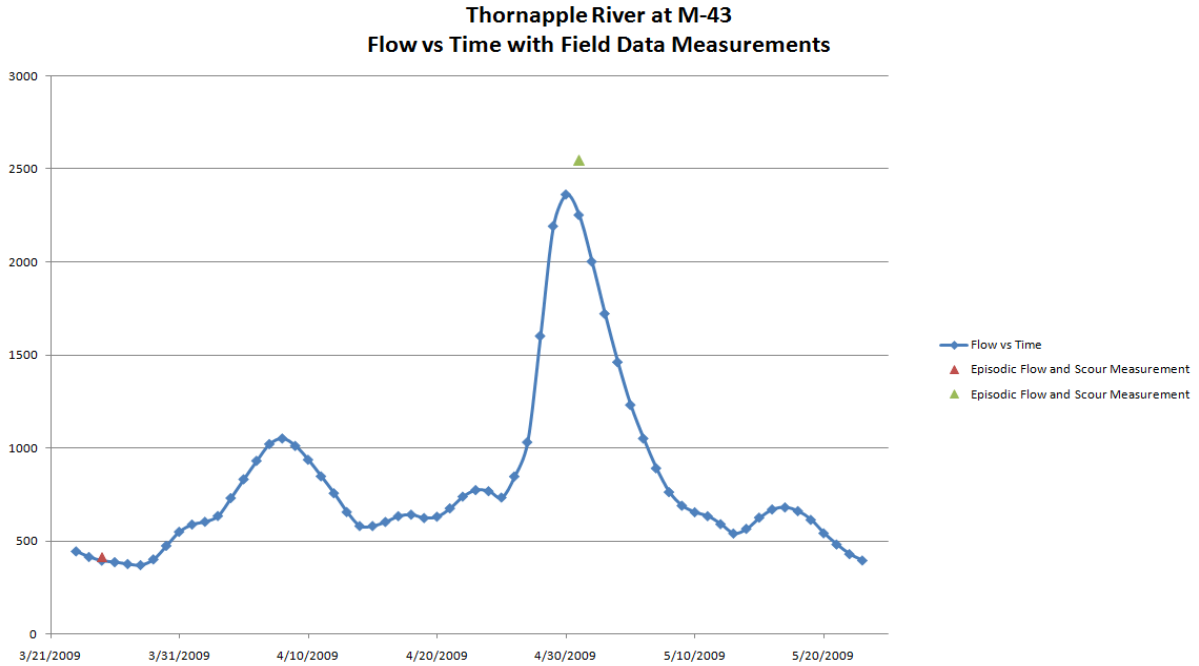


Figure 8.6 Thornapple River hydrograph at M-43 Hydrograph (USGS data) with time of measurement and associated discharge of depicted as triangles

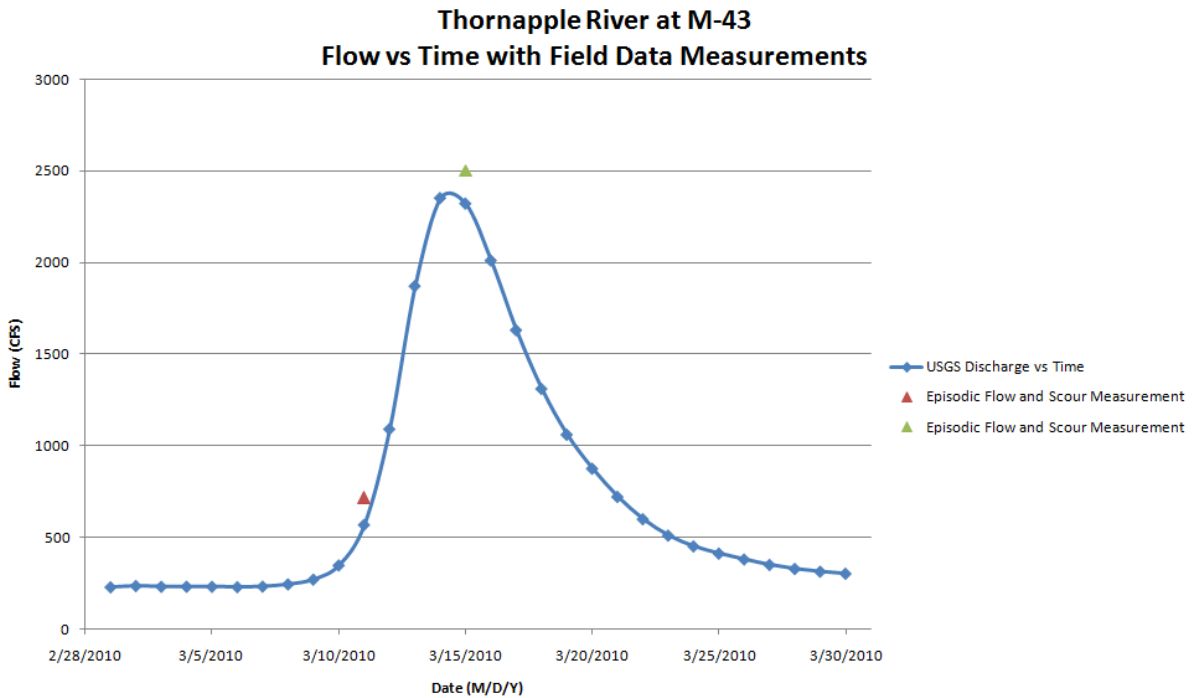


Figure 8.7 Thornapple River hydrograph at M-43 Hydrograph (USGS data) with time of measurement and associated discharge of depicted as triangles

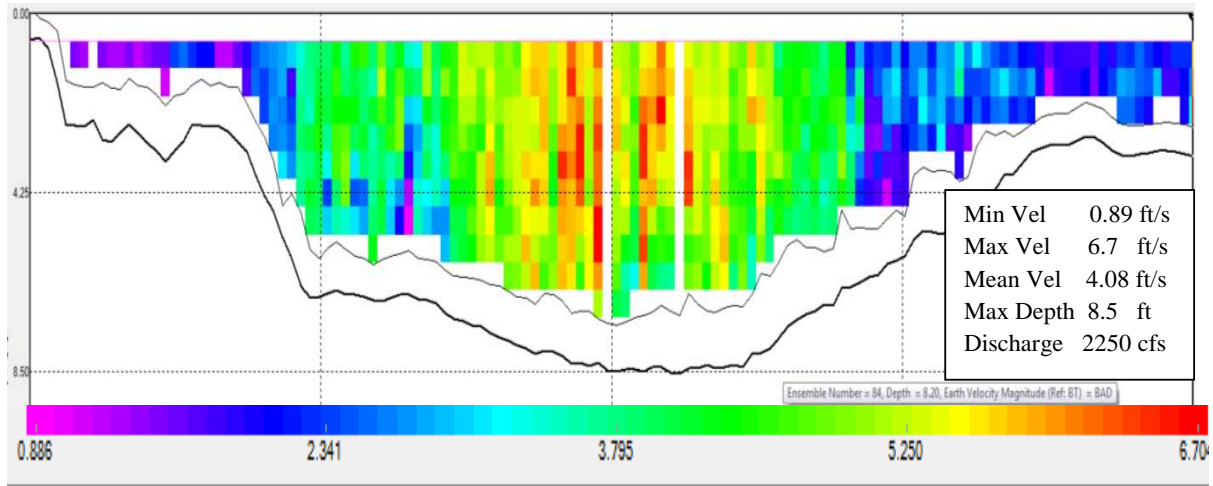


Figure 8.8 Velocity contours (ft/sec) for the Thornapple River at M-42 5/1/2009

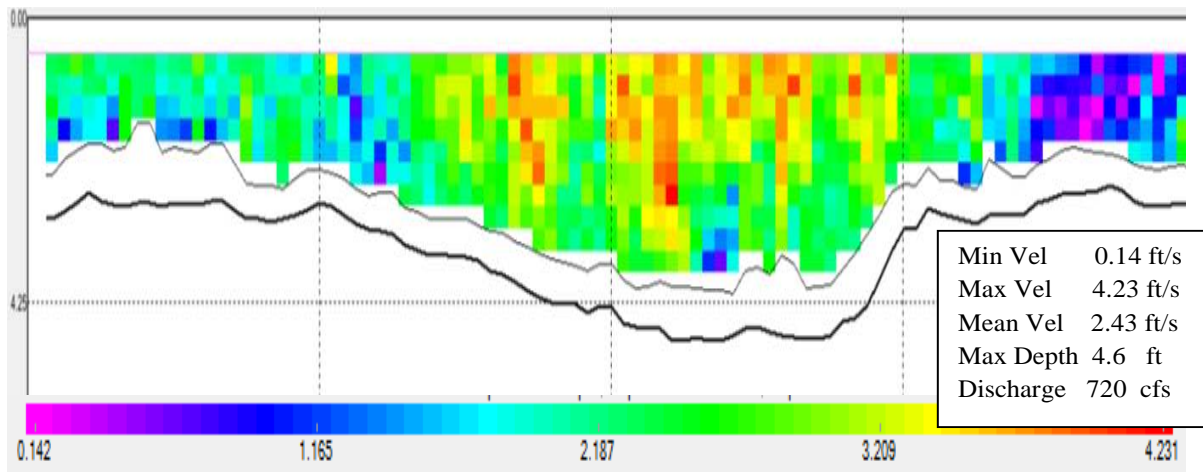


Figure 8.9 Velocity contours (ft/sec) for the Thornapple River at M-43 3/11/2010

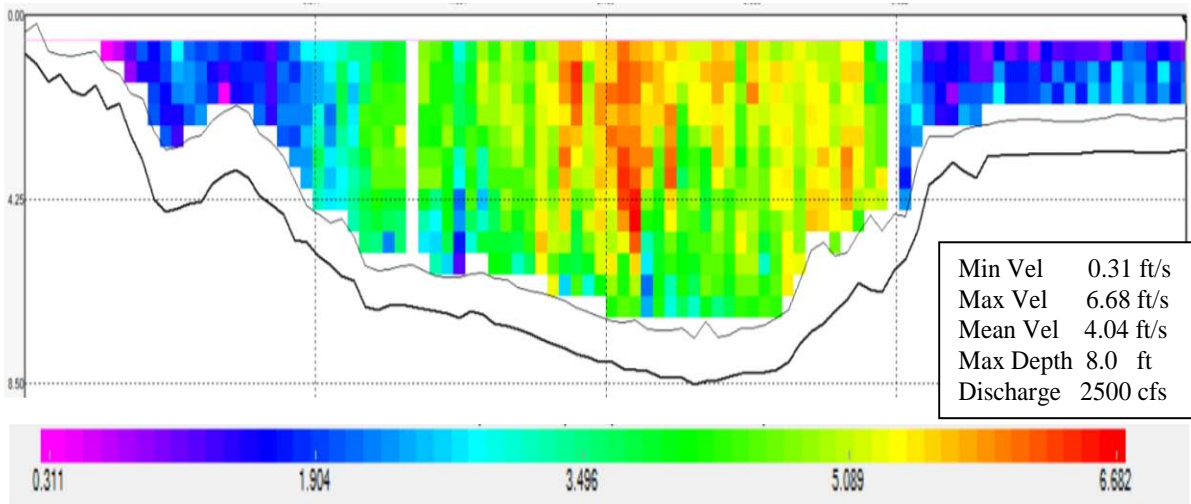


Figure 8.10 Velocity contours (ft/sec) for the Thornapple River at M-43 3/15/2010

8.1.3 Thornapple River at McKeown Road

The Thornapple River at McKeown Road has a real-time USGS gauge. Eight episodic measurements were taken at this site including four during elevated discharges. The largest flow recorded during the monitoring period had a two-year return period which occurred twice. The two major differences between this site and the M-43 location are debris on the pier and the number of measured scour events. This location had significant debris on the pier during the entire monitoring period. Measurements at some profile stations were not obtainable depending on debris location on the day of the measurement. The debris field likely contributed to the overall degradation of the bed in the vicinity of the pier and maximum measured scour at this location was closer to the edge of the debris pile. While debris likely contributed to the overall degradation of the bed, the exact amount of scour attributed to the pier geometry versus the debris field cannot be determined. The maximum measured scour at this location was 0.9ft. (Figure 8.11). Figure 8.12 provides the USGS hydrograph associated with this measurement with the time of the measurement and the local discharge indicated as triangles. Finally, Figure 8.13 and Figure 8.14 are the ADCP velocity contours that provided the discharge.

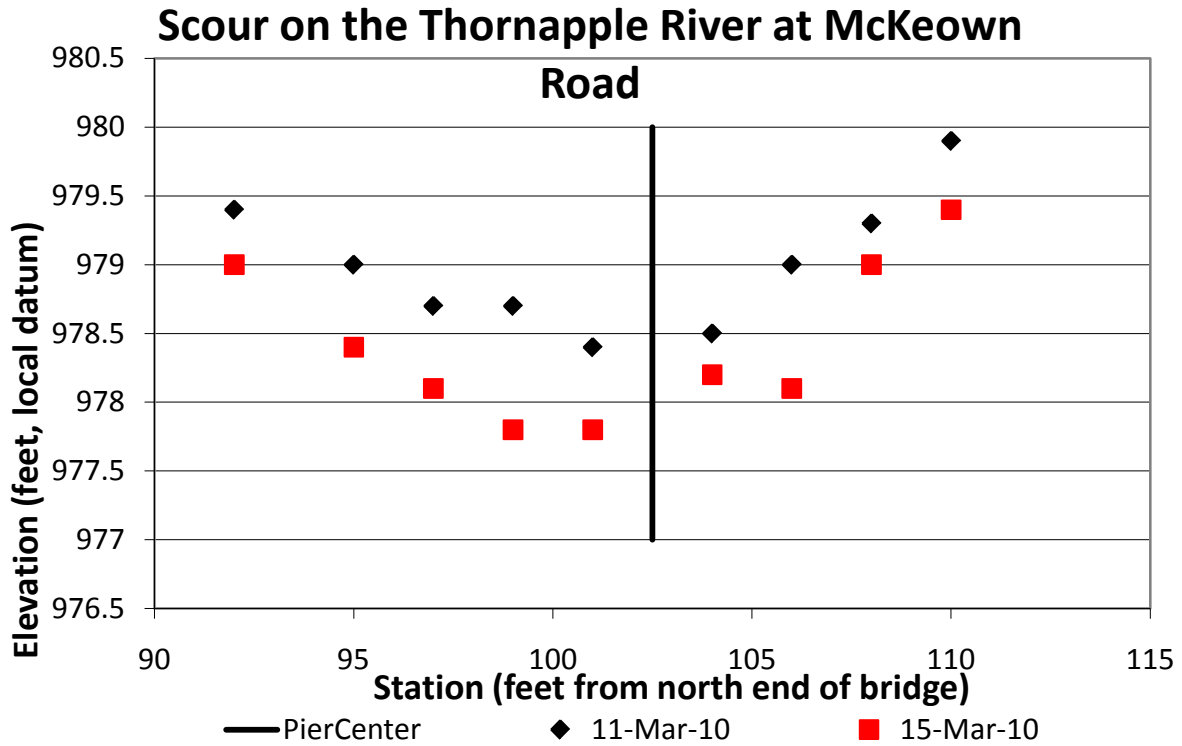


Figure 8.11 Measured bed elevation on the Thornapple River at McKeown Road during 2 year return event

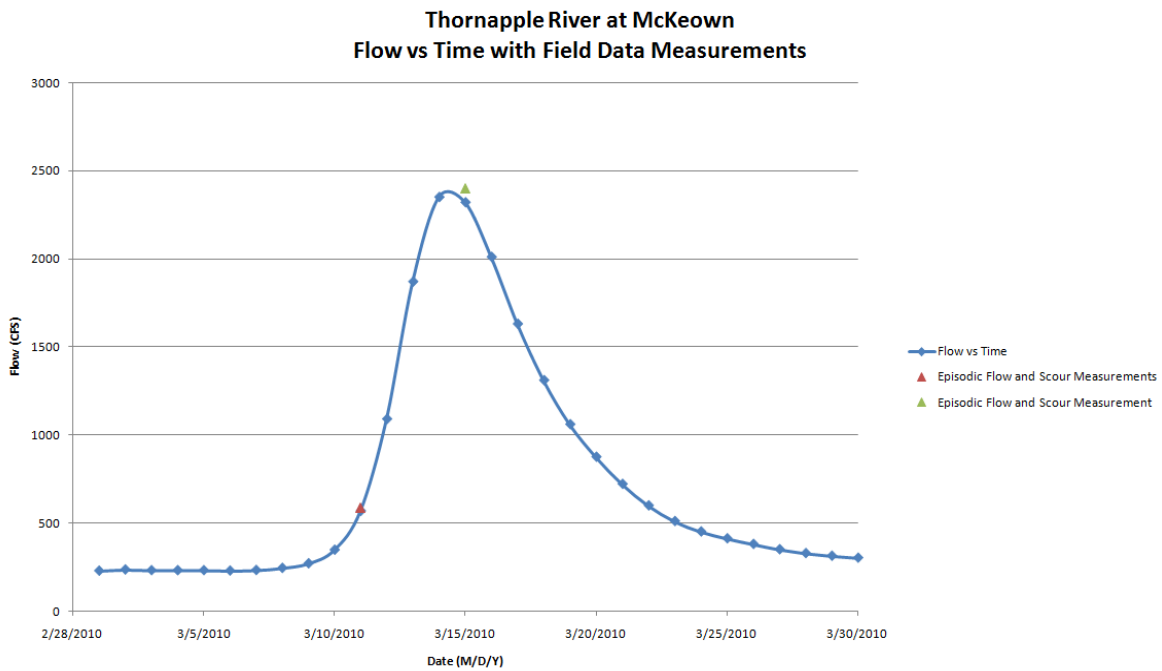


Figure 8.12 Thornapple River hydrograph at McKeown (USGS data) with time of measurement and associated discharge depicted as triangles.

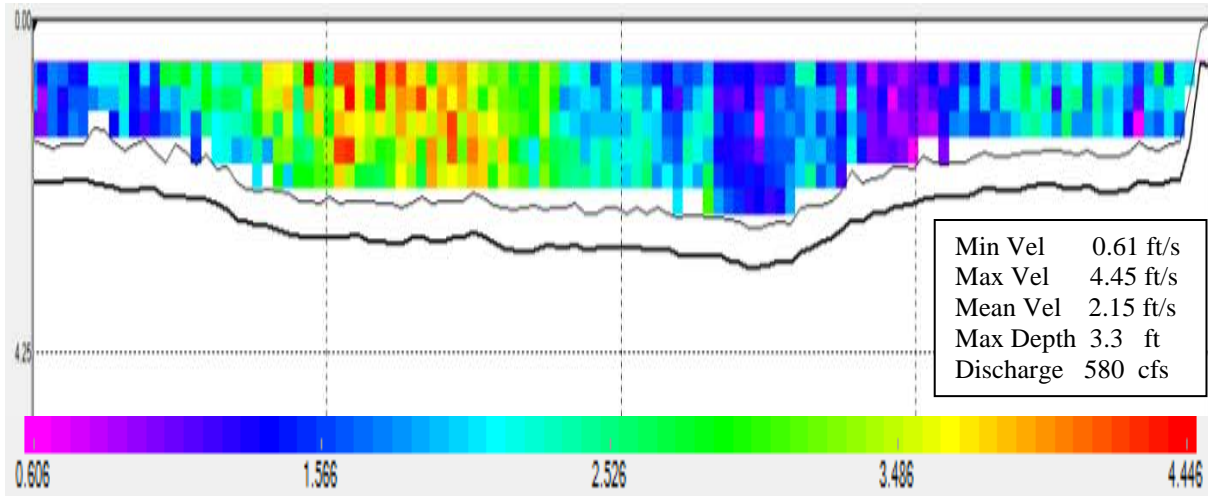


Figure 8.13 Velocity contours (ft/sec) for the Thornapple River 3/11/2010

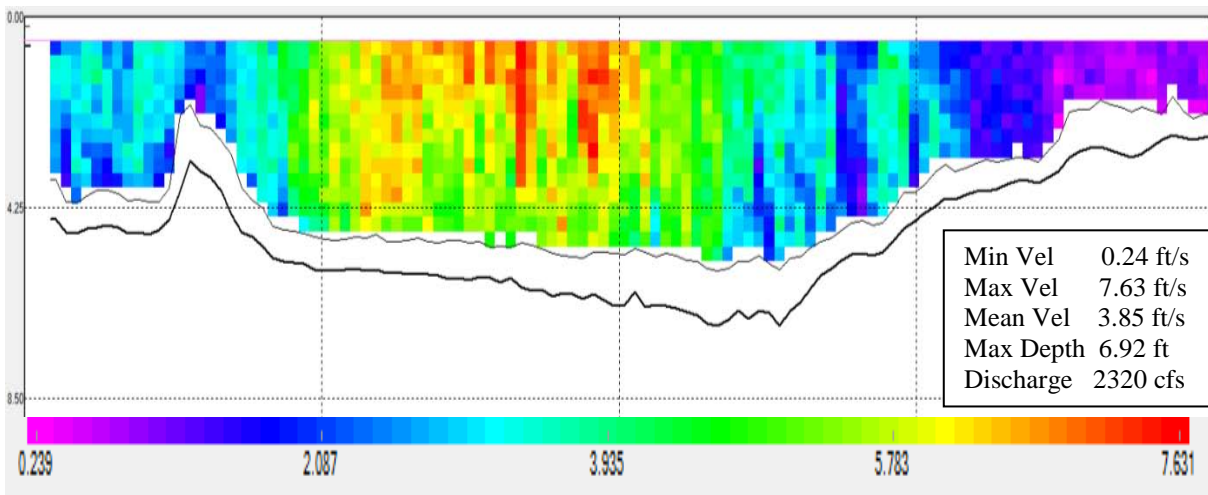


Figure 8.14 Velocity contours (ft/sec) for the Thornapple River 3/15/2010

8.1.4 Pine River at Lumberjack Road

The Lumberjack Road crosses the Pine River in western Gratiot County at three locations. The sites are referred to as the North (most upstream), Middle and South crossings. The nearest real-time USGS gauge is several miles downstream, near Alma, Michigan. ADCP measurements made on April 22, 2009 indicate a 27% increase in flow from the northern crossing to the southern crossing. A similar increase was recorded on April 28, 2009 with an increase of 32% between the north and south crossings. A total of 17 episodic measurements

were completed at these three bridge locations (six measurements at the North and Middle locations and five measurements at the South location with extensive ice at the southern-most crossing in January 2009, prevented data collection at that time). Three measurements were collected from these sites at periods of elevated flow that provided measureable pier scour - one at the North crossing and two at the South crossing. All three scour measurements were collected during the same event which was the largest event observed at this location during the monitoring period (four-year return period). However, the discharge associated with this event will be less at the Lumberjack Road crossings than at the gauge in Alma which is downstream.

The North location is just north of M-46 at Lumberjack Park. A large, well developed, mid-channel bar is located approximately 70ft. upstream of the bridge (Figure 8.15). This bar influences the channel morphology near the bridge pier and the channel has two thalwegs (one around each side of the pier) with the high point between the two coincident with the bridge pier (Figure 8.16). During the scour event on April 28, 2009, 1.2ft. of scour was measured (Figure 8.16) as determined by the difference in bed elevation between the two bed profiles. Figure 8.17 provides the hydrograph associated with this event and where the measurements were made relative to the peak discharge. At this location, the USGS gauge is not coincident with the study site so measured discharge is lower than USGS-recorded discharge.



Figure 8.15 Mid-channel bar upstream of Pine River, north.

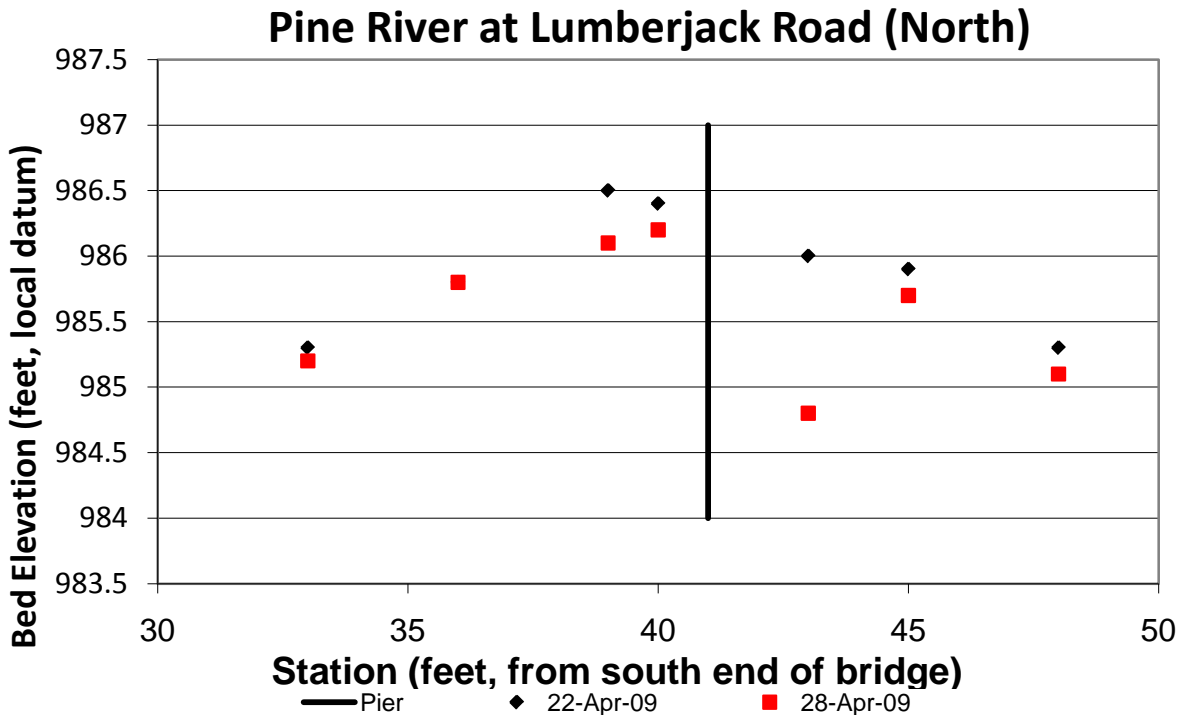


Figure 8.16 Measured bed elevation on the Pine River (north) near Lumberjack during 3 year return event.

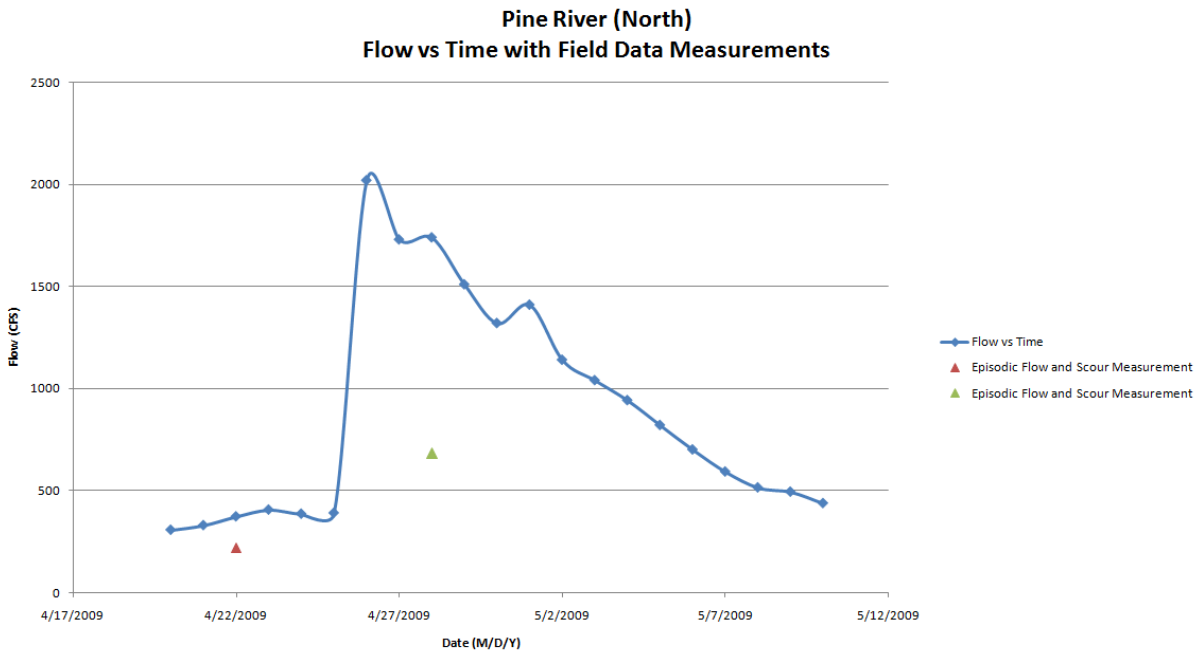


Figure 8.17 Pine River (north) hydrograph during 3 year return event with time of measurement and associated discharge depicted as triangles

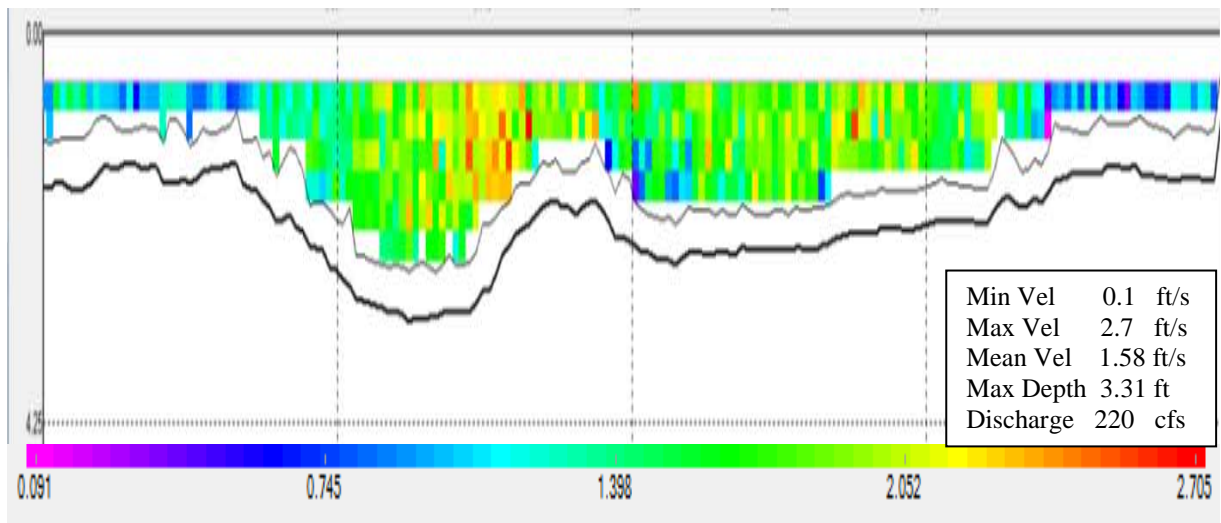


Figure 8.18 Velocity contours (ft/sec) for the Pine River (north) 4/22/2009

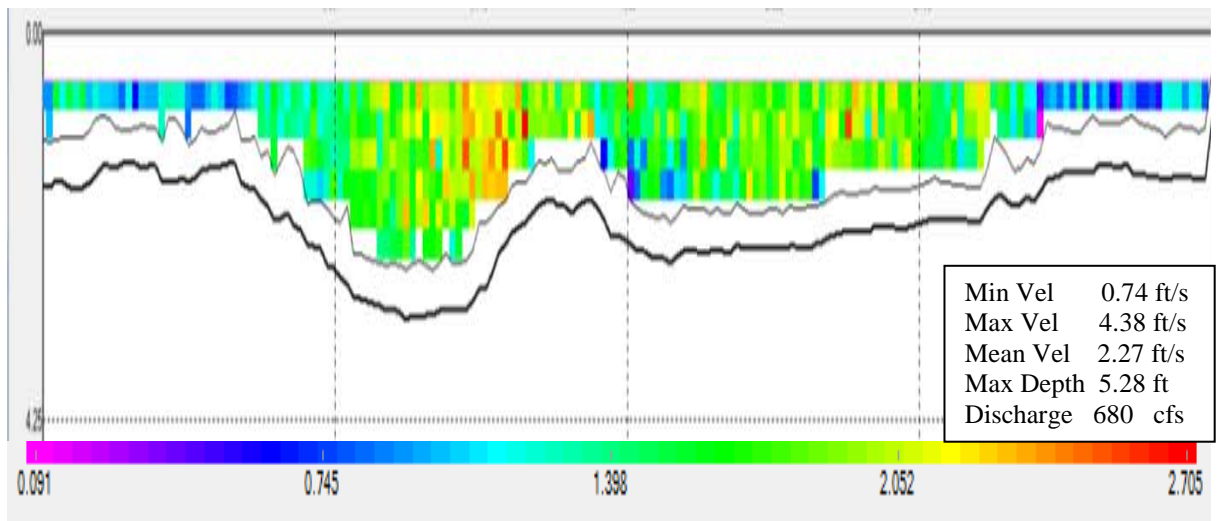


Figure 8.19 Velocity contours (ft/sec) for the Pine River (north) 4/28/2009

On April 29, 2009, two scour measurements, one measurement from each pier, were obtained from the Pine River South location. The far (north) pier in Figure 8.20 was covered with debris during the entire study and sometimes hampered data collection around this pier. However, on April 22 and 28, measurements were made at both piers revealing 0.8ft. of scour at the north pier and 0.7ft. of scour at the south pier (Figure 8.21). Figure 8.22 shows when the

episodic measurements were collected relative to the flow peak. Average velocity at this cross section increased from 0.9 ft/s on April 22, 2009 to 2.1 ft/s on April 28, 2009 (Figure 8.23 and Figure 8.24).



Figure 8.20 Pine River at Lumberjack Road (south) with debris pile on north pier.

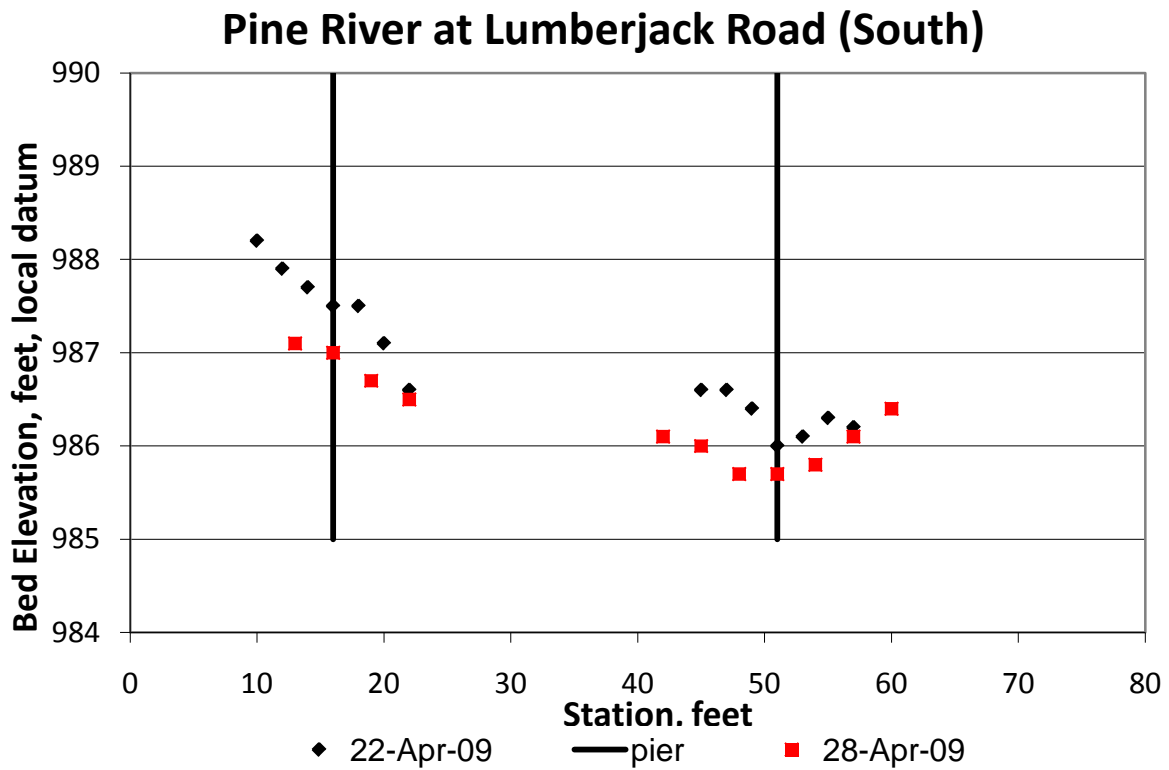


Figure 8.21 Measured bed elevation for Pine River (south) during 3 year return event.

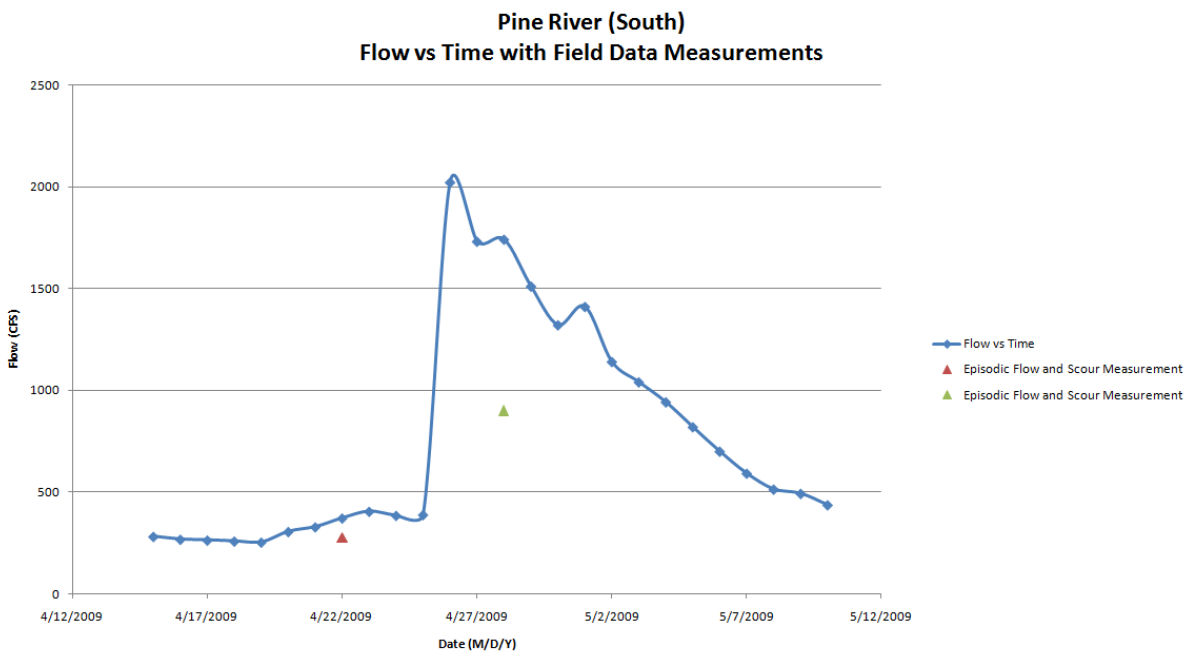


Figure 8.22 Pine River (south) hydrograph during 3 year return event with time of measurement and associated discharge of depicted as triangles

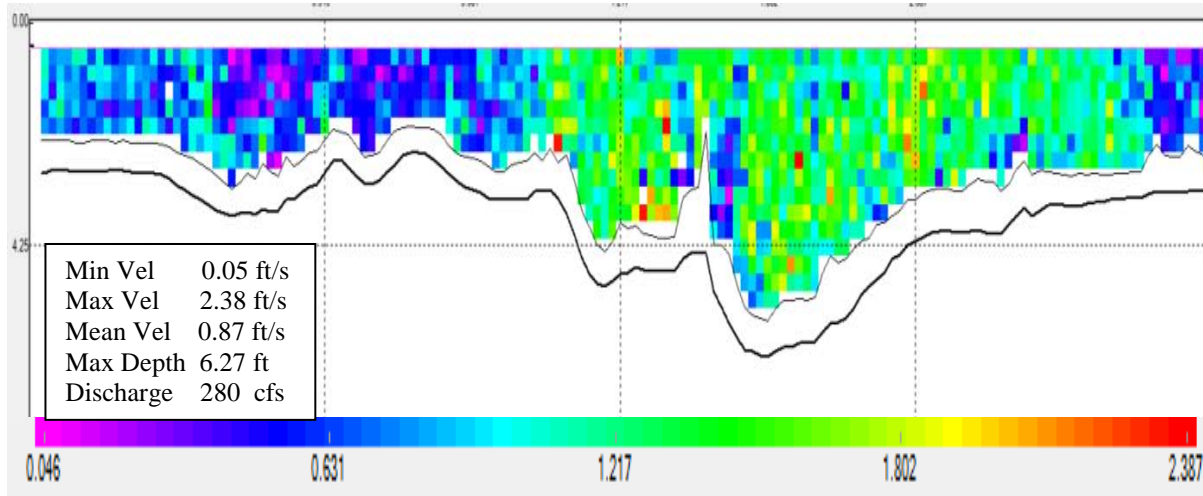


Figure 8.23 Velocity contours (ft/sec) for the Pine River (south) 4/22/2009

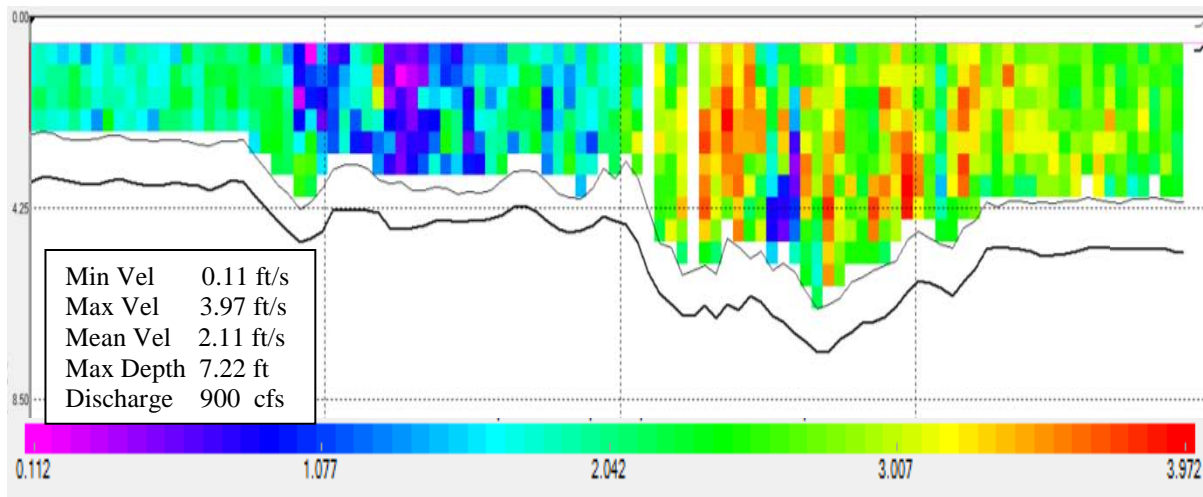


Figure 8.24 Velocity contours (ft/sec) for the Pine River (south) 4/28/2009

8.2 Continuous Measurements

Continuous measurements started in July 2008 on the Flint River at M-15 just north of the MDOT Transportation Service Center in Davison. The continuous monitoring program was piloted at this location until the spring of 2009. During this time, the monitoring equipment was field-tested for consistency and accuracy of data collection. The study team was specifically interested in testing the power supply system and the system's ability to handle the physical environment. The data telemetry and sensor suite had previously undergone successful laboratory testing.

The most valuable lesson learned from the pilot program concerned equipment deployment and placement. The site characteristics, presence of USGS monitoring and safe working conditions made the Flint River a desirable location for the study. However, equipment placement was a challenge. The easiest, most cost efficient way to position the equipment was beneath the bridge deck. The study team found two potential problems with this deployment. First, a pressure flow event would submerge the data logger, telemetry and power systems which would ruin the equipment. The second risk was due to site geometry: the equipment was not accessible during a flood. However, the team felt both of these risks were worth taking in order to collect meaningful scour measurements.

During the first season of measurement a fuse blew in the data logger (January 2009). Several attempts were made to fix the problem; however, water levels were too high to safely access the data logger until May of 2009. During the monitoring period, a seven-year event occurred which was not captured with continuous monitoring because of equipment malfunction. However, it was captured using episodic measurement. Future installations of continuous monitoring equipment were deployed in locations where the entire system, except for the sensor suite, was accessible regardless of the weather or flow condition.

8.2.1 Flint River

The Flint River data record covers the period from July 2008 to October 2010 with the only significant outage from the period of January 2009 through May 2009. Data exists at either hourly or every-other-hour intervals. Data collection was reduced to every other hour in the winter months due to the reduced hours of daylight available to charge the battery. However, we found that at this sampling interval led to maintenance-free operation from May 2009 through 31 October 2010. The largest event captured by the continuous monitoring system at this location occurred in December 2008. The total flow was 3,060 cfs which corresponds to a three-year event (Figure 8.25).

Flint River Continuous Scour Monitoring

Maximum Recorded Event, December 2008 to January 2009

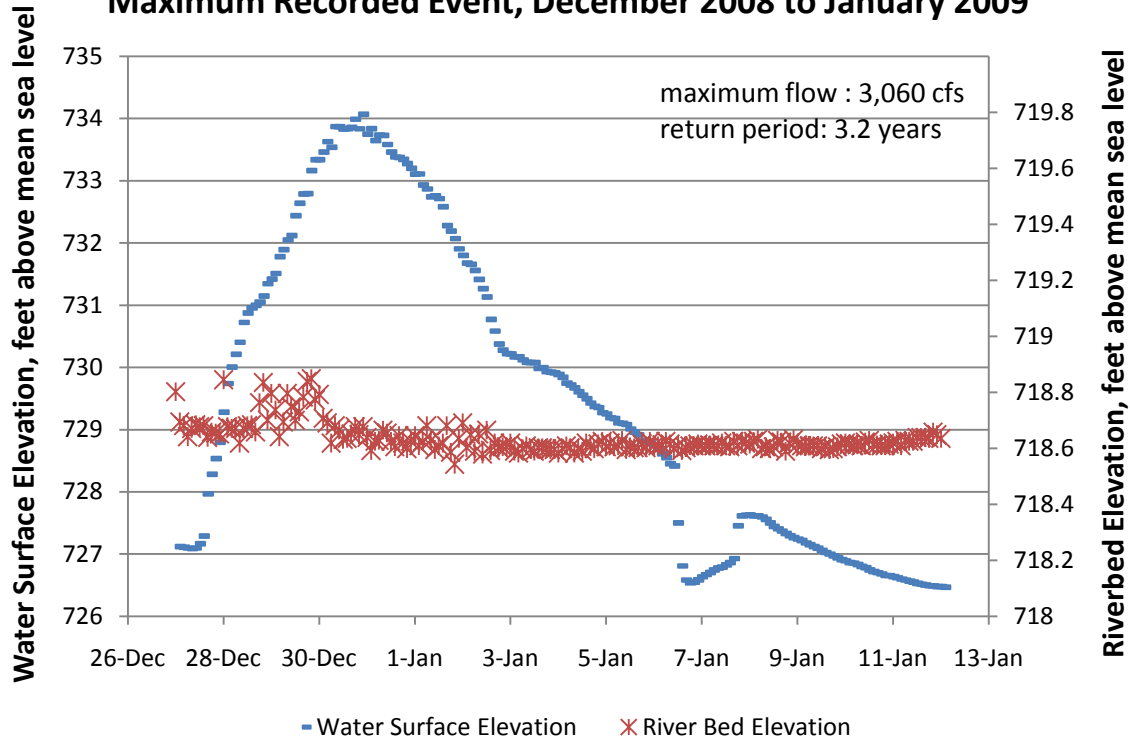


Figure 8.25 Bed elevation measured during maximum recorded flow event

8.2.2 Grand River

Continuous monitoring on the Grand River at M-99 was installed on July 28 2009. Data runs through November 30 2010. The piers on the upstream side of this bridge extend several feet beyond the bridge deck. This extra length of pier was used to mount the data collection platform (Figure 8.26). With the bulk of the equipment mounted on the side of the bridge and the extra length of the pier, the system components are accessible from above the bridge rather than below the bridge, as is the case with the Flint River installation (Figure 8.27).



Figure 8.26 Extended pier with data collection platform on the upstream side of bridge on M-99 over the Grand River

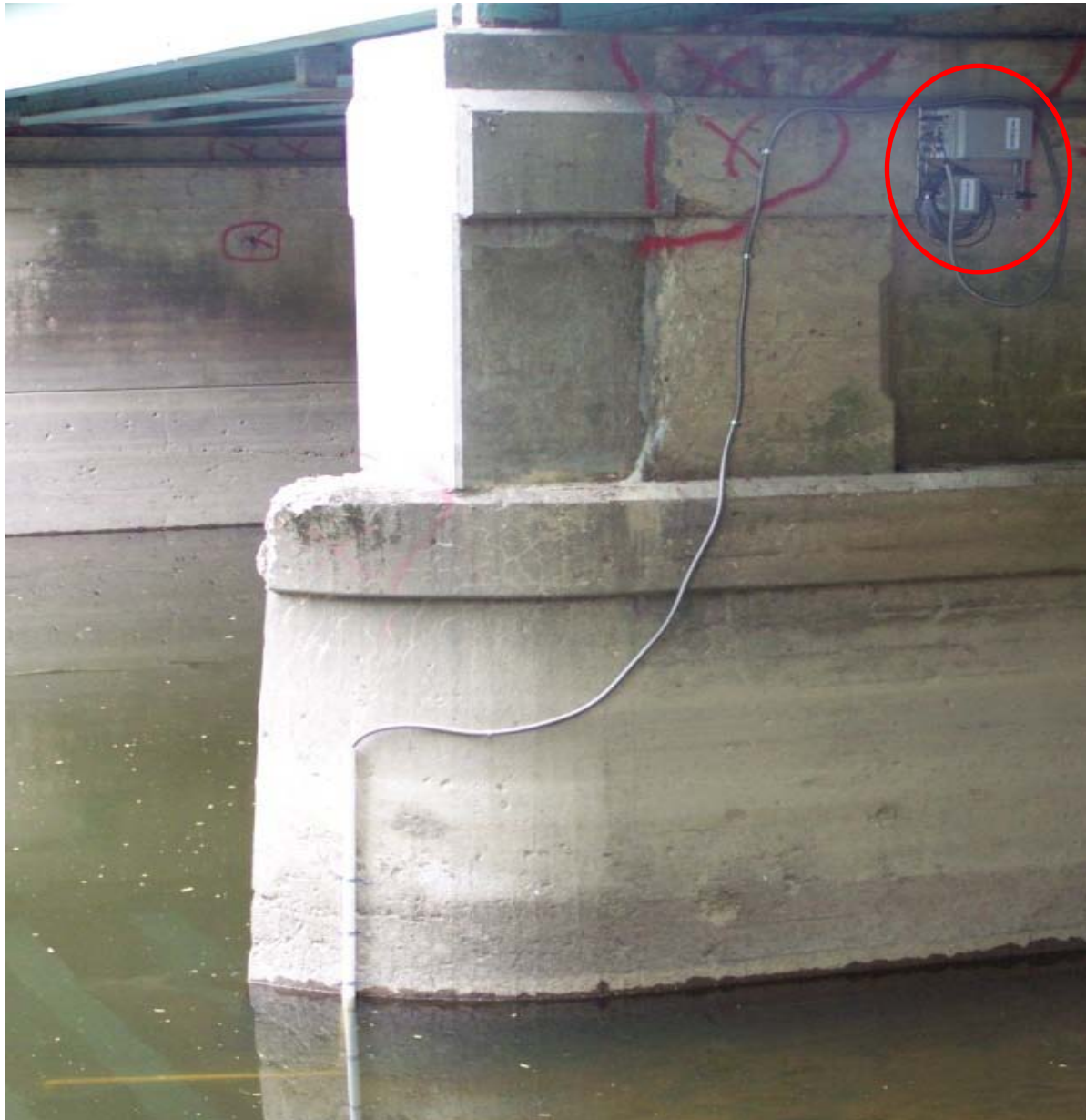


Figure 8.27 Continuous monitoring on the Flint, setup under the bridge deck and inaccessible during high flows

The largest event during the monitoring period occurred in March 2009. It was a three-year event with a total flow approximately 6,500 cfs. The largest event continuously captured at the Grand River location was a 1.5-year event with a flow of 4,160 cfs which occurred on March 14 2010 (Figure 8.28). While the variability in the elevation of the river bed seems to increase near the peak of the hydrograph, but no appreciable scour was measured. However, this increase

in variability associated with the peak of the hydrograph indicates that the method will record scour for larger return period events.

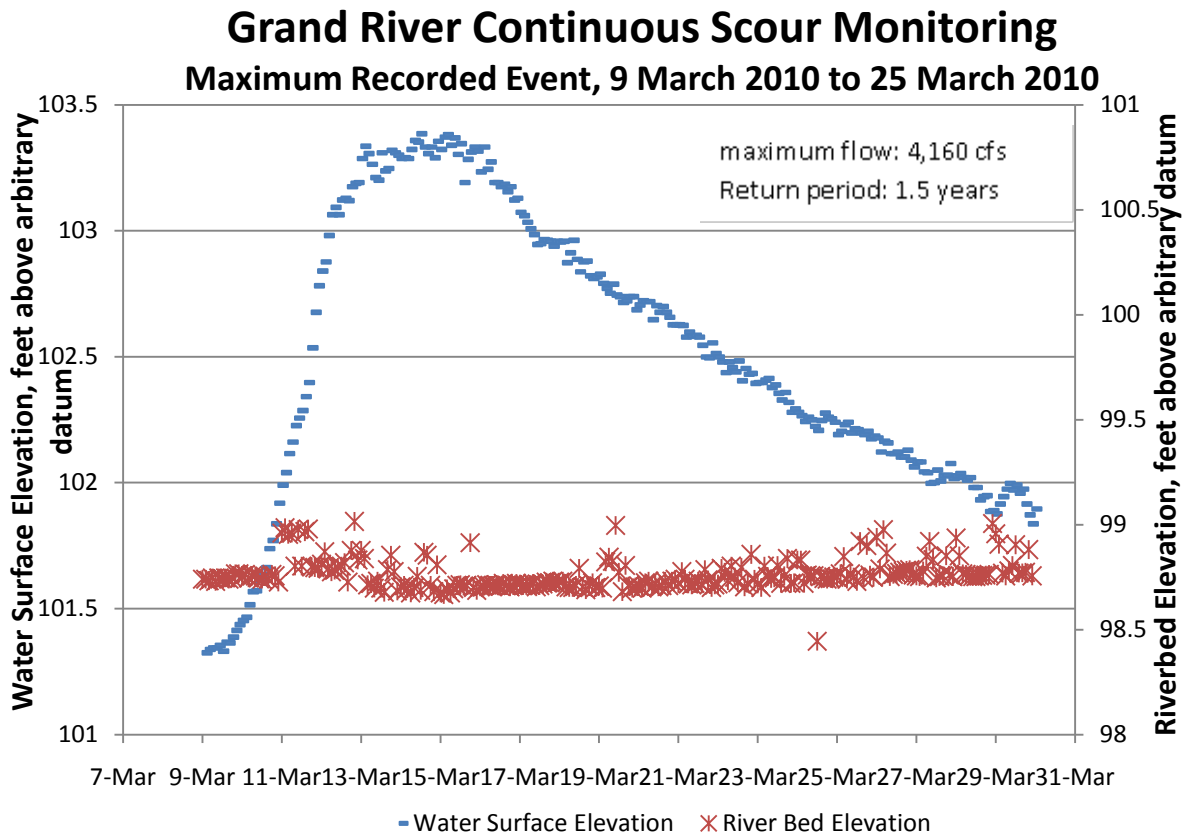


Figure 8.28 Bed elevation measured during maximum recorded flow event

8.2.3 Paw Paw River

The Paw Paw River at Coloma Road was monitored with continuous data collection only. The piers extend 12 to 15ft. in both upstream and downstream directions. The extended pier lengths made useful episodic measurements at this location impossible since the maximum scour would take place near the nose of the pier. This site was fit with continuous monitoring equipment on May 28, 2009 and worked with minimal interruptions and maintenance. The largest event occurred in October 2009 and represented a two-year event with a discharge of 1,410 cfs (Figure 8.29). No appreciable scour was measured during this event.

Paw Paw River Continuous Scour Monitoring Maximum Recorded Event, October and November 2009

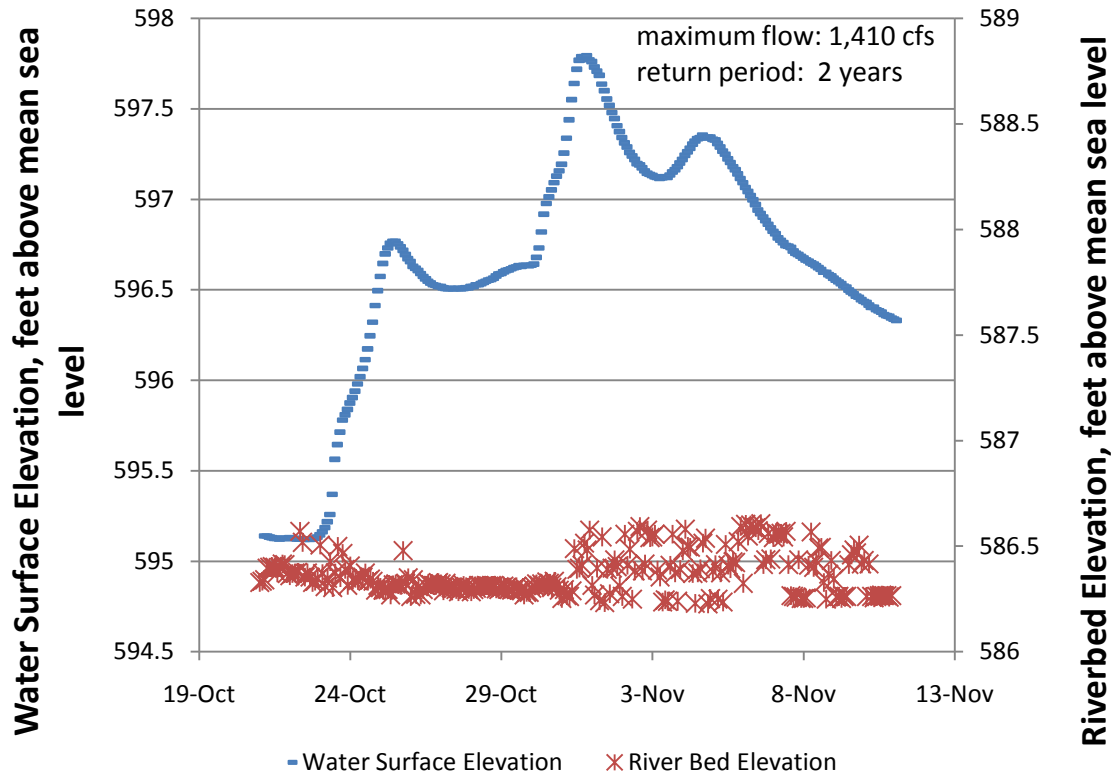


Figure 8.29 Bed elevation measured during maximum recorded flow event

9.0 HEC-18 EQUATION MODIFICATION

The Federal Highway Administration requires engineers to design bridges over waterways to withstand the effects of a 500-year super flood or a series of smaller floods if the series simulation causes greater scour depths (Richardson & Davis, 2001). The Federal Highway Administration issued Hydraulic Engineering Circulars (HEC) 18 (Richardson & Davis, 2001), HEC-20 (Lagasse et al., 2001) and HEC-23 (Lagasse et al., 2000) to provide guidance for local scour determinations. HEC-18 provides specific guidance regarding the prediction of local pier scour depth primarily through the empirically derived Equation 9.1 (Richardson & Davis, 2001):

$$\frac{y_s}{y_1} = 2.0K_1K_2K_3K_4\left(\frac{a}{y_1}\right)^{0.65} Fr^{0.43} \quad (\text{Equation 9.1})$$

where y_s is the scour depth, a is the pier width, K_1 is the correction factor for pier nose shape, K_2 is the correction factor for the angle of attack (the angle at which the flow impinges upon the pier), K_3 is the correction factor for bed condition (plane bed, dune, ripple), K_4 is the correction factor for armoring by bed material size, y_1 is the flow depth directly upstream of the pier and Fr is the Froude number. The remainder of this work refers to (a/y_1) as the normalized pier width (NPW). Equation 9.1 represents the state of the practice in most states including Michigan (see Chapter 4) and is included in one-dimensional hydraulic models such as the Hydraulic Engineering Center-River Analysis System (Brunner, 2008).

Attempts to improve fit and reduce uncertainty in commonly used scour prediction equations appeared in the 1990s when researchers, such as Johnson (1995) tried using field data to determine valid ranges for typical parameters. Johnson (1995) also compared several competing models based on computed bias in predictions. She concluded some equations were not fit for design purposes because they often under predict scour. Conversely, equations used for design purposes over predict with a large, positive bias leading to an improved design from a safety perspective, while unnecessarily increasing construction costs (Johnson, 1995).

For this effort, the National Bridge Scour Database (NBSD) was used in an attempt to improve the scour prediction capabilities of the HEC-18 local pier scour equation. The NBSD, last updated in 2004 and maintained by the U.S. Geologic Survey (USGS), provides data from 20 sites in eight states (Landers et al., 1996). Records were chosen for this analysis based on

completeness. For selection, a record must contain enough data to apply the current version of the HEC-18 scour equation. In an effort to reduce the amount of variance in the scour prediction, records were also restricted to live bed, non-cohesive sites.

The goal of this effort is to develop a family of equations similar in form to HEC-18, but with various exponents applied to the normalized pier width and Froude number. Currently, these exponents are fixed in HEC-18 and apply for all conditions. In this chapter, several pairs of exponents will be developed for a variety of situations that cover the same broad range of conditions the current HEC-18 equation covers. Specifically, this effort will develop two pairs of exponents (Case 1 and Case 2) applicable to live-bed scour where the median particle size is in the sand fraction, Equation 9.2. The choice between pairs of exponents will be determined by the value of the normalized pier width as determined by the parameters at the study site. Case 1 is defined as live-bed scour, median particle size in the sand fraction and a normalized pier width less than 0.3. Case 2 is defined the same as Case 1, but the normalized pier width ranges from 0.3 to 1.25. A normalized pier width of 0.3 was chosen because it represents the median value in the data set.

$$\frac{y_s}{y_1} = K \left(\frac{a}{y_1} \right)^{b_1} Fr^{b_2} \quad (\text{Equation 9.2})$$

The parameters in Equation 9.2 are defined the same as in Equation 9.1 where K is the collection of K_1 through K_4 and b_1 and b_2 are regression coefficients to be determined. The K values were assigned using the approach described in the HEC-18 Manual and varied from 0.99 to 4.92 for the records in this investigation.

9.1 Data Description

The first step in the data filtering process was to query the National Bridge Scour Database for live-bed scour occurring with the median grain size in the sand fraction. This yielded 148 records with enough data to apply HEC-18 equation. The queried records represent 20 unique sites from eight states (Alaska, Colorado, Georgia, Indiana, Louisiana, Missouri, Mississippi and Ohio). There were eleven records with a NPW greater than or equal to 1.25 which were removed from the dataset. It was decided by the research team that 11 records were

not sufficient to derive a third case ($NPW \geq 1.25$). Table 9.1 provides descriptive statistics from the remaining queried data.

Table 9.1: Descriptive statistics

Variable	Mean	Median	Standard Deviation	Min	Max
Normalized pier width	0.35	0.29	0.22	0.043	1.18
Froude	0.25	0.24	0.12	0.04	0.55
Median grain size (mm)	0.81	0.90	0.45	0.15	1.82

This analysis requires two datasets from the queried records: one set to derive and validate exponents for Case 1 (described above), and the other dataset to derive and validate exponents for Case 2. The median normalized pier width was determined and the values used to split the 137 records into two datasets. From Table 9.1, the median normalized pier width is 0.29 and rounded to 0.3 for this analysis. Currently, HEC-18 uses a special correction factor for wide piers which are defined by HEC as having normalized pier widths greater than 1.25. This criterion provides a natural upper bound for the normalized pier widths for Case 2. Analyses for Case 1 and Case 2 were performed with 71 and 66 records, respectively.

Ideally, regression equations are derived from one set of data and validated on a different set. This ensures the usefulness of the equation at locations not used in the deriving data. Therefore, each dataset was parsed into derivation and validation datasets for each case. If the resulting datasets (the 71 record dataset for Case 1 and the 66 record dataset for Case 2) were randomly split into derivation and validation data, site-specific processes in the derivation data would also be present in the validation data set and the resulting equations would have artificially high performance on the validation data. To ensure the family of equations does not rely on site-specific processes to predict scour, all records from the same site were placed into the validation datasets. For example, if a specific location contributes five records to a dataset and is chosen to contribute to the validation dataset, then all five records will be in the validation dataset. This method prevents the same site from simultaneously contributing records to both the derivation and validation datasets.

The process of splitting the data into derivation and validation data was repeated four times. For each trial, the sites or combination of sites, contributing records to the validation dataset changed. The process continued until each site was used in both the derivation and

validation datasets. This re-sampling technique ensured the equations developed with this process did not rely on the records chosen to be in the derivation and validation datasets.

In conclusion, a basic outline of the approach taken is as follows:

- Query the National Bridge Scour Database for appropriate records;
- Stratify data based on normalized pier width;
- Split the data into a deriving data set and a validation data set;
- Modify the HEC-18 equation through non-linear regression;
- Validate the revised equation.

9.2 Regression Types

In this effort, the HEC-18 pier scour equation was re-derived with nonlinear regression analysis. This process optimizes parameters to a user-defined functional form. The resulting parameters minimize the error between predicted and observed values through an ordinary least-squares procedure. This nonlinear regression yields a best-fit model that both under- and over-predicts scour. Therefore, an adjustment factor is applied to the best-fit equation to minimize the number of under-predictions. Two adjustment factors were considered in this study, a multiplicative adjustment as in the current HEC-18 equation and an additive adjustment as in the Froehlich Design Equation (Froehlich, 1988). Equation 9.3 (a) and 9.3 (b) provide the two forms of the adjusted equations examined in this study.

$$\frac{y_s}{y_1} = K \left(\frac{a}{y_1} \right)^{b_1} Fr^{b_2} * adjustment$$

(Equation 9.3 a)

$$\frac{y_s}{y_1} = K \left(\frac{a}{y_1} \right)^{b_1} Fr^{b_2} + adjustment$$

(Equation 9.3 b)

The adjustment factors are computed by examining the maximum under-prediction of scour from the deriving data set. The multiplier required to increase the most under-predicted value in the deriving data set to the observed value was determined. Relative scour depth ratios

in the validation data set were predicted using the best-fit equation and increased by the multiplicative adjustment from the under-predictions in the deriving data set. Similarly, the additive adjustment was determined and added to each best-fit prediction in the validation set.

This study applied four different regression techniques to Equation 9.2 and investigated the ability of equations 9.3a and 9.3b (Case 1 and Case 2) to over predict observed scour but by a lesser margin than the current HEC-18 local pier scour equation. Regression techniques include:

- unrestricted, ordinary least-squares;
- unrestricted, weighted least-squares;
- restricted, ordinary least-squares;
- restricted, weighted least-squares.

The National Bridge Scour Database includes information describing the accuracy for each scour measurement. Accuracy ranged from ± 0.25 feet to ± 2 feet. The weighted regression schemes considered the measurement accuracy for each record to determine the regression parameters. Restricted regression helped maintain intuitive ranges on regression parameters.

9.3 Results

This work developed a series of equations based on various regression forms and types. The mean-square error and number of over predictions were determined for each case and for each trial. Not all regression types or forms resulted in over-predicted scour depths or a reduced mean square error compared to the original HEC-18 equation. However, the restricted, ordinary, least-squares (OLS) regression applied to equation 9.3 (b) consistently over-predicted scour depth (at least as often as the current HEC-18 model) but with less residual error than the current HEC-18 implementation. The remainder of this chapter focuses on comparisons between the restricted OLS equation 9.3 (b) and the current HEC-18 local pier scour equation.

In every trial for Case 1 records, the current HEC-18 approach as well as the modified version over predicted the observed scour. However, for Case 2, each model (current and modified) under predicted the observed scour once. The mean square error for each trial was also determined for both Case 1 and Case 2. Mean square errors for the original HEC-18 ranged from 0.06 to 1.55 and from 0.01 to 0.38 for the modified version and were generally higher for Case 2. Table 9.2 provides a summary of over prediction and mean square errors for both the original and modified models.

Table 9.2: Shows the average mean square error across all four trials is lower for the modified equation than for the original HEC-18. The number of over predictions on validation data sets for each model is also displayed.

	NPW < 0.30			0.30 ≤ NPW < 1.25		
	Original	Modified	P-value	Original	Modified	P-Value
MSE	0.23	0.03	0.0001	1.05	0.30	0.001
Over Prediction	71/71	71/71		65/66	65/66	

In order to maximize the number of records used in equation development, all available data was used to derive a final pair of equations, but only after a regression type (restricted OLS) and model form (Equation 9.3 (b)) were determined through the four re-sampled trials. The first case with $a/y_1 < 0.3$ is predicted with Equation 9.4 (a) and Case 2 with $0.3 < a/y_1 < 1.25$ predicted by Equation 9.4 (b).

$$\frac{y_s}{y_1} = K \left(\frac{a}{y_1} \right)^{1.78} Fr^0 + 0.28 \quad \text{(Equation 9.4 a)}$$

$$\frac{y_s}{y_1} = K \left(\frac{a}{y_1} \right)^{0.39} Fr^{1.38} + 1.05 \quad \text{(Equation 9.4 b)}$$

Residuals from both the original HEC-18 model and the final modified versions are in Figure 9.1. These residuals show some records were better predicted with the original HEC-18 model, but other records indicate an improved fit with the modified version. Overall, the family of equations better predicts the observed field-scale scour measurements based on mean-square error.

Physically, pier scour will depend on various factors including pier geometry, flow depth, approach velocity, and bed material characteristics (Mueller & Wagner, 2005). However, not all bridge pier scour design equations explicitly account for all of these factors. For example, Mueller and Wagner (2005) found that the Mississippi Equation was one of the best predictive equations for pier scour yet that equation only includes pier width and flow depth as significant predictive variables.

In the case of Equation 9.4a, the Froude number does not play a factor in scour prediction (Fr exponent is zero). However, the Froude number is a significant factor in the scour predictions of Equation 9.4b (for NPW greater than 0.3). In this case the exponent on the Froude number is 1.38. The absence of the Froude number in the scour predictions associated with Equation 9.4a is counter-intuitive and physically inappropriate. It results as an artifact of the regression procedure used to develop these equations. The project team is not suggesting that the approach velocity (a component of the Froude number) is not a factor in the resulting scour depth. Instead, in an effort to simplify a complex physical system into predictive empirical equations, some variables will be discounted as having lesser significance than others.

Another apparent anomaly is the discontinuity that occurs in scour prediction between use of Equation 9.4a and 9.4b as is evidenced by the considerable change in regression parameters and the additive adjustment. Again, this discontinuity is a product of the statistical formulation of the equations and designers would have to apply these equations with some engineering judgment if the case being evaluated is very close to the transition point (NPW = 0.30). One option would be to apply a smoothing function between the two design equations such that large deviations in predicted scour depth do not occur near a normalized pier width of 0.3. Another option would be to adjust the transition point of the two cases (currently NPW = 0.3 which is the median of the dataset used for derivation) such that the discontinuity between the two equations is less significant. Finally, as additional field data becomes available, the regression processes will likely lead to a smoother, and more continuous function.

The additive adjustments included in Equations 9.4a and 9.4b preserve over prediction of scour, thereby ensuring the conservative nature of scour prediction. Recall that the goal of this exercise was to limit the over prediction of scour caused by the HEC-18 equation. The additive adjustment approach would indicate that with no flow ($Fr = 0$) the equations would still predict scour. While this is obviously not physically possible, it is a common artifact of empirically derived scour prediction equations. For example, the Froehlich Equation predicts a scour depth equal to pier width at a zero velocity and it is considered one of the best predictive equations (Mueller & Wagner, 2005).

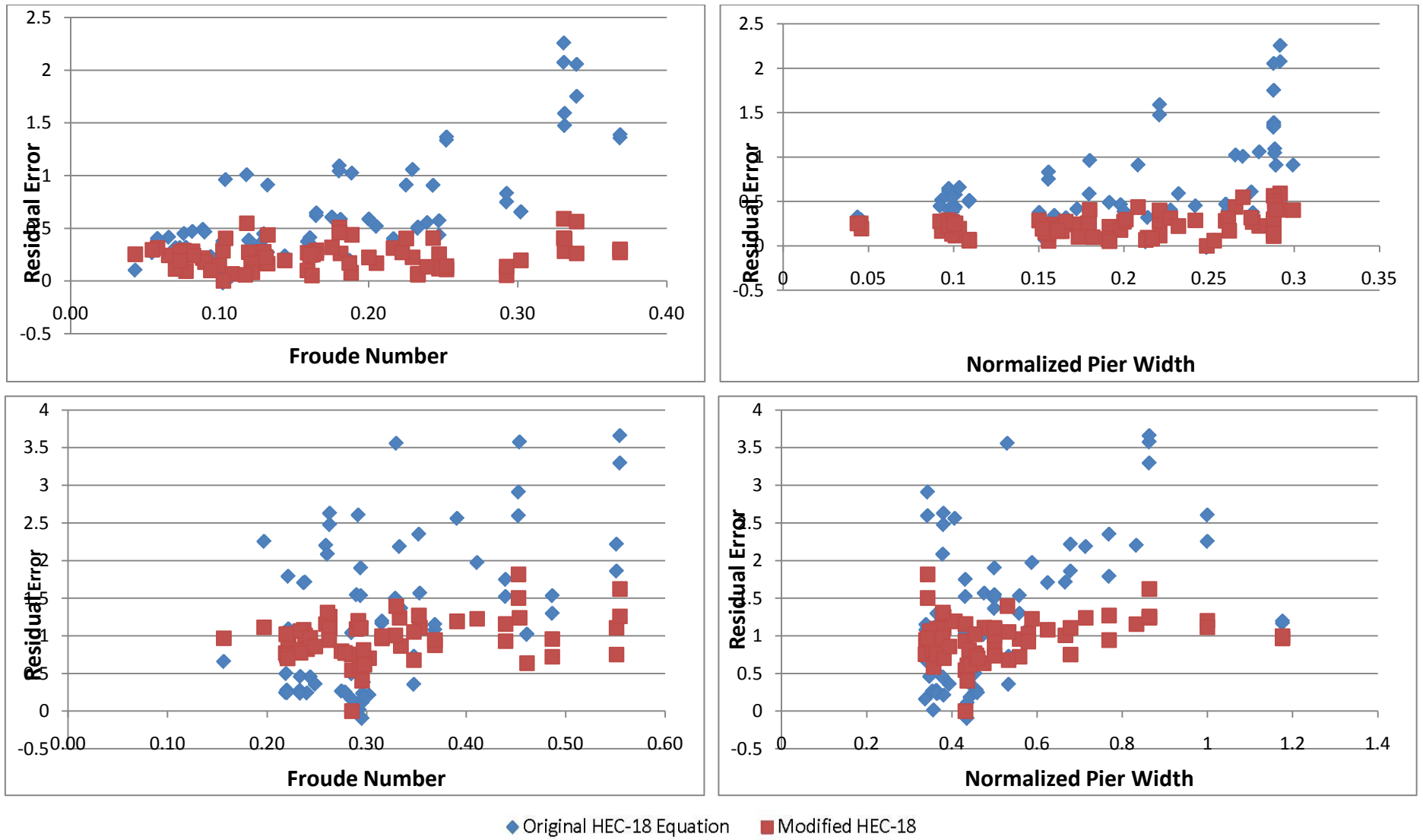


Figure 9.1: Residual comparisons for the final version of the modified HEC-18 family of equations case 1 (top) and case 2 (bottom).

9.4 Conclusion

Four regression types were examined to develop members of a family of scour equations, where each member (Equation 9.3(b) Case 1 and Case 2) of the family is applicable under a narrow set of conditions. The family as a whole covers a broad range of conditions currently covered by HEC-18. A brief summary of the four investigated regression types follows with full description in Appendix 9.A:

- 1) A simple *ordinary, unrestricted, non-linear regression* was applied first. A negative exponent was determined for one equation in the family. The negative exponent did not make physical sense.
- 2) A *weighted, unrestricted regression* was attempted next. This family of equations under predicted several observations in the validation data set.
- 3) An application of an *ordinary, restricted regression* resulted in significantly smaller mean square errors when compared to the original HEC-18 scour equation. The appropriate member of the modified scour equation also over predicted observations in the validation data set at least as often as the original HEC-18 model.
- 4) A *weighted, restricted regression* was also performed for thoroughness of approach. While the mean square errors were quite similar to the ordinary, restricted regression, under predictions occurred more frequently than the original HEC-18 model.

This analysis shows that developing a family of equations in a similar format to the current HEC-18 equation (Equation 9.1) reduces the mean square error of prediction and reduces the overall amount of over-prediction. The current HEC-18 equation has been shown in this and other studies to significantly over predict scour in most cases, resulting in increased construction costs. As shown in this study, using field-scale data, partitioning the data set and defining regression parameters for specific conditions leads to significant reductions in estimated scour depths while maintaining scour over prediction.

The National Bridge Scour Database provided data for this analysis. The database provides public access to field-scale scour measurements. However, the ultimate scour depths for these piers are unknown. Ultimate scour depth is easily determined with laboratory data but they usually represent idealized conditions not seen in the field. The study team encourages application of the newly developed approach to other datasets both laboratory and field-scale to further validate the approach.

While the study team is optimistic about the family of equations approach, a word of caution is necessary. These equations were developed and validated with a limited number of data points from the National Bridge Scour Database. With additional field-scale data, the family can be expanded to include more approach ratios, sediment conditions and scour types (clear water) and more confidence built for the two members developed in this work. Additionally, the current approach does not include scour data from Michigan, which is currently not included in the National Bridge Scour Database. However, scour measurements collected during this project and obtained from wire-weighted gauge surveys (Section 8.1) were used during final verification (Section 9.5).

9.5 Application to Michigan-Specific Conditions

Equations 9.4 (a) and (b) were applied to events that caused scour during this study and predicted an increase of scour compared to the original HEC-18 scour equation for all but one instance of the Michigan data. However, residuals from the Michigan data as computed with Equations 9.4 (a) and (b) compare well with those from the Nation Bridge Scour Database (Figure 9.2). Table 9.3 provides the data from the scour database generally represents the Michigan data well, which justifies the use of this approach in Michigan. The minimum and maximum values for the Michigan data fit between the minimum and maximum values from the National Bridge Scour Database with the exception of the Froude number in Case 2.

Table 9.3: Descriptive statistics for Michigan sites versus the National Bridge Scour Database

	National Bridge Scour Database-Froude				Michigan Data- Froude			
	Mean	Std. Dev	Min	Max	Mean	Std. Dev	Min	Max
Case 1	0.18	0.09	0.04	0.37	0.17	0.13	0.07	0.26
Case 2	0.32	0.10	0.16	0.55	0.18	0.04	0.13	0.23
	National Bridge Scour Database – D_{50}				Michigan Data- Froude – D_{50}			
Case 1	0.74	0.33	0.16	1.82	0.20	0.00	0.2	0.2
Case 2	0.89	0.54	0.15	1.80	1.28	0.99	0.20	2

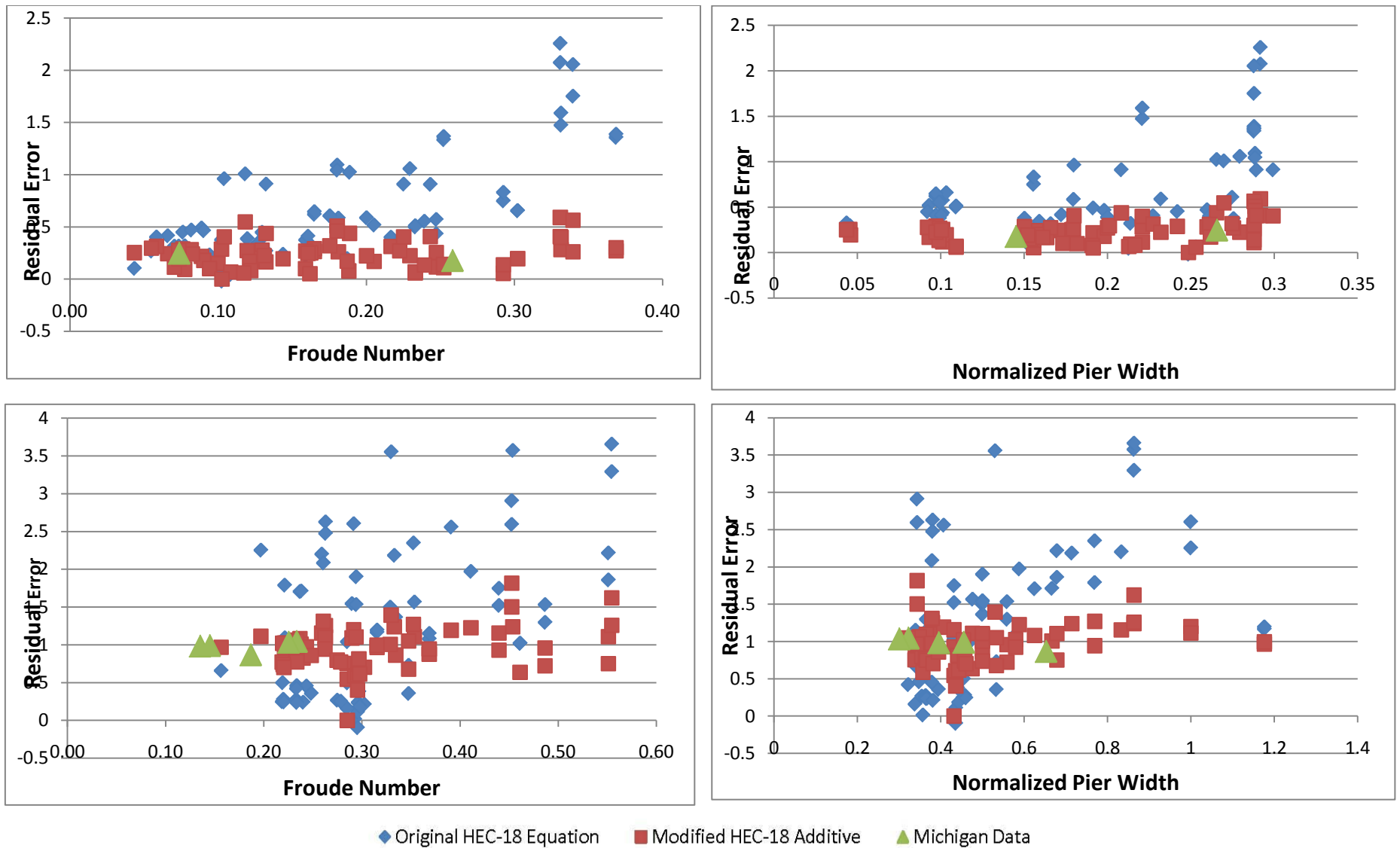


Figure 9.2: Residual comparisons for the final version of the modified HEC-18 family of equations case 1 (top) and case 2 (bottom). Michigan data were predicted with equation 9.4 (a) and 9.4 (b) on the top and bottom, respectively.

9.6 Recommendations for future work

This effort developed two members from a proposed family of scour prediction equations. This showed that the family approach is capable of reducing the mean square error while maintaining the over prediction criterion. Equation 9.4a and 9.4b could be improved with the collection of additional field data. In addition, several approaches could be taken (such as applying a smoothing function or moving the transition point) to minimize the discontinuity in scour prediction between the two equations. In addition, development of new family members (i.e. equations for additional cases) will increase the range of conditions for which this method applies. As this method becomes more diverse, it will approach the range of applicability found with the current HEC-18 local pier-scour equation. Additional family members for clear-water scour, wide pier situations and possibly further divisions based on the Froude number will lead to still smaller mean square errors. The flow chart in Figure 9.3 indicates completed and proposed work.

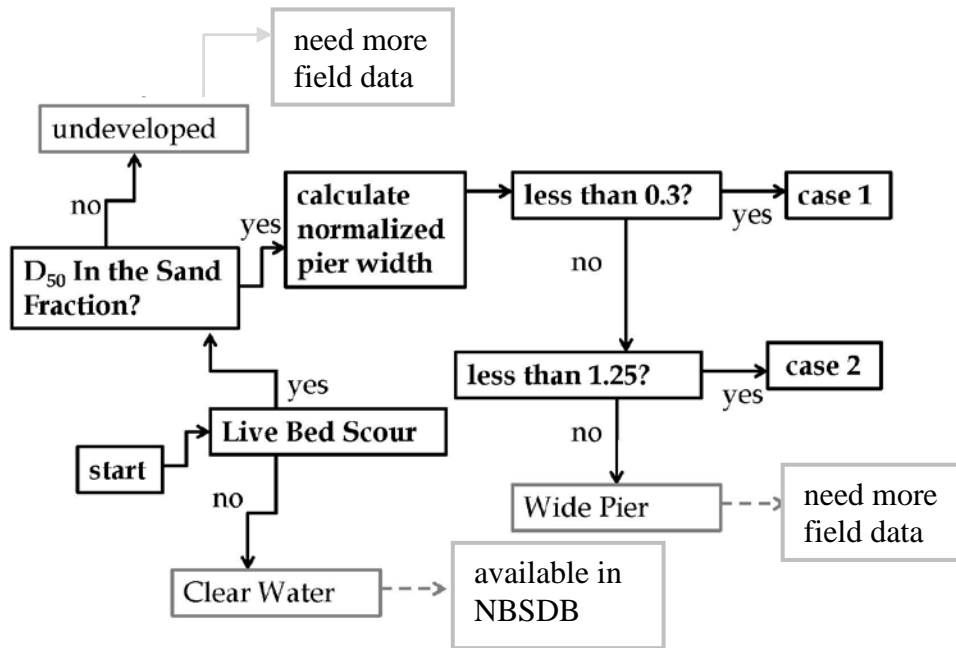


Figure 9.3: Flow chart depicting currently derived equations and conditions where equations still need to be derived

10.0 SCOUR PREDICTIONS USING HEC-RAS

10.1 Introduction

The US Army Corps of Engineers' Hydrologic Engineering Center River Analysis System (HEC-RAS) (Brunner, 2010) is the most common model used for river backwater analysis. In this investigation, the model was used to simulate the hydraulics in the vicinity of the bridge crossings and to calculate the scour at the bridge with a user-selected equation from among several options available in HEC-RAS. Although there are many assumptions inherent in the HEC-RAS hydraulics calculations, the one most important to the calculation of scour at the bridge crossing, is the limitation to a one-dimensional flow field. The assumption is that the velocity vector is perpendicular to the channel cross-section and is uniform across the entire depth. This assumption is a reasonable assumption in a majority of open channel flow cases. However, in the case of complex geometries, such as those found at bridge crossings and around bridge piers, the two- or three- dimensional flow field may be important to the prediction of system response.

A HEC-RAS model was developed for ten of the twelve bridge crossings considered in the field evaluation. Two crossings were not adequately characterized to provide all the key information, necessary for the present analysis. This analysis was conducted to demonstrate how the prediction of scour by a popular and common model is not consistent with measured scour and to compare our modified HEC-18 equation with the original HEC-18 equation for flood events.

10.2 Procedure

The procedure for conducting the HEC-RAS simulation began with the development of a HEC-RAS model for 10 of the bridge crossings using data gathered during the field investigations for the Level 2 analysis, augmented by information (structural and other) maintained by MDOT. The minimum number of cross-sections entered at each bridge crossing is six, although additional sections were interpolated as needed using the internal interpolation functions of HEC-RAS, as well as generated from data taken from the USGS Topographic Maps between cross-section stations.

The next step of the procedure was to select flow values to simulate events of interest. For the present study, this included the peak discharge recorded for the period of USGS records at each site and the peak discharge measured at each bridge crossing by the project team during the study period. Boundary conditions, as appropriate were applied. In most cases, the normal depth condition with subcritical flow produced good results; although for several crossings the mixed flow regime was specified.

Finally, the procedure used HEC-RAS to model the two flows at the 10 bridge crossings. The output of HEC-RAS includes the computer generated solution to the HEC-18 scour equation, as well as the stage information necessary for use in the manual calculation of scour.

A variety of site characterization data was required for the HEC-RAS simulations including bridge geometry, cross-sectional bed elevations, bed stream slope, roughness, and sediment size. The bridge geometric information and cross-sections were determined from construction prints and field measurements. The stream slope was determined using USGS Topographic maps, as well as field verification. The Manning's n values were determined based on field observations and use of FHWA guidelines for roughness assignment. Finally, The D_{50} and D_{95} sizes were determined as part of the geotechnical investigations at each site.

The HEC-18 Equation, as described in Chapter 4, is based on the Colorado State University (CSU) equation which is one of the options for bridge scour calculation in HEC-RAS. This was the option adopted by the study team and was the base equation for subsequent refinement. Although the HEC-RAS screen shots presented subsequently identify the scour equation as CSU, it is the same as presented in Equation 4.4 of this report.

10.3 Modeling Details

Figure 10.1 provides an example of the scour data input screen for the HEC-RAS scour calculations. This particular “screen shot” is for the Cass River bridge crossing. The modeled HEC-RAS geometries for each of the ten bridge crossings are indicated in Figures 10.2 to 10.11.

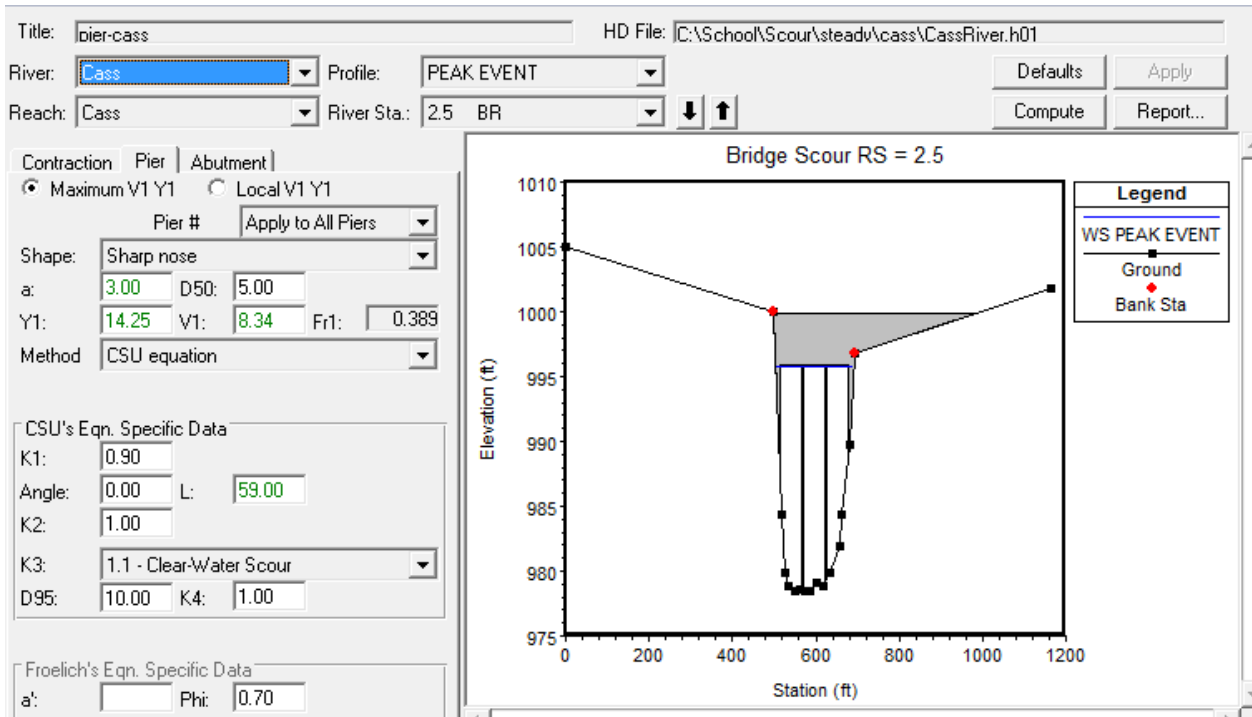


Figure 10.1 HEC-RAS scour evaluation input Cass River Crossing

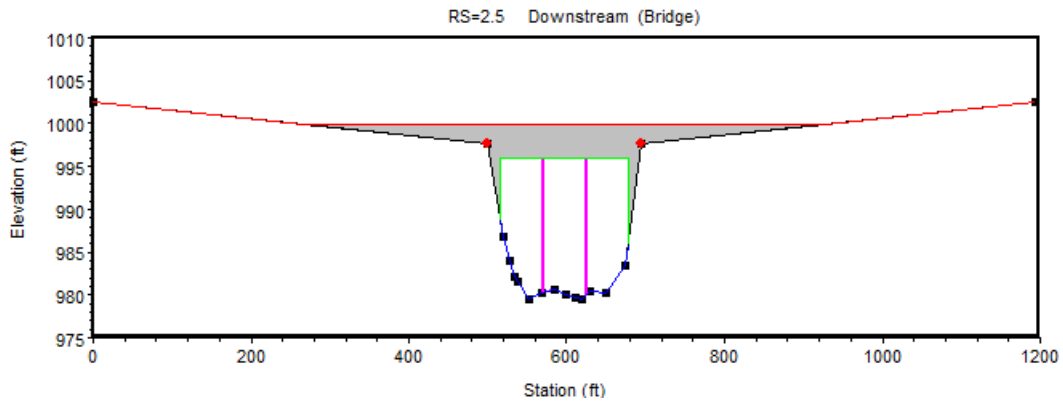


Figure 10.2 Cass River Crossing

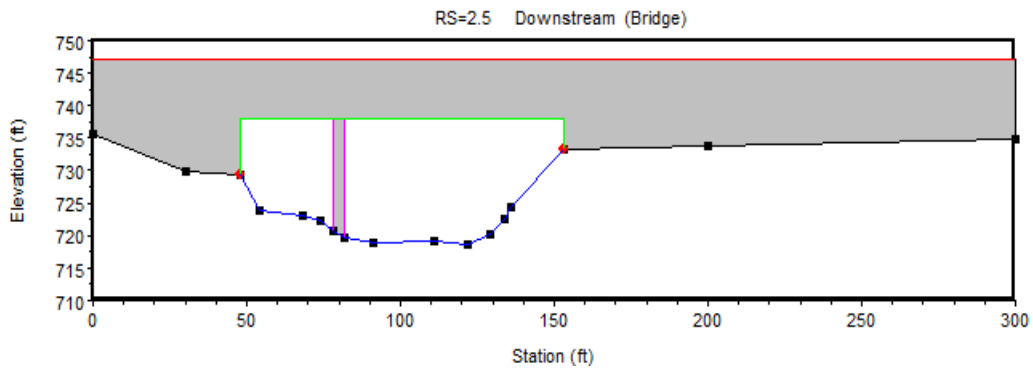


Figure 10.3 Flint River Crossing

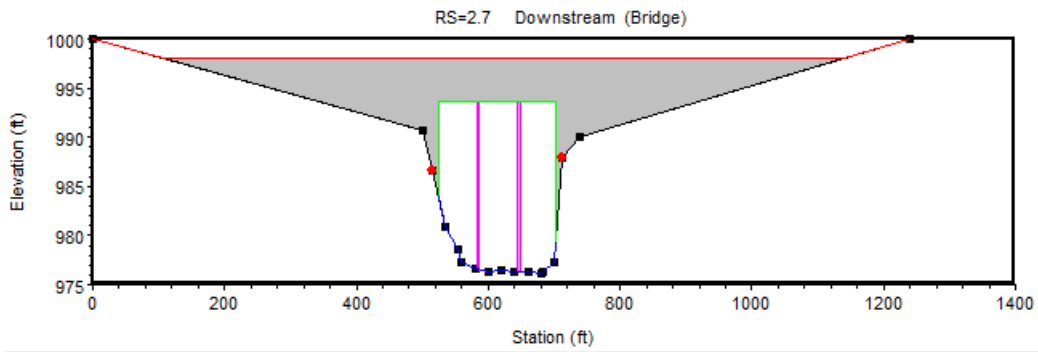


Figure 10.4 Grand River

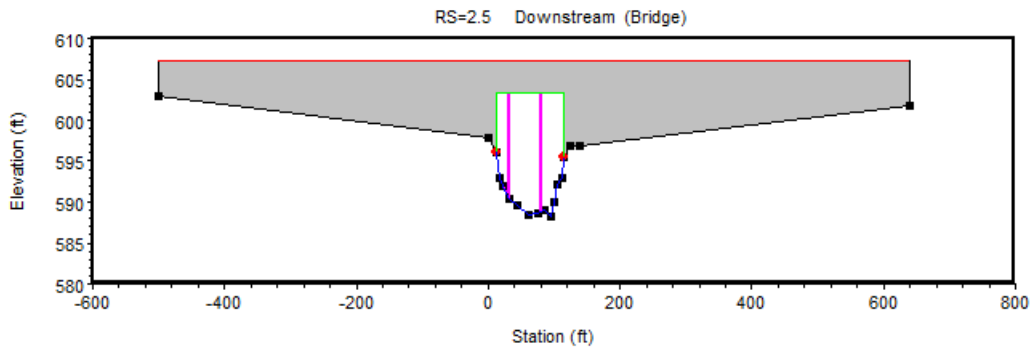


Figure 10.5 Paw Paw River

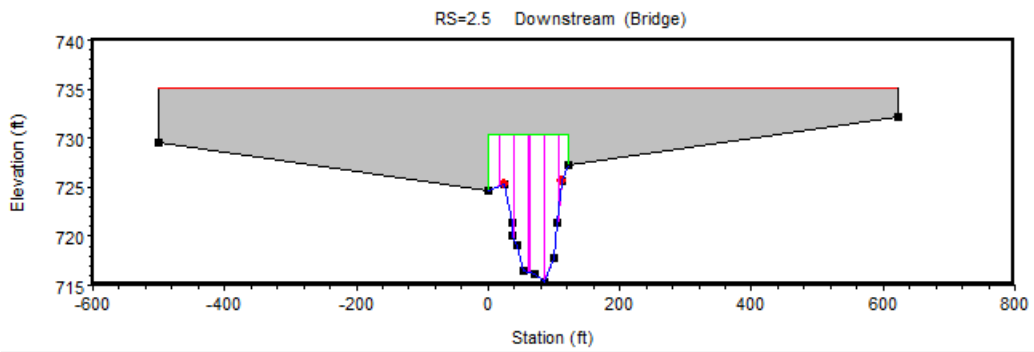


Figure 10.6 Raisin River

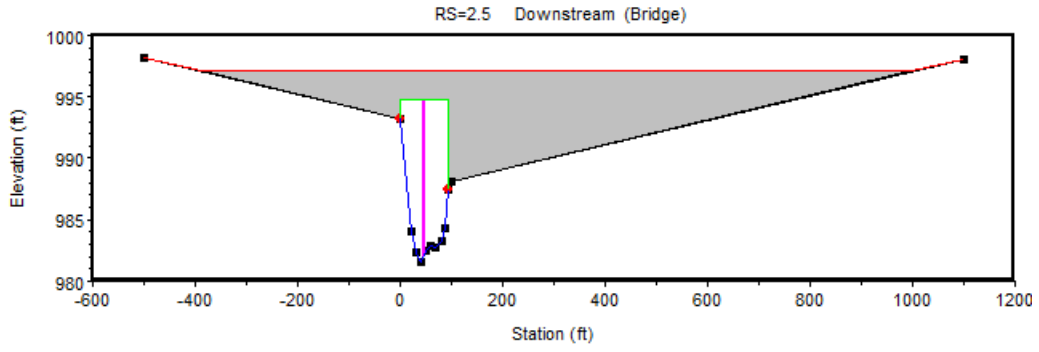


Figure 10.7 Rogue River

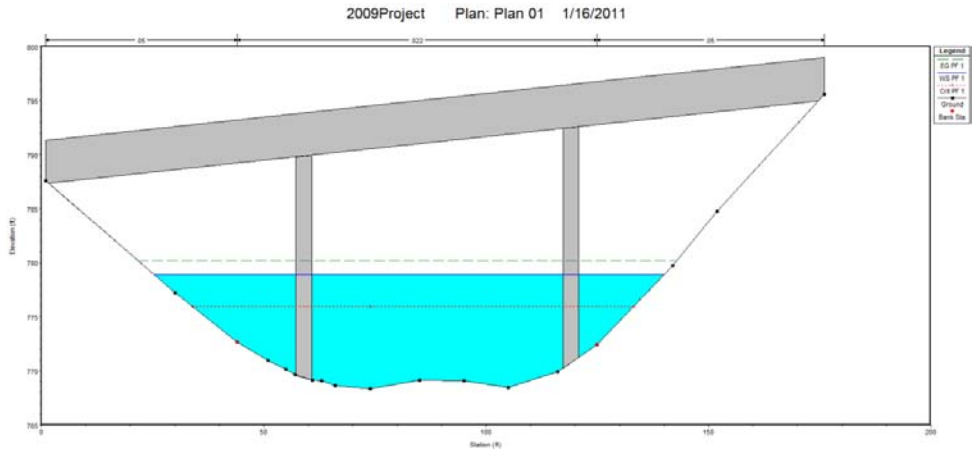


Figure 10.8 Thornapple River at M-43

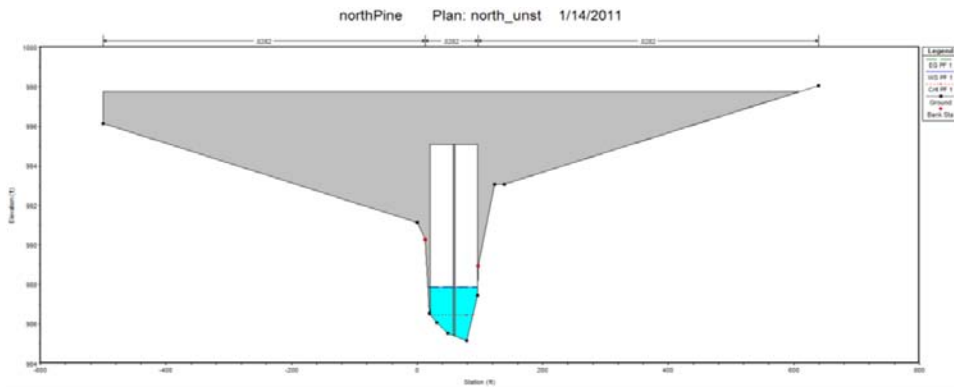


Figure 10.9 Pine River (North)

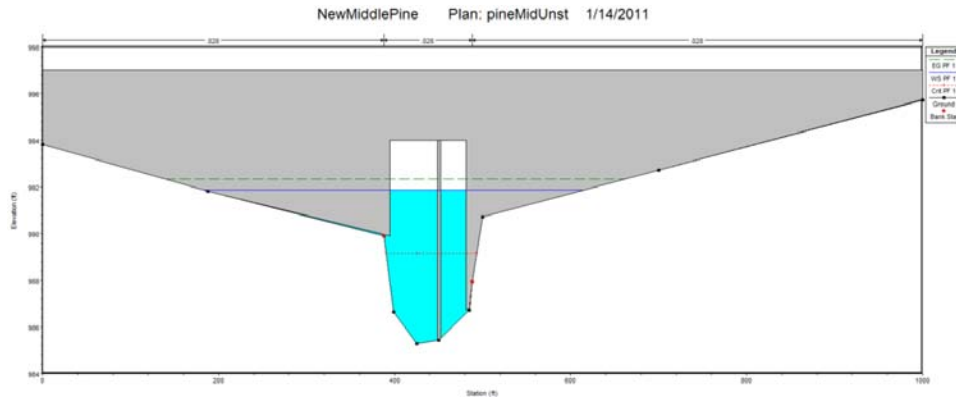


Figure 10.10 Cross Section of Pine River (Middle)

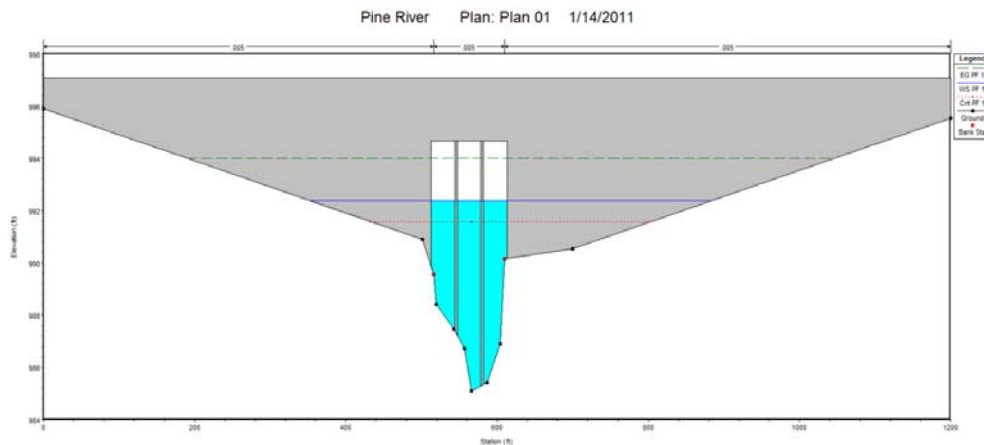


Figure 10.11 Pine River (South)

10.4 Simulation Results

The discharge values associated with each bridge crossing for the two modeled events, the *peak event of record* and the *peak event of the study period*, are recorded in Table 10.1 along with the HEC-RAS calculated bridge scour for each crossing and event. As anticipated, at each crossing the predicted scour from the period of record is greater than that calculated for the peak event of the study period. As previously noted, over-prediction of scour is common when using the HEC-18 Scour Prediction Equation. The Pine River South Crossing (North Pier) the calculated scour for the peak event of record and peak event of the study period are identical even though the discharge values are significantly different. One explanation for this seeming inconsistency is that the eroded scour hole reached an "equilibrium" condition, beyond which further scour was limited.

As further evidence of possible over-prediction of scour, compare the observed maximum scour at the monitored bridge crossings to the calculated scour using the HEC-18 methodology embedded in the HEC-RAS scour simulation (Table 10.2). In all cases, the calculated scour is greater than the measured scour. For bridge crossings that experienced any significant scour during the study period, the predicted scour was between 25% and 650% greater than the observed scour.

Table 10.1 HEC-RAS Scour Predictions

Bridge Crossing	Pier Shape	<i>Peak Event of Record Analysis</i>			<i>Peak Event of Study Period Analysis</i>		
		Date	Predicted Scour (ft)	Flow (cfs)	Date	Predicted Scour (ft)	Flow (cfs)
Cass River	Sharp nose	09/12/1986	6.84	22200	05/14/2010	5.33	4055
Flint River	Sharp Nose	01/24/1996	6.59	7470	04/22/2009	3.96	1090
Grand River	Group of cylinders	03/26/1904	8.87	24500	05/14/2010	5.04	1835
Paw Paw River	Round nose	09/17/2008	5.15	3,870	05/20/2009	2.78	573
Raisin River	Group of cylinders	03/15/1982	3.49	6660	05/12/2010	2.52	1170
Rogue River	Group of cylinders	03/06/1976	5.92	3540	05/01/2009	5.06	1075
Pine River (North)	Sharp Nose	09/12/1986	1.57	5160	04/26/2009	1.55	2790
Pine River (South, South Pier)	Sharp Nose	09/12/1986	1.54	5160	04/26/2009	1.48	2790
Pine River (South, North Pier)	Sharp Nose	09/12/1986	1.59	5160	04/26/2009	1.59	2790
Thornapple River at M-43	Sharp Nose	04/07/1947	7.21	6810	05/10/2008	6.05	3470

Table 10.2 Period of Study Comparisons

Bridge Crossing	Observed Scour, Maximum (feet)	HEC-RAS Calculated Scour (feet)
Cass River	Negligible	5.33
Flint River	Negligible	3.96
Grand River	Negligible	5.04
Paw Paw River	Negligible	2.78
Raisin River	Negligible	2.52
Rogue River	Negligible	5.06
Pine River (North)	1.2	1.55
Pine River (South, South Pier)	0.7	1.48
Pine River (South, North Pier)	0.8	1.59
Thornapple River at M-43	0.8	6.05

To evaluate the modified HEC-18 Equation, the predicted scour for the *period of record* using the Modified HEC-18 Equation was compared to that of the HEC-RAS simulations using the original HEC-18 Pier Scour Equation. Table 10.3 shows that in all cases except one, the Modified HEC-18 Equation is a less conservative prediction tool than HEC-18 which was the goal of the modification.

Table 10.3 Period of Record Comparison

River Crossing	Calculated Scour, Feet	
	HEC-RAS	Modified HEC-18
Cass	6.83	4.87
Flint	6.59	5.31
Grand	8.88	4.68
Paw Paw	5.15	3.42
Raisin	3.49	2.53
Rogue	5.92	7.50

10.5 Conclusion

The HEC-18 equation embedded in HEC-RAS was used to calculate scour at each of the 10 modeled bridge crossing sections. Two flow conditions were analyzed: the *peak flow of record* and the *peak flow measured* during the study period. For all crossings, the predicted scour for the period of record was equal to or greater than the predicted scour for the peak flow of the study period. In those cases where the scour associated with the period of record was not significantly greater than the period of study scour, the eroded scour hole likely reached an "equilibrium" condition.

The HEC-RAS predictions were compared to the observed maximum scour at each of the crossings. In all cases, the HEC-RAS prediction was significantly greater than the observed scour. This corresponds to findings of MDOT that HEC-18 is overly conservative. The modified HEC-18 equation (9.4a and 9.4b) was found to provide less conservative scour predictions for the large discharges represented by the peak discharge of record.

11.0 CONCLUSION

The overall goal of this research was to improve the Michigan Department of Transportation (MDOT) bridge scour prediction capability. Project tasks included evaluating scour prediction methods utilized by regional state DOTs, conducting a field data collection effort, and proposing an alternative approach for pier scour prediction based on field measurements and statistical analyses.

The study team contacted transportation departments in sixteen states in the Midwest and mid-Atlantic to determine scour evaluation methods used in regions adjacent to Michigan. This process was first conducted in 2007 to inform the investigation and then was repeated in 2010 to determine if any states had updated their procedures or research programs. It was determined that most states procedures and protocols were comparable to the scour estimation practices used by Michigan with the HEC manuals as standard procedures for scour estimation. Several states did incorporate guidance from either state drainage manuals or the AASHTO Drainage Manual into their evaluation procedures. Regarding research, ten of the states surveyed have conducted scour related research in the past or currently have scour research programs, but none of those have led to a uniformly accepted version of the HEC-18 Scour Prediction Equation. The research being conducted could generally be categorized as either field measurement of scour in an effort to improve scour prediction or laboratory investigation of soil borings (SIRCOS-EFA) to determine scour rates of cohesive soils.

To determine bridge locations for field data collection, the project team visited 56 bridge spans at 42 unique locations across the southern half of the Lower Peninsula of Michigan. From those visits, nine locations and twelve unique spans were selected for monitoring. The selection criteria included:

- Bridges on the MDOT scour critical list;
- Lower peninsula locations;
- Soil characteristics that exhibited cohesion;
- Proximity to a USGS gauge for discharge monitoring;
- Access and ease of data collection;
- Absence of extensive scour counter measures;
- Low flow conditions that allowed for detailed profiling.

Of the twelve unique spans, eleven were monitored episodically with a wire-weighted gauge across the entire cross section and three were monitored continuously with an acoustic device and a data logger mounted to a bridge pier. This two part data collection strategy maximized the number of sites included in the study and offered spatially and temporally varied data. In addition, a complete soil characterization was performed for the samples collected at the selected monitoring locations. Finally, all monitoring locations have a USGS gauge within several river miles of the study to monitor hydrologic conditions.

A total of 79 episodic measurements from eleven sites and more than 40 months (total) of continuous data from three different sites were collected during the project. During the investigation, seven episodic measurements indicated measureable pier scour. Scour depths ranged from 0.7 to 1.5f.t with the maximum return period corresponding to a seven-year flood event. No measureable scour events occurred at the continuous scour monitoring locations. The measured scour depths were used to evaluate the predictive capabilities of the original and revised HEC-18 Equation.

The field investigation also included the use of a Jet Erosion Test (JET) to experimentally determine if *in situ* soil conditions could be correlated with measured bridge scour. Out of the three JET-related objectives identified in the proposal, only the first objective (i.e. correlate erodibility to other geotechnical properties) was satisfactorily met. It was determined that:

- the dry unit weight of a material has an inverse relationship with the log of its erodibility;
- soil classification is an indicator of erodibility;
- the log of erodibility is inversely related to the friction angle of a soil.

The second objective (use JET results to supplement the data necessary for the process of calibration/verification of scour equations) and the third objective (correlate observed scour with *in situ* soil conditions) were not met due to an overall lack of measureable scour events occurring during the project period. However, an important outcome was the development of a laboratory procedure for JET testing which could use soil borings at scour-critical locations for erodibility analysis.

Another important outcome of this investigation was the modification of the HEC-18 pier scour prediction equation using the National Bridge Scour Database (NBSD). This investigation

demonstrated that field-scale data could be partitioned and regression parameters generated for specific conditions. Specifically, four regression types were examined to determine which would provide the most accurate set, or “family”, of equations using the current HEC-18 equation formulation as the basic structure. The four regression types investigated were:

- 5) A simple *ordinary, unrestricted, non-linear regression* which yielded a negative exponent for one equation in the family. The negative exponent did not make physical sense.
- 6) A *weighted, unrestricted regression* which under predicted several observations in the validation data set.
- 7) An *ordinary, restricted regression* that resulted in significantly smaller mean square errors when compared to the original HEC-18 scour equation. The appropriate member of the modified scour equation also over predicted observations in the validation data set at least as often as the original HEC-18 model.
- 8) A *weighted, restricted regression* resulted in mean square errors that were quite similar to the ordinary, restricted regression, but under predictions occurred more frequently than the original HEC-18 model.

Therefore, an ordinary restricted regression approach led to the development of a family of equations formatted similarly to the current HEC-18 equation. The revised HEC-18 equations exhibited a reduced mean square error of prediction and reduced the overall level of over-prediction. While the study team is optimistic about the *family of equations* approach, a word of caution is necessary. These equations were developed and validated with a limited number of data points from the National Bridge Scour Database. However, scour measurements collected during this project were used during final verification of the equations and demonstrated their potential use in Michigan. With additional field-scale data, the family can be expanded to include more approach ratios, sediment conditions and scour types (clear water) and more confidence built for the two equations developed in this work.

The US Army Corps of Engineers' Hydrologic Engineering Center - River Analysis System (HEC-RAS) model was used to compute bridge scour for flood events at ten of the twelve locations associated with the field measurements. The HEC-18 Equation was the predictive method selected for the HEC-RAS calculations. Each of computer-predicted scour predictions was compared to the measured scour occurring during the field study and found to

exceed the observed scour by a significant amount. A subset of these bridge crossing simulations (six in total) were used to compare to the revised predictive equations of Chapter 9. The modified HEC-18 equation was an improvement to the HEC-RAS scour calculation in all cases, except one.

In conclusion, a modified HEC-18 pier scour prediction equation was developed for application in Michigan. This revised scour prediction procedure could allow MDOT to more accurately predict bridge scour and subsequently more efficiently and confidently design new bridge crossings and/or modify existing bridges. Finally, experimental and analytical approaches were developed during this investigation that provides a foundation for future research in the field of scour prediction.

References

- AASHTO (2005). "American Association of State Highway and Transportation Officials Model Drainage Manual (3rd Ed)." CD-ROM, Washington, DC.
- Allen, P.M., Arnold, J., Jakubowski, E. (1999). "Prediction of Stream Channel Erosion Potential." *Environmental and Engineering Geoscience*, 5(3), 339-351.
- Benedict, S.T. and Caldwell, A.W. (2005). *Development and Evaluation of Clear-Water Pier and Contraction Scour Envelope Curves in the Coastal Plain and Piedmont Provinces of South Carolina*, USGS Scientific Investigations Report 2005-5289, Washington, D.C.
- Brandimarte, L., Montanari, A., Braiud, J.-L., D'Odorico, P. (2006), "Stochastic Flow Analysis for Predicting Scour of Cohesive Soils." *Journal of Hydraulic Engineering*, 132(5).
- Briaud J., Ting, F., Chen, H., Gudavalli, R., Kwak, K., Philogene, B., Han, S., Perugu, S., Wei, G., Nurtjahyo, P., Cao, Y., and Li, Y. (2001). *Prediction of Scour Rate and Bridge Piers*, Texas Transportation Institute Report, College Station, TX.
- Brunner, G. (2010). *HEC-RAS Hydraulic Reference Manual*, U.S. Army Corps of Engineers-Hydraulic Engineering Center, Davis, CA.
- Calappi, T.J., Miller, C.J., and Savolainen, P.T. (2009). "Impact of Grain Size Characterization on the Froehlich Pier Scour Equation." *Proc. of ASCE IFCEE*, Orlando, FL.
- Croskey, H.M. (1985). *MDNR/USGS Peak Flow Regression*, Water Management Division, Michigan Department of Natural Resources, Lansing, MI.
- Ettema, R., Mostafa, E.A., Melville, B.W. and Yassin, A.A. (1998). "On Local Scour at Skewed Rectangular and Oblong Piers." *Journal of Hydraulic Engineering*, 124(7), 756-760.
- Gotvald, A. J. (2003). "Field Monitoring of Bridge Scour at Four Sites in Georgia." *Proc. of Georgia Water Resources Conference*, Atlanta, GA.
- Hanson, G.J. and Hunt, S. (2007). "Lessons learned using laboratory jet test method to measure soil erodibility of compacted soils." *Applied Engineering in Agriculture*. 23(3):305-312.
- Hopkins, G.R., Vance, R.W., and Kasraie, B. (1980). *Scour around bridge piers*, Federal Highway Administration Report FHWA-RD-79-103, Washington DC.
- Holtschlag, D.J. and Croskey, H.M. (1984). *Statistical Models for Estimating Streamflow Characteristics of Michigan Streams*, U.S. Geological Survey Water-Resources Investigations Report 84-4207, 80 p., Lansing, MI

- Holtschlag, D.J. and Miller, R.L. (1997). *Streambed Stability and Scour Potential at Selected Bridge Sites in Michigan*, U.S. Geological Survey Water-Resources Investigations Report 98-4024. Lansing, MI.
- Jain, S.C. and Fischer, E.E. (1979). *Scour around bridge piers at high Froude Numbers*. Federal Highway Administration Report FHWA-RD-79-104, Washington, DC.
- Johnson P. (1995). "Comparison of Pier-Scour Equations Using Field Data." *Journal of Hydraulic Engineering*, 12(8), 626-629.
- Lagasse, P.F., Richardson, E. V., and Sabol, S. A. (1994). "Bridge Scour Instrumentation." *Proc. of the 1994 ASCE National Conference on Hydraulic Engineering*, Buffalo, NY.
- Lagasse, P. F., Schall, J. D., and Richardson, E. V (2001a). *Stream Stability at Highway Structures, Hydraulic Engineering Circular No. 20 (HEC-20)*, Federal Highway Administration Report FHWA-HH1-002, Washington, D.C.
- Lagasse, P. F., Zevenbergen, L. W., and Schall, J. D. (2001b). *Bridge Scour and Stream Instability Countermeasures, Hydraulic Engineering Circular No. 23 (HEC-23)*, Federal Highway Administration Report FHWA-NH1-003, Washington, D.C.
- Lagasse, P.F. and Richardson, E.V. (2001). "ASCE Compendium of Stream Stability and Bridge Scour Papers", *Journal of Hydraulic Engineering*, 127(7) 531-533.
- Landers, M.N., and Mueller, D.S. (1996). *Channel scour at bridges in the United States*, Federal Highway Administration Report FHWA-RD-95-184. Washington, D.C.
- Laursen, E.M. and Toch A. (1956). *Scour around bridge piers and abutments*, Bulletin No. 4, Iowa Highway Research Board, Ames, IA.
- Mellville, B.W. and Sutherland, A.J. (1988). "Design Method for Local Scour at Bridge Piers." *Journal of Hydraulic Engineering*, 114(2) 126-136.
- Melville, B.W. (1997). "Pier and Abutment Scour: Integrated Approach." *Journal of Hydraulic Engineering*, 123(2) 126-136.
- MDOT (2006). *MDOT Drainage Manual, Chapter 6 – Bridges*, Michigan Department of Transportation Lansing, MI.
- Molinas, A. (2004). *Bridge scour in non-uniform sediment mixtures and in cohesive materials*, Federal Highway Administration Report FHWA-RD-03083, Washington, DC.
- Mueller, D.S. (1996) *Local scour at bridge piers in nonuniform sediment under dynamic conditions*, Ph.D. Dissertation, Colorado State University, Fort Collins, CO.

Mueller, D.S., and Wagner, C.R. (2005). *Field Observations and Evaluations of Streambed Scour at Bridges*, Federal Highway Administration Report FHWA-RD-03-052, Washington, D.C.

NBSD (2004). National Bridge Scour Database, U.S. Geologic Survey, <http://water.usgs.gov/osw/techniques/bs/BSDMS/>.

Parola, A. C., Hagerty, D. J., Kamojjala, S. (1998). "Highway Infrastructure Damage Caused by the 1993 Upper Mississippi River Basin Flooding." National Cooperative Highway Research Program, Transportation Research Board. Washington, D.C.

Paaswell (1973) "Causes and Mechanisms for Cohesive Soil Erosion," *Soil Erosion Causes and Mechanisms*, D.H. Grey, Ed., Highway Research Board, Special Report 135, 52-74.

Richardson, E.V. and Davis, S.R. (2001). *Evaluating Scour At Bridges, Fourth Edition, Hydraulic Engineering Circular No. 18 (HEC-18)*, Federal Highway Administration Report FHWA-IP-90-017, Washington, D.C.

Raudkivi, A.J. (1998). "Functional trends of scour at bridge piers." *Journal of Hydraulic Engineering*, 112(6), 1-13.

Sheppard, M. and Miller, W.J. (2006). Live-bed local pier scour experiments." *Journal of Hydraulic Engineering*, 132(7), 635-642.

Sorrell, R. (2001). *Computing Flood Discharges for Small Ungaged Watersheds*, Michigan Department of Environmental Quality, Lansing, MI.

USDOT (1991). *Evaluating Scour at Bridges*, U.S. Department of Transportation Technical Advisory T5140.23, Washington, DC.

Thoman, R.W., and Niezgod, S. (2008). "Determining Erodibility, Critical Shear Stress, and Allowable Discharge Estimates for Cohesive Channels: Case Study in the Powder River basin of Wyoming." *Journal of Hydraulic Engineering*, 134(12), 1677-1687.

Walker, J.F., Hughes, P.E. (2005). *Bridge Scour Monitoring Methods at Three Sites in Wisconsin*, U.S. Geologic Survey Open File Report 2005-1374, Washington, D.C.

Williams-Sether, T. (1999). *Estimated and Measured Bridge Scour at Selected Sites in North Dakota*, U.S. Geological Survey Water-Resources Investigations Report 99-4124, Bismark, ND.

Wagner, C.R., Mueller, D.S., Parola, A.C., Hagerty, D.J., and Benedict, S.T. (2006). *Scour at Contracted Bridges*, National Cooperative Highway Research Program Project 24-14, Transportation Research Board, Louisville, KY.

Wang, J., (2004) *The SRICOS Method for Complex Pier and Contraction Scour*, Ph.D. Dissertation, Texas A&M University, College Station, TX.

Appendix 4.A

Appendix 6D from MDOT Guidelines for Evaluation of Scour

Appendix 6-D
(updated January 2004)

**MDOT Guidelines for Evaluation of Scour
and Scour Analysis Worksheets**

Rev: September 13, 2002

MICHIGAN DEPARTMENT OF TRANSPORTATION
GUIDELINES FOR EVALUATION OF SCOUR AT EXISTING STRUCTURES

INTRODUCTION

These guidelines are proposed for the evaluation of scour at existing bridge structures for the Michigan Department of Transportation (MDOT) and local agencies. The guidelines supplement the following Federal Highway Administration (FHWA) publications and directives on scour:

1. "Evaluating Scour at Bridges," HEC -18 (Fourth Edition)
2. Technical Advisory T 5140.23
3. "Stream Stability at Highway Structures," HEC - 20 (Third Edition)

Scour is a dynamic sediment transport process. Research on scour is ongoing, and revisions to the methods of scour and stream stability analyses may occur.

These guidelines are organized to discuss the priority of evaluation, the three levels of analysis, the National Bridge Inventory System (NBIS), the plan of action, and design of scour countermeasures for scour critical bridges. It is important that an interdisciplinary team consisting of hydraulic, geotechnical, and structural engineers be involved in all levels of analysis and the evaluation process.

Chapter 10 of FHWA's HEC-18 outlines a scour evaluation process for existing bridges. HEC-18 recommends documentation of each level of analysis. Documentation for Michigan includes updating Item 113 of the NBIS at each level of analysis and action and retaining the Level One and Level Two Worksheets. The Level Two Worksheet should include, if needed, recommended scour countermeasures and a "Plan of Action." The Plan of Action should include a timetable to implement the design and construction of accepted scour countermeasures.

PRIORITY OF EVALUATION

In 1991, MDOT developed a scour screening procedure for development of an initial priority list. This procedure was approved by FHWA and distributed to local agencies. Each agency should now have a "priority list" based on this procedure to start its scour evaluation program. An agency should use this priority list to schedule the proposed Level One analysis given in these guidelines. The Level One analysis must be completed to determine the need for a Level Two analysis.

Structures with unknown foundations will have Item 113 coded as a "U" in the NBIS. MDOT recommends as a minimum a Level One analysis, and the hydrologic, hydraulic, and scour calculations of a Level Two analysis be done. The findings can be used to evaluate the potential risk to these structures once the type of foundation is determined.

LEVEL ONE - QUALITATIVE ANALYSIS

A Level One analysis is an information gathering effort consisting of office and field reviews of the structure. The following information should be obtained, reviewed, and commented on:

- Bridge Inspection Reports
- Underwater Inspection Reports (if available)
- Items 60, 61, 71, 92, 93, and 113 of the NBIS (see HEC-18, Appendix J, for definitions)
- Construction, design, and maintenance files for repair and maintenance work done on the structure
- Hydraulic Data (Flood Insurance Study or original design analysis)

The Level One analysis procedure is outlined in Chapter 3 of HEC-20. It is a six-step process that covers stream characteristics, land use, stream stability, lateral stability, vertical stream stability, and channel response to change. Items used in the initial screening procedure should be verified, corrections made to the screening database, and the priority list updated accordingly.

A field investigation will be required to obtain the above stream characteristics and confirm the minimum hydraulic parameters, i.e., channel slope, channel and overbank roughness coefficients, plan elevations and dimension of structure, foundation conditions, etc.

If a Level Two analysis is recommended, a code of "6" should be entered for Item 113.

LEVEL TWO - BASIC ENGINEERING ANALYSIS

The Level Two scour analysis is an eight-step process to define stream stability and scour problems. These steps cover:

1. Hydrology or flood history
2. Hydraulic conditions
3. Geotechnical - bed and bank material evaluation
4. Watershed sediment yield
5. Incipient motion analysis
6. Armoring potential
7. Rating curve shifts
8. Scour conditions

Appendix B of these guidelines provides a worksheet for a Level Two scour analysis. The following is a discussion of each of these eight steps:

HYDROLOGY

The discharge estimate used in the scour screening procedure should not be used for scour design. The Michigan Department of Environmental Quality (MDEQ) will not provide flood frequency discharge estimates for scour evaluation studies. Therefore, it is recommended that a range of flood discharges that approximate the 2 percent, 1 percent, and 0.2 percent chance floods be used. If flood estimates are not readily available, the MDEQ recommends the following methods for estimating flood discharges:

- For drainage areas less than 20 square miles use:

"Computing Flood Discharges for Small Ungaged Watersheds," by Rick Sorrell, P.E., Michigan Department of Environmental Quality, October 2001.
- For drainage areas greater than twenty square miles use:

"DNR/USGS Peak Flow Regression," by Hope Meyers Croskey, Engineering-Water Management Division, Michigan Department of Natural Resources, February 1985. The accompanying report is "Statistical Models for Estimating Flow Characteristics of Michigan Streams," U.S. Geological Survey, Water-Resources Investigations Report 84-4207.
- Drainage area ratio method on gaged streams can be used where USGS gages exist, or recent MDEQ discharge estimates at or near the bridge may be used. The ratio of the drainage areas should be raised to the 0.89 power when estimating the discharge. This method should only be used if the hydrologic characteristics of the two drainage basins are similar.

Estimated discharges are for evaluation purposes only. Design and construction of structure repair, replacement, or scour countermeasures requires a discharge estimate from MDEQ with a permit application for the proposed work. The MDEQ discharge estimate should be compared with the range of discharges used in the scour evaluation. Engineering judgement should be used to determine if the scour evaluation is adequate.

NOTE: The use of a flood hydrograph is beneficial to scour analysis since it can illustrate the time and duration that hydraulic forces are present to transport bed material. However, development of flood hydrographs for the recommended range of flood flows is beyond the scope of a Level Two analysis and is recommended for Level Three.

HYDRAULICS

Chapter 2 of HEC-18 recommends the utilization of existing hydraulic studies. If these studies are not available, a "worst-case analysis" is suggested. It is assumed that a detailed hydraulic survey of the channel cross sections will not be done. Channel cross sections can be developed based on existing bridge plans, topographic maps, and data gathered during the Level One field investigation. These cross sections should have a minimum of eight station points to define the cross section. A sufficient number of cross sections downstream of the structure should be input to achieve a normal water surface. Duplication of existing cross sections is an acceptable technique.

MDOT recommends the use of the U.S. Army Corps of Engineers Hydrologic Engineering Center HEC-RAS computer program for the computation of water surface profiles and the hydraulic parameters needed in the scour calculations.

GEOTECHNICAL

A soil gradation curve of streambed and overbank material is needed to determine the D_{50} and D_{84} particle sizes for use in the respective contraction scour and pier scour equations. Gradation curves or soil boring information used in the original plans of the structure can be used. A geotechnical engineer should be consulted for an estimation of the D_{50} and D_{84} .

If existing plans or soil information are not available, analyze based on the worst-case scenario. It is recommended that Laursen's live bed contraction scour equation be used with a $K_1=0.69$.

WATERSHED SEDIMENT YIELDS

The availability of watershed yield is imprecise. Information on Michigan streams is limited and, therefore, not used in the overall evaluation of a Level Two Analysis.

INCIPIENT MOTION ANALYSIS

Use of the Shields relation (Chapter 6 of HEC-20) for the range of discharges may provide information on the channel stability and what flood may cause stream channel instability. This relation is recommended for gravel or cobble stream systems only.

ARMORING POTENTIAL

Determination of the potential armoring of a streambed is discussed in Chapter 6 of HEC-20.

RATING CURVE SHIFTS

USGS stream gage data is limited to a few locations on Michigan streams. Analyses of rating curve shifts have not been completed in Michigan. Therefore, this portion of a Level Two analysis cannot be done.

SCOUR CALCULATIONS

Scour has three additive components: local scour at abutments and piers, contraction scour, and aggradation/degradation of the streambed. HEC-18 provides detailed computational procedures. The total scour depth should be reviewed by geotechnical and structural engineers to evaluate the stability of the structure.

LEVEL THREE - MATHEMATICAL AND PHYSICAL MODEL STUDIES

A detailed evaluation and assessment of stream stability can be completed by either mathematical or physical model studies. However, such studies are beyond the scope and monies available for a majority of Michigan projects.

NATIONAL BRIDGE INVENTORY SYSTEM (NBIS)

The scour evaluation program should result in the proper code for Item 113 of the NBIS. For state trunkline structures, the worksheet with the appropriate code should be forwarded to the Hydraulics/Hydrology Unit for review after each level of analysis. A copy of the Structure Inventory and Appraisal (SI&A) form (MDOT form Q1717A) will then be forwarded to the Bridge Operations Unit of MDOT. Local Agencies should send the SI&A form to the Bridge Operations Unit, Construction and Technology Division, Michigan Department of Transportation, P.O. Box 30049, Lansing, Michigan, 48909. Local agencies may also submit the form electronically.

PLAN OF ACTION AND SCOUR COUNTERMEASURES

Scour countermeasures are needed at the bridge to make it less vulnerable to either damage or failure from scour. For existing bridges, recommended countermeasures include:

- Riprap at piers and abutments with monitoring (visual, cross sections, instrumentation, etc.) during and after flood events
- Guide banks
- Channel improvements
- Strengthening bridge foundations
- Relief bridges

A plan of action is needed and can be part of the Level Two documentation. The plan of action should be developed among the hydraulic, geotechnical, and structural engineers. Examples include the following:

- Monitor for scour during regular bridge inspection
- Increase monitoring frequency
- Temporary countermeasures - riprap and monitor
- Selection of scour countermeasures
- Scheduling of scour countermeasure construction

LEVEL ONE WORKSHEET

Revised 5/06/02

MICHIGAN DEPARTMENT OF TRANSPORTATION
LEVEL ONE SCOUR ANALYSIS WORKSHEET

Date: _____ By: _____ Structure No: _____ Control Section: _____

Job No. _____ Route: _____ Watercourse: _____

All references are to HEC-20, 3rd Edition.**Data Collection**

- _____ Plans
 _____ Bridge Inspection Reports (Maintenance Division)
 _____ Underwater Inspection Reports (Maintenance Division)
 _____ Review existing items 60, 61, 71, 92, 93, and 113 of the NBIS
 _____ Review available construction, design, and maintenance files for repair and maintenance work done on structure

Field Investigation Date: _____

_____ Channel bottom width approximately one bridge span upstream = _____ feet

_____ Overbank and channel Manning's roughness coefficients

_____ Left _____ Channel _____ Right

_____ Is there sufficient riprap? Abutments _____ Piers _____

_____ Photographs

_____ Cross sections at upstream and downstream faces of bridge

Comments:

Stream Characteristics

_____ Complete the attached Figure 2.6 from HEC-20.

Comments:

Land Use: Identify the existing and past land use of the upstream watershed:

Urban Area	Yes__	No__	Comments:
Sand and Gravel Mining	Yes__	No__	Comments:
Undeveloped Land	Yes__	No__	Comments:

Lateral Stability: Refer to HEC-20, Section 2.3.9 on Channel Boundaries and Vegetation for channel bank stability. Comment:

Vertical Stability:

- streambed elevation change from as-built plans? Yes _____ No _____
- exposed pier footings (degradation)? Yes _____ No _____
- exposed abutment footings (degradation)? Yes _____ No _____
- channel bank caving in (degradation)? Yes _____ No _____
- eroding floodplain (aggradation)? Yes _____ No _____
- crossing at confluence or tributaries? Yes _____ No _____
- bridge sites upstream and downstream? Yes _____ No _____
- grade or hydraulic controls, i.e. dams, weirs, diversions? Yes _____ No _____
- foundation on rock Yes _____ No _____
- channel armoring potential Yes _____ No _____

Comments:

Stream Stability: Make a qualitative assessment of the overall stream stability by referring to the above information and Figure 2.6 and Table 3.2 from HEC-20 (attach copies of figures).

Stable _____ Unstable _____ Degrading _____ Aggrading _____

Comments:

RECOMMENDED NBIS ITEM 113 CODE: _____

LEVEL TWO ANALYSIS NEEDED: YES ___ **NO** ___

Worksheet approved by: _____ P.E. License # _____ Date _____

LEVEL TWO WORKSHEET

Revised: 5/06/02

MICHIGAN DEPARTMENT OF TRANSPORTATION
LEVEL TWO SCOUR ANALYSIS WORKSHEET

Date: _____ By: _____

Structure No: _____ Control Section: _____ Job No. _____

Route: _____ Watercourse: _____

Page numbers refer to HEC-20, 3rd Edition and HEC-18, 4th Edition. Attach water surface profile modeling printouts with pertinent variables highlighted. Scour calculations automatically done by HEC-RAS are not acceptable. All calculations must be attached or on the back of their respective pages.

1. **Hydrology:**

Method of Analysis: DEQ estimate, SCS, Regression, DAR to gage, other

Drainage Area: _____ square miles

Q₅₀ = _____ cfs Q₁₀₀ = _____ cfs Q₅₀₀ = _____ cfs2. **Hydraulics:** Water surface profiles by: HEC-2 ___ WSPRO ___ HEC-RAS ___3. **Geotechnical:** Bed and overbank material values:D₅₀ ___ D₈₄ ___ (ft) Left OverbankD₅₀ ___ D₈₄ ___ (ft) Right OverbankD₅₀ ___ D₈₄ ___ (ft) Main Channel

Source of information:

4. **Incipient motion analysis:** For gravel and cobble streams only. Refer to Page 6.14 of HEC-20.5. **Armoring potential:** Refer to Page 6.16 of HEC-20.

LEVEL TWO SCOUR ANALYSIS WORKSHEET

Str. No. ____ C.S. _____ Job No. _____ By: _____ Date: _____

6. **Scour calculations**

LONG-TERM BED ELEVATION CHANGES - AGGRADATION/DEGRADATION

___ Use information from **Level One** Analysis

___ Use information from bridge inspection reports

___ Estimate change during the next 100 years if enough information exists

Estimated aggradation/degradation = ____ feet

*** Do not adjust fixed bed hydraulics for contraction scour and local scour. If channel has aggraded, do not adjust the estimated scour depth.

CONTRACTION SCOUR (Section 5.2, HEC-18)

Bridge Site Condition:

CASE: 1a__ 1b__ 1c__ 2__ 3__ 4__

Compare critical velocity V_c to the mean velocity V .

$$V_c = 11.17 y^{1/6} D^{1/3} \text{ (p. 5.2, HEC-18)}$$

$y =$

$D_{50} =$

$V_c =$

If $V_c < V$, use Laursen's Live-Bed contraction scour.

If $V_c > V$, use Laursen's Clear-Water contraction scour.

If coarse sediments in bed material, see p 5.12, HEC-18.

LEVEL TWO SCOUR ANALYSIS WORKSHEET

Str. No. _____ C.S. _____ Job No. _____ By: _____ Date: _____

Laursen's live-bed scour equation (p 5.10, HEC-18):

$$y_2/y_1 = (Q_2/Q_1)^{6/7} (W_1/W_2)^{k_1} \text{ and}$$

$$y_s = y_2 - y_0 = \text{average contraction scour depth (feet)}$$

y_1	= _____ ft	V^*	= _____ ft/s
y_2	= _____ ft	ω	= _____ ft/s
y_0	= _____ ft	S_1	= _____ ft/ft
W_1	= _____ ft	V^*/ω	= _____
W_2	= _____ ft	k_1	= _____
Q_1	= _____ cfs	y_s	= _____ ft
Q_2	= _____ cfs		

Laursen's Clear-Water Contraction Scour (p. 5.12, HEC-18)

$$y_2 = (0.0077 Q^2 / (D_m^{2/3} W^2))^{3/7}$$

$$y_s = y_2 - y_0 = \text{average scour depth (feet)}$$

y_0	= _____ ft	D_m	= _____ ft
y_2	= _____ ft	D_{50}	= _____ ft
Q	= _____ cfs	y_s	= _____ ft
W	= _____ ft		

LOCAL SCOUR**ABUTMENTS**

Froehlich's live-bed scour equation. (If $L'/y_1 > 25$, use HIRE equation, p. 7.8, HEC-18.)

$$\text{Froehlich's equation: } y_s / y_a = 2.27 K_1 K_2 (L'/y_a)^{4.3} (Fr)^{0.61} + 1 \quad (\text{p. 7.8, HEC-18})$$

LEVEL TWO SCOUR ANALYSIS WORKSHEET

Str. No. _____ C.S. _____ Job No. _____ By: _____ Date: _____

		<u>Left Abutment</u>	<u>Right Abutment</u>
K_1	=	_____	_____
K_2	=	_____	_____
L'	=	_____ ft	_____ ft
A_e	=	_____ ft ²	_____ ft ²
Q_e	=	_____ cfs	_____ cfs
V_e	=	_____ ft/s	_____ ft/s
Fr	=	_____	_____
y_a	=	_____ ft	_____ ft
y_s	=	_____ ft	_____ ft

PIER(S)

Colorado State University equation (p. 6.2, HEC-18):

$$y_s/y_1 = 2.0 K_1 K_2 K_3 K_4 (a/y_1)^{0.65} (Fr_1)^{0.43}$$

Pier #:		_____	_____	_____
y_1	=	_____ ft	_____ ft	_____ ft
K_1	=	_____	_____	_____
K_2	=	_____	_____	_____
K_3	=	1.1	1.1	1.1
K_4	=	_____	_____	_____
a	=	_____ ft	_____ ft	_____ ft
V_1	=	_____ ft/s	_____ ft/s	_____ ft/s
Fr_1	=	_____	_____	_____
y_s	=	_____ ft	_____ ft	_____ ft

Note: If there is a possibility of channel migration, use the worst-case condition for all piers. For complex pier foundations, see Section 6.4, HEC-18.

SUMMARY

LEVEL TWO SCOUR ANALYSIS WORKSHEET

Str. No. ____ C.S. _____ Job No. _____ By: _____ Date: _____

100 YEAR

Element	Long-term (ft)	Contraction (ft)	Local (ft)	Total (ft)
Left Abutment				
Right Abutment				
Pier #				
Pier #				
Pier #				

Adjust total scour depth as needed if scour holes overlap.

500 YEAR

Element	Long-term (ft)	Contraction (ft)	Local (ft)	Total (ft)
Left Abutment				
Right Abutment				
Pier #				
Pier #				
Pier #				

____ Attach sketch or marked copy of existing design plan showing 100-year and 500-year total scour depths in relation to foundation. Foundation elevations must be shown.

Geotechnical Evaluation of scour results by: _____

Structural Evaluation of scour results by: _____

Is the structure stable under the estimated scour depth presented in this scour evaluation?

Yes ___ No ___

RECOMMENDED NBIS ITEM 113 CODE: ____ (p. J.14, HEC-18)

LEVEL TWO SCOUR ANALYSIS WORKSHEET

Str. No. ____ C.S. _____ Job No. _____ By: _____ Date: _____

ATTACHMENTS:

1. Calculations
2. Water surface profile computer output with pertinent values highlighted
3. Sketch of bridge with scour depths in relation to foundation
4. Scour countermeasure calculations with plans showing limits of countermeasures
5. Recommended plan of action

Worksheet approved by: _____ Date: _____

P.E. LICENSE # _____

Additional comments:

Appendix 4.B

Scour Evaluation Methods Practiced by Other States

Illinois

Website: <http://dot.state.il.us/default.asp>

Contact: William M. Kramer
State Foundations and Geotechnical Engineer
(217) 782-7773
William.Kramer@illinois.gov

Matt O'Connor
Bridge Hydraulic Engineer
matthew.oconnor@illinois.gov

Manuals: Illinois Drainage Manual, HEC-18, HEC-20 and HEC-23 Highways and River Environment (HIRE).

Scour Calculation Method: Utilizes methods from HEC-18 outlined within Illinois Drainage Manual.

Description: Three manuals are currently available to provide guidance for bridge scour and stream stability analyses. They are part of a set of Hydraulic Engineering Circulars (HEC) issued by FHWA. HEC 18, Evaluating Scour at Bridges Fourth Edition, contains equations for computing scour depths and designing countermeasures. HEC 20, Stream Stability at Highway Structures Third Edition, provides a guide for identifying stream instability problems. HEC 23, Bridge Scour and Stream Instability Countermeasures Second Edition, provides guidelines for the selection and design of appropriate countermeasures to mitigate potential damage to bridges and other highway components at stream crossings. HEC 18 forms the primary basis of the text in this chapter and is an excellent reference for more in-depth information.

Current Research: Illinois DOT has a study under way on the SRICOS- EFA. The Erosion Function Apparatus (EFA) is used in conjunction with the Scour Rate in Cohesive soils (SRICOS) method of scour prediction. The SRICOS method is a site specific method that involves collecting soil samples and testing them in the EFA. This research includes field verification of SRICOS-EFA and Synthetic Hydrograph generation for Illinois Streams. The Scour rate in cohesive soils Erosion function apparatus methodology provides potentially useful methodology for assessing scour in cohesive soils. The overall objective of this study is to test the SRICOS-EFA method for estimating scour depth of cohesive soils in Illinois Streams.

Past Research: None

Indiana

Website <http://www.in.gov/dot/>

Contact: Bill Dittrich
Hydraulics Engineer Supervisor
317-232-5474
bdittrich@indot.in.gov

Manuals: The Indiana Design Manual: Hydrology and Hydraulics, HEC-18 and HEC-20, AASHTO Model Drainage Manual.

Scour Calculation Method: Utilizes methods from HEC-18 and AASHTO Model Drainage Manual.

Description: Before the various scour forecasting methods for contraction and local scour can be applied, it is necessary to obtain the fixed bed channel hydraulics, estimate the profile and plan form scour or aggradation, adjust the fixed bed hydraulics to reflect these changes and compute the bridge hydraulics. Refer to Ch. 10 AASHTO Model Drainage Manual, Chapter 10 for combining the contraction and local scour components to obtain a total scour. There are two methods described within this manual, Indiana DOT typically uses method one. Method one, armoring is not a concern or precise scour estimates are not necessary and method two armoring is of concern and more precise scour estimates are pertinent. IDOT typically utilizes method one. Method one is:

1. Estimate the natural channel's hydraulics for a fixed bed condition based on existing conditions.
2. Assess the expected profile and plan form changes.
3. Adjust the fixed bed hydraulics to reflect any expected profile or plan form changes.
4. Estimate contraction scour using the empirical contraction formula and the adjusted fixed bed hydraulics assuming no bed armoring.
5. Estimate local scour using the adjusted fixed bed channel and bridge hydraulics assuming no bed armoring.
6. Add the local scour to the contraction scour to obtain the total scour. If contraction scour is negative, then use zero for contraction scour.

General Description of Scour Analysis and Computations:

Decide which analysis method is applicable. Method 1 shall be used to evaluate existing bridges to identify significant potential scour hazards or, where armoring is obviously not of concern, on a proposed bridge. Method 2 should be used to evaluate bridges where

significant armoring may occur. Step 2. Determine the magnitude of the 100-year flood and the 500-year super flood. Step 3. Develop a water surface profile through the site's reach for fixed bed conditions using WSPRO or HEC-2. Step 4. Obtain the variables necessary to perform contraction and local scour. Step 5. Compute the predicted scour depths using the equations in HEC 18 for contraction and pier scour for the 100-year and 500-year floods or an overtopping flood of a lesser recurrence interval.

Current Research: None

Past Research: None

Additional Sources: Through a conversation with Bill Dittrich, many printed sources not updated and limited financial resources therefore no research is being conducted.

Iowa

Website: <http://www.dot.state.ia.us/>

Contact: Dave Claman, P.E.
Preliminary Bridge Engineer
Office of Bridges and Structures, Iowa DOT
david.claman@dot.iowa.gov
(515) 239 - 1487

Manuals: Use Appendix C from Office of Bridges and Structures HEC-18

Scour Calculation Method: At this time, IDOT recommends not using FHWA's abutment scour equations or, at most, use them with caution. However, be aware that abutment scour can occur. Concerning pier scour, the equation in HEC-18 generally gives reliable results. However, a much simpler method that gives very similar results is found in Iowa Highway Research Board's Bulletin No. 4, "Scour Around Bridge Piers and Abutments," by Emmett M. Laursen and Arthur Toch, May 1956. This method for estimating pier scour can be used in most cases instead of the methods in HEC-18.

Description: The Federal Highway Administration has attempted to find the best equations and published them in HEC-18. HEC-18 contains equations for contraction scour, abutment scour and pier scour. The contraction scour equations are the best available equations of their type and sometimes provide reliable estimates, although these estimates still need to be evaluated considering soil types, site scour history, etc. The abutment scour equations frequently give questionable estimates. Because of comments similar to this from various states, FHWA is conducting additional research to develop new methods. Contraction Scour Use HEC-18, Most Iowa stream channels will be live-bed. In other words, the velocities in the channel will be high enough to cause movement of the soil particles in the streambed. In order to be sure if the channel is live-bed, Chapter 2 in HEC-18 gives a simple equation to calculate the velocity needed to cause

movement of the soil, Live-bed scour From HEC-18, Clear-water scour From HEC-18, do not calculate abutment scour at this time due to this questionable equation.

Current Research: Research is being performed at the University of Iowa's Hydraulic Institute, NCHRP 24-20 which is reviewing abutment scour in compound channels.

Past Research: The Center for Transportation Research and Education at Iowa State University has released a report that examines the first integral abutment bridge in the state of Iowa that utilized precast, prestressed concrete piles in the abutment. Use "Scour Around Bridge Piers and Abutments", Emmett M. Laursen Highway Research Board, Bulletin No. 4, 1956. This report outlines procedures both field and laboratory for investigation of scour around piers and abutments. The material used was sand. "Scour at Bridge Crossings," Emmett M. Laursen Iowa Institute of Hydraulic Research

Kansas

Website: <http://www.ksdot.org/>

Contact: Tom Allen
Publications Writer
thallen@ksdot.org

Manuals: KU-HR Bridge Scour Program User's Manual First Edition

Description: This study was performed to develop a computer program for analyzing bridge scour. The program is referred to as KU-BSP. The visual basic program used the methods presented in HEC-18 and the hydraulic modeling results of HEC-RAS Version 3.1.2. The program allows users to compute contraction, abutment and pier scour at bridges using hydraulic and geometry parameters from HEC-RAS output. The complex pier scour calculations presented in HEC-18 can be used with this program. This option is not available in scour module of HEC-RAS 3.1.2. This document outlines the functions of KU-BSP, the compatibility with HEC-RAS, and is an overall step-by-step user-friendly manual for the KU-BSP program.

There are three types of scour incorporated into KU-BSP, Contraction Scour, Pier Scour, and Abutment Scour. Contraction Scour is based off of HEC-18 and incorporates either Live Bed Scour or Clear Water Scour. The Pier Scour is based off of HEC-18 and incorporates the CSU equation. In addition complex pier scour analysis is included, where either the footing (pile cap) or the footing and the pile group are exposed to flow. Each of these factors can be contributors to pier scour. Therefore utilizing superposition a total pier scour may be determined by adding the three components (pile cap, pier stem, and pile group). Abutment Scour is based off of HEC-18 Foehlich's live-bed abutment scour equation and the HIRE live bed abutment scour equation. The KU-BSP may be used to account for the hydraulic effect of contraction scour before computing pier scour and/or abutment scour.

Current Research: None

Past Research: None

Kentucky

Website: <http://www.transportation.ky.gov/default2.html>

Contact: David Moses
Chief Drainage Engineer
david.moses@ky.gov

Manuals: Drainage Guidance Manual Ch.8 Bridges, Correlation of Rock Quality and Rock Scour Around Bridge Piers and Abutments Founded on Rock, HEC-18, and HEC-20.

Scour Calculation Method: Refer to HEC-18 and HEC-20 for bridge scour evaluation.

Description: Calculate the 100-year and 500-year storm and design bridge according to larger scour potential.

Additional Sources: Kentucky Transportation Center, <http://www.ktc.uky.edu/>

Current Research: An investigation on three sided bottomless culvert scour countermeasures research.

Past Research: Correlation of Rock Quality and Rock Scour Around Bridge Piers and Abutments Founded on Rock. There is much information on local for unconsolidated alluvial material, however there is a lack of information pertaining to scour on abutments and piers located on rock. The purpose is to study is to evaluate scour around bridge piers and abutments founded on rock.

http://www.ktc.uky.edu/Reports/KTC_99_57_SPR_94_157.pdf

Maryland

Website: <http://www.mdt.state.md.us/mdta/servlet/dispatchServlet?url=/Home/main.jsp>

Contact: Stan Davis
410-545-8362
SDavis6@sha.state.md.us

Andrzej Kosicki
Assistant Division Chief - Bridge Design Division
akosicki@sha.state.md.us

Manuals: Manual of Hydrologic and Hydraulic Design Ch. 11, HEC-18, HEC-20, HEC-23, HIRE, AASHTO Model Drainage Manual, 1998, AASHTO Standard Specifications for Highway Bridges, Sixteenth Edition, 1996 and including all Interim Revisions through 2002, Corps of Engineers Hydraulic Engineering Center, UNET—One Dimensional Unsteady Flow Through a Full Network of Open Channels, User's Manual, CPD-66, Version 3.1, 1996.

Scour Calculation Method: Reference Manual of Hydrologic and Hydraulic Design Ch. 11 which refers to HEC-18.

Description: This Chapter is based on and incorporates the recommendations and policy guidance of various FHWA, AASHTO and ASCE manuals and guidelines. The FHWA Manuals have served as basic guidelines in the preparation of Chapter 11. The FHWA guidance has been expanded on or modified where necessary in keeping with the experience and practices of the Office of Bridge Development (OBD) as set forth in this Manual for Hydrologic and Hydraulic Design.

One-dimensional hydraulic models such as the Corps of Engineers HEC-RAS model is commonly used for this purpose. However, sites with complex flood flow patterns may warrant the use of a two dimensional model, such as the FESWMS model, to establish the hydraulic flow conditions. The ABSCOUR Program is to be used to estimate scour at bridges and bottomless arch culverts.

Current Research: None to date

Past Research: Estimation of Long-term bridge pier scour in cohesive soils at Maryland bridges using EFA/ SRICOS. This study consisted of three stages, using the erosion function apparatus (EFA) to characterize cohesive soils at selected bridge crossing sites in Maryland, developing a method to generate synthetic discharge hydrographs for ungaged sites in Maryland to provide the required inputs to SRICOS; and based on inputs from the first two stages, using the SRICOS method to predict bridge pier scour at the selected sites. This thesis comprises stages 1 and 3. Stage 2 was performed at the University of Maryland by other personnel, and is briefly described in this thesis as relevant to stages 1 and 3.

Minnesota

Website: <http://www.dot.state.mn.us/>

Contact: Andrea Hendrickson
State Hydraulic Engineer
651-366-4466
andrea.hendrickson@dot.state.mn.us

Manuals: Minnesota Department of Transportation Bridge Scour Evaluation Procedure for Minnesota Bridges. General guidelines for monitoring bridges are included in the

Mn/DOT Flood Response Plan for state bridges and the Bridge Scour Monitoring Plan for Local Roads. Bridge Inspection Manual contains FHWA National Bridge Inventory Rating System and Sufficiency Rating, MNDOT Smart Flag Coding.

Scour Calculation Method: HEC 18 and HEC 20. Additional considerations provided in, Practical Methods for Calculating Scour Practical Method for Calculating Scour. E.V. Richardson J. R. Richardson, located within the appendix of Bridge Scour Evaluation Procedure for Minnesota Bridges, and utilizes the same equations as HEC-18 but gives detailed instructions and examples.

Description: MnDOT has a primary screening process this process leads to determining whether the bridge is low risk, scour susceptible, or unknown. Next, a secondary screening process determines whether the bridge should be monitored, or move to a level 1 evaluation. The secondary screening process evaluates seven key parameters, historical scour performance, scour resistant foundations, debris and blockage, geomorphic conditions, hydraulic conditions, structural conditions, and special low risk conditions. The level 1 evaluation then determines the MnDOT Scour Codes or determines a level 2 evaluation is necessary. Within the Level 2 evaluation the MnDOT scour codes can be determined.

Current Research: None

Past Research: Analysis of Real Time Data by FHWA in response to flooding in 1997. USGS bridge scour data collection team to collect real-time scour (contraction and local) measurements at contracted bridge openings. An analysis of two sites that were surveyed during the April 1997 flooding is presented. Research for Bridge Scour Evaluation Procedure for Minnesota Bridges March 1995. Effects of Footing Location on Bridge Pier Scour. J. Sterling Jones Roger T. Kilgore Mark P. Mistichelli. This was a laboratory study conducted to investigate the effects of placement of footing versus pier scour.

Missouri

Website: <http://www.modot.mo.gov/>

Contact: Keith Ferrell
Structural Hydraulics Engineer
keith.ferrell@modot.mo.gov

Manuals: HEC 18, Bridge Design Manual Section 8.2 Missouri Department of Transportation. (2004), HEC-20.

Scour Calculation Method: Utilize HEC-18 and are presented in section 8.2 of Missouri DOT Bridge Design Manual.

Description: The methods used to calculate those depths are based on the FHWA HEC-18 publication (13), Abutment scour calculated using FHWA publication Highways in

the River Environment (HIRE), this is consistent with the required location of the approach cross-section in both HEC-RAS and WSPRO. If the threshold is exceeded for any one of the categories, the second stage of the risk analysis process, the Least Total Economic Cost (LTEC) design, should be employed. The FHWA publication HEC-17 provides detailed procedures for performing a LTEC design.

Current Research: None

Past Research: None

Nebraska

Website: <http://www.nebraskatransportation.org/>

Contact: Don Jisa
Hydraulics Engineer
djisa@dor.state.ne.us

Manuals: Nebraska Department of Roads. Bridge Operations and Procedures. (2005).

Scour Calculation Method: Currently use HEC-18 and HEC-20.

Description: In process of updating Bridge scour documents.

Current Research: None

Conducted Research: None

New Jersey

Website: <http://www.nj.gov/transportation/eng/>

Contact: Jose A. Lopez
Supervising Engineer
Dot.state.nj.us

Manuals: Current (2002) AASHTO Manual for Condition Evaluation of Bridges, Current (2002) AASHTO Standard Specification for Highway Bridges, Current FHWA Bridge Inspector Reference Manual, 1987 AASHTO Manual for Bridge Maintenance, 1994 NJDOT Underwater Inspection and Evaluation Guidelines Manual, 2003 FHWA Recording and Coding Guide for the Structure Inventory & Appraisal (SI&A) of the Nation's Bridges, 2003 NJDOT Recording and Coding Guide, 2003 NJDOT Pointis/Seismic manual, 1998 AASHTO Movable Bridge Inspection Maintenance Evaluation Manual and Standard Specifications for Movable Highway Bridges, 2006

Pointis Lite Users Manual. HEC-18 and HEC-23, Bridge Scour Evaluation Program Plan of Action Report.

Scour Calculation Method: Refer to Plan of Action Report which refers to HEC-18

Description: Bridge Scour Evaluation Program Plan of Action Report
Scour evaluation program started with the selection of a technical and Management Consultant to assist the department in the development and implementation of the program.

Divided into 4 stages, Stage 1 screening and prioritization process was developed to establish a logical sequence and focus on most critical needs. This process included the use of standard data forms and criteria for coding appraisal factors related to each bridge's potential susceptibility to scour damage. These key scour factors were, Type of Foundation, Bridge Characteristics, Collapse Vulnerability, Waterway Characteristics and History of Scour Problems. The tasks for the Stage 1 program included, the collection of readily available data and field visits by an interdisciplinary team of experienced hydraulic, structural and geotechnical engineers. Based upon these efforts numerical appraisal ratings were coded for the previously defined key scour factors. The ratings for the key scour factors were used to determine an overall numerical Scour Sufficiency rating from 0 to 100 which was used to assess the structures potential sufficiency to resist scour damage. In addition the scour evaluation consultants coded each bridge with a prioritization Category rating of 1 to 4, which assessed the necessity for in-depth scour evaluations. These ratings were then used to identify the bridges that were most susceptible to scour and required an in-depth evaluation to determine whether they were scour critical. Stage 2 In depth scour evaluation

The procedure recommended by HEC-18 for conducting a scour evaluation study includes a determination of waterway characteristics for flood flow conditions and the calculation of potential scour depths at the substructure units, followed by an assessment of the stability. Use Bridge Scour Evaluation Program Guidelines Manual for Stage 2 in depth scour evaluation (1994) for procedures and scope of work for scour analysis. The scope of work included within Stage 2 includes, Data collection and review, Field investigation, determination of scour analysis variables, scour analysis and evaluation, evaluation of countermeasures, bridge scour evaluation report.

Current Research: None.

Past Research: None.

New York

Website: <https://www.nysdot.gov/portal/page/portal/index>

Contact: Scott Lagace
Bridge Safety Assurance Unit

slagace@dot.state.ny.us

Wayne Gannett
Hydraulic Engineer
wgannett@dot.state.ny.us

Manuals: Bridge Manual NYDOT Structures design and Construction Division River Engineering for Highway Encroachments. FHWA. HEC18, 20 23 Highways in the River Environment. FHWA.

Scour Calculation Method: Utilize methods outlined in HEC-18, Nordin (1971) Straub (1940), Colorado State University's (CSU) equation, Jain and Fisher's equation, Graded and/or armored streambeds equations, Froehlich's equations.

Description: All bridges over water in New York State are assessed for scour vulnerability using the procedures outlined in the NYSDOT Hydraulic Vulnerability Manual. New bridges are evaluated for scour according to FHWA Hydraulic Engineering Circular No. 18 (HEC-18). HEC-23 is used for Countermeasure Design. The NYSDOT Hydraulic Vulnerability Assessment (HVA), Scour Analysis (if available), Countermeasure Installed (if present), and Bridge Inspection Erosion ratings are all taken into account when assigning a code for FHWA Item 113 - Scour Critical Bridges. In accordance with FHWA Technical Advisory T 5140.23, a Plan of Action will be developed for each bridge in New York State which is coded '0'-'3' (Scour Critical), '7' (Countermeasures Installed), or 'U' (Unknown Foundation) for Item 113. Part of the Plan of Action for NYSDOT bridges include placing the bridge on the Flood Watch list, which would then be monitored during a flood event. In addition, some bridges have a post flood inspection performed after a flood event.

Current Research: None

Past Research: None

Ohio

Website:

<http://www.dot.state.oh.us/Divisions/HighwayOps/Structures/Pages/default.aspx>

Contact: Bill Krouse, P.E.
Bridge Hydraulic Engineer
(614) 466-2398
Bill.Krouse@dot.state.oh.us

David Riley, P.E.
State Hydraulic Engineer
david.riley@dot.state.oh.us

Manuals and Papers: Bridge Design Manual (BDM) in section 203. 3 Scour and FHWA publication NHI 01-001 Evaluation Scour at Bridges fourth edition. ODOT Manual of Bridge Inspection, HEC-18.

Scour Calculation Method: Utilizes methods from HEC-18 referred to in Ohio Bridge Design Manual.

Description: The Department developed an alternative method of scour assessment based upon the observance of geomorphic, hydrologic and hydraulic features at the bridge site. This assessment is seen as a cost effective approach meeting the NBIS requirements for evaluating existing bridges without analytical scour computations.

A scour assessment of a bridge using the theoretical scour calculations is a method based on hydrologic and hydraulic analyses of the stream and bridge opening. The method is described in the Bridge Design Manual in section 203. 3 Scour and FHWA publication NHI 01-001 Evaluation Scour at Bridges fourth edition (HEC-18).

Current Research: None

Past Research: Time Domain Reflectometry (TDR) scour monitoring.

Pennsylvania

Website: <http://www.dot.state.pa.us/>

Contact: Lance Savant
PENNDOT – BQAD
717-783-7498
lsavant@state.pa.us

Scour Calculation Method: Use DM4 Chapter 7 and FHWA Technical Advisory. Evaluating Scour at Bridges. (T 5140.23 October 1991) for guidance on the methodology.

Manuals: Procedures for Bridge Scour Assessments. Peter J. Cinotto and Kirk E. White. Bridge Safety Inspection Manual 238, AASHTO Manual for the Condition Evaluation of Bridges, DM4 Chapter 7 and FHWA Technical Advisory. Evaluating Scour at Bridges. (T 5140.23 October 1991), Scour Calculator Manual.

Description: Pennsylvania with the assistance of USGS has developed Procedures for Bridge Scour Assessments at Bridges in Pennsylvania: This document outlines procedures for assessing bridge scour. Focusing on two methods, field reviewed bridge sites and office reviewed field sites. The field reviewed procedures identify appropriate methodologies and data to collect to analyze bridges susceptibility to bridge scour. Both these methods then enable the evaluator to identify an appropriate Scour-Critical Bridge

Indicator Code (Code) and a Scour Assessment Rating (Rating). This then enables a decision to be made on the appropriate scour countermeasures that are applicable, if any.

In addition publication 238 was developed and includes inspection methods, scour assessments recommendations and calculations. To combat this loss of structures from the transportation system and protect our valued infrastructure, PA uses a threefold approach:

- Underwater inspection of bridge substructure units are used to verify the structural condition of the underwater elements, to verify integrity of their foundations and to identify critical anti-scour maintenance needs.
- An assessment of the bridges vulnerability to scour is made so that critical bridges can be identified for closer monitoring and scour countermeasures.
- During high water events, bridges whose safety is very susceptible to scour are required to be monitored.

The two acceptable methods of performing scour assessments in PA are:

1. Theoretical Scour Calculations Use DM4 Chapter 7 and FHWA Technical Advisory. Evaluating Scour at Bridges. (T 5140.23 October 1991) for guidance on the methodology.
2. PA's Observed Scour Assessment for Bridges methodology. (Procedures for Bridge Scour Assessments at Bridges Pennsylvania outlines this methodology).

The PA OSAB uses an algorithm in a Department software program named SCBI/SAR Calculator to determine the value for BMS Item W06 Scour Critical Bridge Indicator. If the W06 SCBI value from the PA OSAB is based on conditions valid at the time of inspection, it should be used in the inspection as the value for BMS. In addition, a new data item call Scour Assessment Rating (SAR) was developed for the PA OSAB to assist bridge owners with another measure of threat for hydraulic failure of the bridge. The SCBI/SAR Calculator also computes the SAR that ranges from 0 to 100, extremely vulnerable to scour resistant. The SAR analysis also provides a list of potential scour-related deficiencies at the bridge.

Software User's Guide for Determining the Pennsylvania Scour Critical Indicator Code and Streambed Scour Assessment Rating for Roadway Bridges The Scour Critical Bridge Indicator (SCBI) Code and Scour Assessment Rating (SAR) use algorithms to rate bridge sites for observed and potential streambed scour on the basis of USGS field observations and or existing PennDOT data. SCBI Code indicates the vulnerability of the bridge to future scour. The SCBI is based on the FHWA code (NBI Item 113) and PennDOT's interpretation of the FHWA Code. The SCBI Code contains a whole number between 9 and 2. Each code number has one or more cases. Codes and cases are not a straightforward numeric sequence; they describe a specific type of site condition only; for example a code 6 isn't necessarily better or worse than a code 5. The SCBI Code and SAR calculator uses various factors from the field or office scour evaluations to

determine the SCBI Code for individual subunits and the bridge. The data fields that must be complete to determine the SCBI Code for each substructure unit.

The SAR is composed of component values for each bridge subunit and selected site conditions that are combined to provide an overall bridge rating from 0 to 100. It was designed by PennDOT and USGS to incorporate all factors that could lead to hydraulic failure at a bridge site. The SAR indicates the observed scour condition of a bridge site and generally can be interpreted as 100 to 80 =good, 79 to 51, average, 50 to 20= potential problems and 19 to 0= poor; however, all bridge-site data must be reviewed before making this interpretation.

Current Research: None

Past Research: Scour Calculator Code This report presents the instructions required to use the Scour Critical Bridge Indicator (SCBI) Code and Scour Assessment Rating (SAR) calculator developed by the Pennsylvania Department of Transportation (PennDOT) and the U.S. Geological Survey to identify Pennsylvania bridges with excessive scour conditions or a high potential for scour. Procedures for Scour Assessments at Bridges in Pennsylvania. This report describes procedures for the assessment of scour at all bridges that are 20 feet or greater in length that span water in Pennsylvania. There are two basic types of assessment: field-viewed bridge site assessments, for which USGS personnel visit the bridge site, and office-reviewed bridge site assessments

Virginia

Website: <http://www.virginiadot.org/>

Contact: Mr. Kendal Walus
State Structure and Bridge Engineer
Kendal.Walus@VDOT.Virginia.gov

Mr. John Matthews, P.E.
Assistant State Hydraulic Engineer
John.Matthews@VDOT.Virginia.gov

Mr. Stephen Kindy, P.E.
State Hydraulic Engineer
Stephen.Kindy@VOT.Virginia.gov

Manuals:HEC-18 Evaluating Scour at Bridges and Hec-20 Stream Stability at Highway Structures” HEC-23 Bridge Scour and Stream Instability Countermeasures Experience, Selection, and Design Guidance

Scour Calculation Method: Reference Virginia DOT Drainage Manual which references HEC-18 methods.

Description: The VDOT Drainage manual refers to procedures and criteria presented in the FHWA's "Evaluating Scour at Bridges" (HEC-18) and "Stream Stability at Highway Structures" (HEC-20) to determine and counteract the impact of scour and long term aggradation/degradation on bridges.

Current Research: None

Past Research: None

West Virginia

Website: <http://www.transportation.wv.gov/>

Contact: Douglas Kirk
State Hydraulics Engineer
douglas.w.kirk@wv.gov

Manuals: Bridge Design Manual Federal Highway Administration Technical Advisory T5140.23, "Evaluating Scour at Bridges, Design of Riprap Revetment, Hydraulic Engineering Circular No.11, (HEC11), Evaluating Scour at Bridges, Fourth Edition, Hydraulic Engineering Circular No. 18, (HEC 18), Stream Stability at Highway Structures, Third Edition, Hydraulic Engineering Circular No. 20, (HEC 20), Bridge Scour and Stream Instability Countermeasures Experience, Selection, and Design Guidance, Second Edition, Hydraulic Engineering Circular No. 23, (HEC 23) The WVDOH Drainage Manual, 3rd Edition, 2007 is online at: <http://www.transportation.wv.gov/highways/engineering/Pages/publications.aspx>. Relevant chapters are 7 and 10.

Scour Calculation Method: References HEC-18 for Scour computations, no drainage manual available on website.

Description: All designs will be performed in accordance with the Federal Highway Administration Technical Advisory T5140.23, "Evaluating Scour at Bridges". A DS-34 form will be completed during the design phase of the project. Refer to WVDOH Bridge Maintenance Directive (BMD) S-102-2 for additional information regarding the DS-34 form. Stated in the WV DOT Bridge Design Manual, scour calculations are based upon the discharge created by the flood of 1% annual incidence of return (Q100) and the "super flood" defined as 0.2% annual incidence of return (Q500). Scour depth, average stone size (D50) and any necessary designs shall be based upon the provisions of the following FHWA publications:

- Design of Riprap Revetment, Hydraulic Engineering Circular No.11, (HEC11)
- Evaluating Scour at Bridges, Fourth Edition, Hydraulic Engineering Circular No. 18, (HEC 18)
- Stream Stability at Highway Structures, Third Edition, Hydraulic Engineering Circular No. 20, (HEC 20)

- Bridge Scour and Stream Instability Countermeasures Experience, Selection, and Design Guidance, Second Edition, Hydraulic Engineering Circular No 23, (HEC 23)

Current Research: None

Past Research: None

Wisconsin

Website: <http://www.dot.wisconsin.gov/>

Contact: Najoua Ksontini
Bridge Hydraulic Engineer
najoua.ksontini@dot.state.wi.us

Manuals: Bridge Manual, HEC-18 and HEC-20

Scour Calculation Method: Utilizes methods from HEC-18, outlined within Wisconsin Bridge Manual.

Description: Evaluating scour potential at bridges is based on recommendations and background from FHWA Technical Advisory “Evaluating Scour at Bridges” dated October 28, 1991 and procedures from the FHWA Hydraulic Engineering Circular No. 18, Evaluating Scour at Bridges revised April 1993 (English), November 1995 (Metric), and Hydraulic Engineering Circular No. 20 Stream Stability at Highway Structures, February 1991 (English), November 1995 (Metric).

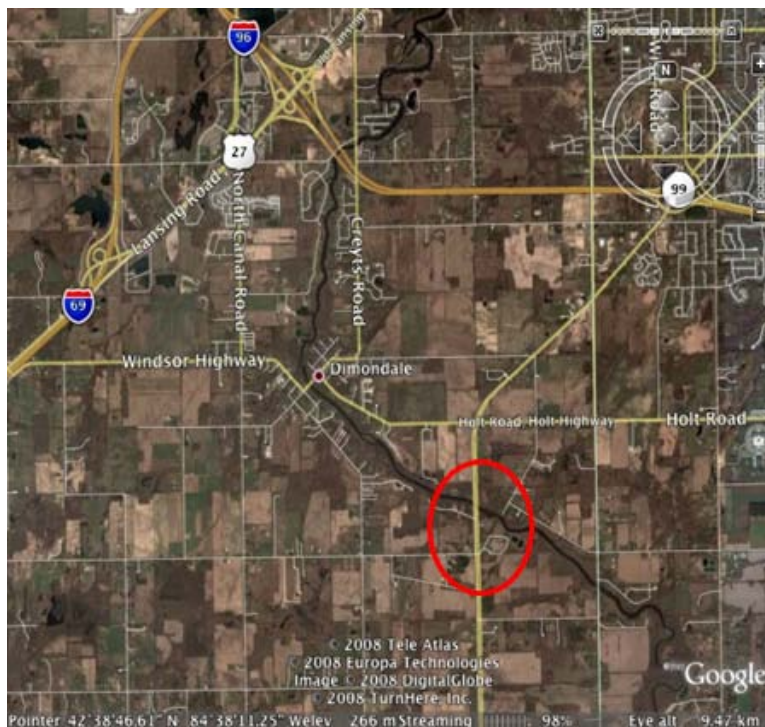
The bridge design manual contains all formulas used to calculate the three primary forms of scour, aggradation and degradation, local and contraction scour. Local scour is computed utilizing Colorado State University equation. Abutment scour is calculated utilizing Froelich’s Live-Bed Scour at Abutments and Highways and River Environment (HIRE) equation.

Current Research: None

Past Research: Bridge Scour Monitoring Methods at Three Sites in Wisconsin USGS Report. Two monitoring approaches were employed: (1) manual monitoring using moderately simple equipment, and (2) automated monitoring, using moderately sophisticated electronic equipment.

Appendix 4.C
Bridge Fact Sheets for Selected Sites

Figure 4.C.1 Grand River Site





Abutment Rating Comments

10 sft area of delam under beam 1w at the north abutment. Open vertical cracks in both abutments. Spalling from fires on both abutments approximately 10 sft total. Leaching map and diagonal cracking in all wing walls.

Pier Rating Comments

Pier 1s - Areas of STS and delam. Large area of leaching and delam in cantilevered section. Pier 2s areas of STS and few areas of horizontal, leaching random cracks.

Channel Rating Comments

Rocks and deep.

USGS Station Details

Ingham County, Michigan, Hydrologic Unit 04050004

USGS Station Location

--Lat 42°45'02", long 84°33'19" referenced to North American Datum of 1927, in NW ¼ sec.9, T.4 N., R.2 W., Ingham County, MI, Hydrologic Unit 04050004, on right bank 30 ft upstream from bridge on North Grand River Avenue in Lansing, 2.0 mi downstream from Red Cedar River, and at mile 152.

DRAINAGE AREA

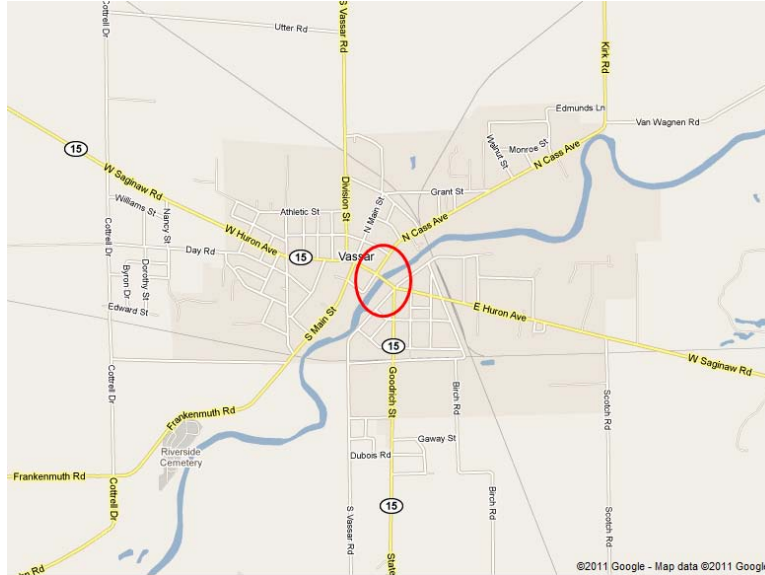
1,230 mi²

USGS URL

<http://wdr.water.usgs.gov/wy2009/pdfs/04113000.2009.pdf>

Figure 4.C.2 Cass River Site





Abutment Rating Comments

Vert, horiz & random crking in abuts also see other jts, N. backwall has numerous leaching cracks.

Pier Rating Comments

Repaired areas in S backwall.
 STS pier 3S E end. Light scale on nose of pier 1S. at the E.

Channel Rating Comments

5yr. underwater.

USGS Station Details

STREAMS TRIBUTARY TO LAKE HURON
 04151500 CASS RIVER AT FRANKENMUTH, MI

USGS Station Location

--Lat 43°19'40", long 83°44'53", in NW1/4 SE1/4 sec.27,
 T.11 N., R.6 E., Saginaw County, Hydrologic Unit 04080205, on right bank
 2,000 ft downstream from dam in Frankenmuth, 3,600 ft upstream from
 highway bridge on Dehmel Road, 3.4 mi upstream from Dead Creek,
 and 17 mi upstream from mouth.

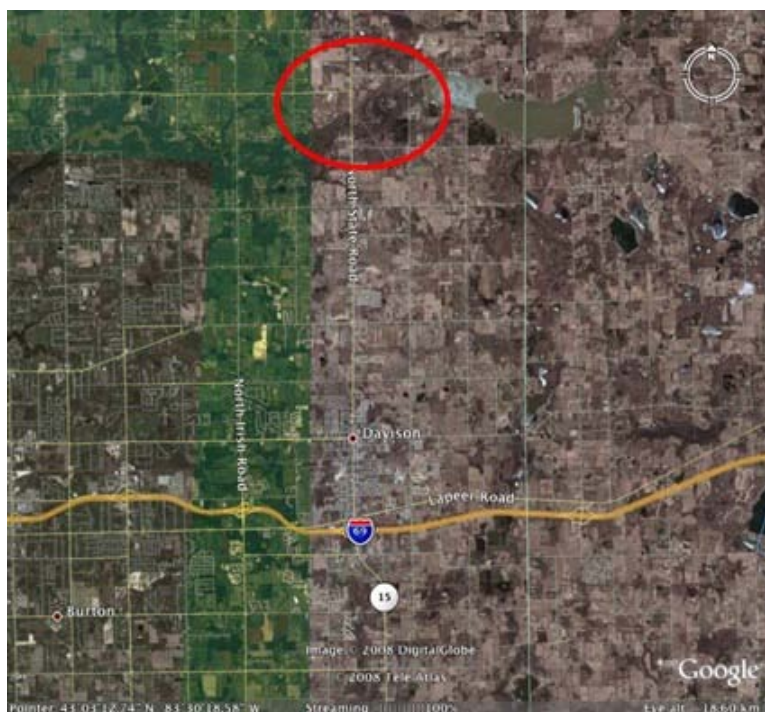
DRAINAGE AREA

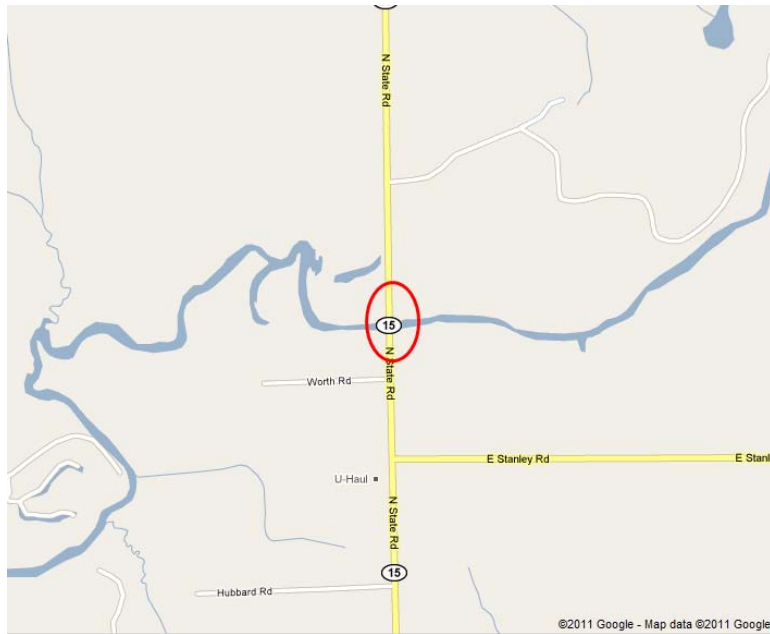
841 mi²

USGS URL

http://waterdata.usgs.gov/mi/nwis/uv/? site_no=04151500&PARAMeter_cd=00065,00060

Figure 4.C.3 Flint River Site





Abutment Rating Comments

Map and wet leaching cracks at South abutment.

Pier Rating Comments

Leaking and horizontal map cracks along the top of the pier on both sides. Top of pier has heavy scale and spalls under beams 3, 4, & 6, South side. Minor loss of section of exposed rebar.

Channel Rating Comments

Waded and probed - minor stream bed movement North side of pier. Top of footing exposed full length South side of pier 1s. Erosion of the south bank at Southeast and southwest quadrants.

USGS Station Details

STREAMS TRIBUTARY TO LAKE HURON
04147500 FLINT RIVER NEAR OTISVILLE, MI

USGS Station Location

Lat 43°06'40", long 83°31'10", in SE1/4 sec.9, T.8 N.,
R.8 E., Genesee County, Hydrologic Unit 04080204, on left bank 20 ft
downstream from bridge on State Highway 15, 1.5 mi downstream from
Holloway Reservoir, 3.5 mi upstream from Powers-Cullen Drain, and
3.8 mi south of Otisville.

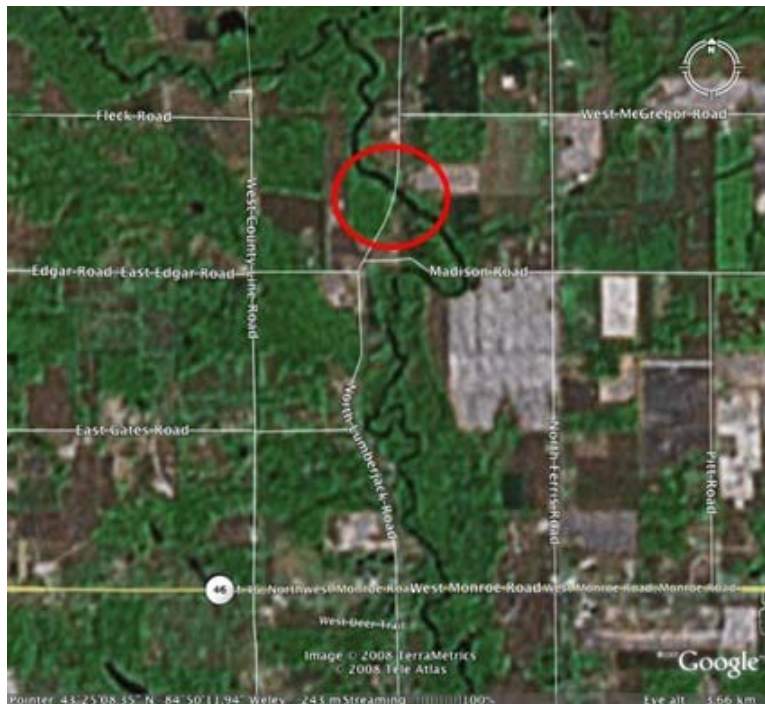
DRAINAGE AREA

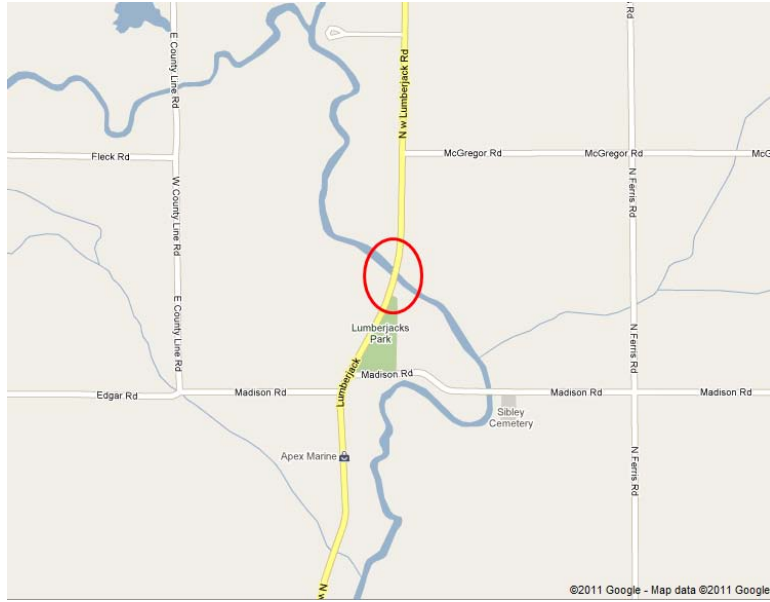
530 mi²

USGS URL

http://waterdata.usgs.gov/mi/nwis/uv/?site_no=04147500&PARAMeter_cd=00065,00060

Figure 4.C.4 Pine River (North) Site





Abutment Rating Comments

Noted minor vertical crack in center of both abutments.

Pier Rating Comments

Minor spall , 2 sft, on north and south face of pier wall. No exposed resteel

Channel Rating Comments

No Comments

USGS Station Details

Gratiot County, Michigan, Hydrologic Unit 04080202

USGS Station Location

-- Lat 43°22'46", long 84°39'20" referenced to North American Datum of 1927, in SW ¼ SE ¼ sec.34, T.12 N., R.3 W., Gratiot County, MI, Hydrologic Unit 04080202, on right bank 270 ft downstream from Superior Street Bridge in Alma, 0.6 mi downstream from municipal reservoir, and 38 mi upstream from mouth.

DRAINAGE AREA

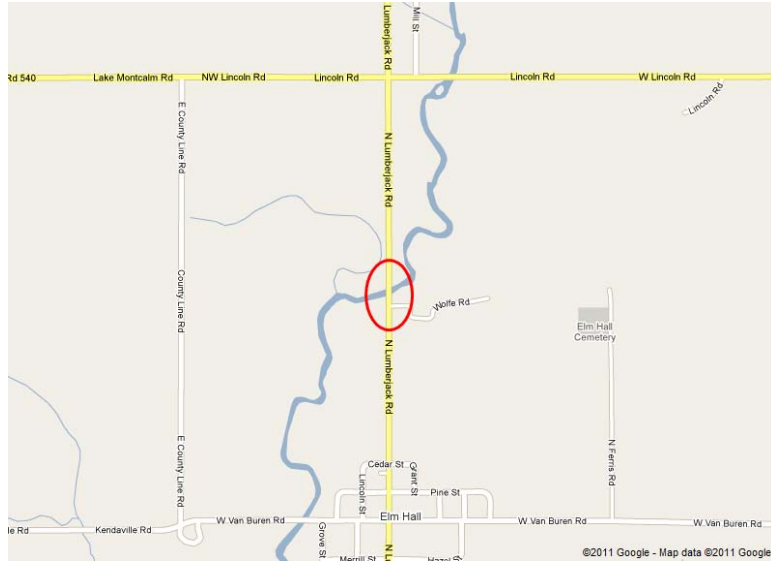
288 mi²

USGS URL

[Http://waterdata.usgs.gov/nwis/uv?04155000](http://waterdata.usgs.gov/nwis/uv?04155000)

Figure 4.C.5 Pine River (Middle) Site





Abutment Rating Comments

Noted minor vertical crack in center of both abutments.

Pier Rating Comments

Minor spall , 2 sft, on north and south face of pier wall. No exposed resteel

Channel Rating Comments

No Comments

USGS Station Details

Gratiot County, Michigan, Hydrologic Unit 04080202

USGS Station Location

-- Lat 43°22'46", long 84°39'20" referenced to North American Datum of 1927, in SW ¼ SE ¼ sec.34, T.12 N., R.3 W., Gratiot County, MI, Hydrologic Unit 04080202, on right bank 270 ft downstream from Superior Street Bridge in Alma, 0.6 mi downstream from municipal reservoir, and 38 mi upstream from mouth.

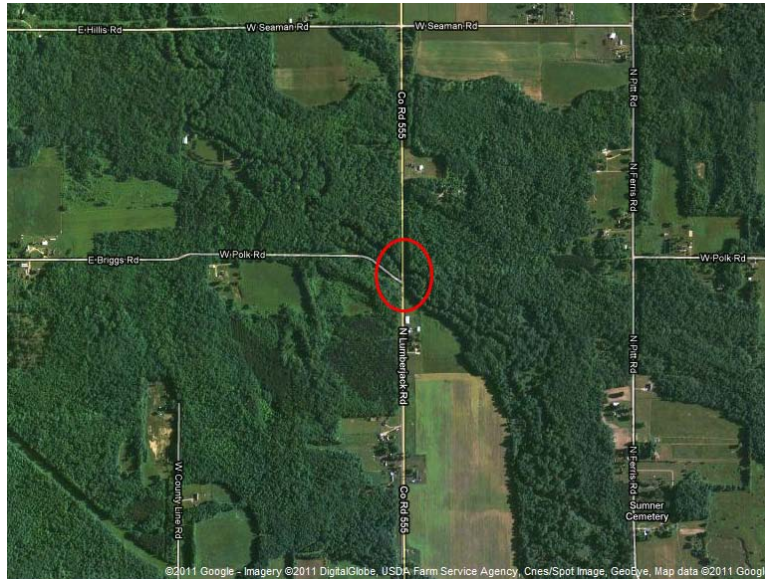
DRAINAGE AREA

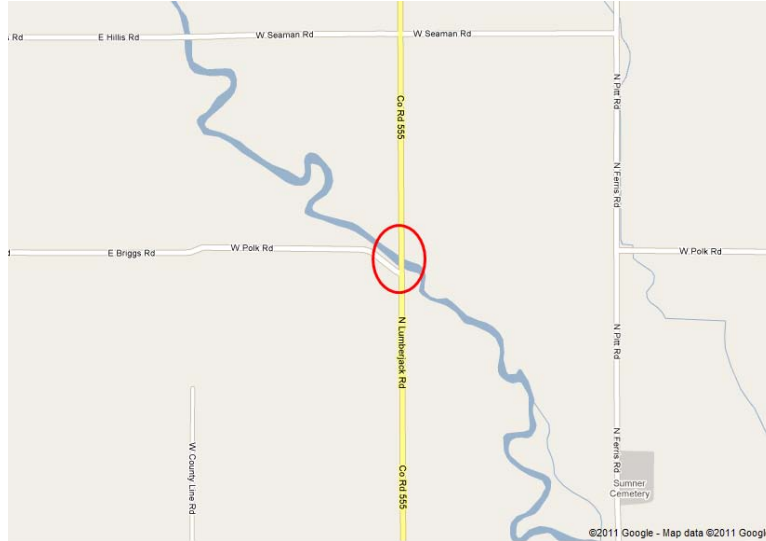
288 mi²

USGS URL

[Http://waterdata.usgs.gov/nwis/uv?04155000](http://waterdata.usgs.gov/nwis/uv?04155000)

Figure 4.C.6 Pine River (South) Site





Abutment Rating Comments

Noted minor vertical crack in center of both abutments.

Pier Rating Comments

Minor spall , 2 sft, on north and south face of pier wall. No exposed resteel

Channel Rating Comments

No Comments

USGS Station Details

Gratiot County, Michigan, Hydrologic Unit 04080202

USGS Station Location

-- Lat 43°22'46", long 84°39'20" referenced to North American Datum of 1927, in SW ¼ SE ¼ sec.34, T.12 N., R.3 W., Gratiot County, MI, Hydrologic Unit 04080202, on right bank 270 ft downstream from Superior Street Bridge in Alma, 0.6 mi downstream from municipal reservoir, and 38 mi upstream from mouth.

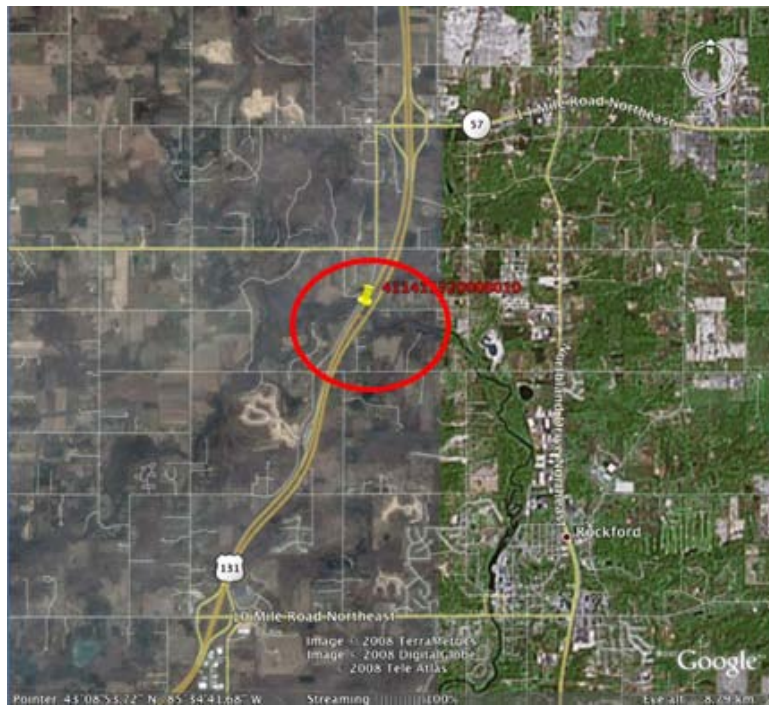
DRAINAGE AREA

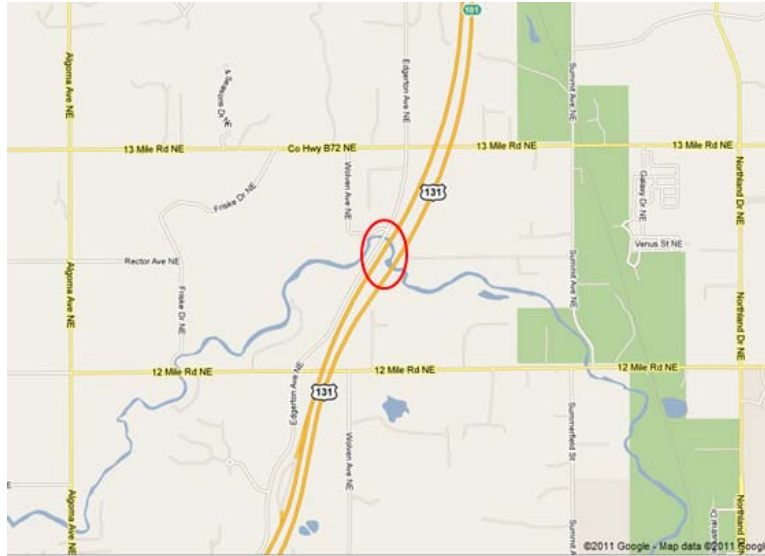
288 mi²

USGS URL

[Http://waterdata.usgs.gov/nwis/uv?04155000](http://waterdata.usgs.gov/nwis/uv?04155000)

Figure 4.C.7 Rogue River Site





Abutment Rating Comments

South abutment has 4" of footing exposed on the east end from the sand washing from slope. Joint 1S needs to be sealed up the curb and sand replaced on the slope to repair this problem. Few vertical shrinkage cracks.

Pier Rating Comments

Horizontal leaching cracks in cap ends of pier 1s. Pier 2s has a full length horizontal crack in cap with spall under beam 5w and spall near beam 6w. Steel column casings beginning to rust. Pier caps have debris on them from recent joint repair.

Channel Rating Comments

Waded through, no scour apparent, Large amount of debris along bents at pier 1s.

USGS Station Details

Kent County, Michigan, Hydrologic Unit 04050006

USGS Station Location

--Lat 43°04'56" long 85°35'27" referenced to North American Datum of 1927, in NE ¼ sec.15, T.8 N., R.11 W., Kent County, MI, Hydrologic Unit 04050006, on left bank at downstream side of bridge on Packer Drive, 2.2 mi upstream from mouth, and 3.0 mi southwest of Rockford.

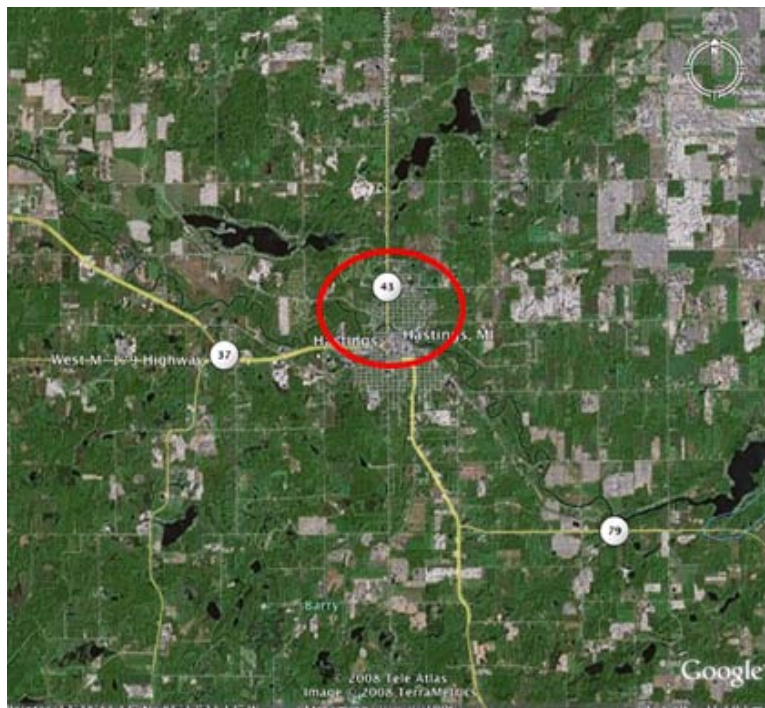
DRAINAGE AREA

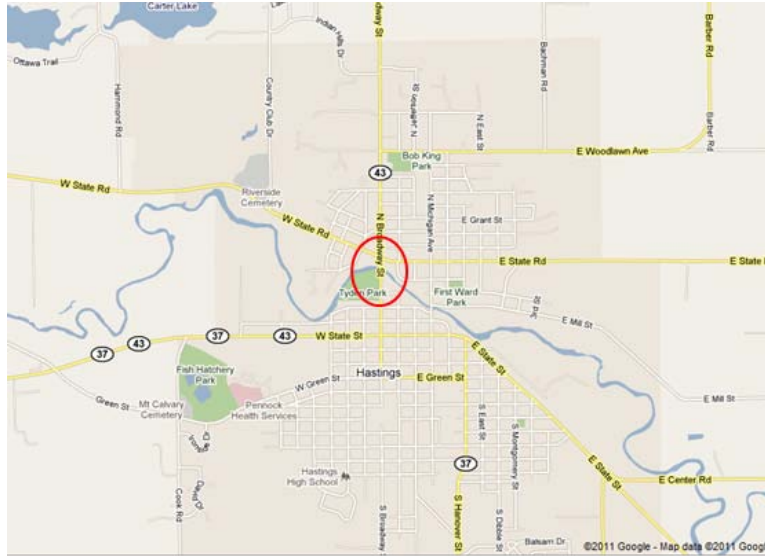
234 mi²

USGS URL

<http://waterdata.usgs.gov/nwis/uv?04118500>

Figure 4.C.8 Thornapple River at M-43 Site





Abutment Rating Comments

No Comments

Pier Rating Comments

No Comments

Channel Rating Comments

No Comments

USGS Station Details

Barry County, Michigan, Hydrologic Unit 04050007

USGS Station Location

--Lat 42°36'57", long 85°14'11" referenced to North American Datum of 1927, in SE ¼ sec.27, T.3 N., R.8 W., Barry County, MI, Hydrologic Unit 04050007, on right bank 100 ft upstream from bridge on McKeown Road, 0.6 mi downstream from Cedar Creek, 2.0 mi downstream from Thornapple Lake, and 3.2 mi southeast of Hastings.

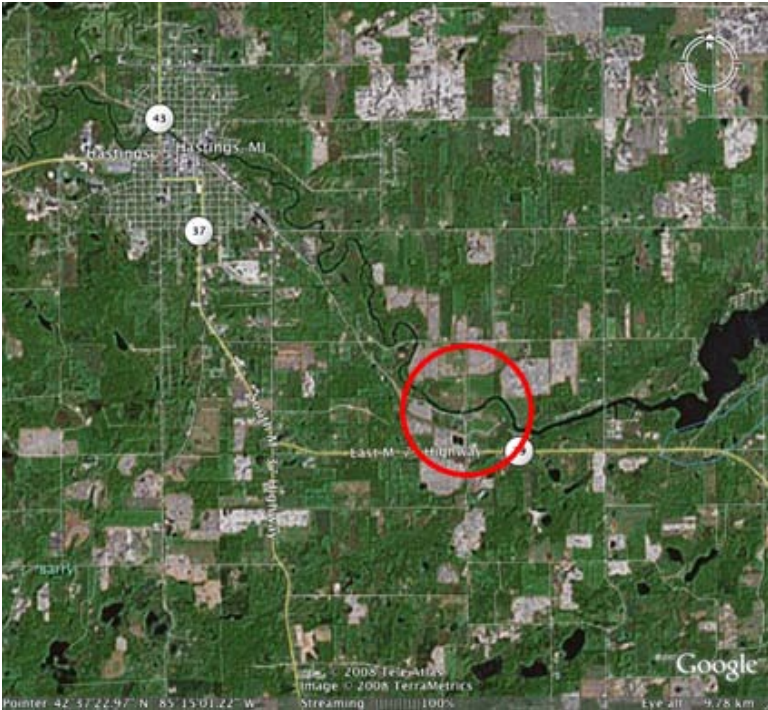
DRAINAGE AREA

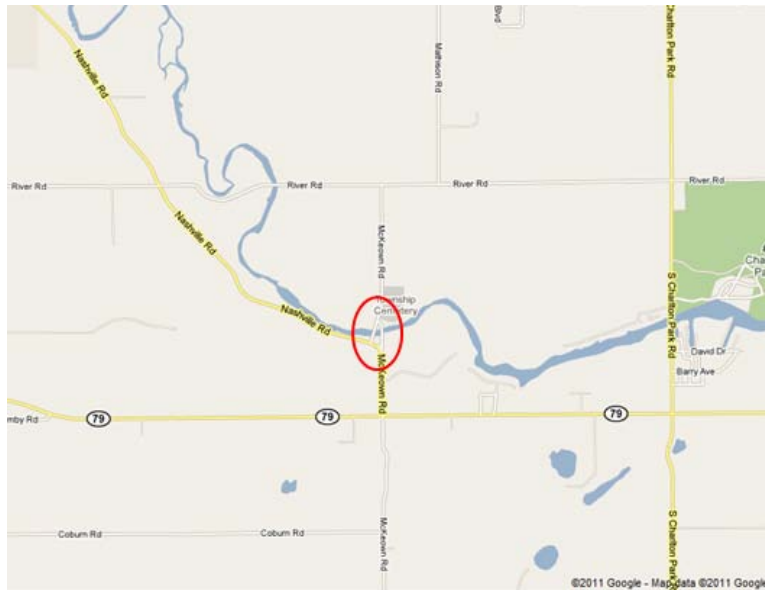
385 mi²

USGS URL

<http://waterdata.usgs.gov/nwis/uv?04117500>

Figure 4.C.9 Thornapple River at McKeown Site





Abutment Rating Comments

No Comments

Pier Rating Comments

No Comments

Channel Rating Comments

No Comments

USGS Station Details

Barry County, Michigan, Hydrologic Unit 04050007

USGS Station Location

--Lat 42°36'57", long 85°14'11" referenced to North American Datum of 1927, in SE ¼ sec.27, T.3 N., R.8 W., Barry County, MI, Hydrologic Unit 04050007, on right bank 100 ft upstream from bridge on McKeown Road, 0.6 mi downstream from Cedar Creek, 2.0 mi downstream from Thornapple Lake, and 3.2 mi southeast of Hastings.

DRAINAGE AREA

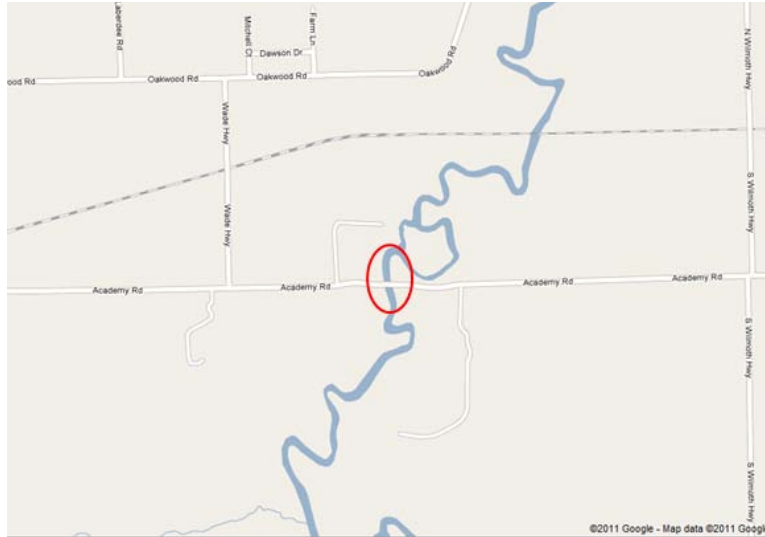
385 mi²

USGS URL

<http://waterdata.usgs.gov/nwis/uv?04117500>

Figure 4.C.10 River Raisin Site





Abutment Rating Comments

No comments

Pier Rating Comments

No comments

Channel Rating Comments

No comments

USGS Station Details

Lenawee County, Michigan, Hydrologic Unit 04100002

USGS Station Location

LOCATION.--Lat 41°54'17", long 83°58'51" referenced to North American Datum of 1927, in NW ¼ sec.5, T.7 S., R.4 E., Lenawee County, MI, Hydrologic Unit 04100002, on right bank at downstream side of bridge on Academy Road, 1.7 mi east of Adrian, and 2.6 mi downstream from South Branch.

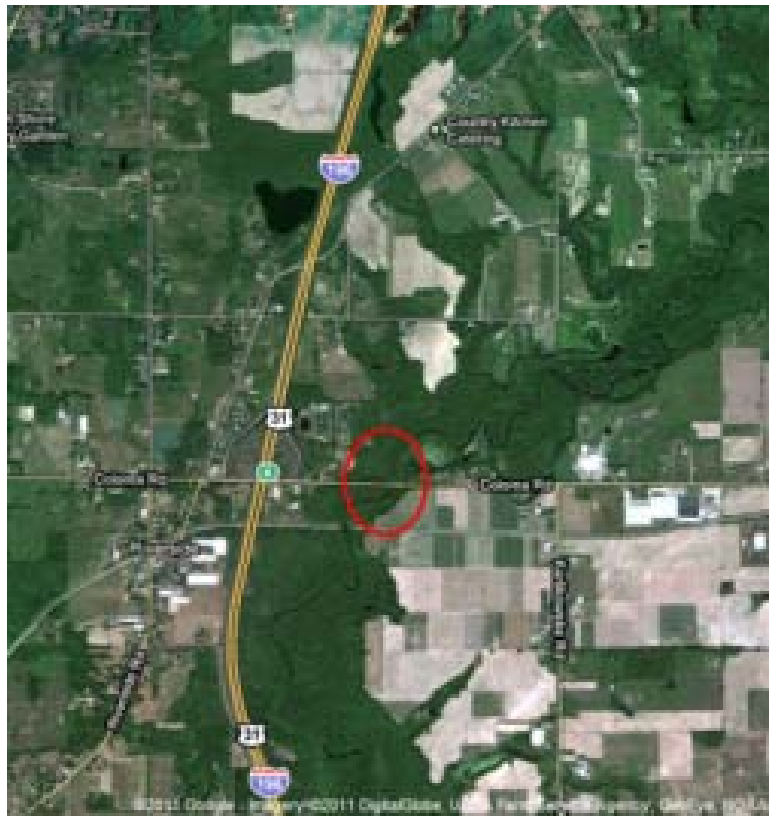
DRAINAGE AREA

463 mi²

USGS URL

<http://waterdata.usgs.gov/nwis/uv?04176000>

Figure 4.C.11 Paw Paw River Site





Abutment Rating Comments

No comments

Pier Rating Comments

No comments

Channel Rating Comments

No comments

USGS Station Details

Berrien County, Michigan, Hydrologic Unit 04050001

USGS Station Location

--Lat 42°11'11", long 86°22'08" referenced to North American Datum of 1927, in SW ¼ SE ¼ sec.23, T.3 S., R.18 W., Berrien County, MI, Hydrologic Unit 04050001, on left bank 40 ft upstream from bridge on Coloma Road, 0.8 mi east of Riverside.

DRAINAGE AREA

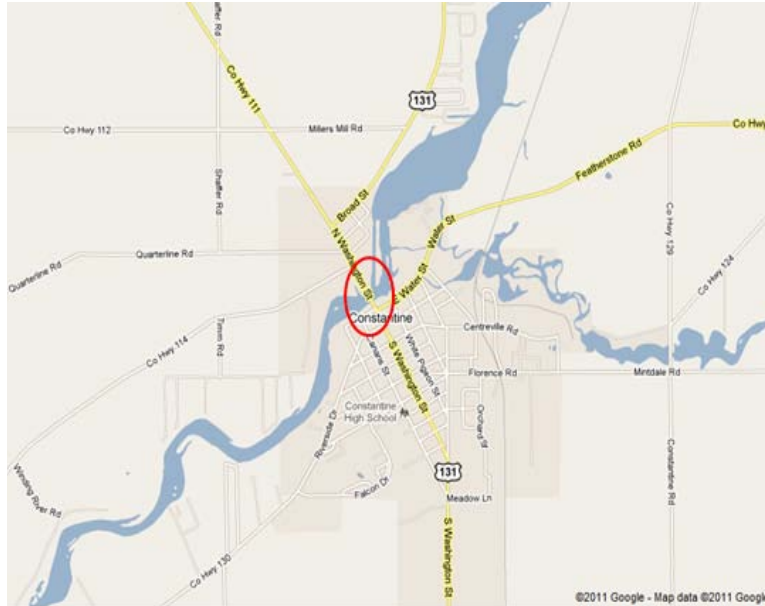
390 mi²

USGS URL

<http://waterdata.usgs.gov/nwis/uv?04102500>

Figure 4.C.12 Pigeon River Site





Abutment Rating Comments

No comments

Pier Rating Comments

No comments

Channel Rating Comments

No comments

USGS Station Details

Lagrange County, Indiana, Hydrologic Unit 04050001

USGS Station Location

--Lat 41°44'56" long 85°34'5" referenced to North American Datum of 1927, in SE¼ NW ¼ sec.14, T.38 N., R.8 E., Lagrange County, IN, Hydrologic Unit 04050001, on right bank 20 ft downstream from bridge on County Road 750 North, 1,200 ft downstream from Page Ditch, 0.7 mi south of Indiana-Michigan State line, and 1.2 mi northwest of Scott.

DRAINAGE AREA

361 mi²

USGS URL

<http://waterdata.usgs.gov/nwis/uv?04099750>

Appendix 6.A

JET Apparatus Specifications

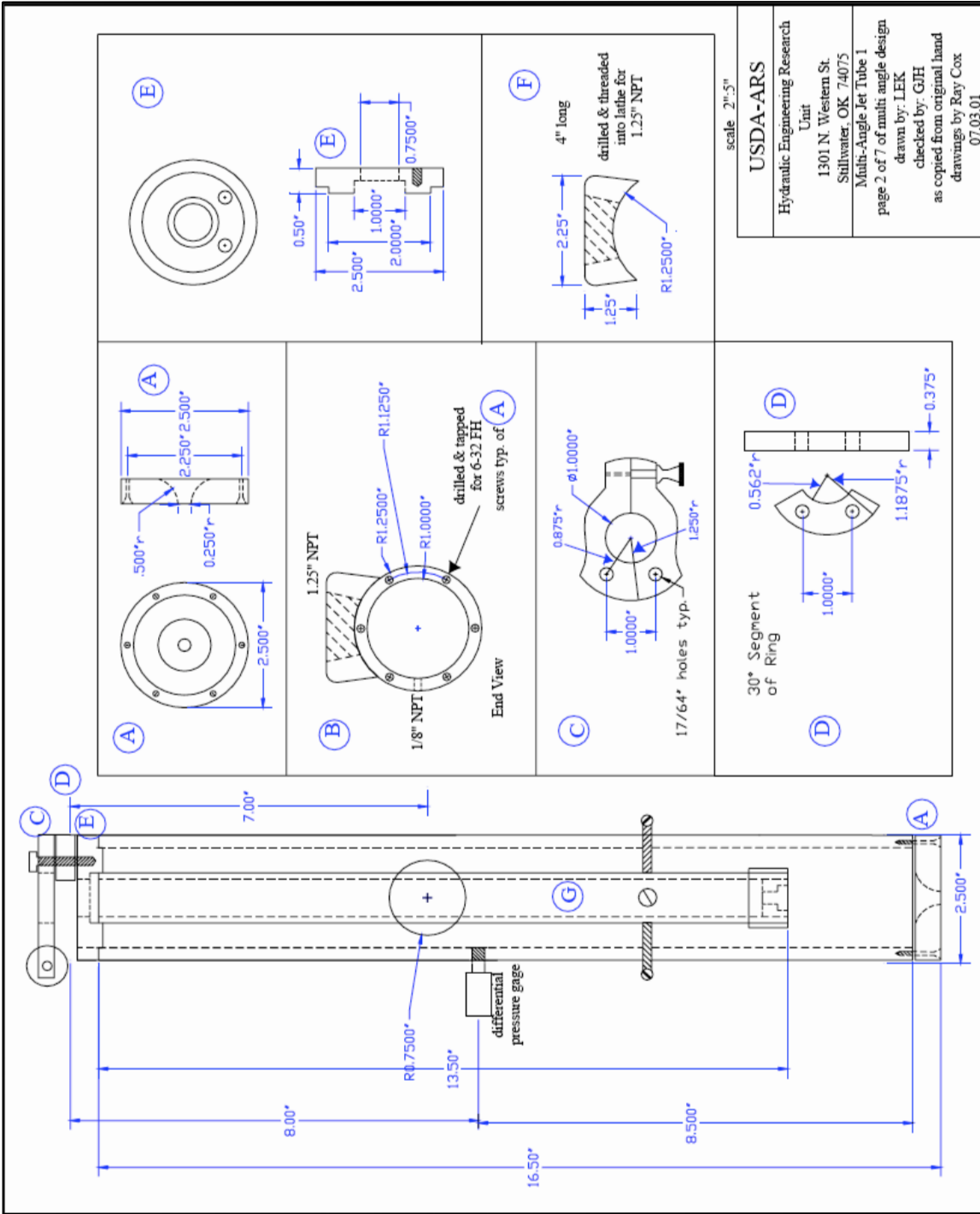
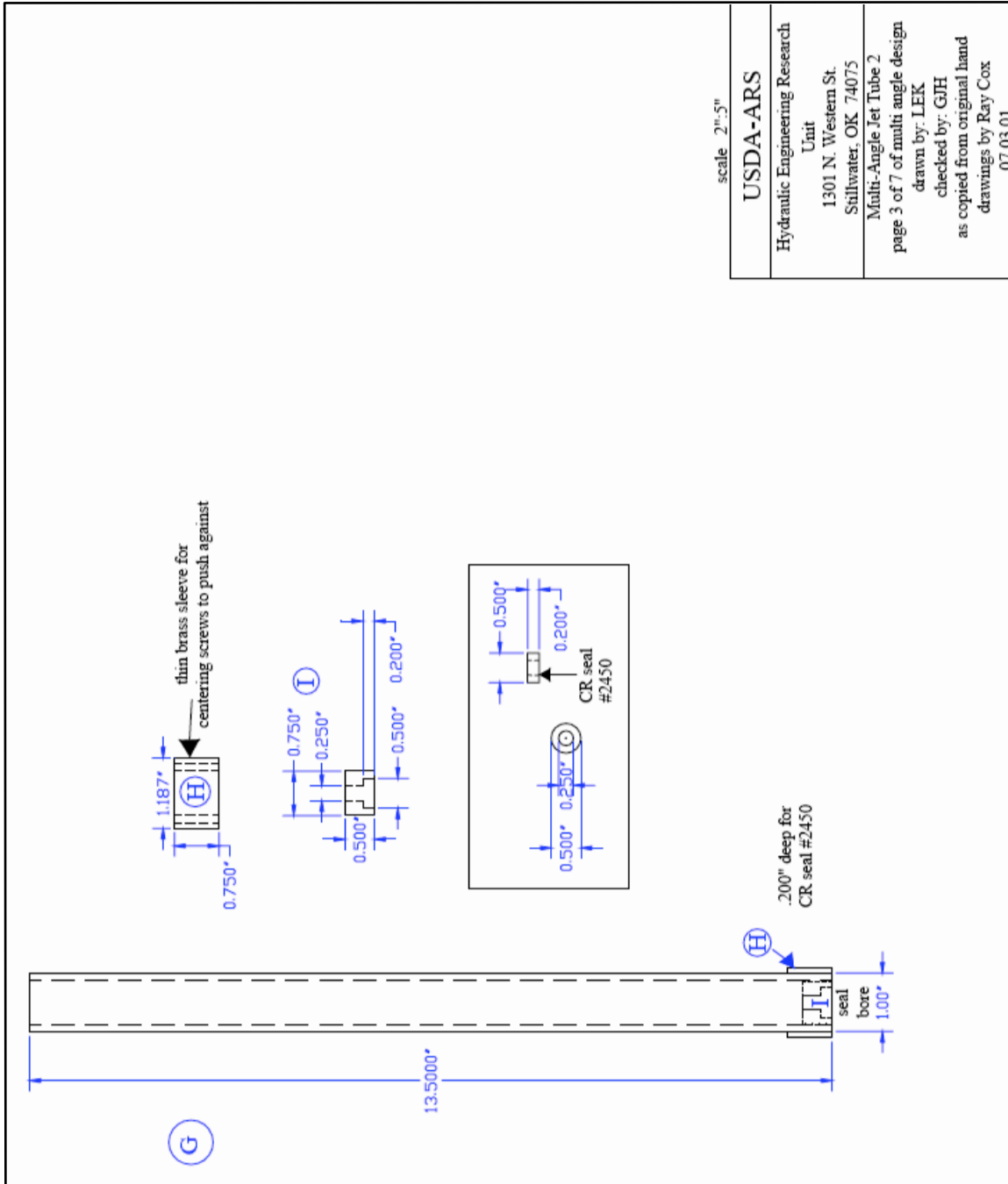


Figure 6.A.2 Jet tube assembly (Dr. Greg Hanson, USDA Stillwater, OK)



scale 2"=5"

USDA-ARS

Hydraulic Engineering Research
Unit
1301 N. Western St.
Stillwater, OK 74075

Multi-Angle Jet Tube 2
page 3 of 7 of multi angle design
drawn by: LEK
checked by: GJH
as copied from original hand
drawings by Ray Cox
07.03.01

Figure 6.A.3 Jet tube guide assembly (Dr. Greg Hanson, USDA Stillwater, OK)

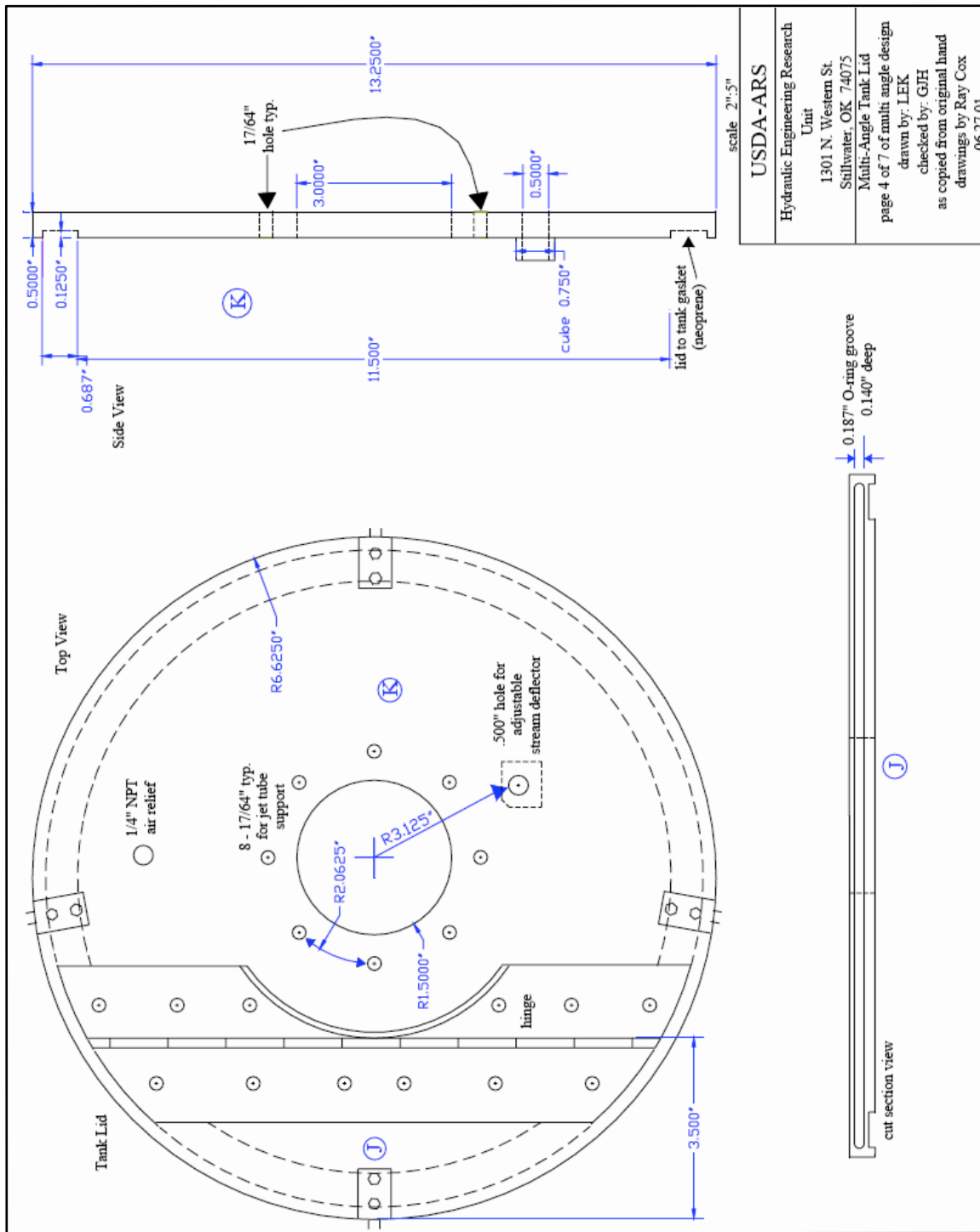


Figure 6.A.4 Lid assembly (Dr. Greg Hanson, USDA Stillwater, OK)

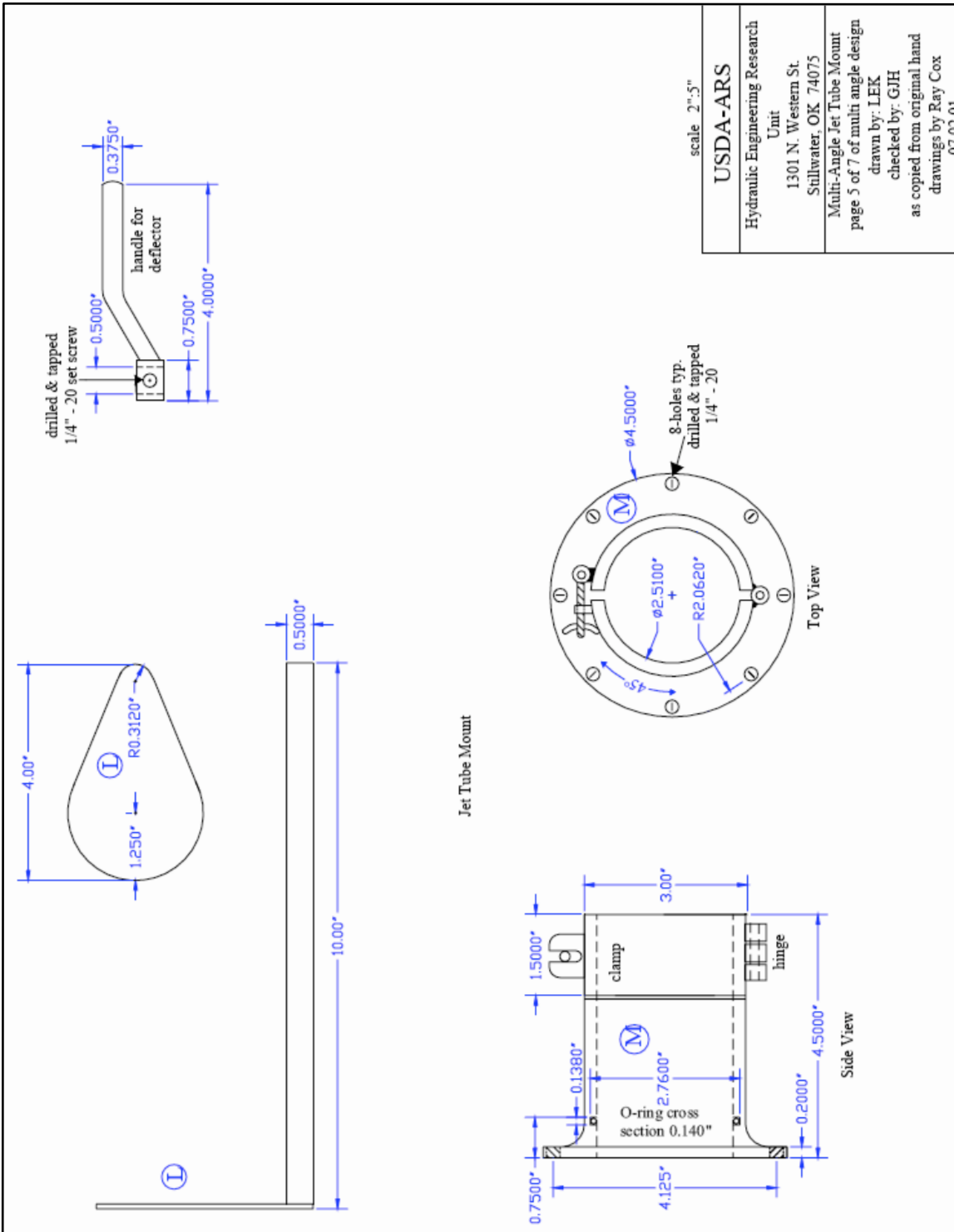


Figure 6.A.5 Stream deflector and jet mount (Dr. Greg Hanson, USDA Stillwater, OK)

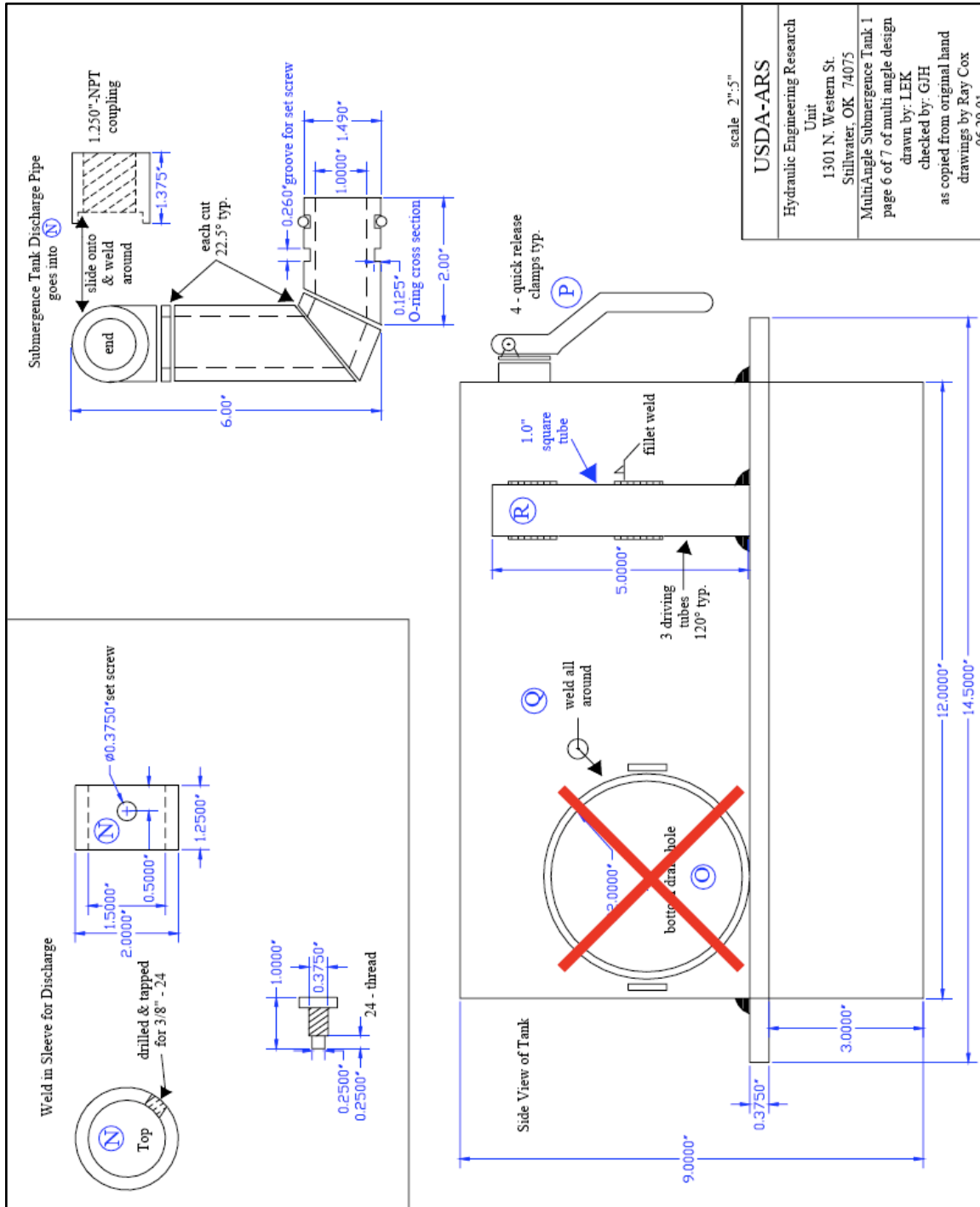


Figure 6.A.6 Tank assembly (Dr. Greg Hanson, USDA Stillwater, OK)

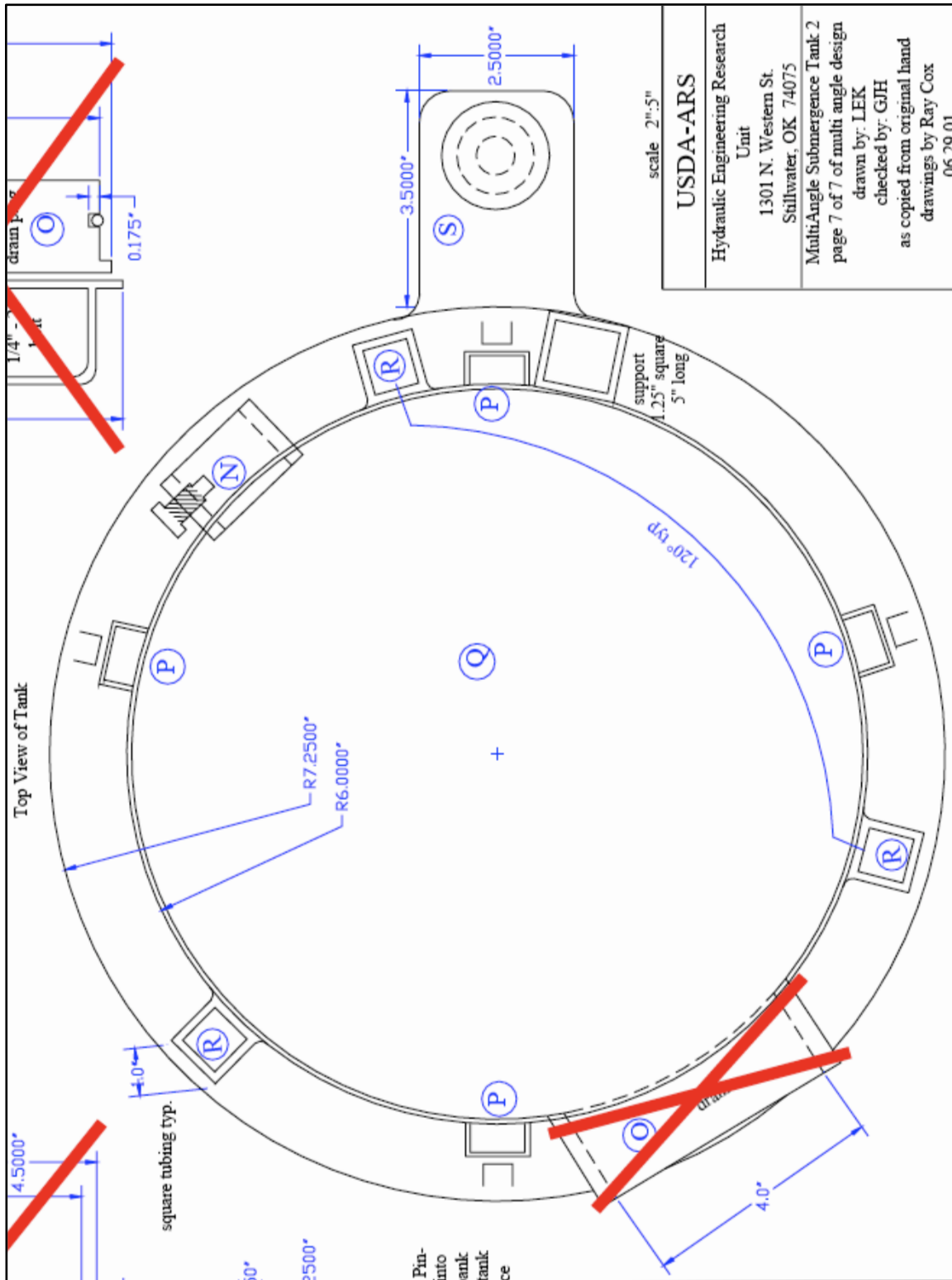


Figure 6.A.7 Tank assembly (Dr. Greg Hanson, USDA Stillwater, OK)

Appendix 6.B

JET Excel Spreadsheet

STREAM BED JET DATA

DATE 5/20/09

JET TEST
LOCATION In-situ Pawpaw River Test

OPERATOR Matt

ZERO POINT GAGE READING 2.504

TEST # 2

PRELIMINARY HEAD SETTING 70

PT GAGE RDG @ NOZZLE 2.921

NOZZLE DIAMETER (IN) 0.25

NOZZLE HEIGHT (FT) 0.417

SCOUR DEPTH READINGS			
TIME (MIN)	DIFF TIME (MIN)	PT GAGE READING (FT)	MAXIMUM DEPTH OF SCOUR (FT)
0	0	2.504	0.000
0.5	0.5	2.497	0.007
1	0.5	2.480	0.024
1.5	0.5	2.480	0.024
2	0.5	2.478	0.026
5	3	2.474	0.030
10	5	2.469	0.035
20	10	2.460	0.044
40	20	2.450	0.054
60	20	2.446	0.058
120	60	2.436	0.068

HEAD SETTING	
TIME (MIN)	HEAD (IN)
0	70.00
0.5	70.00
1	70.00
1.5	70.00
2	70.00
5	70.00
10	70.00
20	70.00
40	70.00
60	70.00
120	70.00

Solve Workbook

COMMENTS Dry Unit Weight 16.44

Figure 6.B.1 JET input worksheet (Dr. Greg Hanson, USDA Stillwater, OK)

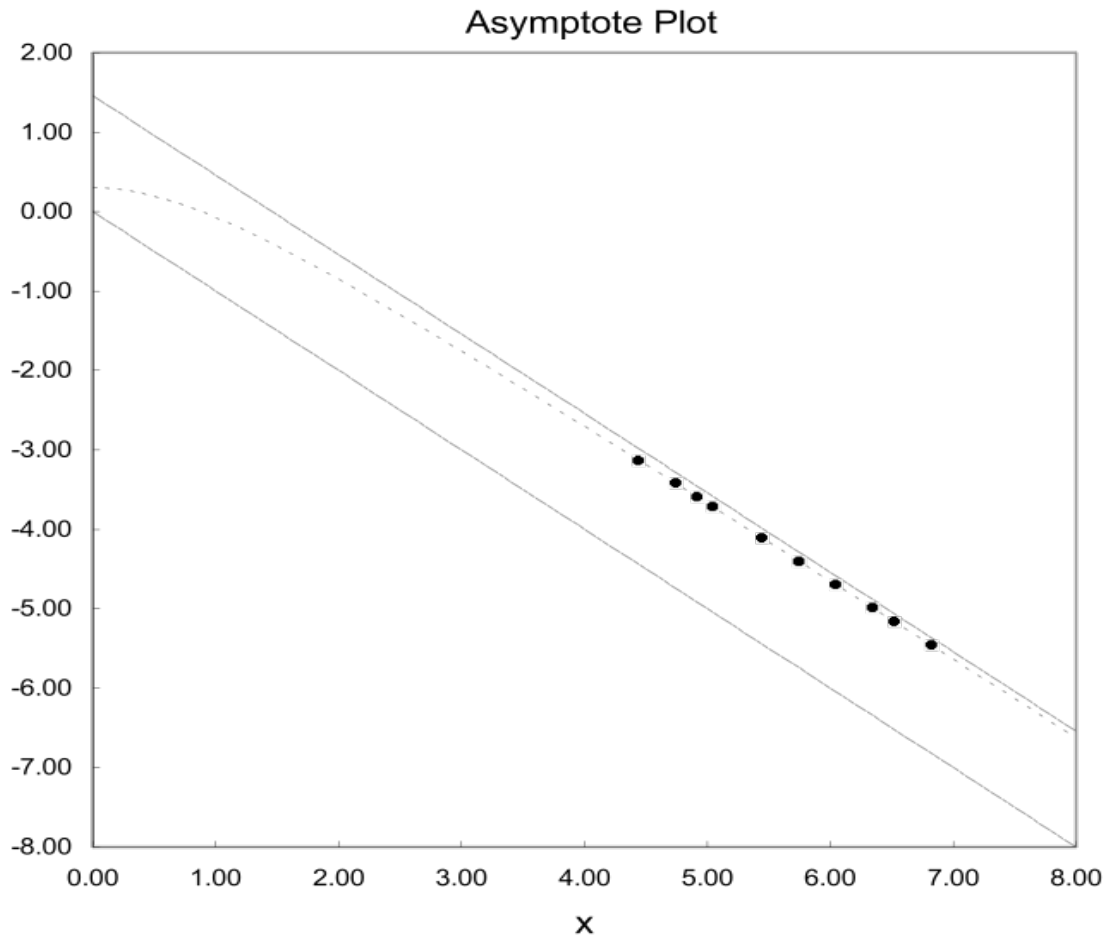


Figure 6.B.2 JET asymptote plot (Dr. Greg Hanson, USDA Stillwater, OK)

Blaisdell Method

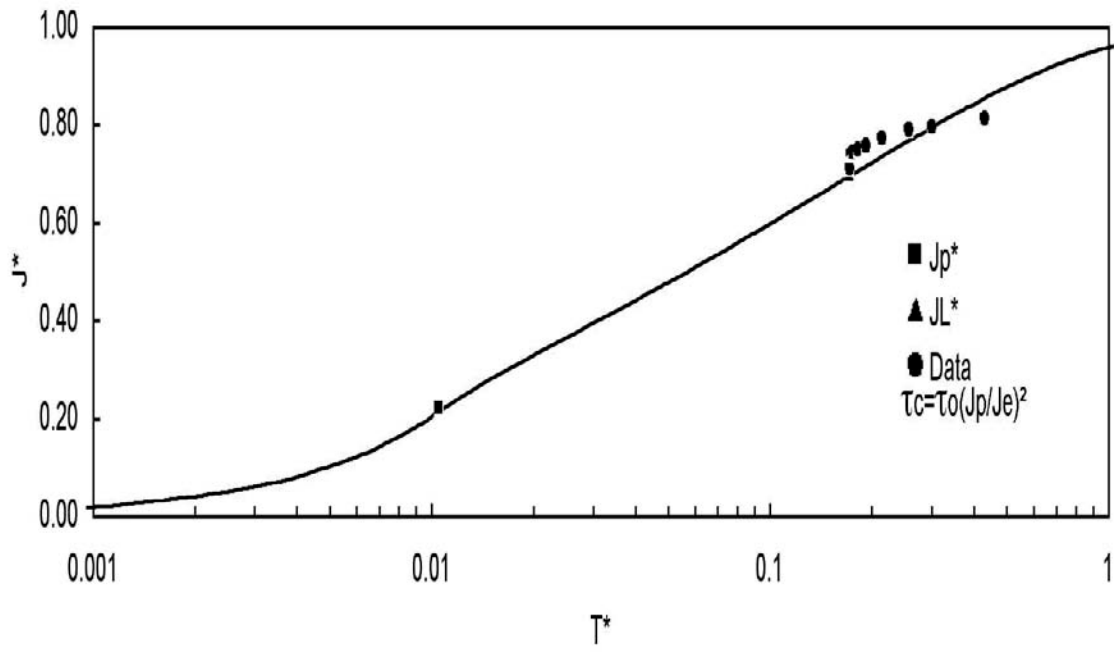


Figure 6.B.3 JET Blaisdell Method plot (Dr. Greg Hanson, USDA Stillwater, OK)

Cd =	6.2		Cf =	0.00416		yo (m) =	0.0064					
		Jo (m) =	0.127		Jp (m) =	0.039		τo (Pa) =	145.119			
Run	Elapsed	Head	J	Uo	Je	τc	K	Tr	J*	JL*	Tm pre	Err ²
#	Time	Reading	(m)	(m/s)	(m)	(Pa)	m ³ /N-s					
	(sec)	(m)										
1	30	1.78	0.129	5.906	0.182	6.757	9.77E-07	27640.8	0.70834	0.69665	315.01	81232
2	60	1.78	0.134	5.906					0.73674		1173.8	1E+06
3	90	1.78	0.134	5.906					0.73674		1173.8	1E+06
4	120	1.78	0.135	5.906					0.74008		1284.5	1E+06
5	300	1.78	0.136	5.906					0.74677		1512.7	1E+06
6	600	1.78	0.138	5.906					0.75512		1811.3	1E+06
7	1200	1.78	0.141	5.906					0.77015		2389.4	1E+06
8	2400	1.78	0.144	5.906					0.78686		3100.3	490442
9	3600	1.78	0.145	5.906					0.79354		3407.4	37080
10	7200	1.78	0.148	5.906					0.81025		4240	9E+06
												Σ Err ²
												17.494

Figure 6.B.4 JET results (Dr. Greg Hanson, USDA Stillwater, OK)

Appendix 7.A

Confidence Interval Development

Sample	Dry Unit Weight (KN/m ³)	k (cm ³ /N-s)	log k	Predicted value + (Standard Error * t-statistic)	Predicted Value Transformed 10 ^k	Predicted value - (Standard Error * t-statistic)	Predicted Value Transformed 10 ^k
Pawpaw River @ Coloma Rd. Lab test 1	18.5	0.598	-0.223	0.451	2.825	-1.555	0.028
Pawpaw River @ Coloma Rd. Lab test 2	17.1	1.01	0.004	1.340	21.879	-0.666	0.216
Pawpaw River @ Coloma Rd. Lab test 3.17.09	18	0.308	-0.511	0.768	5.868	-1.237	0.058
Pawpaw River @ Coloma Rd. Lab Test 3.27.09	17.8	0.365	-0.438	0.895	7.861	-1.110	0.078
Pawpaw River @ Coloma Rd. Lab test 5.20.09 Sample	16.5	27.5	1.439	1.721	52.610	-0.285	0.519
Pawpaw River @ Coloma Rd. Lab test 5.20.09 Sample	17	2.32	0.365	1.404	25.324	-0.602	0.250
Pawpaw River @ Coloma Rd. Lab test 5.20.09 Sample	17.5	3.39	0.530	1.086	12.190	-0.920	0.120
Pawpaw River @ Coloma Rd. Lab test 6.17.09	16.5	1.91	0.281	1.721	52.610	-0.285	0.519
Pawpaw River @ Coloma Rd. Lab test 6.17.09	17	2.07	0.316	1.404	25.324	-0.602	0.250

Figure 7.A.1 Example of the development of the confidence interval for the Pawpaw River

SUMMARY OUTPUT

Regression Statistics	
Multiple R	0.728622902
R Square	0.530891333
Adjusted R Sq	0.463875809
Standard Error	0.434918131
Observations	9

ANOVA					
	df	SS	MS	F	Significance F
Regression	1	1.498460311	1.498460311	7.921915745	0.025974186
Residual	7	1.324076463	0.18915378		
Total	8	2.822536774			

	Coefficients	Standard Error	t Stat	P-value	Lower 95%	Upper 95%	Lower 95.0%	Upper 95.0%
Intercept	11.19653651	3.911089889	2.862766346	0.024241475	1.948278512	20.44479451	1.948278512	20.44479451
X Variable 1	-0.63505413	0.225629371	-2.8145898	0.025974186	-1.16858281	-0.10152544	-1.16858281	-0.10152544

RESIDUAL OUTPUT

Observation	Predicted Y	Residuals	Standard Residuals
1	-0.55196484	0.328666019	0.807873319
2	0.337110942	-0.33278957	-0.81800916
3	-0.23443777	-0.27701151	-0.68090462
4	-0.10742695	-0.33028019	-0.81184101
5	0.718143419	0.721189275	1.772710106
6	0.400616355	-0.03512837	-0.08634684
7	0.083089292	0.447110406	1.099014036
8	0.718143419	-0.43711005	-1.07443279
9	0.400616355	-0.08464601	-0.20806305

PROBABILITY OUTPUT

Percentile	Y
5.555555556	-0.51144928
16.666666667	-0.43770714
27.777777778	-0.22329882
38.888888889	0.004321374
50	0.281033367
61.111111111	0.315970345
72.222222222	0.365487985
83.333333333	0.530199698
94.444444444	1.439332694

t-statistic (double sided)	2.306
Standard Error *	
t-statistic	1.002921209

Figure 7.A.2 Example of the linear regression for the Pawpaw River

Appendix 7.B

Mohr-Coulomb Envelopes

Pawpaw River

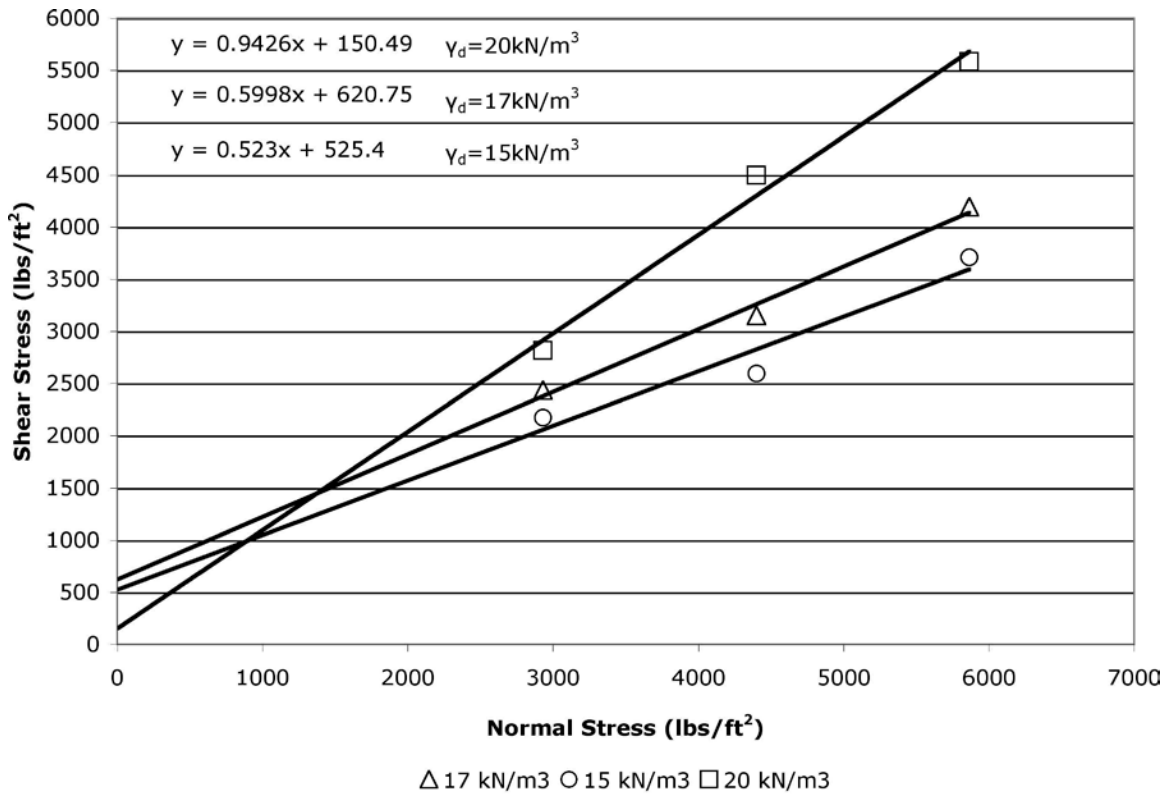


Figure 7.B.1 Pawpaw River Mohr-Coulomb envelope

Grand River

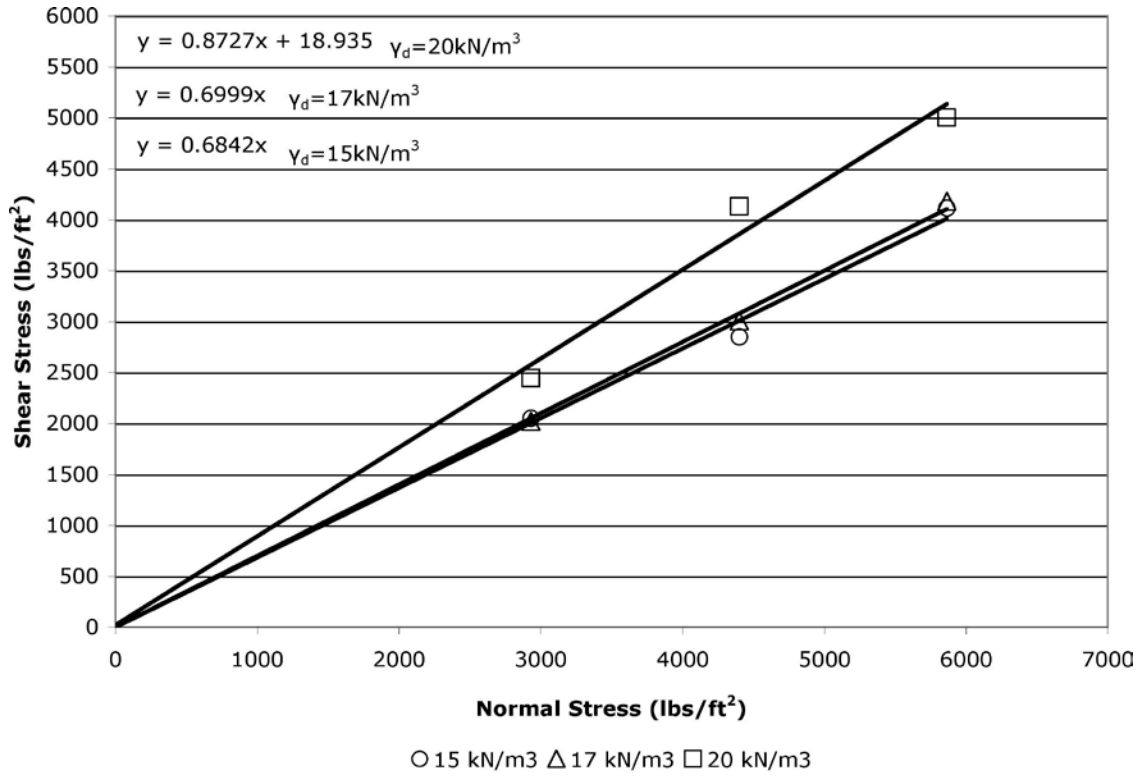


Figure 7.B.2 Grand River Mohr-Coulomb envelope

Appendix 7.C

Erodibility vs. Friction Angle Calculations

Pawpaw River

Friction Angle vs. Dry Unit Weight

$$\phi = 3.2158\gamma_d - 21.774 \Rightarrow \gamma_d = 0.311\phi + 6.771$$

Erodibility vs. Dry Unit Weight

$$k = (2 \times 10^{11})(e^{-1.4623\gamma_d})$$

Erodibility vs. Friction Angle

$$k = (2 \times 10^{11})(e^{(-1.4623*(0.311\phi+6.771))})$$

$$k = (2 \times 10^{11})(e^{(-0.4554\phi-9.901)})$$

Grand River

Friction Angle vs. Dry Unit Weight

$$\phi = 1.3984\gamma_d + 12.587 \Rightarrow \gamma_d = 0.715\phi - 9.00$$

Erodibility vs. Dry Unit Weight

$$k = (2 \times 10^6)(e^{-0.6685\gamma_d})$$

Erodibility vs. Friction Angle

$$k = (2 \times 10^6)(e^{(-0.6685*(0.715\phi - 9.00))})$$

$$k = (2 \times 10^6)(e^{(-0.478\phi + 6.02)})$$

Appendix 8.A

Hydrographs for Sites during Measurements

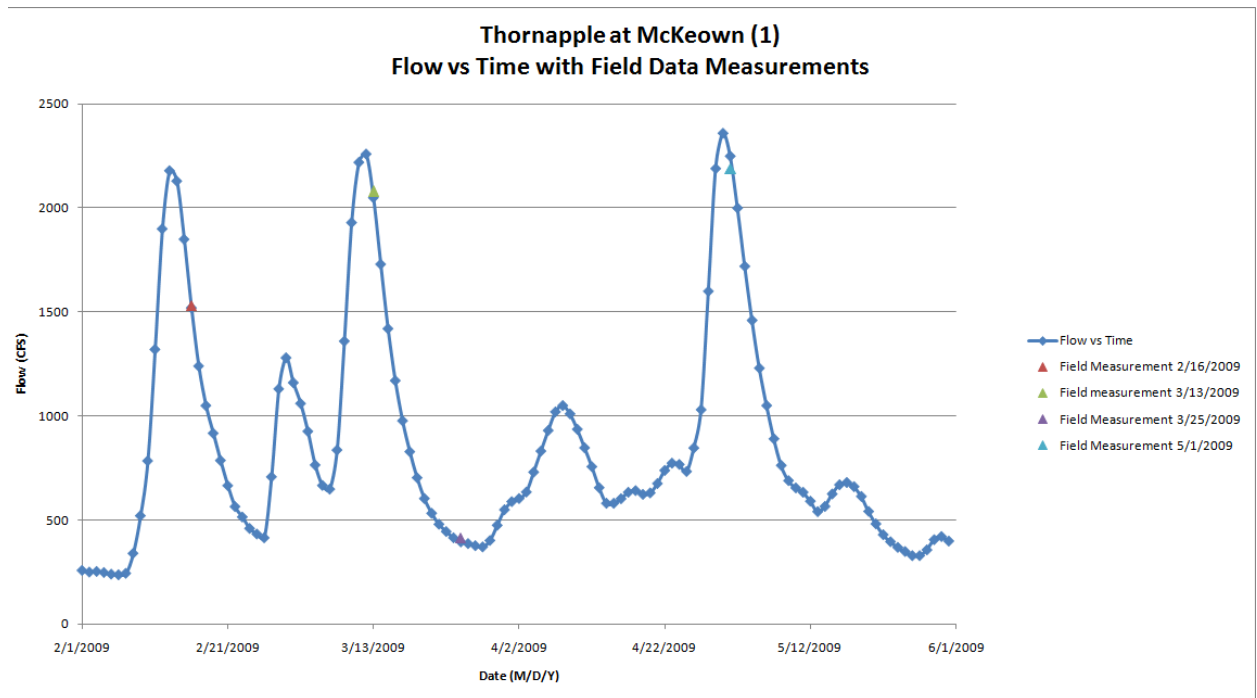


Figure 8.A.1 Hydrograph for Thornapple at McKeown (1) with time of measurement and associated discharge of depicted as triangles

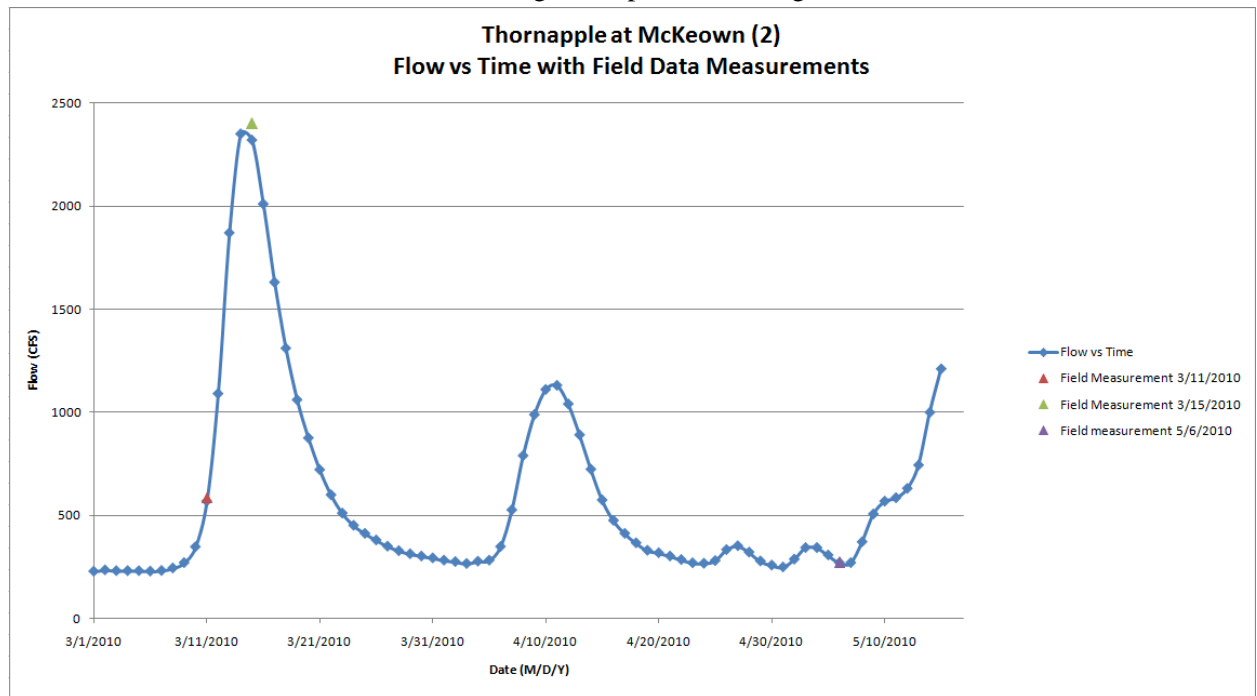


Figure 8.A.2 Hydrograph for Thornapple at McKeown (2) with time of measurement and associated discharge of depicted as triangles

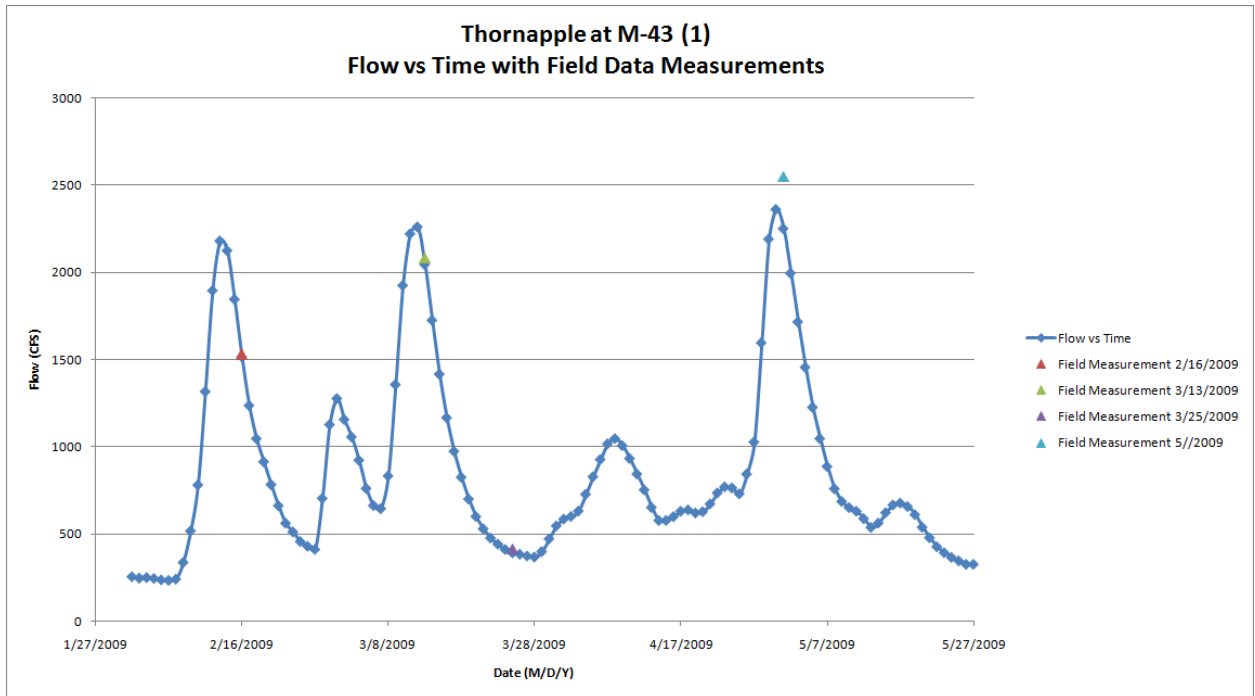


Figure 8.A.3 Hydrograph for Thornapple at M-43 (1) with time of measurement and associated discharge of depicted as triangles

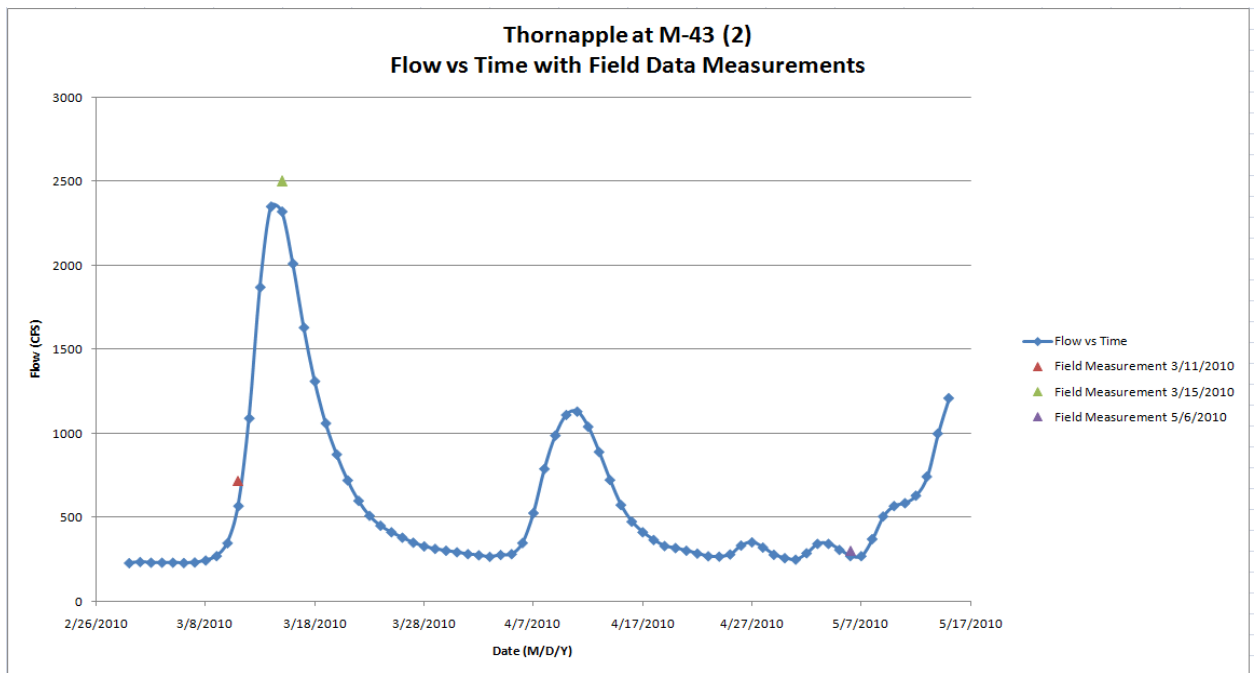


Figure 8.A.4 Hydrograph for Thornapple at M-43 (2) with time of measurement and associated discharge of depicted as triangles

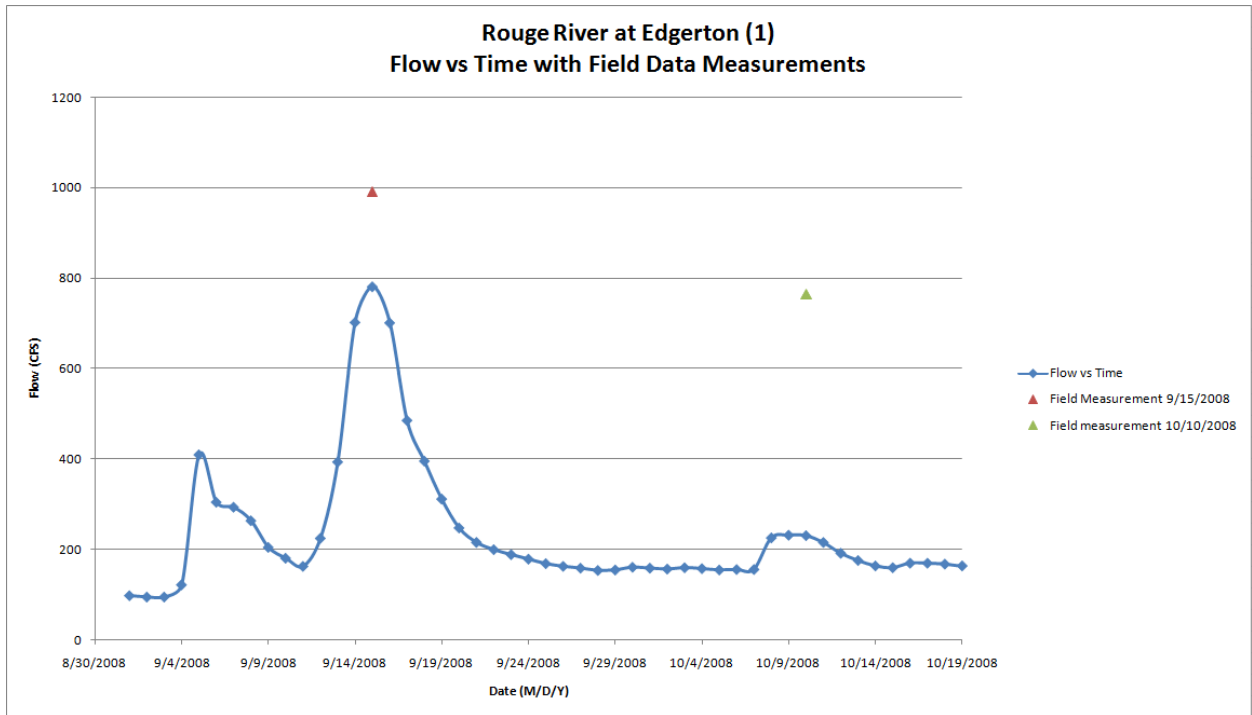


Figure 8A.5 Hydrograph for Rouge River at Edgerton (1) with time of measurement and associated discharge of depicted as triangles

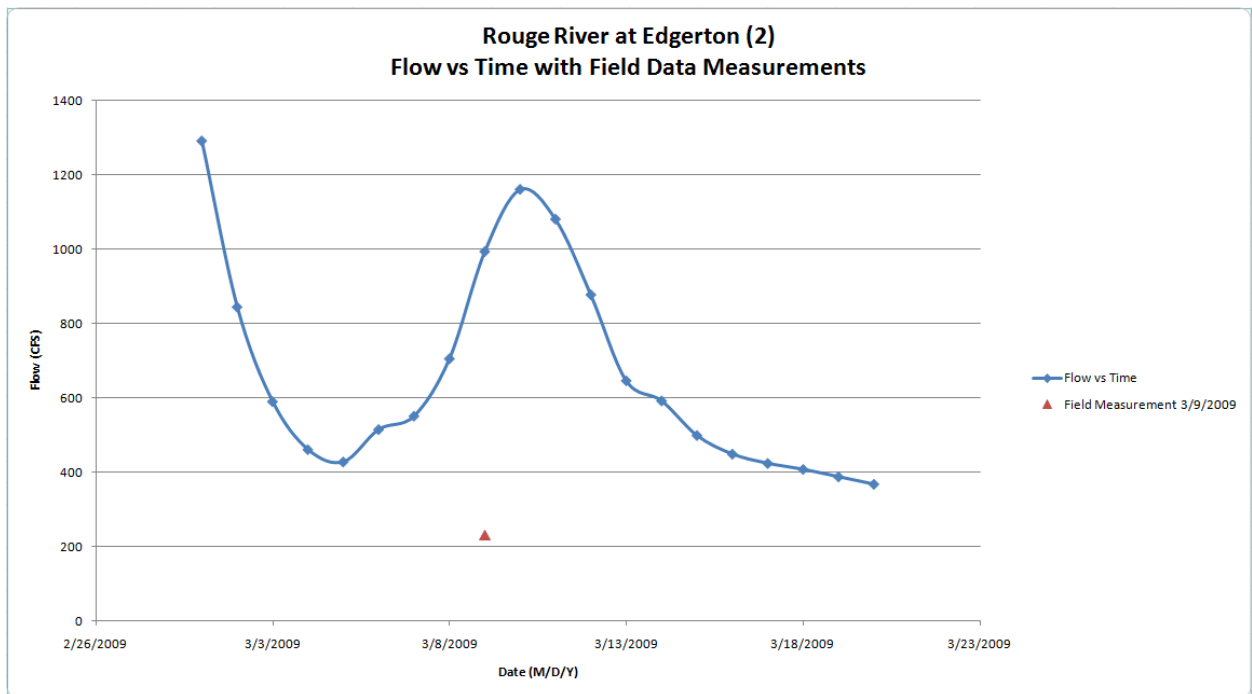


Figure 8.A.6 Hydrograph for Rouge River at Edgerton (2) with time of measurement and associated discharge of depicted as triangles

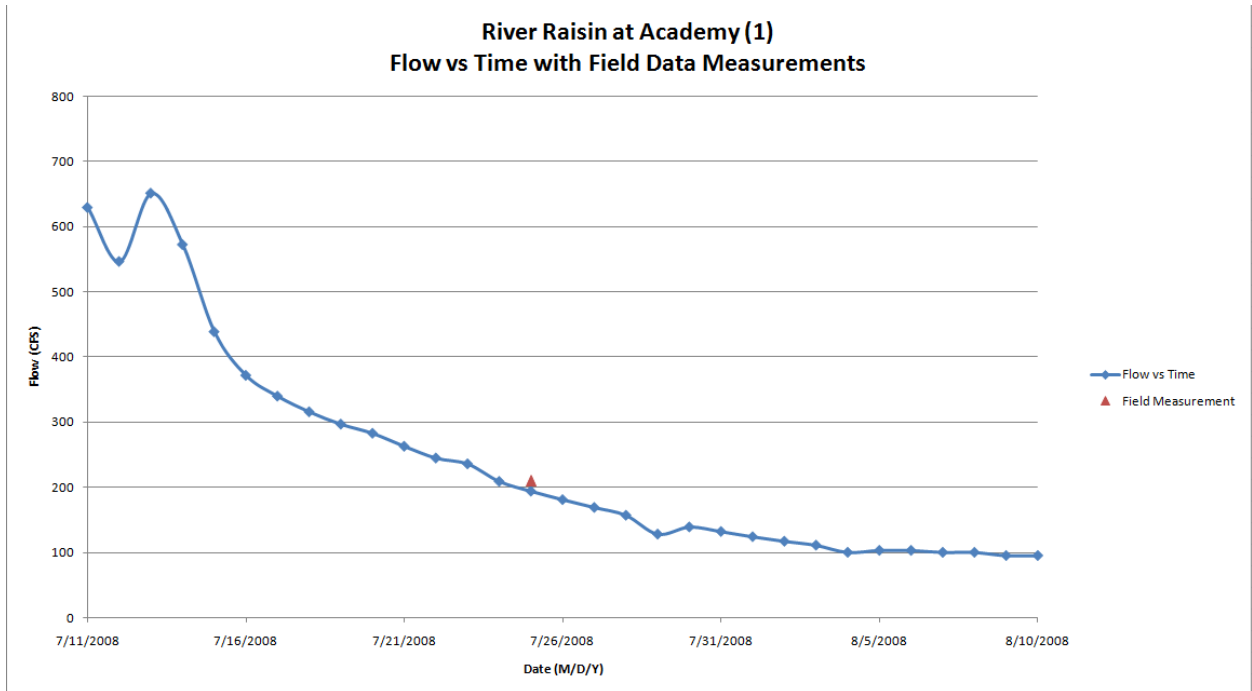


Figure 8.A.7 Hydrograph for River Raisin at Academy (1) with time of measurement and associated discharge of depicted as triangles

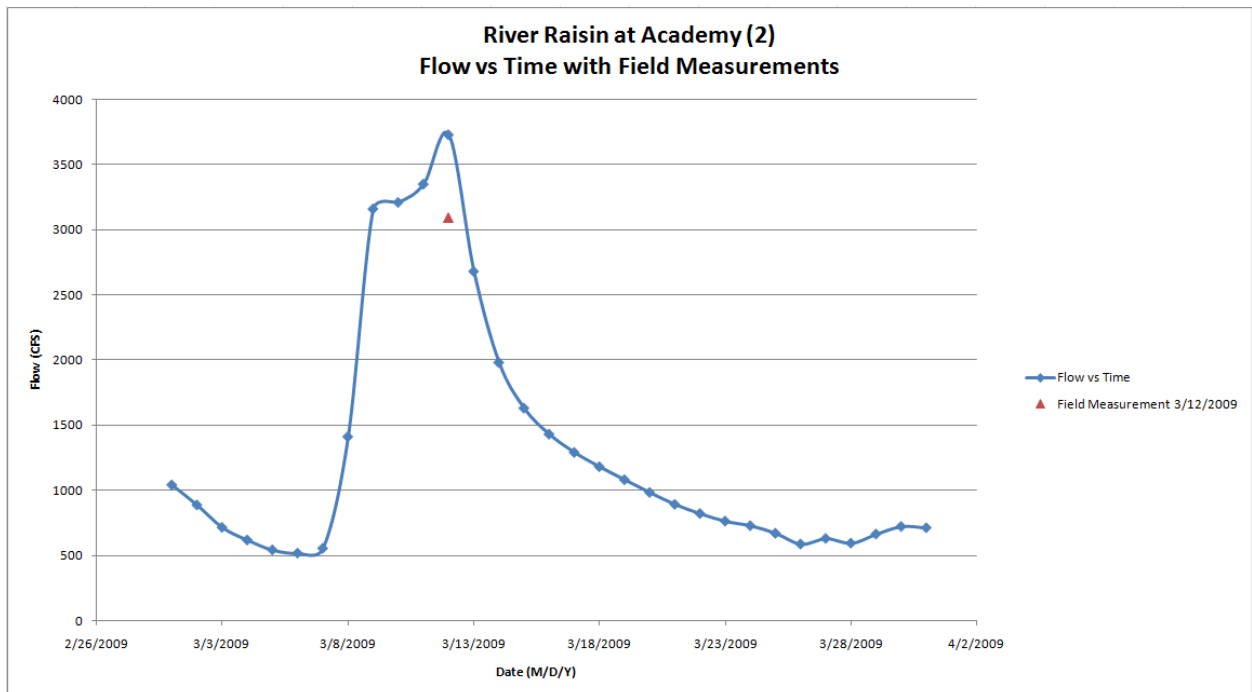


Figure 8.A.8 Hydrograph for River Raisin at Academy (2) with time of measurement and associated discharge of depicted as triangles

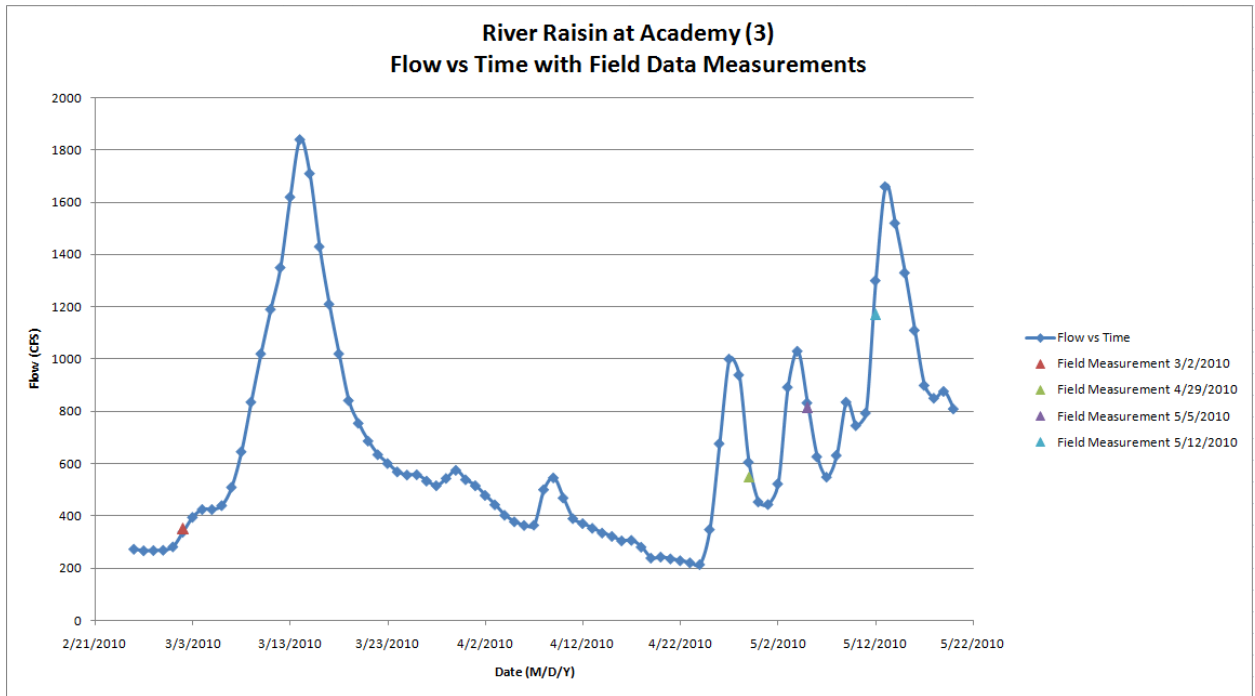


Figure 8.A.9 Hydrograph for River Raisin at Academy (3) with time of measurement and associated discharge of depicted as triangles

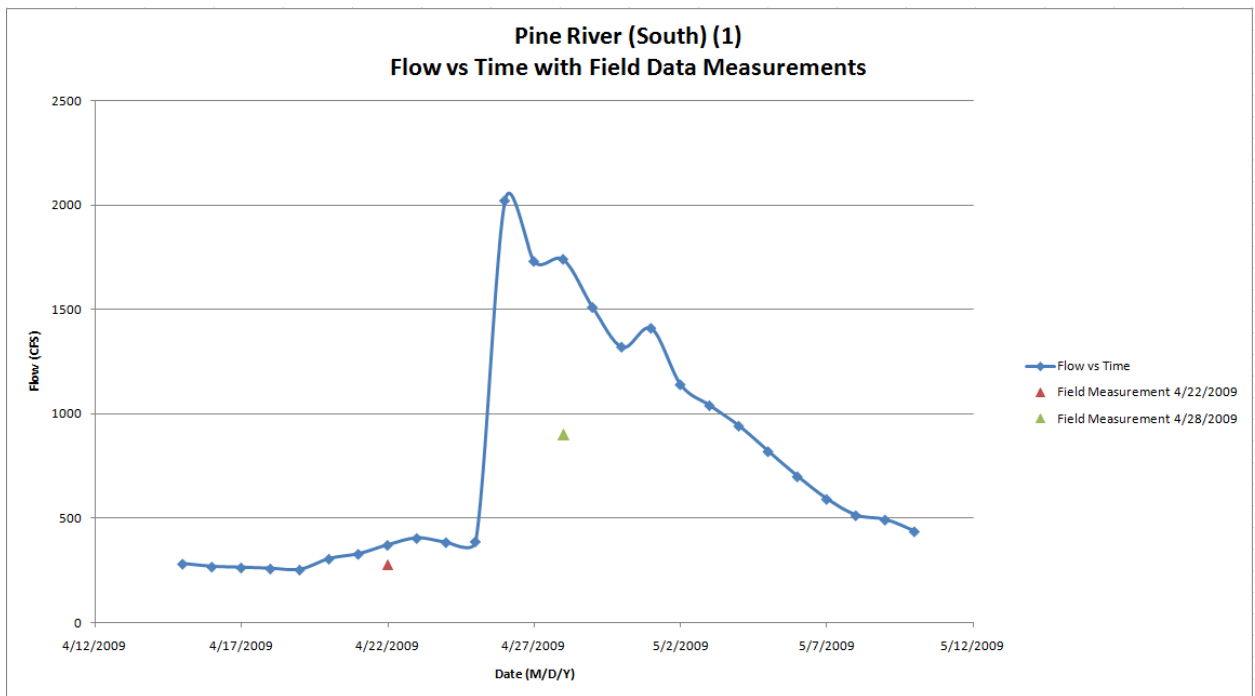


Figure 8.A.10 Hydrograph for Pine River (South) (1) with time of measurement and associated discharge of depicted as triangles

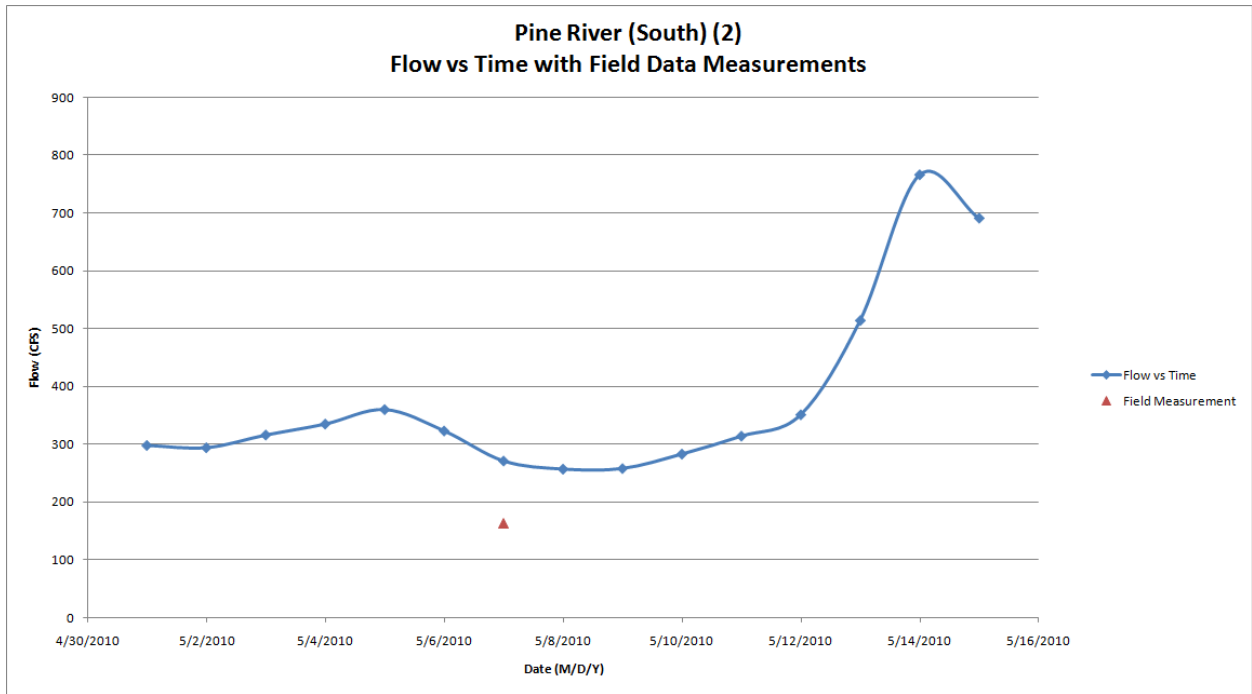


Figure 8.A.11 Hydrograph for Pine River (South) (2) with time of measurement and associated discharge of depicted as triangles

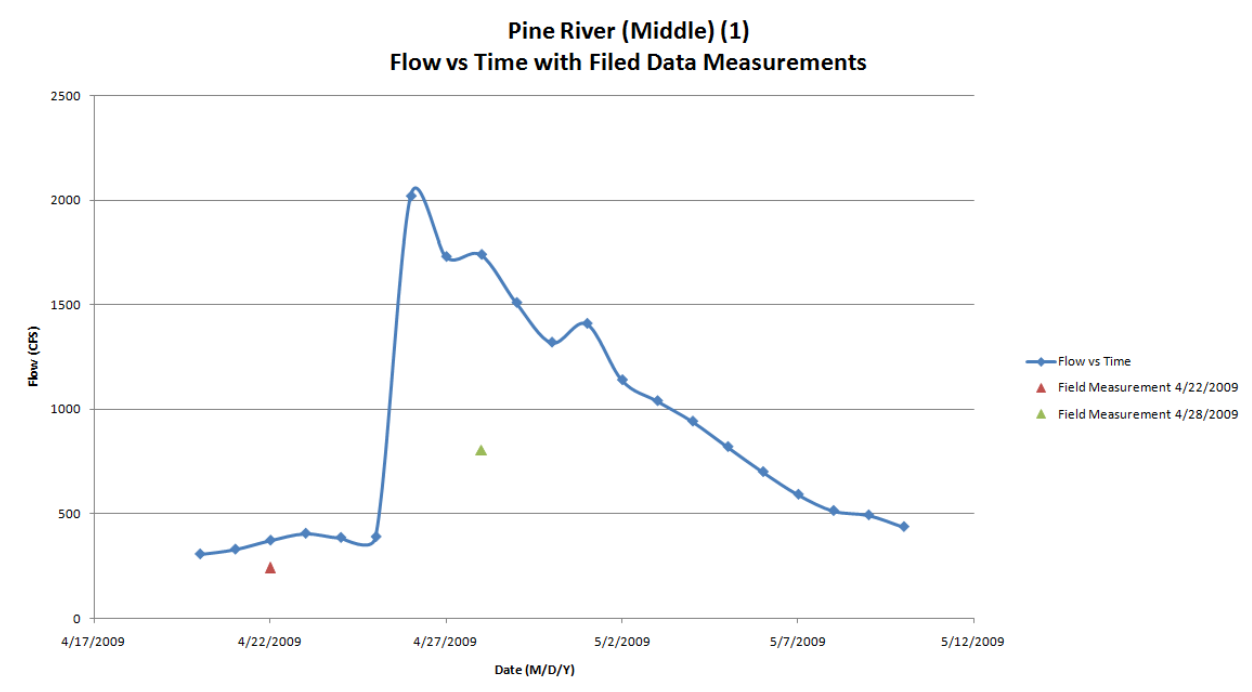


Figure 8.A.12 Hydrograph for Pine River (Middle) (1) with time of measurement and associated discharge of depicted as triangles

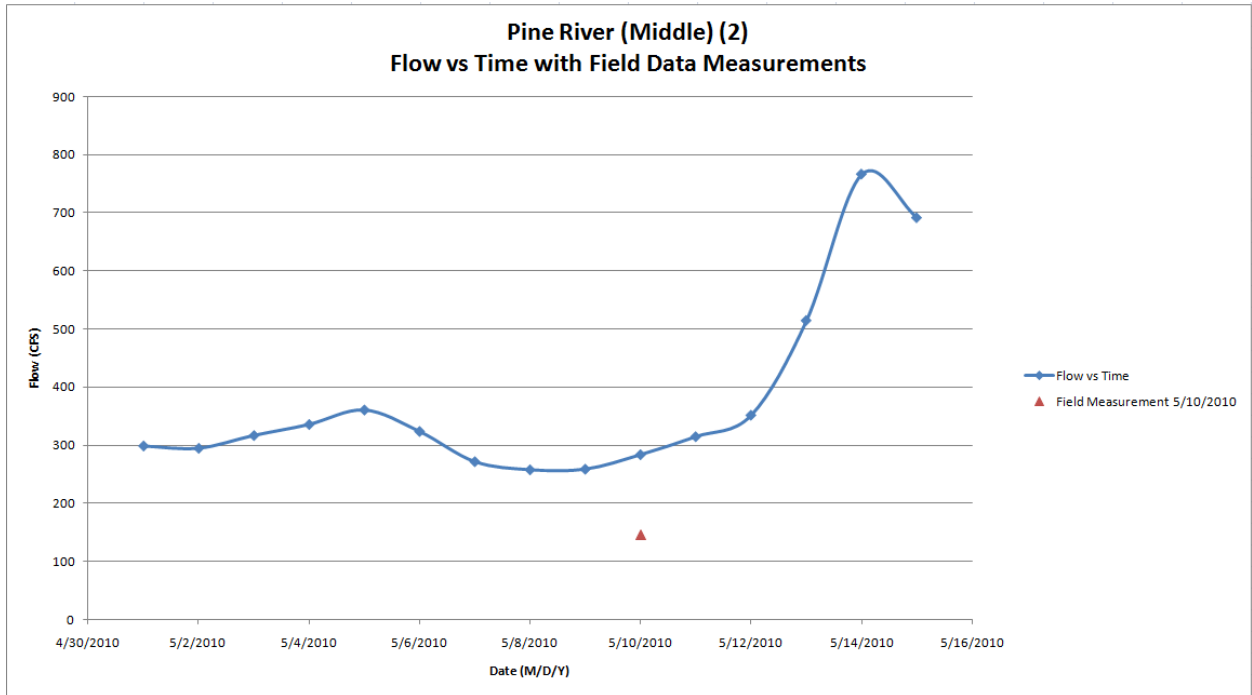


Figure 8.A.13 Hydrograph for Pine River (Middle) (2) with time of measurement and associated discharge of depicted as triangles

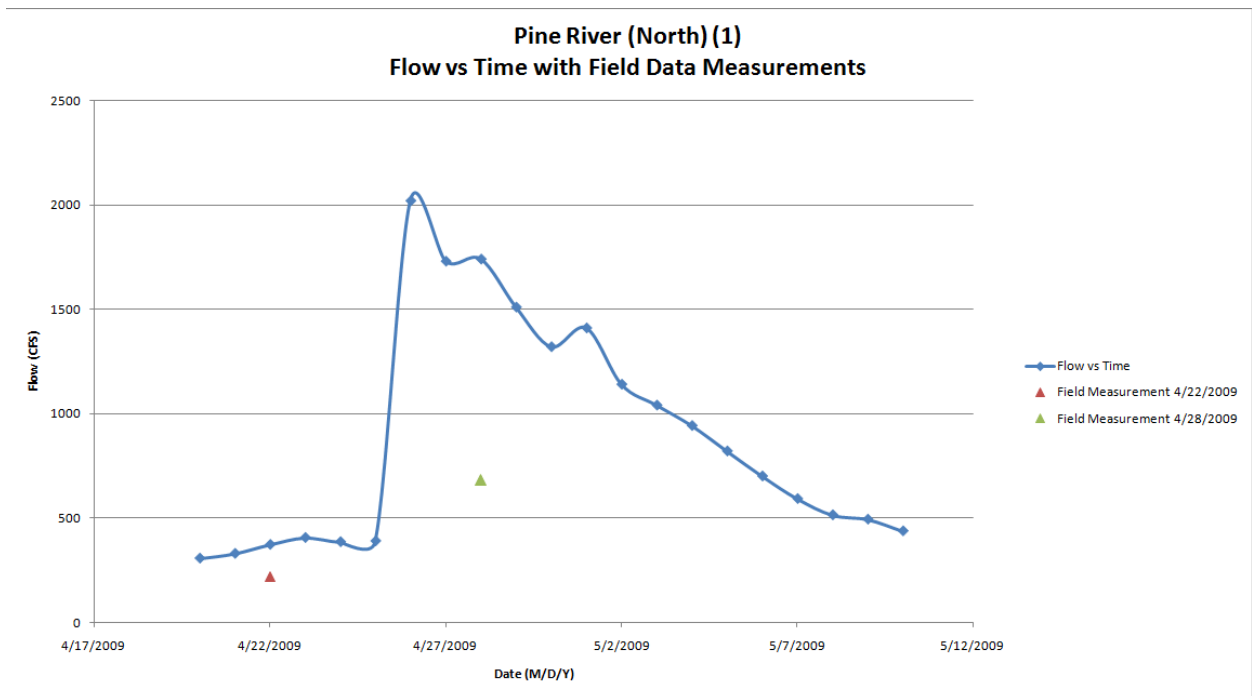


Figure 8.A.14 Hydrograph for Pine River (North) (1) with time of measurement and associated discharge of depicted as triangles

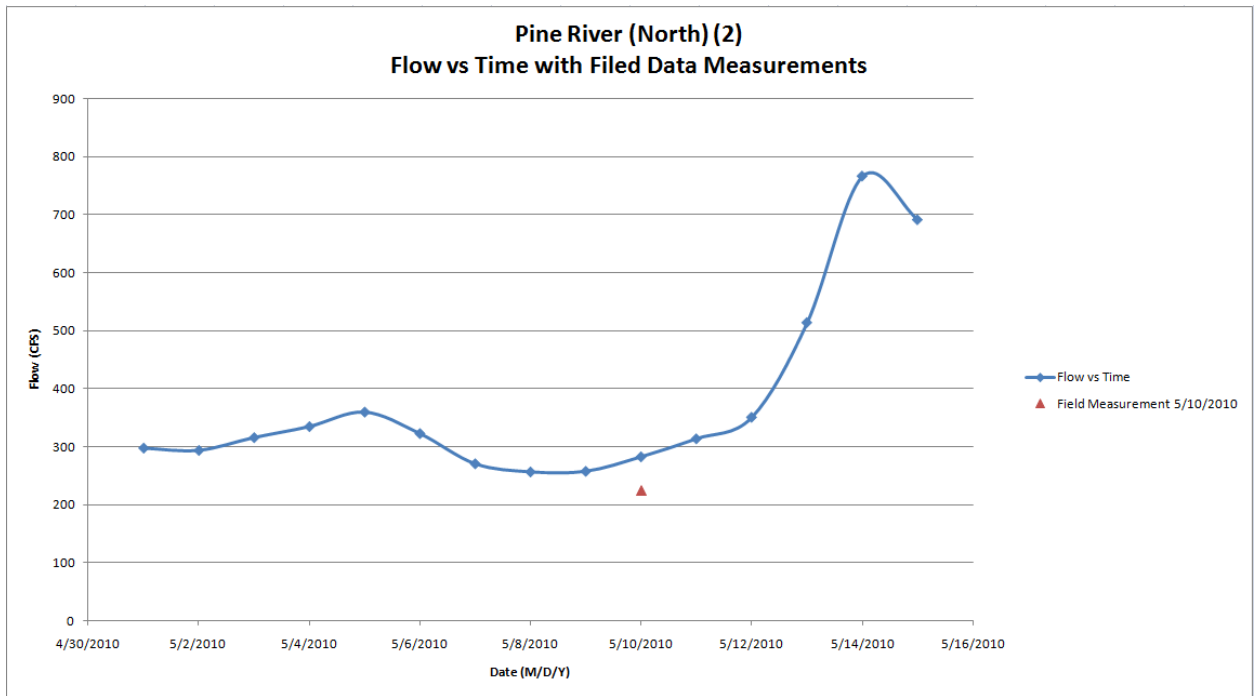


Figure 8.A.15 Hydrograph for Pine River (North) (2) with time of measurement and associated discharge of depicted as triangles

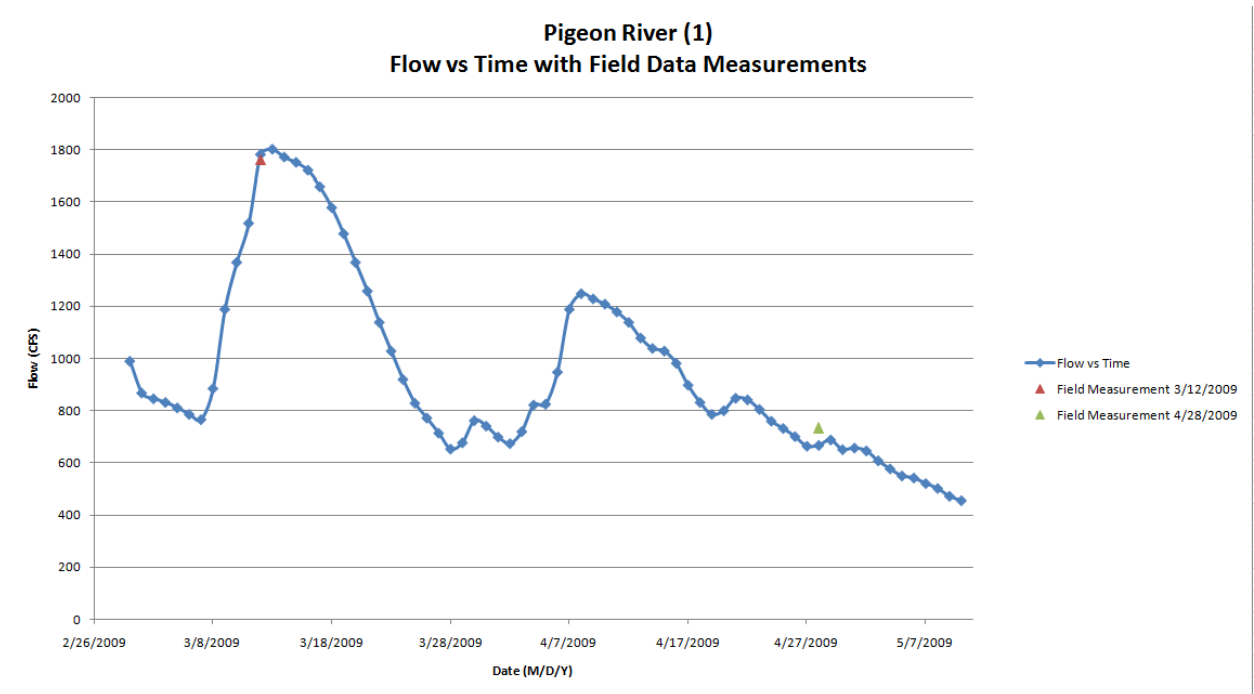


Figure 8.A.16 Hydrograph for Pigeon River (1) with time of measurement and associated discharge of depicted as triangles

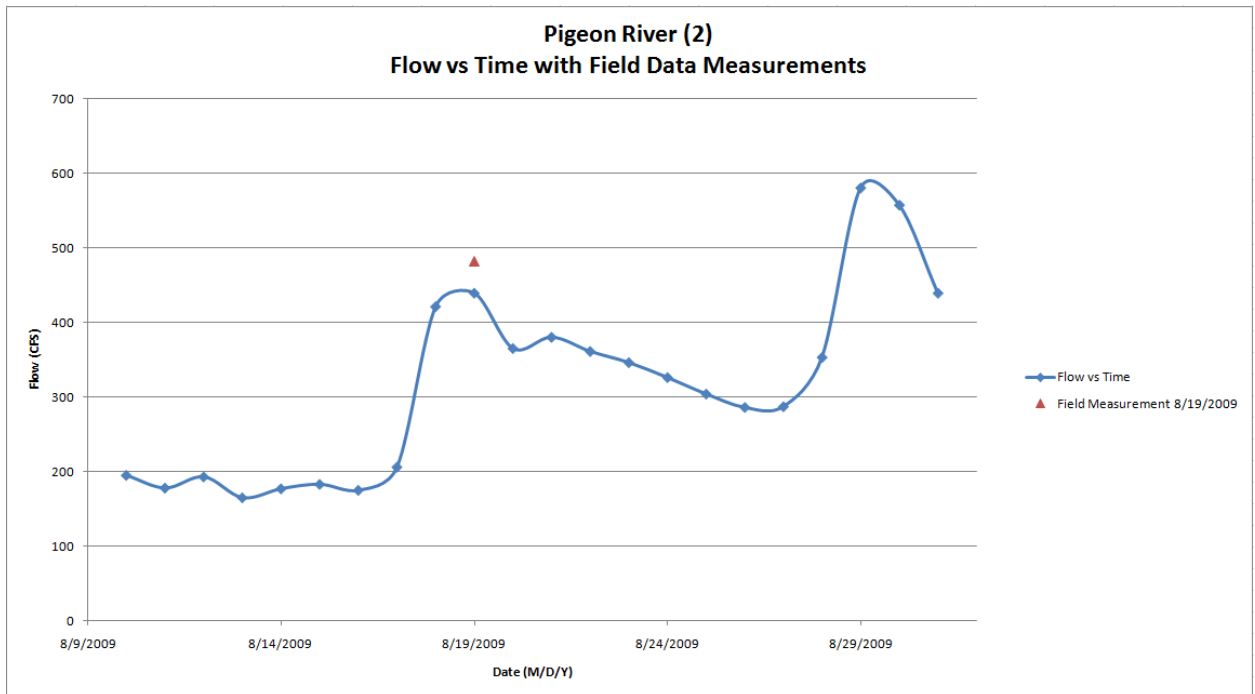


Figure 8.A.17 Hydrograph for Pigeon River (2) with time of measurement and associated discharge of depicted as triangles

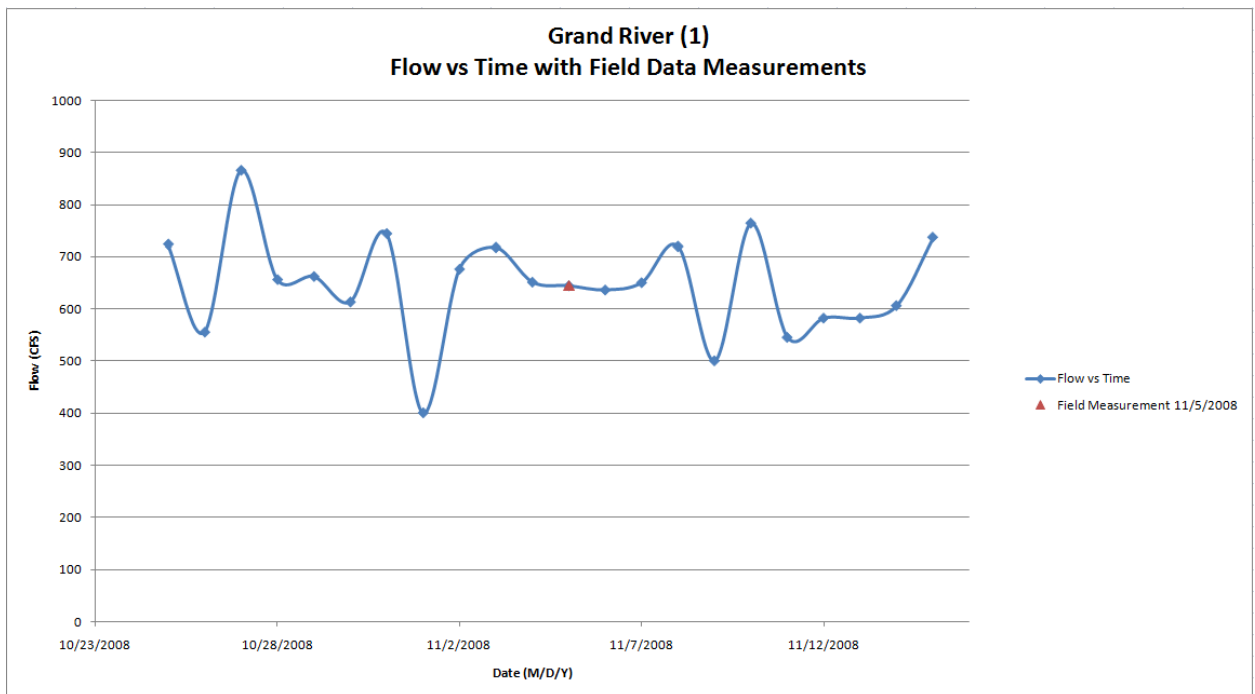


Figure 8.A.18 Hydrograph for Grand River (1) with time of measurement and associated discharge of depicted as triangles

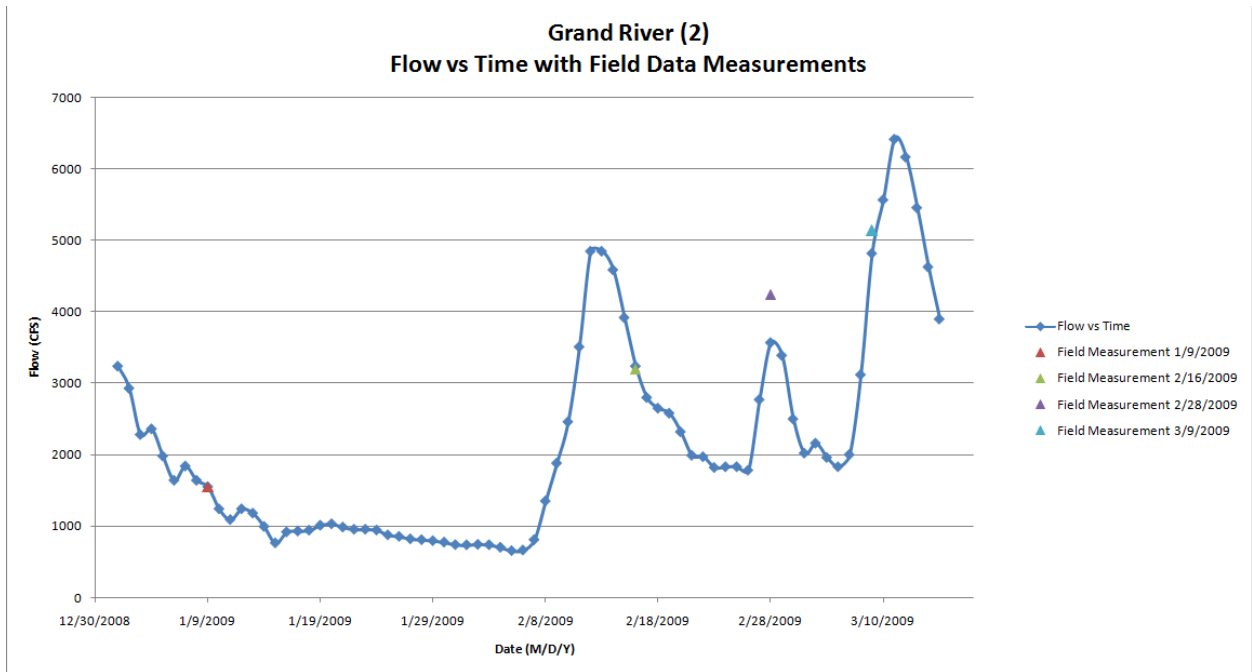


Figure 8.A.19 Hydrograph for Grand River (2) with time of measurement and associated discharge of depicted as triangles

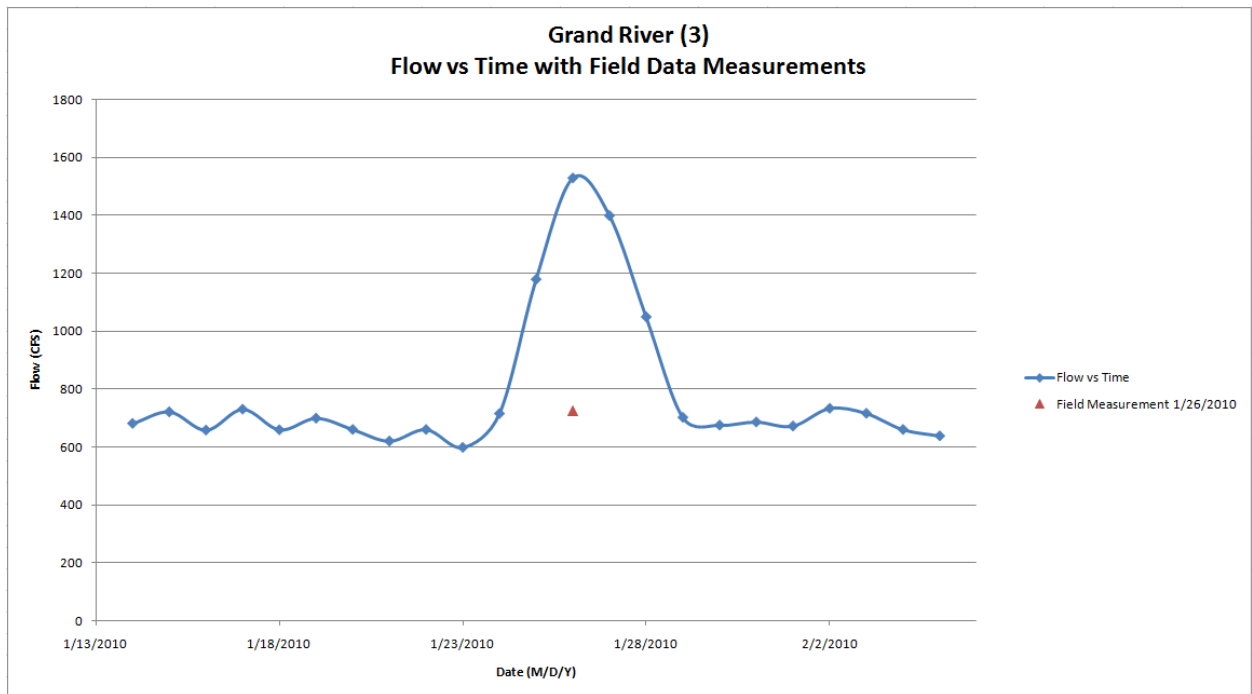


Figure 8.A.20 Hydrograph for Grand River (3) with time of measurement and associated discharge of depicted as triangles

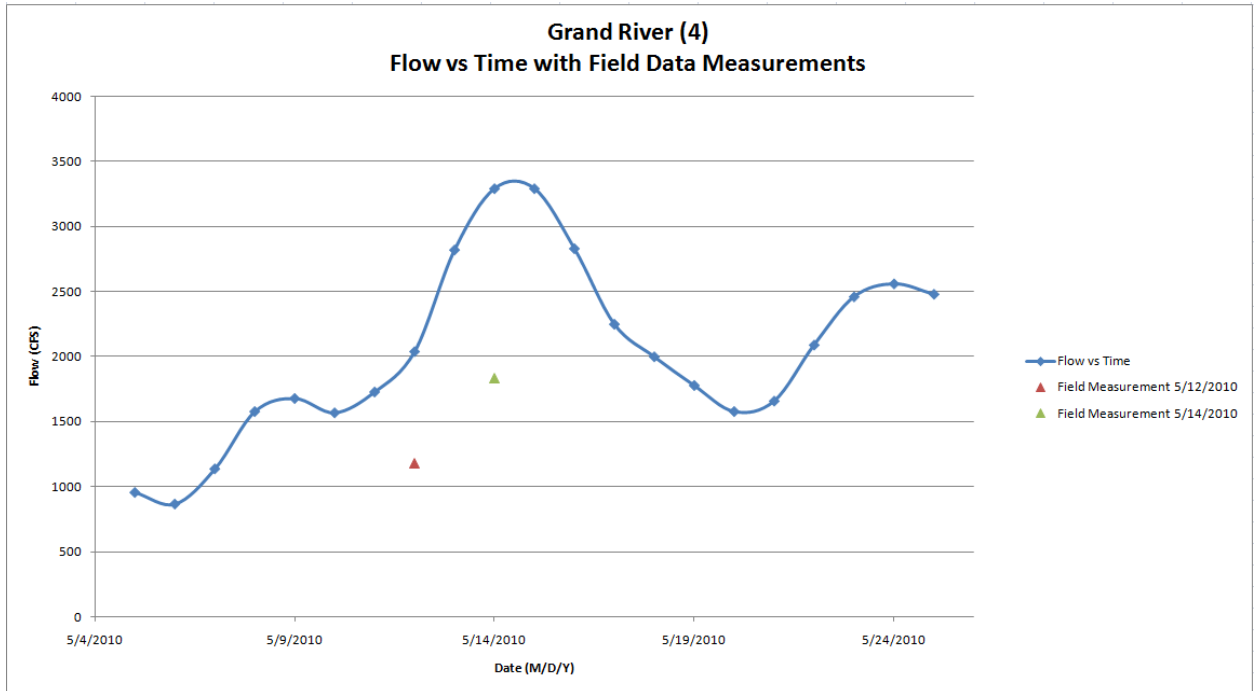


Figure 8.A.21 Hydrograph for Grand River (4) with time of measurement and associated discharge of depicted as triangles

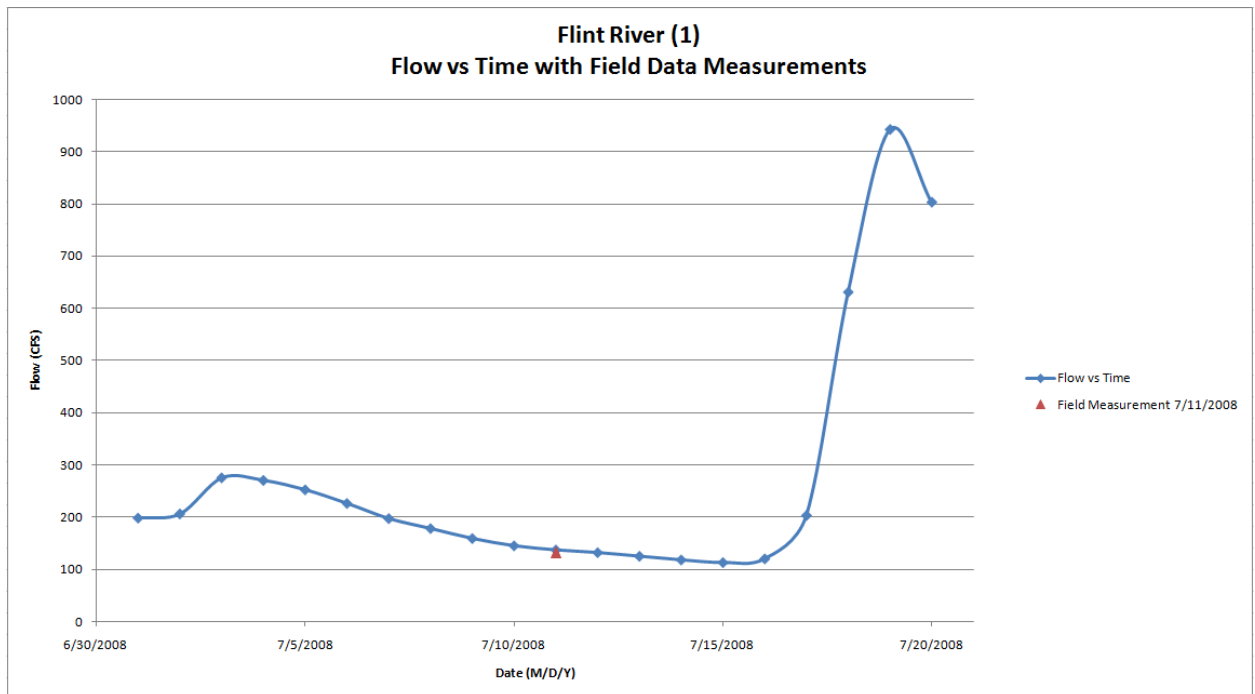


Figure 8.A.22 Hydrograph for Flint River (1) with time of measurement and associated discharge of depicted as triangles

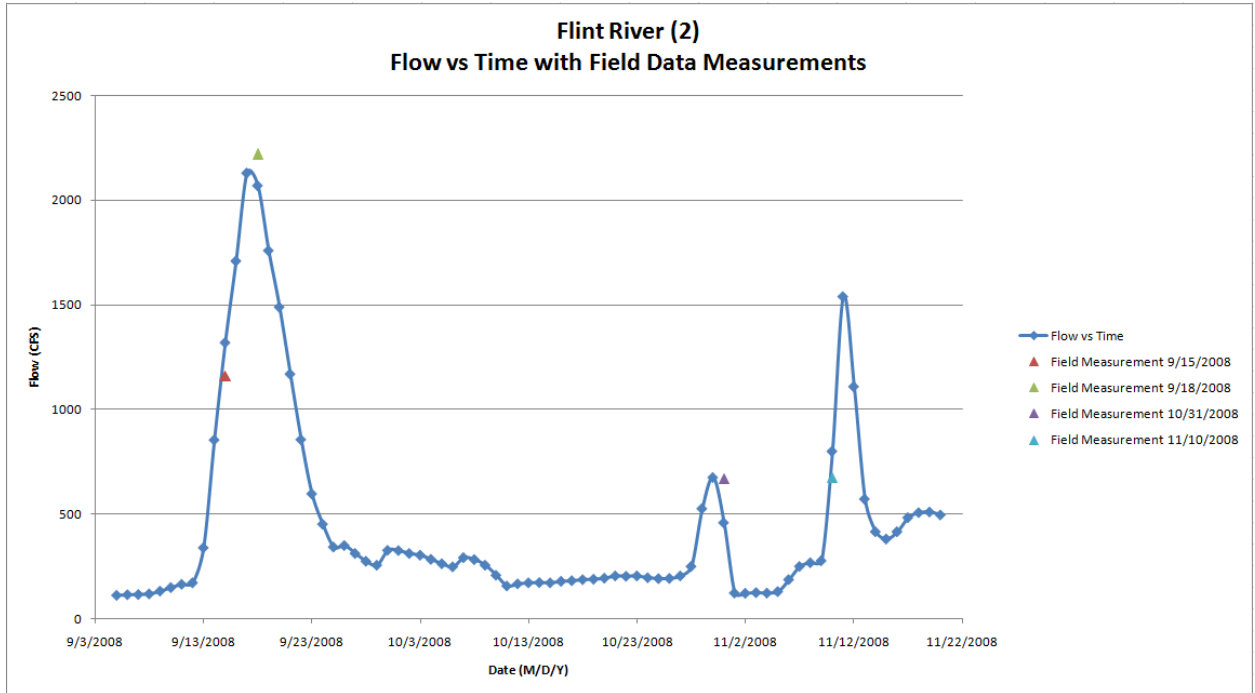


Figure 8.A.23 Hydrograph for Flint River (2) with time of measurement and associated discharge of depicted as triangles

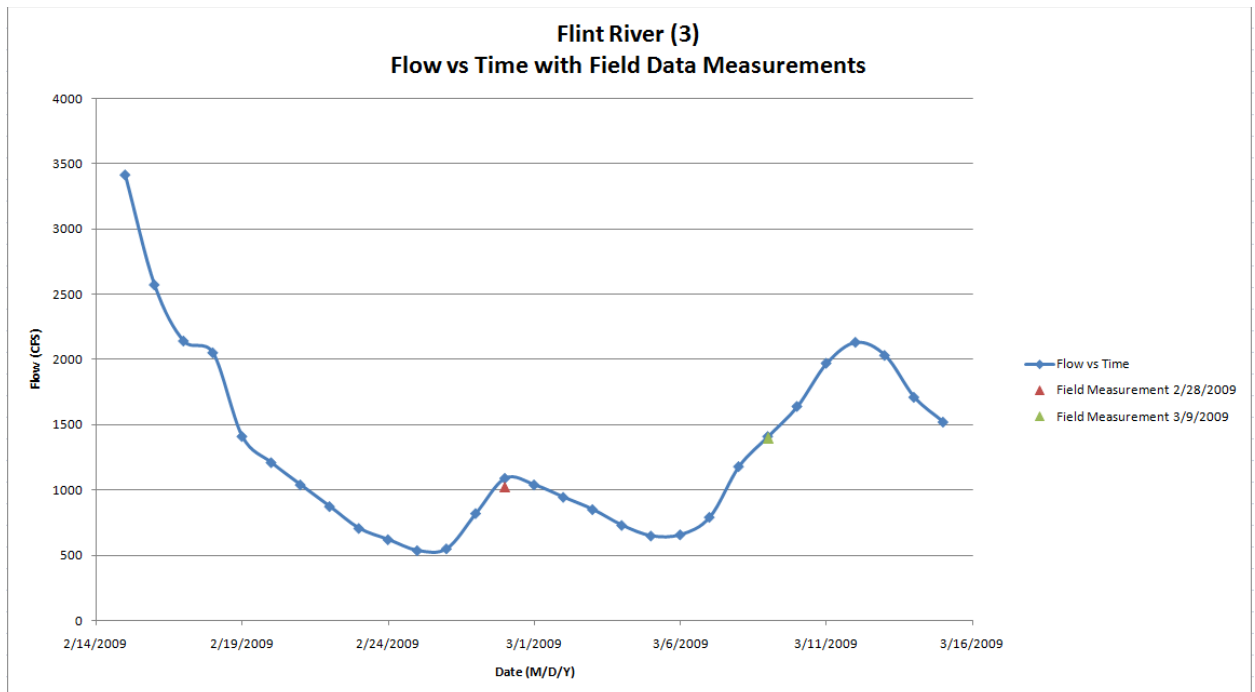


Figure 8.A.24 Hydrograph for Flint River (3) with time of measurement and associated discharge of depicted as triangles

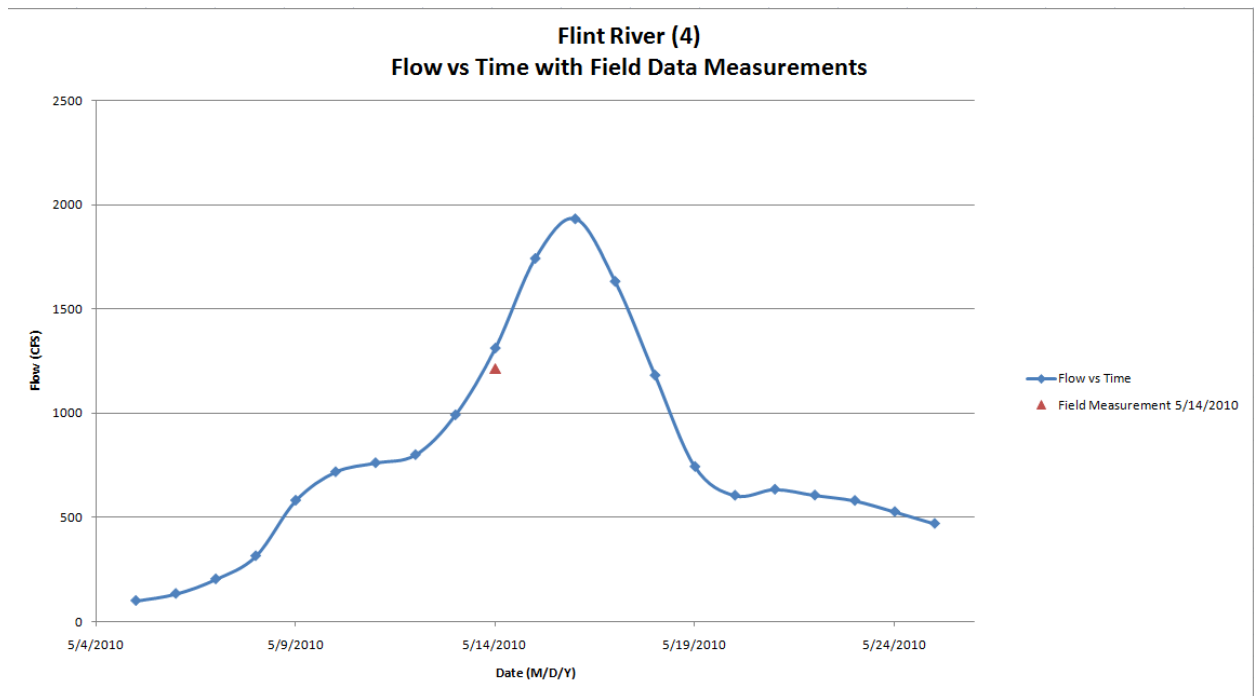


Figure 8.A.25 Hydrograph for Flint River (4) with time of measurement and associated discharge of depicted as triangles

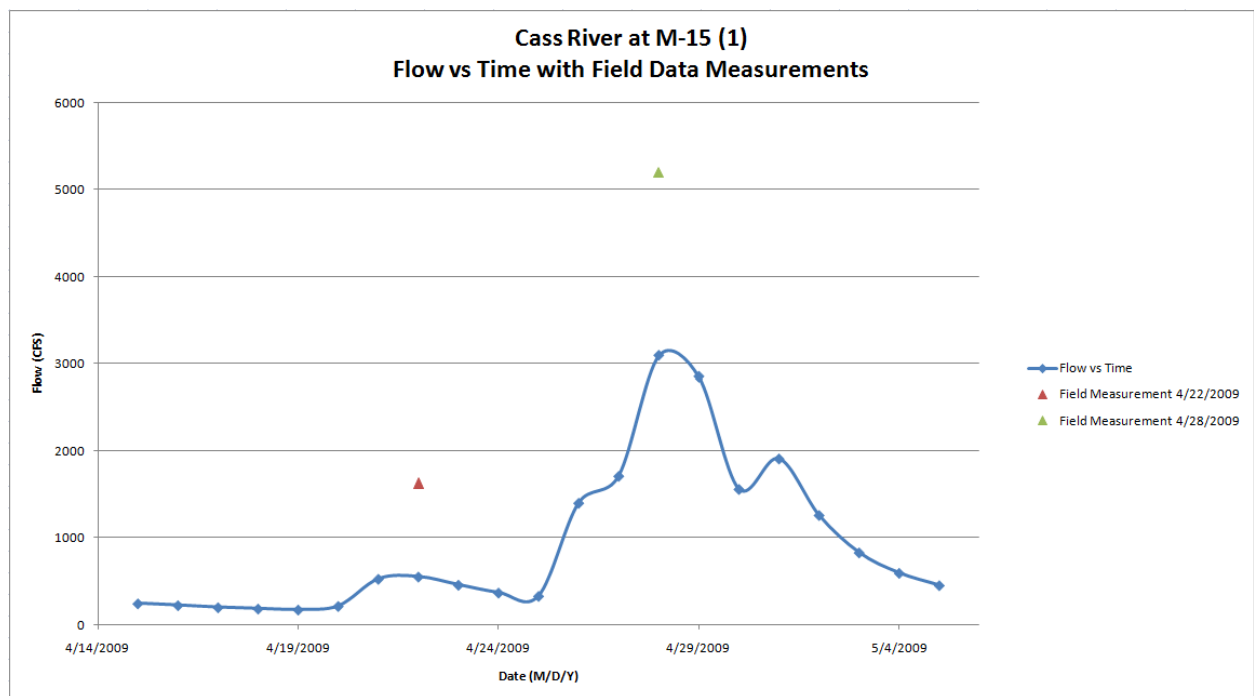


Figure 8.A.26 Hydrograph for Cass River at M-15 (1) with time of measurement and associated discharge of depicted as triangles

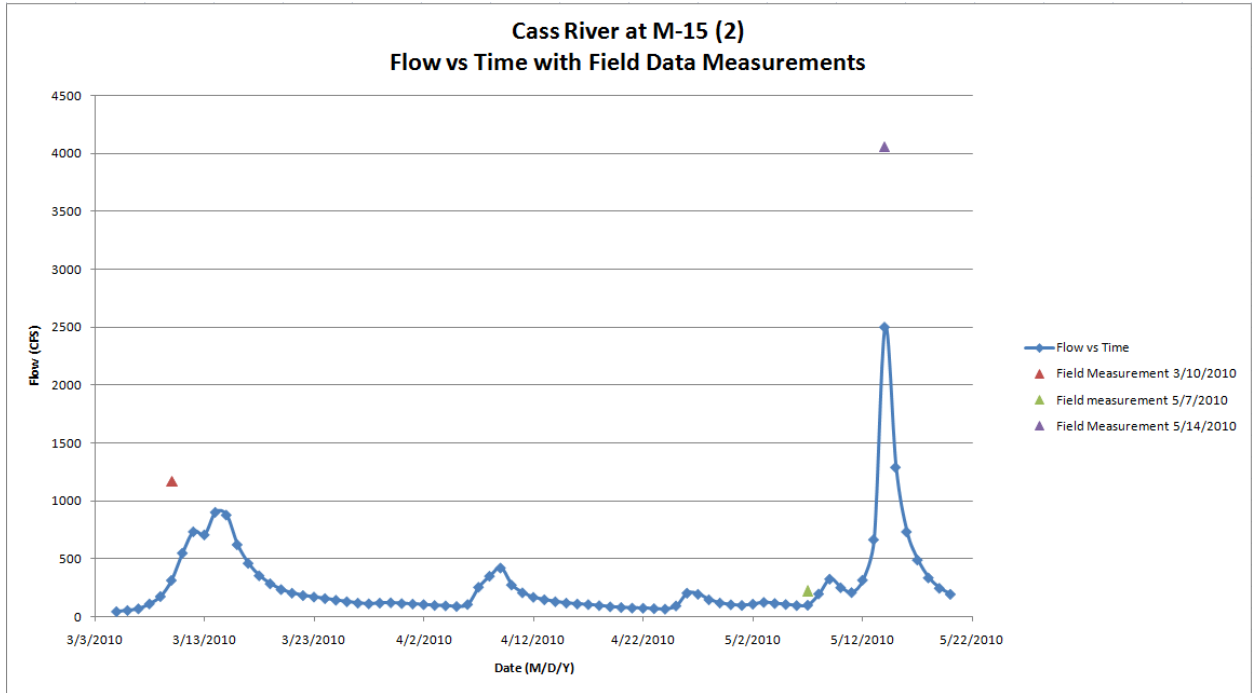


Figure 8.A.27 Hydrograph for Cass River at M-15 (2) with time of measurement and associated discharge of depicted as triangles

Appendix 9.A

Detailed Results from Regression Analyses

Three of the four regression types investigated failed to meet both selection criteria of lower mean-square error compared to the original HEC-18 equation and over-predict scour at least as often as HEC-18. The following tables and graphs show results from these modification attempts for all four trials. Table 9A.1 provides a key to reading the subsequent tables. Each table describes a parameter used to compare various models. Parameters include mean-square error (MSE), number of over predictions and the model exponents b_1 and b_2 including confidence intervals.

Table 9.A.1 : Key to following tables. Rep is the repetition number ranging from 1 to 4

Parameter trials 1 to 4	Original HEC-18		Multiplicative Adjustment		Additive Adjustment	
Case 1	Trial 1	Trial 2	Trial 1	Trial 2	Trial 1	Trial 2
	Trial 3	Trial 4	Trial 3	Trial 4	Trial 3	Trial 4

Unrestricted Ordinary Least-Squares Regression

Both equations, (9.3a and 9.3b) for Case one and Case two based on an unrestricted, ordinary least squares regression, yield a reduction in mean-square error when compared to predictions based on the original HEC-18 local pier scour equation (Table 9A.2). However, in Case one for trials one through four, the modified HEC-18 equation with the multiplicative adjustment under predicted relative scour depths in 18 instances where the original equation over predicted results, Table 9A.3. The modified equation with the additive adjustment under predicted scour in one additional instance when compared to the original HEC-18 model, Table 9A.3. Similarly, in Case two, the modified model with the multiplicative adjustment under predicted scour in five additional instances, compared to the original HEC-18 model, Table 9A.3. The modified model with the additive adjustment under predicted scour once in trial one, while the original model under predicted scour once in trial three, Table 9A.3. The unrestricted, ordinary least-squares regression for Case two, with an additive adjustment, in terms of over prediction capability both the original HEC-18 and the modified family member produced equivalent results. However, due to the under predictions described above and the negative exponents on the Froude number (regression parameter b_2), Table 9A.4, the family of equations produced with the unrestricted, ordinary least-squares regression is inferior in comparison to the original HEC-18 model.

Table 9.A.2: Mean square error for trials 1 to 4 from models developed with unrestricted, ordinary least-squares regression for both Case one and Case two.

MSE trials 1 to 4	Original HEC-18	Multiplicative Adjustment	Additive Adjustment
-------------------	-----------------	---------------------------	---------------------

Case 1	0.46	0.15	0.07	0.07	0.01	0.04
	0.25	0.06	0.36	0.03	0.03	0.01
Case 2	1.55	1.09	7.26	0.50	0.14	0.39
	0.96	0.14	1.36	0.04	0.44	0.29

Table 9.A.3: Number of over predictions for original and modified models.

Over Predictions trials 1 to 4	Original HEC-18		Multiplicative Adjustment		Additive Adjustment	
Case 1	17	19	9	15	16	19
	17	17	17	11	17	17
Case 2	19	15	19	15	18	15
	13	18	10	16	14	18

Table 9.A.4: Modified exponents b_1 and b_2 with corresponding 95% confidence limits for each trial.

Regression Coefficients trials 1 to 4	Lower		Best Fit		Upper	
b_1 Case 1	1.59	1.51	2.35	1.95	3.12	2.40
	0.69	1.43	1.22	1.87	1.76	2.31
b_2 Case 1	-0.91	-0.57	-0.38	-0.20	0.16	0.16
	-0.03	-0.43	0.50	-0.05	1.03	0.33

b₁ Case 2	0.24	-0.08	0.80	0.50	1.36	1.08
	-0.83	-0.15	-0.34	0.38	0.14	0.92
b₂ Case 2	0.90	0.81	1.27	1.26	1.64	1.71
	1.32	1.05	1.67	1.45	2.01	1.84

Unrestricted Weighted Least-Squares Regression

Both equations for Case one and Case two based on an unrestricted, weighted least-squares regression, yield a reduction in mean-square error when compared to predictions based on the original HEC-18 local pier scour equation for most trials but not all, Table 9A.5. Additionally, in Case one trials one through four, the modified HEC-18 equation with the multiplicative adjustment under predicted relative scour depths in three net instances compared to the original equation, Table 9A.6. The modified equation with the additive adjustment, under predicted scour in one additional instance when compared to the original HEC-18 model, Table 9A.6. Similarly, in Case two, the modified model with the multiplicative adjustment under predicted scour once compared to the original HEC-18 model, Table 9A.6. Whereas the modified model with the additive adjustment over predicted scour once (in trial three) when compared to the original model, Table 9A.6. Due to the number of under predictions generated with this regression type, this family of equations does not perform as well as the original model. Table 9A.7 provides the regression exponents b_1 and b_2 for these models.

Table 9.A.5: Mean square error for trials 1 to 4 from models developed with unrestricted, weighted least-squares regression for both Case one and Case two.

MSE trials 1 to 4	Original HEC-18	Multiplicative Adjustment	Additive Adjustment
-------------------	-----------------	---------------------------	---------------------

Case 1	0.46	0.15	0.13	0.08	0.02	0.04
	0.25	0.06	0.21	0.07	0.04	0.01
Case 2	1.55	1.09	12.33	0.89	0.54	0.55
	0.96	0.14	98.47	0.93	18.72	0.54

Table 9.A.6: Number of over predictions for original and modified models.

Over Predictions trials 1 to 4	Original HEC-18		Multiplicative Adjustment		Additive Adjustment	
Case 1	17	19	14	18	17	19
	17	17	17	18	17	16
Case 2	19	15	19	15	19	15
	13	18	14	18	14	18

Table 9.A.7: Modified exponents b_1 and b_2 with corresponding 95% confidence limits for each trial.

Regression Coefficients trials 1 to 4	Lower		Best Fit		Upper	
b_1 Case 1	1.54	1.51	1.72	1.65	1.91	1.78
	1.05	1.59	1.22	1.72	1.75	1.84
b_2 Case 1	-0.22	-0.17	-0.10	-0.07	0.01	0.02
	0.04	-0.17	0.25	-0.08	0.45	0.01
b_1 Case 2	0.28	0.39	0.53	0.66	0.78	0.92
	-0.67	0.11	-0.45	0.39	-0.21	0.68

b₂ Case 2	0.93	0.62	1.11	0.82	1.29	1.03
	1.39	1.06	1.56	1.23	1.73	1.48

Restricted Ordinary Least-Squares Regression

Both equations (Case one and Case two), based on a restricted, ordinary least-squares regression, yield a reduction in mean square error when compared to predictions based on the original HEC-18 local pier scour equation for all but one trial in Case 2, Table 9A.8. Additionally, in Case one in trials one through four, the modified HEC-18 equation with the multiplicative adjustment under predicted relative scour depths in 11 net instances, compared to the original equation, Table 9A.9. The modified equation with the additive adjustment over predicts scour in the same number of instances as the original HEC-18 model, Table 9A.9. Similarly, in Case two, the modified model with the multiplicative adjustment under predicted scour in five additional instances, when compared to the original HEC-18 model, Table 9A.9. Whereas the modified model with the additive adjustment under predicted scour once (in trial two) when compared to the original model, it over predicted scour once in trial three compared to the original model, Table 9A.9. This regression type and model form was chosen for use in the final model due to a significant decrease in mean-square error, Table 2 and the number of over predictions, Table 9A.9. Table 9A.10 provides the regression exponents b_1 and b_2 and the respective confidence intervals for each trial.

Table 9.A.8: Mean square error for trials 1 to 4 from models developed with restricted, ordinary least-squares regression for both Case one and Case two.

MSE trials 1 to 4	Original HEC-18	Multiplicative Adjustment	Additive Adjustment
--------------------------	------------------------	----------------------------------	----------------------------

Case 1	0.46	0.15	0.18	0.09	0.02	0.04
	0.25	0.06	0.36	0.03	0.03	0.01
Case 2	1.55	1.09	7.26	0.50	0.14	0.39
	0.96	0.14	1.04	0.04	0.39	0.29

Table 9.A.9: Number of over predictions for original and modified models.

Over Predictions trials 1 to 4	Original HEC-18		Multiplicative Adjustment		Additive Adjustment	
Case 1	17	19	14	18	17	19
	17	17	17	10	17	17
Case 2	19	15	19	15	18	15
	13	18	10	16	14	18

Table 9.A.10: Modified exponents b_1 and b_2 with corresponding 95% confidence limits for each trial.

Regression Coefficients trial 1 to 4	Lower		Best Fit		Upper	
b_1 Case 1	1.13	1.27	1.86	1.72	2.59	2.18
	0.69	1.37	1.22	1.81	1.75	2.26
b_2 Case 1	-0.55	-0.40	0	0	0.55	0.40
	-0.03	0.39	0.50	0	1.03	0.39

b₁ Case 2	0.24	-0.08	0.80	0.50	1.36	1.08
	-0.48	-0.15	0	0.38	0.48	0.92
b₂ Case 2	0.93	0.81	1.27	1.26	1.64	1.71
	1.14	1.05	1.46	1.45	1.78	1.84

Restricted Weighted Least-Squares Regression

Both equations (Case one and Case two), based on a restricted, weighted least-squares regression, yield a reduction in mean square error when compared to predictions based on the original HEC-18 local pier scour equation for most trials in both Case one and case two, Table 9A.11. Additionally, for Case one in trials one through four, the modified HEC-18 equation with the multiplicative adjustment under predicted relative scour depths in four net instances compared to the original equation, Table 9A.12. The modified equation with the additive adjustment under predicts scour once relative to the original HEC-18 model, Table 9A.12. Similarly, in Case two, the modified model with the multiplicative adjustment under predicted scour in five additional instances when compared to the original HEC-18 model, Table 9A.12. Whereas the modified model with the additive adjustment over predicted scour as often as the original, Table 9A.12. Table 9A.13 provides the regression exponents b_1 and b_2 and the respective confidence intervals for each trial.

Table 9.A.11: Mean square error for trials 1 to 4 from models developed with restricted, weighted least-squares regression for both Case one and Case two.

MSE trials 1 to 4	Original HEC-18	Multiplicative Adjustment	Additive Adjustment
-------------------	-----------------	---------------------------	---------------------

Case 1	0.46	0.15	0.17	0.09	0.03	0.04
	0.25	0.06	0.36	0.03	0.04	0.01
Case 2	1.55	1.09	4.42	0.55	0.20	0.43
	0.96	0.14	0.91	0.04	0.40	0.26

Table 9.A.12: Number of over predictions for original and modified models.

Over Predictions trials 1 to 4	Original HEC-18		Multiplicative Adjustment		Additive Adjustment	
Case 1	17	19	14	18	17	19
	17	17	17	17	17	16
Case 2	19	15	19	15	18	15
	13	18	10	16	14	18

Table 9.A.13: Modified exponents b_1 and b_2 with corresponding 95% confidence limits for each trial

Regression Coefficients trials 1 to 4	Lower		Best Fit		Upper	
b_1 Case 1	1.39	-1.41	1.57	1.54	1.74	1.67
	1.05	1.48	1.26	1.61	1.47	1.73
b_2 Case 1	-0.11	-0.09	0	0	0.11	0.09
	0.04	-0.09	0.25	0	0.45	0.09

b₁ Case 2	0.28	0.39	0.53	0.66	0.78	0.92
	-0.23	0.11	0	0.39	0.23	0.68
b₂ Case 2	0.93	0.62	1.11	0.82	1.29	1.03
	1.13	1.06	1.28	1.27	1.43	1.48